Sheffield Hallam University

The phase behaviour and structure of binary lipid/water systems.

PEEL, William Edward.

Available from the Sheffield Hallam University Research Archive (SHURA) at:

http://shura.shu.ac.uk/20215/

A Sheffield Hallam University thesis

This thesis is protected by copyright which belongs to the author.

The content must not be changed in any way or sold commercially in any format or medium without the formal permission of the author.

When referring to this work, full bibliographic details including the author, title, awarding institution and date of the thesis must be given.

Please visit http://shura.shu.ac.uk/20215/ and http://shura.shu.ac.uk/information.html for further details about copyright and re-use permissions.

PONDS STREET
SHEFFIELD S1 1WB

TELEPEN

100250766 9

SHEFFIELD POLYTECHNIC
LIBRARY SERVICE

MAIN LIBRARY

21 DEC 73

29th mar '74

I.L.L.
4th Dec 81

Sheffield City Polytechnic Library

REFERENCE ONLY

Books must be returned promptly, or renewed, on or before the last date stamped above.

FAILURE TO DO SO WILL INCUR FINES

PL/17

ProQuest Number: 10700860

All rights reserved

INFORMATION TO ALL USERS
The quality of this reproduction is dependent upon the quality of the copy submitted.

In the unlikely event that the author did not send a complete manuscript
and there are missing pages, these will be noted. Also, if material had to be removed,
a note will indicate the deletion.

ProQuest 10700860

Published by ProQuest LLC (2017). Copyright of the Dissertation is held by the Author.

All rights reserved.
This work is protected against unauthorized copying under Title 17, United States Code
Microform Edition © ProQuest LLC.

ProQuest LLC.
789 East Eisenhower Parkway
P.O. Box 1346
Ann Arbor, MI 48106 – 1346

A thesis entitled

THE PHASE BEHAVIOUR AND STRUCTURE OF BINARY LIPID/WATER SYSTEMS

presented by

WILLIAM EDWARD PEEL B.Sc.

in part fulfilment of the requirements
for the degree of

DOCTOR OF PHILOSOPHY
of the
COUNCIL FOR NATIONAL ACADEMIC AWARDS

Department of Chemistry and Biology,
Sheffield Polytechnic,
Pond Street,
Sheffield, S1 1WB.

September 1972

SHEFFIELD POLYTECHNIC
LIBRARY
574.192
Q X
73-03994

SHEFFIELD CITY POLYTECHNIC
ERIC MENSFORTH LIBRARY

LOAN OF THESIS

Author PEEL, W.E.

Title The phase behaviour + structure of binary lipid/water systems

I undertake that neither the whole nor any part of the above-mentioned thesis shall be copied, quoted or published without the consent of the Author and of the Sheffield City Polytechnic.

Signature J. Hardman

Address Chemistry Dep.
Reading University

Date 16/11/81

This undertaking is to be signed by the reader consulting the thesis and returned to:-

The Librarian
Eric Mensforth Library
Sheffield City Polytechnic
Pond Street
Sheffield
S1 1WB

ACKNOWLEDGEMENTS

This work was carried out in the Department of Chemistry and Biology, Sheffield Polytechnic, and was supported by a grant from Unilever Research Laboratories. I wish to thank Unilever for making this grant available.

I would like to express my sincere thanks to my supervisor, Dr. M.P. McDonald, for his help and guidance throughout the course of this work.

My thanks also go to the late Professor Lawrence for many interesting discussions and helpful advice, and also for supplying samples of 1-monodecanoin, 1-monododecanoin, and 1-monooctadecanoin.

I am also greatly indebted to Mr. J. Clifford of Unilever Research Laboratories, Port Sunlight, for acting as industrial supervisor, and Dr. G.J.T. Tiddy, Mr. K. Stammers and Mr. J.A. Thompson of Unilever Research Laboratories, Port Sunlight for carrying out the relaxation time and X-ray diffraction measurements.

Finally I would like to thank Professor R.W. Douglas of the Department of Glass Technology, University of Sheffield, for making available broad-line NMR facilities.

W.E. Peel

AUTHOR'S NOTE

Saturated 1-monoglycerides have been abbreviated to MG_n where n is the number of carbon atoms in the parent fatty acid.

1-mono-olein has been abbreviated to MG//18.

n-Octylamine has been abbreviated to OA.

SUMMARY

The polymorphism of five 1-monoglycerides has been studied. Transition temperatures have been determined and the thermal stability of the various polymorphs has been investigated. The structure of several of the polymorphs has been investigated using broad-line NMR and some infra-red spectroscopy.

MG8/D_2O and MG//18/D_2O phase diagrams have been obtained and the structure of the neat phase in these two systems and the MG11/water and OA/water systems has been investigated using X-ray diffraction and broad-line, high resolution and pulse NMR.

High resolution PMR spectra at 60 MHz and 220 MHz have been obtained of 1-monoglycerides in solution. An analysis has been made of these spectra and together with some infra-red measurements they have enabled some conclusions to be drawn about the hydrogen-bonding of 1-monoglycerides in the dissolved state.

CONTENTS

[illegible]

(a) [illegible]

(b) [illegible]

(c) [illegible]

(d) [illegible]

[illegible] ..... [illegible]

[illegible]

(a) [illegible]

(b) [illegible]

(c) [illegible]

(d) [illegible]

(e) [illegible]

(f) [illegible]

(g) [illegible]

[illegible] ..... [illegible]

(a) [illegible]

(b) [illegible]

(c) [illegible]

(d) [illegible]

(e) [illegible]

(f) [illegible]

(g) [illegible]

[illegible]

(a) [illegible]

(b) [illegible]

(c) [illegible]

(d) [illegible]

(e) [illegible]

(f) [illegible]

(g) [illegible]

[illegible]

(a) [illegible]

(b) [illegible]

CHAPTER I

INTRODUCTION

The structure of lipids and their interaction with each other and principally water, cholesterol, and proteins has been the subject of an increasing amount of research over the past fifteen years.

From an academic point of view the above systems afford the opportunity to study the van der Waals' forces between alkyl chains, the electrostatic forces between charged lipids and water, and also hydrogen-bonding between lipids containing one or more polar groups of the type OH, NH_2, COOH, and water.

From an industrial point of view lipids are important as surface-active agents for cleaning purposes, in the production of stable emulsions, and to promote suitable crystallisation.

However, the fundamental importance of these systems is that all membranes found in plants and animals consist of lipids associated with water, and usually cholesterol, other sterols, and proteins. The structures of membranes can be investigated in two different ways. Either actual membranes obtained from plants and animals can be studied, or model systems can be set up to approximate the properties of actual membranes, and these model systems studied. The latter approach has been adopted in this research concerned with the study of simple lipid water systems.

(I) Lipid Systems

(a) Types of lipid and their interaction with water

Lipids can be divided basically into two types, non-polar and polar (1).

1. Non-polar lipids

These lipids are long-chain paraffins or unsubstituted aromatic compounds. They are insoluble in bulk in water and form either oil

droplets or crystals. On the surface of water they appear as either an oil drop or crystals and do not spread to form monolayer films. They will not be considered further in this thesis.

2. Polar lipids

These molecules have alkyl chains which are hydrophobic, terminating in one or more polar groups which are hydrophilic. Hence they are also known as amphiphilic lipids.

In the solid state hydrogen-bonding between the polar groups and the van der Waals' interaction between the alkyl chains hold the lipid molecules in a layer lattice. Figure 1 shows the formulae of some of these amphiphilic molecules.

Amphiphilic lipids can be classified into three groups depending on the way in which they interact with water (1, 2, 3). Group I consists of di- and triglycerides, fatty acids and alcohols, cholesterol, and other sterols. Group II consists of unionised monofunctional alkylamines, bifunctional diols e.g. 1,2-hexadecanediol and 1- and 2-monoglycerides, α-hydroxyacids, and the biologically important lecithins, phosphatidyl ethanolamines and inositols, and sphingomyelins. Group IIIa includes anionic, cationic, and non-ionic detergents and lysolecithin. Group IIIb are generally aromatic compounds with three or more fused rings and are steroids. They consist of the sulphated bile alcohols and bile salts. Other compounds which may belong to this group are the rosin, soaps, saponins and phenanthrene sulphonic acids.

The lipids belonging to group I dissolve small amounts of water but do not form liquid crystalline (l.c.) phases even when heated. They form stable monolayers on the surface of water. Group II lipids dissolve considerable amounts of water and form l.c. phases either at room temperature or on heating. These molecules also form stable monolayers

[illegible]

[illegible]

[illegible]

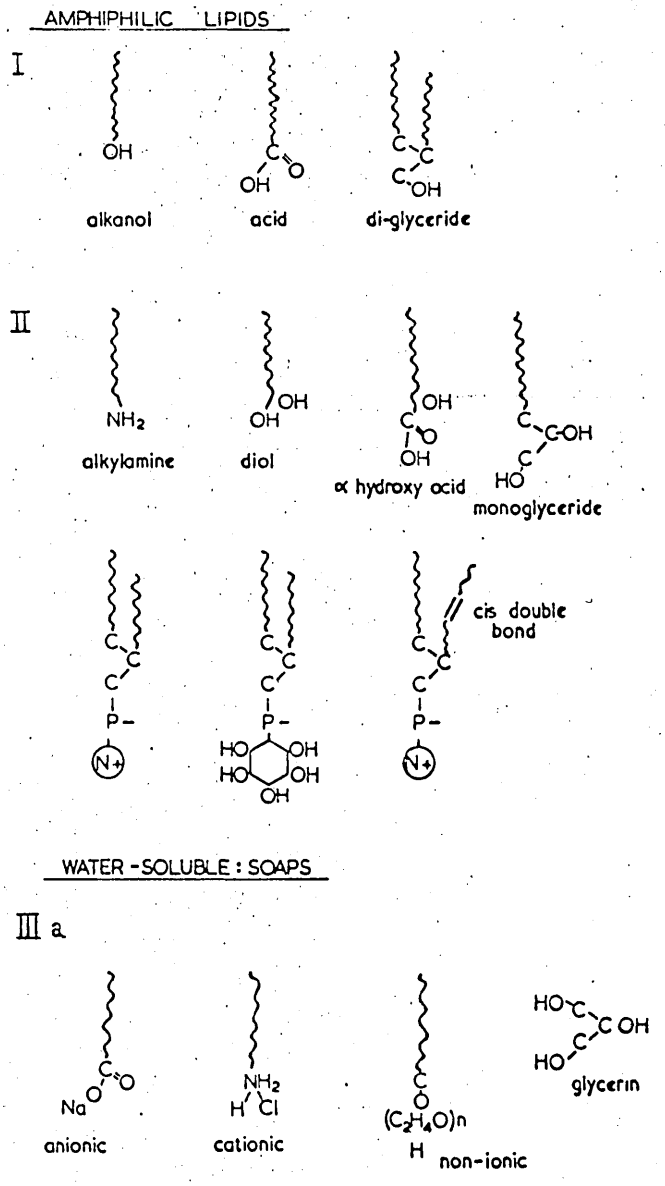

Figure 1. Amphiphilic lipids; skeleton formulae showing shape of molecules and location of hydrophilic groups.

on the surface of water. Group IIIa lipids are soluble in water and also form l.c. phases when small amounts of water are added to them. Group IIIb lipids are soluble in water but do not form l.c. phases. Both group IIIa and b lipids form unstable films at the air-water interface and demonstrate an equilibrium between molecules in the bulk phase and those on the surface. A summary of the above appears in figure 2.

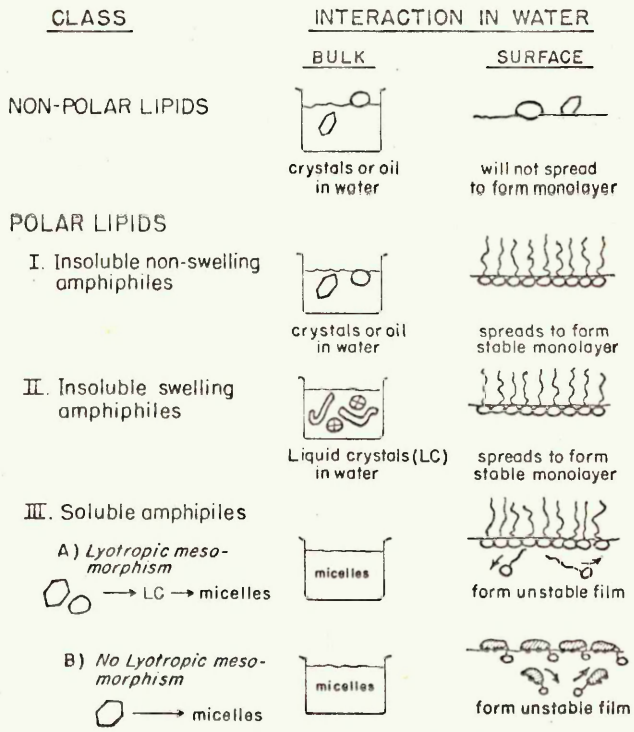

FIG. 2. Classification of biologically active lipids. Column 1 gives the three major lipid classes. Column 2 depicts the physical state of the lipid in bulk aqueous system and on the surface of water. Wavy line represents the aliphatic tails of lipid molecules, and open circles represent polar heads. Cross-hatched area molecules of Type IIIB represent the steroid nucleus of the bile salt.

(b) Binary lipid/water systems

McBain (4) showed that the most complete way of illustrating the interaction of lipids with water is by the construction of a phase diagram. When only one species of lipid is involved a binary lipid/water phase diagram can be constructed.

1. Group I lipids + water

The t/c diagram of the n-butanol/water system is shown in figure 3 and two major facts are indicated. These are the very small change of solubility in water over a wide temperature range, which becomes more pronounced with higher homologues, and the solubility of water in n-butanol which is three times larger than its own solubility in water. The latter effect still occurs in the higher alcohols as shown in figure 4.

The phase diagram of the t-butanol/water system in figure 5 shows two eutectics with a nearly flat top indicative of weak compound formation. No specific hydrate exists however, owing to the prolonged flat between the eutectics.

The alcohol-water interaction in the bulk has been investigated by Lawrence et al. (5). Under a polarising microscope fitted with a heated stage alcohol single crystals from $C_{12}OH$ to $C_{18}OH$ are seen to be penetrated by water. The temperature at which penetration occurs was termed T_{pen} which is dependent on the chain length of the alcohol. This phenomenon has been observed with other lipids and will be described in more detail in part III.

2. Group II lipids + water

These amphiphiles are insoluble in water but form several well defined l.c. phases. The molecules also spread to form stable monolayers on the surface of water. They are described in greater detail in part III.

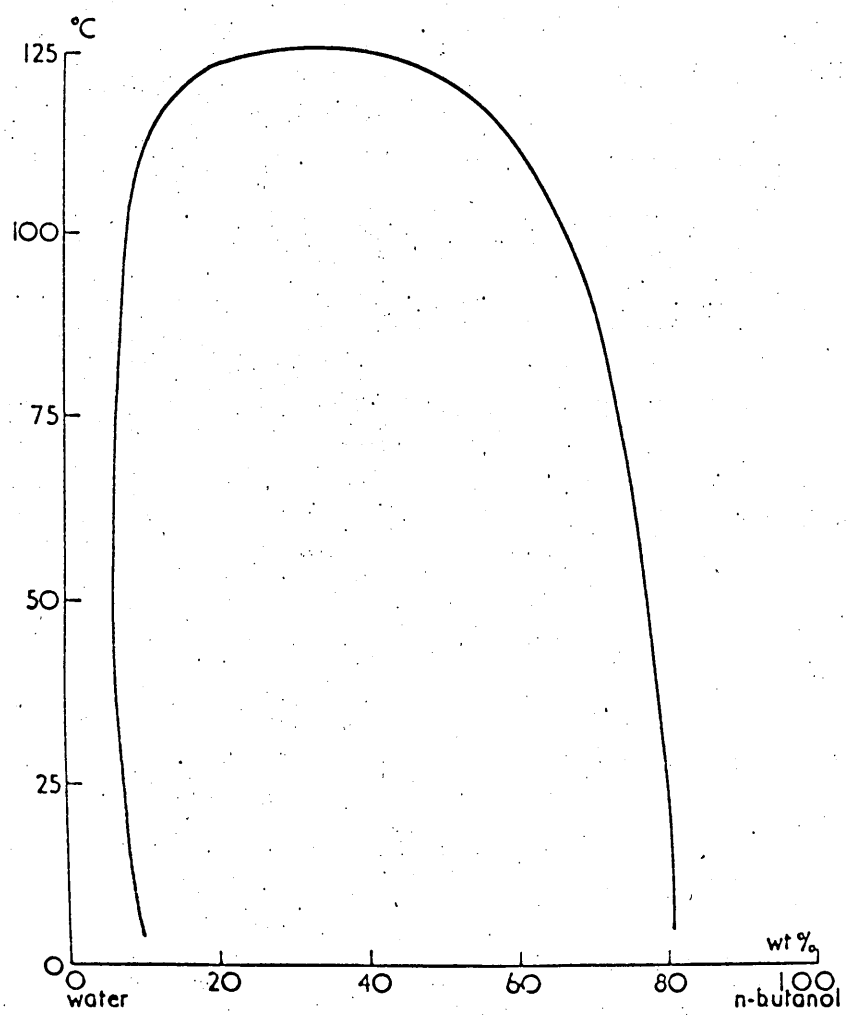

Figure 3. Solubility *vs.* temperature for the *n*-butanol-water system.

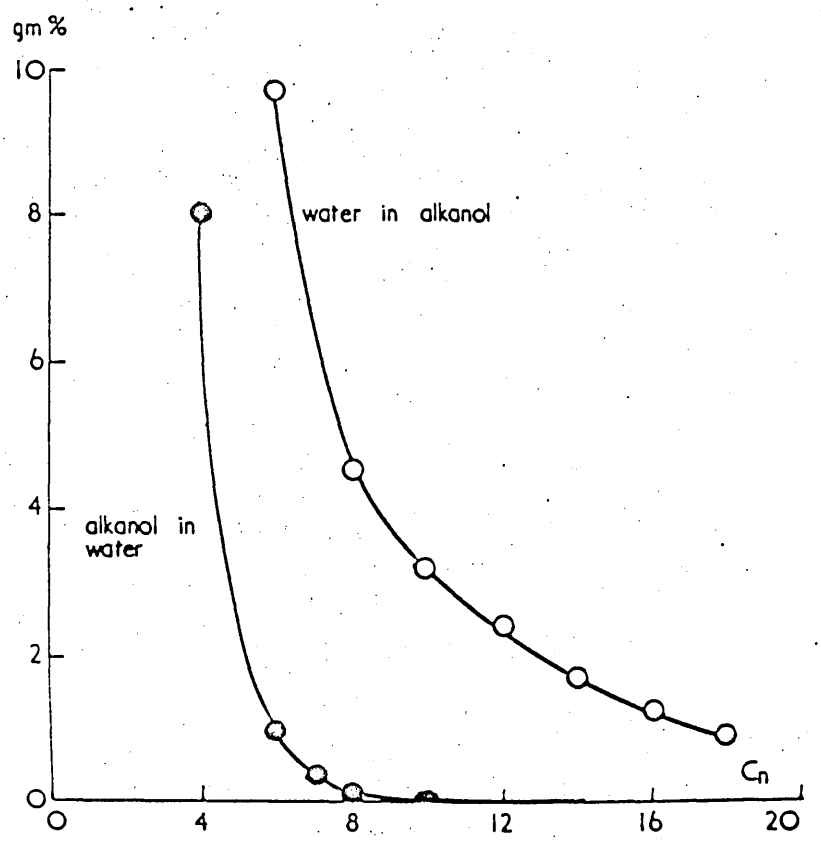

Figure 4. Solubility of *n*-alkanols in water and of water in alkanols as function of number of C atoms in chain.

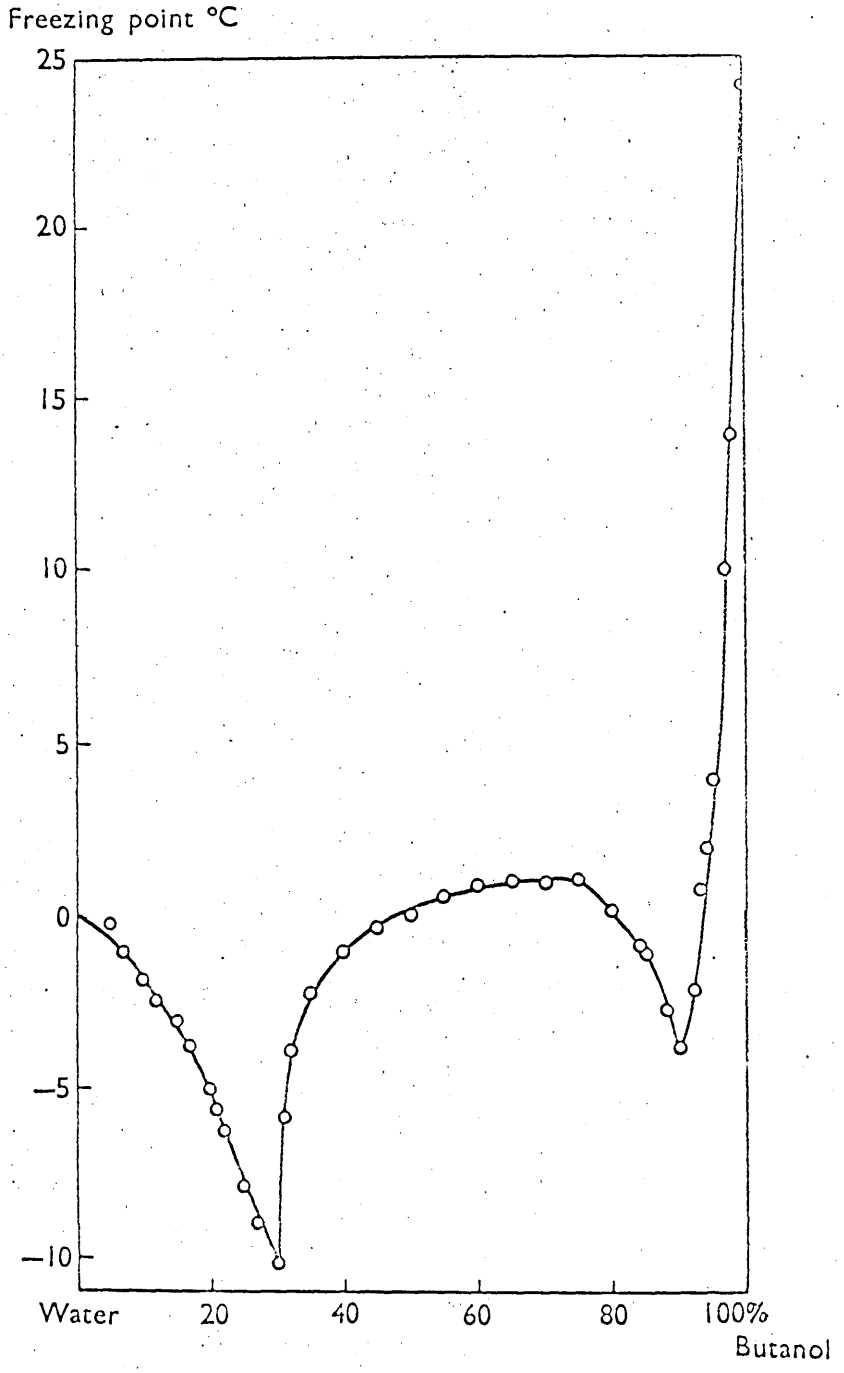

Figure 5. Freezing point diagram for the tert butanol-water system.

3. Group IIIa lipids + water

The phase diagram of a group IIIa soluble amphiphile is shown in figure 6. The diagram has been modified from the work of McBain (4) to show the various l.c. and micellar phases.

The concentration for a specific temperature at which the micelles fall apart giving an ideal solution is called the critical micellar concentration (CMC). Below the line marked 'T_c' there exists a mixture of crystals and water usually termed a gel or coagel. At T_c the gel or coagel melts and either micelles or an l.c. phase are formed. This line has been called the Krafft Point (6) or the critical micellar temperature (7).

4. Group IIIb lipids + water

Figure 7 shows the phase diagram of an amphiphile of this type, the sodium cholate/water system (1). The sodium deoxycholate/water phase diagram has also been published by Vold and McBain (8). In each case no l.c. phases are formed (8, 9, 10) and the Krafft point for most of these lipids is below $0^{o}C$ (11).

(c) Summary

These phase diagrams show that polar lipids vary considerably in their bulk interactions with water. Group I lipids have small solubilities in water, and water is slightly more soluble in them. Group II lipids are insoluble in water but can incorporate water into their various l.c. phases. The classical detergents of group IIIa form several l.c. phases but in the presence of excess water form micellar solutions. Soluble lipids of group IIIb have a high solubility in water, form micellar solutions but do not form l.c. phases.

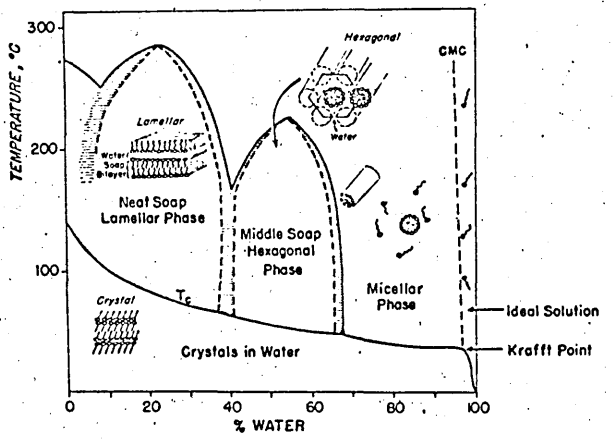

FIG. 6. Soap-water binary-phase diagram (Class IIIA-water),

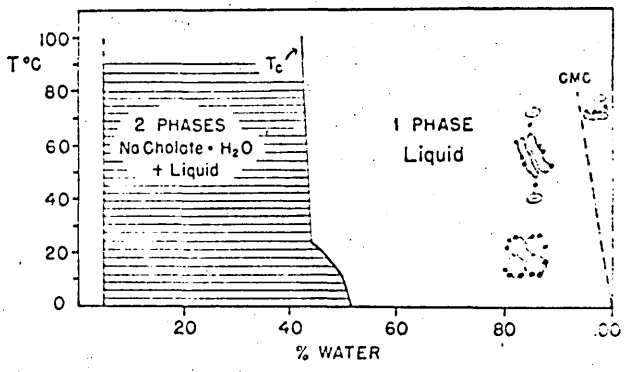

FIG. 7. Sodium cholate-water binary-phase diagram (Class IIIB-water). Vertical axis, temperature degrees C; horizontal axis, percentage of water. The line at about 5% water represents a monohydrate of sodium cholate. This monohydrate is in equilibrium with a liquid phase. The dotted line marked Tc represents the solubility of sodium cholate in water. The solubility increases slightly with increasing temperature. The liquid phase in the dilute region is made up of small micelles.

The nature of the more concentrated liquid phase is not yet certain, but it appears to be an ordered liquid. CMC, critical micellar concentration.

(II) 1-monoglycerides

(a) Polymorphism

The polymorphism of racemic 1-monoglycerides and other glycerides has been reviewed by Chapman (12) and later work by Larsson (13, 14) has provided new information.

The polymorphism was studied first by thermal (15-22) and X-ray diffraction (17,19,20,21,23) methods. Later investigations of the polymorphic forms were carried out using infra-red spectroscopy (24, 25), broad-line N.M.R. spectroscopy (26), and dielectric measurements (27, 28).

The points of controversy between the two main investigators of the polymorphism, Lutton (20) and Malkin (17, 21), are the temperature ranges of existence of the α -forms, whether sub- α forms exist, and whether the α to sub- α transitions are reversible. Some of the above points have been clarified by Larsson (13, 14) who studied single crystals of racemic 1-monoglycerides using X-ray diffraction.

Data reported on the four polymorphic forms of racemic 1-monoglycerides is summarised below.

1. Sub-alpha form

Lutton (20) reported that the α -form is reasonably stable down to a lower transition temperature, about 25°C below the α -melting point, at which it changes reversibly into a new crystalline modification sub-alpha. The reversibility of the transition was confirmed using X-ray diffraction, dilatometry, and microscope observations. The X-ray diffraction pattern consisted of a single strong short spacing at 4.15 Å and other medium spacings at 3.9, 3.75, and 3.55 Å. The long spacings are similar to those of B' forms and the sub-alpha form is thought to have tilted, common orthorhombic packed chains (25). The X-ray data and the reversibility of the transition have been confirmed by Larsson (14) who

[illegible]

[illegible]

[illegible]

found an angle of tilt of the chains towards the end group planes of 55°.

Dielectric constant and loss measurements (28) have indicated that below the alpha $\rightleftharpoons$ sub-alpha transition point rotational freedom of the molecules about their long axes ceases but that segmental reorientation still occurs.

In the infra-red spectrum (25) of the sub-alpha form there are two bands at 719 and 725 cm^{-1} similar to those observed in crystalline polyethylene (29), and an orthorhombic (31) form of solid n-paraffins (30). Stein (32) ascribed the doublet to the in-phase and out-of-phase components of the CH_2 rocking frequency. Chapman (25) deduces that the sub-alpha form has at least a very ordered structure and probably a crystalline lattice. An infra-red spectrum of the sub-alpha form of 1-monopalmitin is shown in figure 8.

The line-widths and second moments of the sub-alpha forms of 1-monomyristin and 1-monostearin from the work of Chapman et al. (26) are given in table I. The large second moments confirm the probability of common orthorhombic packing of the alkyl chains.

Only measurements on three specific sub-alpha forms have been reported, those of 1-monomyristin (26), 1-monopalmitin, and 1-monostearin (20,25,26,28). Therefore, whether 1-monoglycerides with shorter alkyl chains give sub-alpha forms is still open to conjecture. Transition temperatures for the above three 1-monoglycerides and possible transition temperatures for others from the work of Malkin (17), and Lutton (20) are given in table II.

2. Alpha-form

The alpha-form is obtained by cooling the molten 1-monoglycerides (15, 16, 17), and has the lowest complete melting point. On the basis of X-ray data (short spacing 4.2 Å) Malkin (17) described the structure as

[illegible]

Molecular studies have been performed (Ref.) have indicated that below the [illegible] transition point, crystalline [illegible] the material is mostly [illegible] [illegible] [illegible]

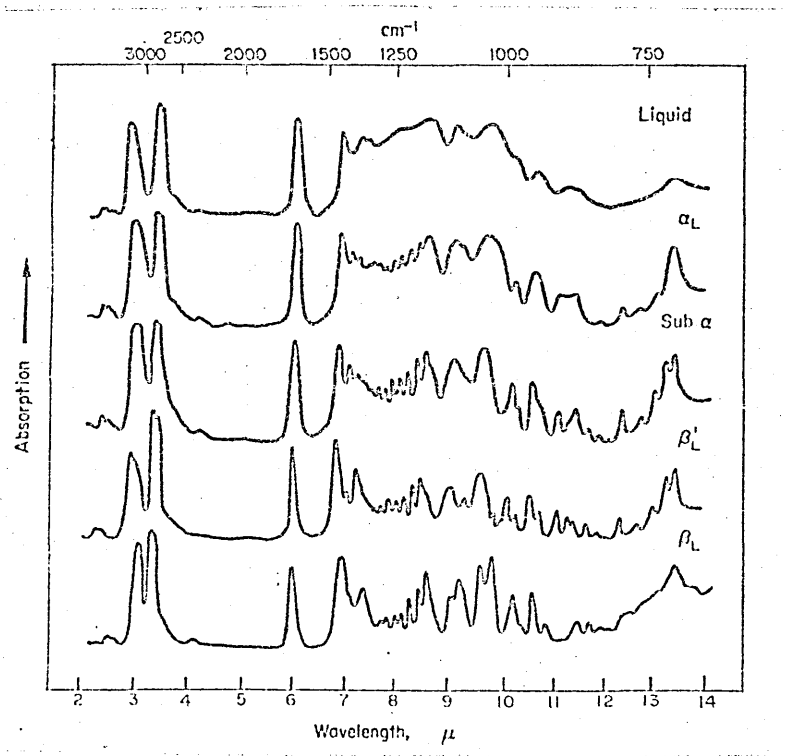

Figure 8

Infra-red spectra of the polymorphic forms of 1-monopalmitin.

Table I

Linewidths (μT)*

1-Monoglyceride	B	B'	α	Sub- α	Temp.(K)
1-Monomyristin	1290 ± 40			1260 ± 40	293
			430 ± 20		303
1-Monostearin	1270 ± 50			1310 ± 20	293
			400 ± 10		323
1-Mono-olein	800 ± 30	750 ± 60			293
			940 ± 80		273

Second Moments ($10^4 \mu T^2$)**

1-Monoglyceride	B	B'	α	Sub- α	Temp.(K)
1-Monomyristin	19.7 ± 1.3			19.8 ± 1.4	293
			5.7 ± 1.0		303
1-Monostearin	19.9 ± 1.7			20.0 ± 1.3	293
			4.5 ± 0.1		323
1-Mono-olein	13.1 ± 0.5	12.9 ± 1.4			293
			13.7 ± 1.2		273

* $1G \cong 100 \mu T$ ** $1G^2 = 10^4 (\mu T)^2$.

Table II

1-Monoglyceride	Transition Temperature (^{o}C)			
	α	B'	B	*
Decanoin	27	49	53	8
Undecanoin	36.5	52	56.5	3
Laurin	44	59.5	63	15
Tridecanoin	50	61	65	9
Myristin	56	67.5	70.5	24
Pentadecanoin	62	69	72	17
Palmitin	66.5(66.9)	74(74.6)	77(77)	34(39)
Heptadecanoin	70	74.5	77	28
Stearin	74(74)	79(78)	81.5(81.5)	47.5, 42(49)

Temperatures from Malkin (17) and those in brackets from Lutton (20)

* These temperatures are regarded by Malkin (17) as transitions to B' and B and by Lutton (20) as transitions to sub-alpha.

Table II

3-Aminotyrosine	[illegible]	[illegible]	[illegible]	[illegible]
Lysine	[illegible]	[illegible]	[illegible]	[illegible]
Cysteine	[illegible]	[illegible]	[illegible]	[illegible]
Leucine	[illegible]	[illegible]	[illegible]	[illegible]
Methionine	[illegible]	[illegible]	[illegible]	[illegible]
Phenol	[illegible]	[illegible]	[illegible]	[illegible]
Tryptophan	[illegible]	[illegible]	[illegible]	[illegible]
Proline	[illegible]	[illegible]	[illegible]	[illegible]
Hydroxyproline	[illegible]	[illegible]	[illegible]	[illegible]
Arginine	[illegible]	[illegible]	[illegible]	[illegible]

[illegible]

vertical rotating chains hexagonally packed similar to that found for the alpha-forms of long chain esters (33), alcohols (34), and n-hydrocarbons (31). The X-ray measurements of Lutton et al. (20) and Larsson (14) indicated however that the chains were tilted.

Additional evidence for the considerable orientational freedom of the alkyl chains has been obtained from dielectric measurements (28), infra-red spectra (25), and broad-line N.M.R. (26), shown in fig. 8 and Table I.

3. B'-form

Malkin (17) obtained the B' form by cooling molten 1-monoglycerides at a suitable rate and found that the melting points alternate as shown in table II. X-ray analysis gave long spacings similar to those of the B form and short spacings of 3.86 and 4.24 Å. The structure was thought to consist of rigid double molecules tilted at an angle of 55°. Lutton (20), Chapman (25), and Larsson (14) could only obtain a B' form by rapid crystallisation from solvents. A single crystal of this B' form was shown by Larsson to give identical X-ray data to that obtained from one form of optically active 1-monoglycerides (14, 35). Larsson therefore stated that the form earlier termed B' is optically active and that the racemic form is separated by rapid crystallisation into antipode crystals, and the B' form has nothing to do with a polymorphic transition in racemic 1-monoglycerides. The structure was found to consist of molecules arranged head-to-head with the alkyl chains packed in a common orthorhombic sub-cell and tilted at 55°, the direction of chain tilt alternating in successive double layers.

The infra-red spectra for the B' forms of three 1-monoglycerides have been reported by Chapman (25), and that of 1-monopalmitin is shown in figure 8.

4. B-form

This form is normally obtained by slow crystallisation from

[illegible]

[illegible]

[illegible]

solvents or by transformation from alpha and B' forms. It is the stable form with the highest melting point, and gives X-ray short spacings of 3.9, 4.4, and 4.6 Å (17, 20). The melting points for a series of 1-monoglycerides are given in table II (17, 20). The structure has been shown by X-ray diffraction (13,14,17,20) to consist of rigid double layers of molecules with the alkyl chains packed in a monoclinic sub-cell and again tilted at 55°, the direction of tilt alternating in successive double layers as in the B' form. The hydroxyl groups are thought to form a hydrogen-bonded square array (14) similar to that found in 2-monoglycerides (36) shown in figure 9.

Dielectric constants (28), N.M.R. line-widths and second moments (26,,table I) of the B-forms of 1-monoglycerides are those expected from rigid structures in which no appreciable motion occurs.

Infra-red spectra of the B-forms of 1-monoglycerides have been reported by Kurht et al. (37), Barcelo and Martin (38), O'Connor et al. (39), and Chapman (25, 40). Chapman notes that the main differences in the spectra of the B-forms of different 1-monoglycerides (figure 10) occur in the 1250 cm^{-1} region associated with the CH_2 vibration patterns.

(b) Monoglycerides in solution

1. Infra-red Spectroscopy

The infra-red spectra of various 1-monoglycerides have been determined as solutions in carbon tetrachloride (38) and chloroform (39). Some of the latter spectra with the most prominent absorption band assignments are given in figure 11.

The spectra show two bands with maxima at about 2.7 and 2.8 microns associated with OH vibrations. The 2.7 micron band was ascribed (39) to a stretching vibration of a free OH group whilst the 2.8 micron band was thought to be from an OH stretching vibration of the single

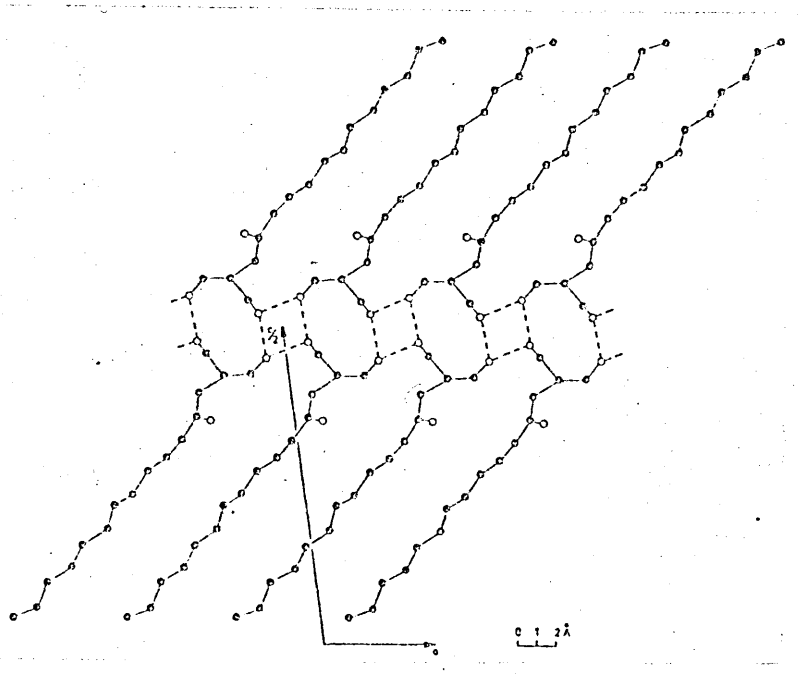

Figure 9

The molecular arrangement in 2-monolaurin as viewed along the b-axis.

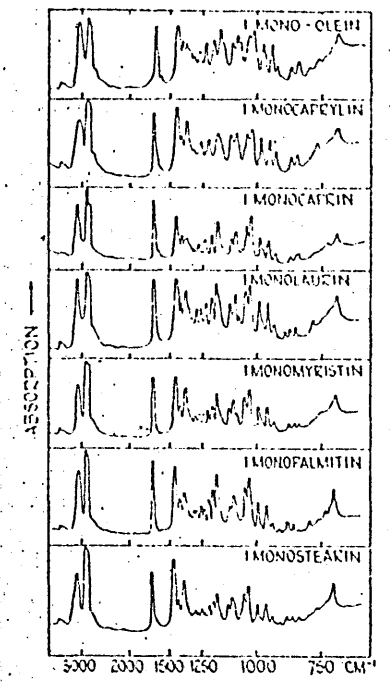

Monoglycerides (β_L-form)	Frequency of bands in the 1250 region (cm^{-1})
1-Mono-olein	1333, 1294, 1255, 1213
1-Monocaprylin	1327, 1283, 1231
1-Monocaprin	1329, 1293, 1256, 1221
1-Monolaurin	1337, 1302, 1275, 1242, 1215
1-Monomyristin	1332, 1306, 1284, 1256, 1230, 1205
1-Monopalmitin	1339, 1314, 1293, 1271, 1248, 1227, 1202
1-Monostearin	1332, 1312, 1297, 1277, 1258, 1233, 1219, 198

Figure 10

The spectra of a series of 1-monoglycerides in the most stable B-form, and identification bands in the 1250 cm^{-1} region.

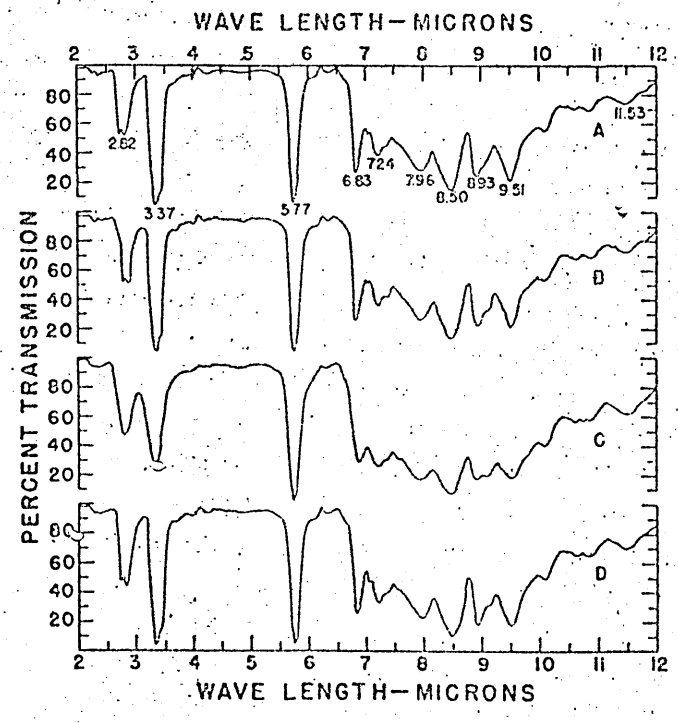

Most Prominent Absorption Bands in the Infrared Spectra of All Mono-, Di-, and Triglycerides

Wavelength position of maximum (microns)	Intensity	Most probable assignment
3.30–3.37	Very strong	C—H stretching (CH_3 and CH_2)
5.71–5.77	Very strong	C=O stretching (COOR)
6.83–6.88	Strong	C—H bending (doubly degenerate deformation of CH_3 and symmetrical deformation of CH_2)
7.23–7.35	Strong	C—H bending (symmetrical deformation of CH_3)
7.93–8.00	Strong	C—H in-plane wagging or rocking of CH_2 groups
8.48–8.58	Very strong	C—O stretching (COOR)

Figure 11

Infra-red spectra of 1-monoglycerides in $CHCl_3$; and band assignments.

A. 1-monostearin

B. 1-monopalmitin

C. 1-mono-olein.

D. 1-monomyristin.

bridged dimer. The stretching vibration of more highly hydrogen bonded OH was thought to be masked by the strong CH stretching vibration at 3.3 microns.

This last conclusion is highly unlikely since even in solid monoglycerides, where stronger hydrogen bonding occurs, the OH bands only appear up to 3.1 microns (25).

2. N.M.R. Spectroscopy

The N.M.R. spectra of various 1-monoglycerides dissolved in chloroform have been determined by Chapman (42) and Hopkins (43) at 40 MHz and 60 MHz respectively. N.M.R. spectra from the work of Chapman are shown in figure 12. The reported chemical shift values and the protons they are assigned to are given in table III.

Table III

τ		Group
Chapman	Hopkins	
5.95	5.8	$\underline{CH_2}.O.CO$
6.25	6.1	$\underline{CH}O$
6.39	6.3	$\underline{CH_2}.OH$
7.9	7.7	$\underline{CH_2}.CO$
8.7	8.7	$(\underline{CH_2})_n$
9.1	9.1	$\underline{CH_3}CH_2$

The chemical shifts observed for the hydroxyl protons are not given since they are strongly concentration and temperature dependent.

Chapman (42) investigated the N.M.R. lines from the glyceride grouping CH_2CHCH_2 on the basis of an approximate AB_4 system. He also studied similar model compounds to see whether and under what conditions a good fit to an AB_4 type pattern could be expected.

[illegible]

[illegible]

[illegible]

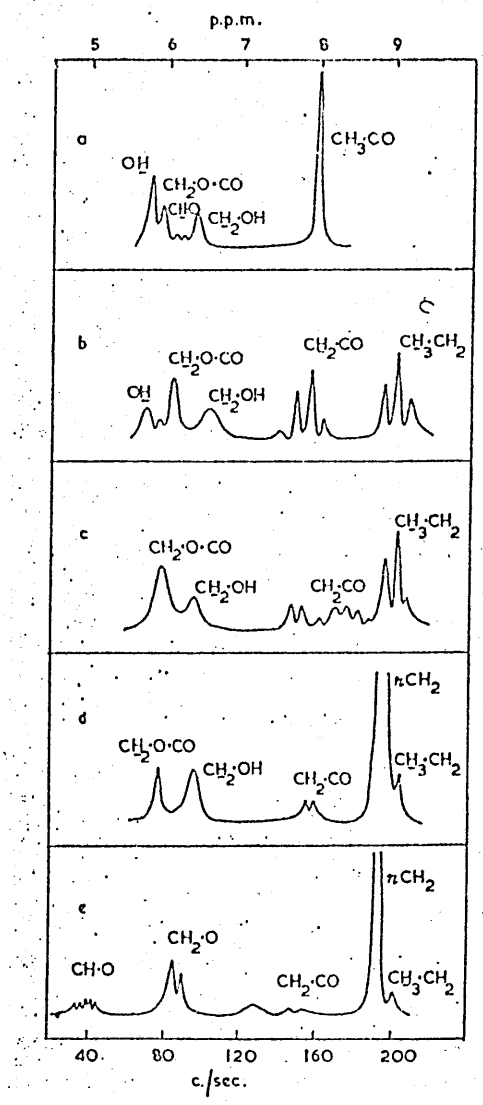

Figure 12

PMR spectra of 1-monoglycerides in $CHCl_3$.

(a) 1-monoacetin

(b) 1-monopropionin

(c) 1-monobutyrin

(d) 1-monostearin

(e) 2-monostearin

(III) Liquid Crystal Systems

The first observation of the lyotropic l.c. state, although he did not realise it at the time, was made by the German physiologist Virchow in 1854 (44). In his own words "he soaked a piece of nerve tissue in water for a long time" and then saw under his microscope this curious "Newgate frill" of tubular excrescences, which are now termed myelins.

In 1863 Neubauer (45, 46) observed myelin formation of lyotropic liquid crystals when ammonium hydroxide solution was brought into contact with oleic acid and the study of liquid crystals began.

The l.c. state has been the subject of four relatively recent reviews by Brown et al. (47a, b), Chistyakov (48), and Winsor (49).

The bulk of this thesis is concerned with the lyotropic neat l.c. state and to some extent the viscous isotropic state.

(a) Formation of the lyotropic neat phase

Lawrence et al. (5,50,51,52) observed that for several group II lipids including 1-monoglycerides, hexadecane-1,2-diol, and α-hydroxypalmitic acid, penetration of water into the solid crystals occurred at or above a specific temperature which was termed T_{pen}. The penetration was observed using a heated stage polarising microscope and T_{pen} was stated to be as sharp as a melting point. The penetration is shown diagramatically in figure 13.

T_{pen} can be considered as that temperature at which thermal motion of the crystal lattice is great enough to allow water to penetrate between the polar end groups of the lipid bilayer structure. The penetration is an equilibration process taking place spontaneously and therefore ΔG is negative above T_{pen}. Lawrence (2) defines T_{pen} as the temperature at which $\Delta H_m = T\Delta S_m$ where H_m and S_m are the heat and entropy of the mixing process, which include the ΔS and ΔH of the

[illegible]

[illegible] observed that the [illegible] i.e. [illegible] [illegible] for the [illegible], was made by [illegible] [illegible] Vickers in [illegible]. In his own words "We obtained a [illegible] [illegible] in water for a [illegible] "[illegible]" [illegible] under his observation [illegible] [illegible] "[illegible] Fall" of [illegible] [illegible], which are now known [illegible].

In [illegible] Kathleen [illegible], who observed again formation of [illegible] liquid crystals when [illegible] [illegible] [illegible] [illegible] with [illegible] acid and [illegible] of [illegible] [illegible].

The [illegible] has been the subject of [illegible] [illegible] [illegible] by [illegible] [illegible], [illegible], Chandrasekhar [illegible], and Kinsley [illegible].

The [illegible] of this [illegible] is concerned with the [illegible] [illegible] [illegible] and to [illegible] [illegible] the [illegible] [illegible] [illegible].

(a) [illegible] of the [illegible] [illegible] [illegible]

[illegible] [illegible], [illegible] observed that [illegible] [illegible] [illegible] liquids [illegible] [illegible] [illegible], [illegible], and [illegible] [illegible], [illegible] of water from the [illegible] [illegible] [illegible] or [illegible] [illegible] [illegible] which [illegible] [illegible]. The [illegible] was [illegible] [illegible] a [illegible] [illegible] [illegible] [illegible]

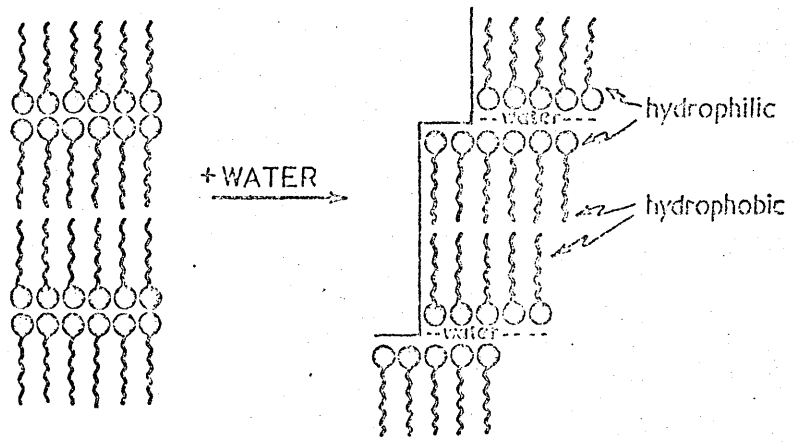

Figure 13
Penetration of water into a bimolecular layer of amphiphilic lipid.

crystalline transition as well as the terms for the hydration process.

The penetration of water will only lead to liquid crystal formation if a sufficiency of water can be incorporated into the bimolecular lipid layer to provide a centre across which the fluid shear, which is required for laminar flow of the liquid crystal, can take place. Therefore a liquid crystal phase will only be formed if this sufficiency is reached before saturation occurs and the system becomes two-phase.

(b) Structure of the Neat Phase

Prior to physical measurements on a particular neat phase it is usually necessary to determine the region over which it exists in the system being studied. This is carried out most easily by determining the phase diagram of the system as a function of temperature and composition. Condensed binary phase diagrams for numerous group II lipid/water systems have been reported, and these include amine/water (53), amine-oxide/water (54, 55), amine-hydrochloride/water (56, 57), alkyl-imide/water (58), dimethylalkylphosphine-oxide/water (101), 1-monoglyceride/water (59,60,61,62,63,64), dodecylhexaoxyethylene glycol monoether ($C_{12}E_6$)/water (65), and lecithin/water (66), two of which are shown in figures 14 and 15. The presence of a neat phase is most easily detected by the birefringent 'textures' which it shows under the polarising microscope (67, 68).

The earliest investigations into the structure of the neat phase were carried out using X-ray diffraction measurements on soap/water systems (69, 70). The structure was thought to be lamellar with the alkyl chains taking up a highly ordered conformation. Since then a large amount of X-ray data has been reported, on the neat phases of soap/water (71-82), amine-hydrochloride/water (76, 81), amine-oxide/water (54, 83), alkyl-imide/water (84), 1-monoglyceride/water (61,62,

experiments [illegible] as well as the cause for the polarizing process.

The presentation of water will only lead to liquid crystal formation if a sufficiency of water can be incorporated into the mesophase in order to provide a medium across which the polar charge water is required for lateral flow of the liquid crystal, and also prior. Therefore a liquid crystal phase will only be formed if the sufficiency of cooling molecular association occurs and the phase becomes [illegible].

(b) Mesogenic Molecular Shape

Based on physical measurements on a particular unit shape it is usually necessary to make the molecule over which it exists in the crystal lattice unstable. This is carried out most easily by a molecular [illegible] in a [illegible] as a function of temperature and concentration. Conformational [illegible] change [illegible] for mesogens [illegible] Thermotropic systems have been researched, and these include azomethines (XXI), azoxy-[illegible] (XX), [illegible] (XIX), [illegible] (XVIII), [illegible] (XVII), [illegible] (XVI), [illegible] (XV), [illegible] (XIV), [illegible] (XIII), [illegible] (XII), [illegible] (XI), [illegible] (X), [illegible] (IX), [illegible] (VIII), [illegible] (VII), and [illegible] (VI), some of which are shown in figures 6 and 7. The presence of a [illegible] is well [illegible] by the [illegible] 'rectangle' which is based [illegible] [illegible] (XI, XX).

In addition [illegible] the [illegible] [illegible] [illegible] water [illegible] (XX, XXI). In [illegible] the [illegible] [illegible] the edge [illegible] is a highly ordered [illegible] [illegible] a [illegible] [illegible] [illegible] [illegible] [illegible] [illegible] (XVIII), [illegible] (XV), [illegible] [illegible] (XIV), [illegible] (XIII), [illegible] (XII), [illegible] (XI), [illegible]

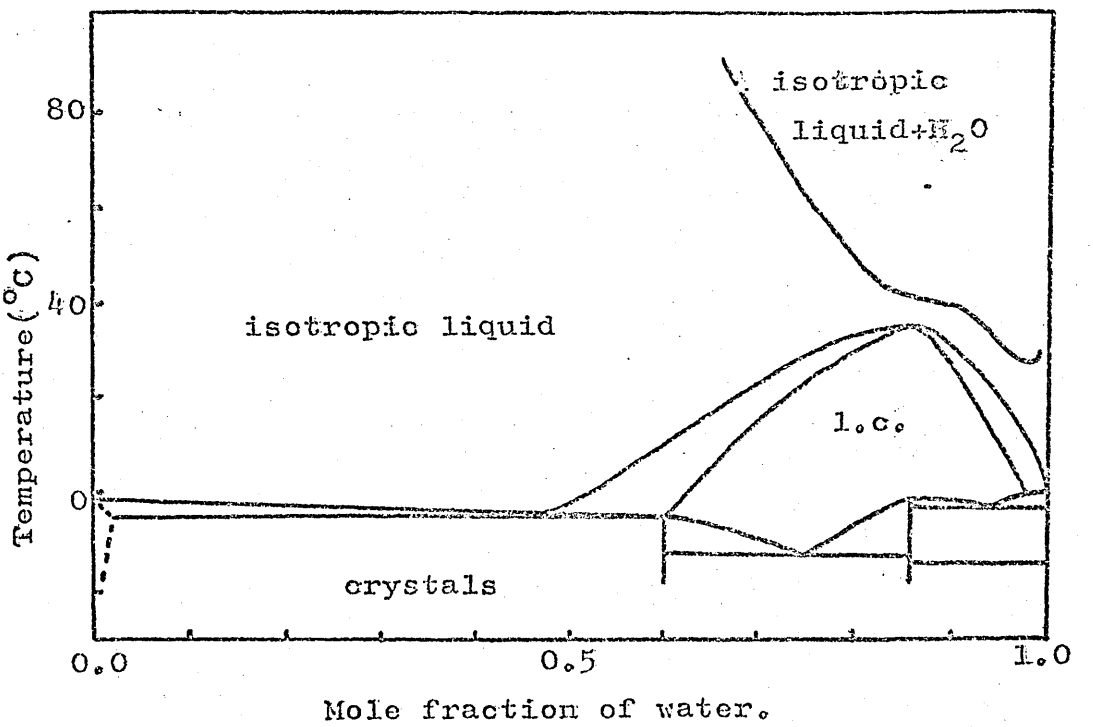

Figure 14

n-Octylamine/water phase diagram

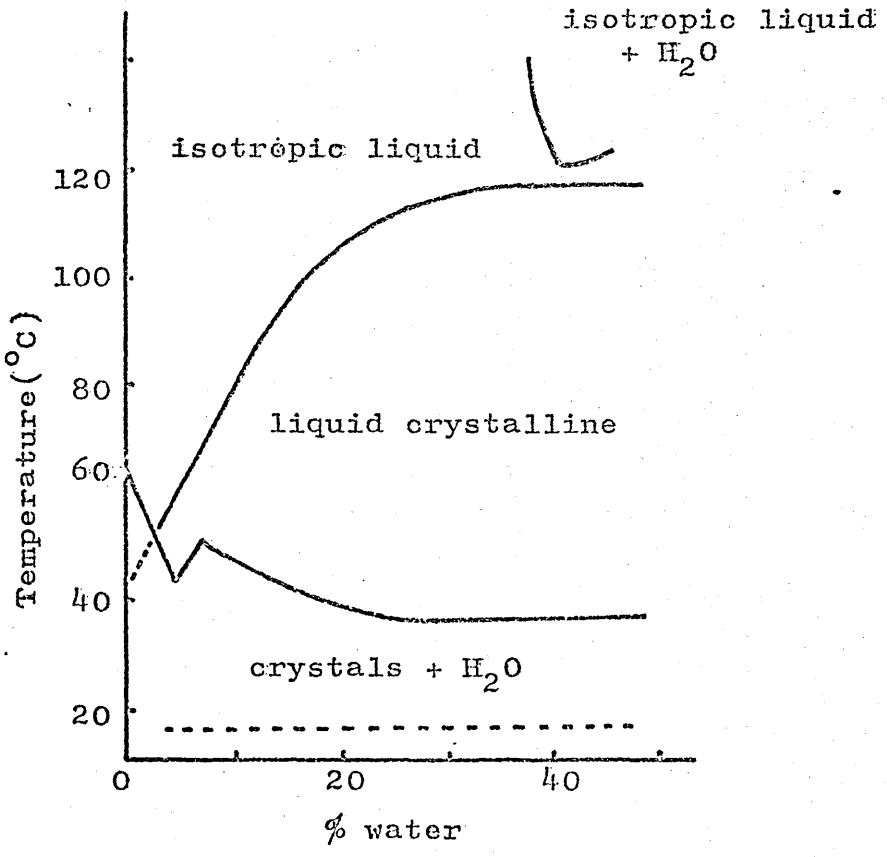

Figure 15

1-monolaurin/H_2O phase diagram.

63,80,82,85,86), $C_{12}E_6$/water (65), and phospholipid/water (66,77,80, 82,87,88) systems. In each system the neat phase was found to have a lamellar structure with layers of water intercalated between the lipid lamellae, as shown in figure 16. The X-ray parameters d_1 and d used to characterise the structure are also shown.

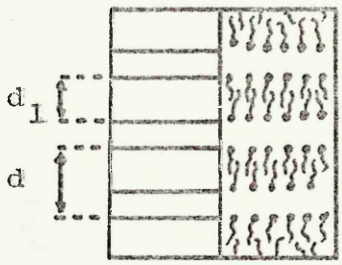

Figure 16
Structure of neat phase showing X-ray parameters d_1 and d.

In the neat phase regions of the above systems, at constant temperature, d and s (the average surface area per hydrophilic group) were found to increase with increasing water content, while d_1 decreases. At constant water content d and d_1 decrease with increasing temperature while s increases. Luzzati and Husson (76) noted that the bulkier the hydrocarbon moiety of the lipid the more extended is the range of existence of the neat phase.

Gallot and Skoulios (77) found that in the neat phase for a number of soaps the area s, at constant temperature and for one cation, is a function of the number of polar groups per volume of water, irrespective of the chain length. They concluded therefore that the dimensions of the structure elements are determined by the interactions at the lipid/water interface, which in turn seem to be dependent on the

61,80,82,85,86). $C_{12}E_6$/water (82), and phosphatidylcholine/water (66,77,80, 82,87,88) systems. In each system the cubic phase was found to have a lamellar structure with layers of water intercalated between the lipid lamellae, as shown in Figure 10. The X-ray parameters d_1 and d used to characterize the structure are also shown.

In the cubic phase regions of the above systems, at constant temperature, d and d_1 (the average surface area per hydrophilic group) were found to increase with increasing water content, while d_1 decreases. At constant water content d and d_1 decrease with increasing temperature while a increases. Luzzati and Husson (77) noted that the bulkier the hydrocarbon moiety of the lipid the more extended is the range of existence of the cubic phase.

Gulik and Scriven (47) found that in the cubic phase for a number of soaps the size a, at constant temperature and for one cation, is a function of the number of polar groups per volume of water, irrespective of the chain length. They concluded therefore that the dimensions of the structure elements are determined by the interactions at the lipid/water interface, which in turn seem to be independent on the

molal concentration of hydrophilic groups.

Lawson et al. (83) studied the neat phase of dimethyldodecylamine-N-oxide ($DC_{12}AO$)/D_2O and noted that their X-ray data indicated that water is associated with and around the polar end groups of the $DC_{12}AO$ molecules, with some kind of ordered structure. They also derive an angle of tilt for the $DC_{12}AO$ molecules of 50-56° from their X-ray long spacing data, based on the assumption that the oxygen of the amine-oxide group is incorporated into an ordered water lattice. Too much significance cannot be attached to this figure however since it depends so much on the structure assigned to the polar interface.

Most workers regard the alkyl chains in neat phases as in a 'liquid-like' state, on the basis of an observed diffuse X-ray diffraction band around 4.5 Å similar to that of a liquid paraffin. However, Luzzati (82) states that in some cases a modulation of the intensity of the band is observed, showing that the motion of the chains is restricted. He also states that since d_1 decreases as the temperature is raised the conformation of the chains must be disordered and the interface must be compressible, or in other words, the organisation of the hydrophilic groups must be disordered. The latter statement is construed as meaning that the hydrophilic groups are disordered with respect to each other in two dimensions laterally in the bimolecular layer. However if they order water around themselves as visualised by Lawson and Flautt (83) then we consider they must also be ordered with respect to the water layer.

Electron microscopy studies have been carried out on the neat phases of soap/water (78,79,84), and phospholipid/water (79,89,90) systems. Electron microscopy studies of membranes have been reviewed by Chapman (91). The layered structure of the neat phase has been confirmed by

radial concentration of a polydisperse system.

Hasson et al. (68) studied the rate of change of concentration in colloidal-sized $(NH_4)_2Cr_2O_7$ and of other small Wegg dye impurities that occur in more dilute with and without the salts and gives in the $Cr_2O_7^{2-}$ molecule with the kind of induced measurements. They also derive an angle of 111° for the Cr_2O molecules of $Na_2Cr_2O_7$ from the X-ray diffraction data, and for the assumption that the oxygen of the water molecule energy is incorporated into an ordered water layer. For such clarification cannot be attached to this figure because it depends on such an arbitrary assumption to the pulse interference.

Our work shows that the ultra violet is most useful in a "liquid-like" state, on the basis of a observed difference being distinguishable from a solution to that of a liquid paraffin. However, Tomasi (69) argues that to some degree a modification of the intensity of the band in question shows that the action of the chelate is restricted. In such cases the chelate, d_2 decreases in the temperature in related the configuration of the chelate and the interaction must be compatible, or in other words, the organization of the hydrophilic groups must be disordered. The latter is found to be increased in assuming that the hydrophilic groups are disordered with respect to each other in two dimensional lattices in the intermediate layer. However, if there other water molecules is considered as elucidated by Lemmon and Ellett (70) then no correlation in such cases be modified this process in the water layer.

Electron paramagnetic studies have been carried out on the [illegible] of manganese (II) (71), and phosphorylcholine (70,69,68) as well as studies of energy for the of membranes were also carried by Chapman (69). A lipoprotein interaction of the water phase has been established by

electron micrographs of anhydrous surface replicas (78,79,84), osmium tetroxide fixed sections (78,79,90), and negatively stained specimens (79, 89). A typical electron micrograph is shown in figure 17. The dark bands are layers of hydrophilic groups and the light bands the central parts of the bimolecular layers originally containing the alkyl chains. The step heights obtained from electron micrographs have been found to be in good agreement with values obtained for the same neat phase using low-angle X-ray diffraction.

At present lyotropic liquid crystals are being studied by Wilford (92) using polarised infra-red and certain conclusions from this work will be used in this thesis where appropriate. Infra-red spectroscopy has also been applied to the study of certain phospholipids in the l.c. state (93, 94), and membranes (94,95,96,97,98). The infra-red spectrum of DL-α-dipalmitoyl cephalin (m. pt. 194-195) at various temperatures (93) is shown in figure 18. At 110-120°C all the fine structure disappears and the spectrum resembles that of a liquid. This is interpreted as indicating that the alkyl chains have melted and that the smearing out of the spectrum is related to oscillation of the methylene groups about the trans configuration or to the occurrence of rotational isomerism. In phospholipids containing an unsaturated alkyl chain e.g. 2-oleoyl-3-stearoyl-L-1-phosphatidyl choline (94) the alkyl chains were shown, by infra-red spectroscopy, to be in a 'liquid-like' state at room temperature.

Seelig (99) has carried out spin-label studies on an oriented neat phase of sodium decanoate/decanol/water. Both amphiphilic and steroid spin labels were used to investigate different regions of the bilayer, and their e.s.r. spectrum was found to depend on the orientation of the sample with respect to the applied magnetic field. The amphiphilic

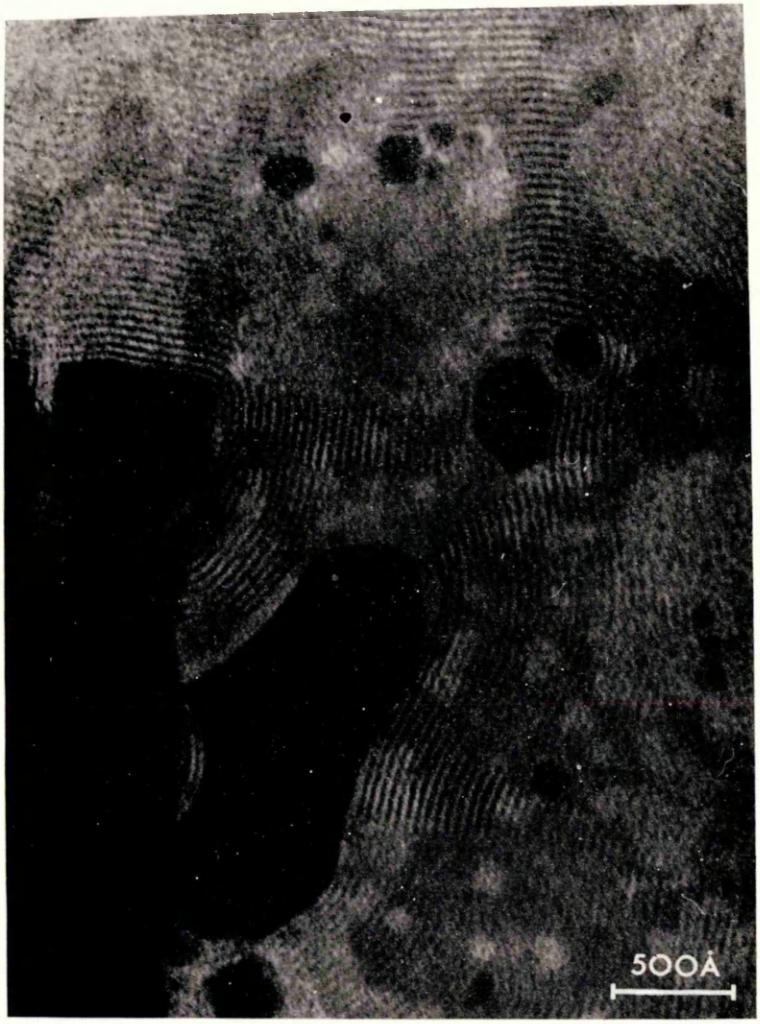

Figure 17. Negatively stained crystals + neat phase from didecanoyl lecithin + water system.

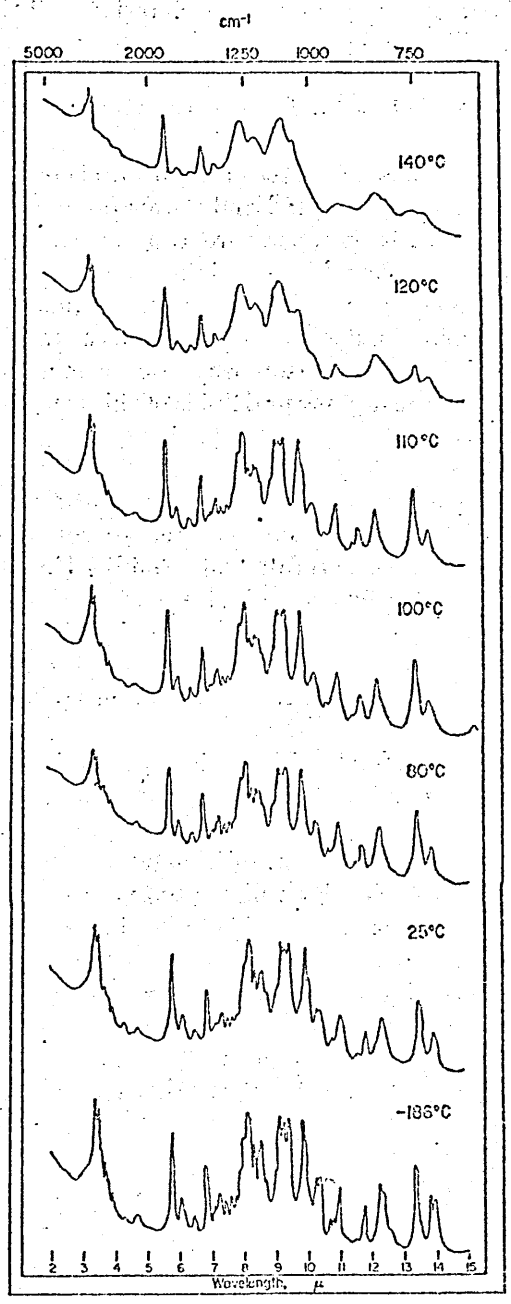

Figure 18

Infra-red spectra of 2,3 dipalmitoyl-DL-1-phosphatidylethanolamine at different temperatures.

spin-labels indicated an exponential decrease in the degree of order down the chain from the polar head group. However it was concluded that the alkyl chains are in an almost extended configuration, and that the polar interface is not restricted to a planar surface, but has a diffuse structure. The latter observation appears to suggest that some water penetrates to a slight extent into the bimolecular lipid layer and therefore the interface consists of perhaps one or two methylene groups, the polar head group and 'ordered' water. The behaviour of spin labels in phospholipid dispersions was found to be very similar to that in the neat phase model system.

The first N.M.R. investigation of lyotropic liquid crystals was carried out by McDonald (100) who studied the neat phases of the octylamine/water, sodium dodecyl sulphate/octanol/water, and sodium dodecyl sulphate/caprylic acid/water systems. For each system when the l.c. state was formed there was a reduction of the intensity of the water proton signal, and the signal from the alkyl chains was completely suppressed. The disappearance of the alkyl proton lines in the l.c. phase was interpreted as indicating a restriction in the freedom of motion of the alkyl chains caused by an increased regularity of structure so that the chains take up ordered positions in liquid crystalline lamellae. Since only one signal was observed from the amine and water protons it was concluded that they are exchanging rapidly. The reduction in intensity and broadening of the water line with the formation of the l.c. phase was interpreted as indicating the effective removal of some water molecules from the liquid state to be used to hold together the lamellar structure by hydrogen bonding between polar groups and/or through a pseudo-crystalline structure within the water layer.

Similar results to the above have been obtained by Gilchrist et al. (102) and Corkhill et al. (103) who studied the neat phases of

alkyl-imide/water and Aerosol OT/water, and $C_{12}E_6$/water systems using high resolution N.M.R. An annealed capillary sample of $C_{12}E_6/H_2O$ neat phase was found to give a smaller line-width and a greater chemical shift compared to a centrifuged sample of the same composition. This was discussed in terms of the effect on the water molecules of the anisotropic magnetic susceptibility difference between the polar head groups of oriented and random lamellar layers of surfactant molecules.

It was also observed that in the absence of orientation effects in the neat phase the chemical shift and T_1 (the spin-lattice relaxation time) are continuous functions of temperature across the liquid crystal-fluid isotropic phase boundary. This was interpreted as indicating that the hydrogen-bonding undergoes no radical change with phase transition, and the mobility of the water molecules is independent of the phase structure.

Lawrence and McDonald (60) have studied the neat phase of 1-monolaurin (MG12)/H_2O and D_2O using broad-line N.M.R. spectroscopy. The second moment of the neat phase was found to decrease with increasing water content. The widths of the four component lines (one narrow 'liquid-like' and three others symetrically about the centre) were also found to decrease with increasing water content. At the melting point of the neat phase the broad lines disappeared and the fine structure of the high resolution spectrum appeared.

Lawson and Flautt have studied the neat phases of the systems sodium palmitate/D_2O (55), and $DC_{12}AO/D_2O$ (55, 104) using proton and deuteron magnetic resonance. For the neat phase of each system they observed 'super Lorentzian' (105) lines of width at half-height c.a. 15μT. The observed line-shapes were attributed to a distribution of correlation times in the alkyl chains and described in terms of a parameter $R(^8/_2)$ which is the ratio of the line-width at one-eighth

height to that at one-half height. The value of $R(^8/_2)$ for a Lorentzian line is 2.64 while values c.a. 6.6 were found for the neat phase lines. The larger values of $R(^8/_2)$ were interpreted as indicating an increase in the relative intensity in the 'wings' of the lines. The polar head group, two or three methylene groups, and ordered water around the polar head group were assumed to be responsible for the 'wings' of the lines. The line-shapes became more Lorentzian in nature with increasing temperature which was interpreted as evidence for a distribution of correlation times in the alkyl chains.

The D_2O in the neat phase of $DC_{12}AO/D_2O$ gave 'powder-type' spectra with an assymetry parameter η of zero. Quadrupole coupling constants c.a. 2.8 kHz obtained from the spectra were observed to decrease with increasing D_2O content. Similar spectra have been obtained by Charvolin and Rigny (106) and Blinc et al. (107) from the neat phases of potassium laurate/D_2O and sodium palmitate/D_2O giving coupling constants c.a. 1.5 - 3 kHz and 100 - 500 Hz respectively. For each system the magnitude of the coupling constants was interpreted as indicating rapid but slightly anisotropic motion of the water molecules, and was thought to be an average of the coupling constants of self-associated and surfactant-associated water molecules.

De Vries and Berendsen (108) have obtained N.M.R. spectra from samples of potassium oleate/D_2O neat phase oriented between glass slides as a function of the angle (θ) between the normal to the slides and the magnetic field B_o. At all angles they observed a small signal from residual HDO. At $\theta = 55^o$ they observed a large additional peak shifted upfield approximately 4 ppm from the water signal and found that the spectra were symmetrical about $\theta = 90^o$. They postulated that the large peak was due to the protons of the alkyl chains, which were

rotating about their optical axes, making the average direction of the CH_2 dipole-dipole interaction along the optical axis of the system. At $\theta = 55^{\circ}$ the dipole broadening term, $3 \cos^2 \theta - 1$, is zero and so the dipolar broadening is effectively reduced to zero. However, Berendsen has misinterpreted the situation slightly since if the molecules are rotating about their optical axes, it is unnecessary for the CH_2 dipole-dipole interactions to be along these axes because θ is now the angle between the axis of rotation and the magnetic field. The CH_2 dipole-dipole interaction is probably in fact at 90° to the axis of rotation.

The line-width at 55° was $2\mu T$ and was interpreted as indicating that the alkyl chains are in motion with respect to each other as well as rotating about their long axes. This is a reasonable conclusion since long chain alcohols (109) give N.M.R. line-widths of c.a. $400\mu T$ in their α-phases in which the molecules are assumed to be rotating only about their long axes with no diffusion occurring. The majority of the work in this thesis is based on using Berendsen's technique to study oriented l.c. samples of non-ionic lipid/water systems.

Drakenberg et al. (110) have studied the neat phase of the system n-octylamine/n-octylamine hydrochloride/water using high resolution N.M.R. They observed a fine structure from the water protons which was different for spinning and non-spinning samples. This was explained in terms of chemical shift differences which were attributed to magnetic susceptibility anisotropies in the neat phase. Theoretical expressions for the line-shapes were deduced with the assumption that the magnetic field experienced by the water protons depends on the orientation of the neat phase lamellae with respect to the external magnetic field.

Several pulse N.M.R. studies have been carried out on lyotropic liquid crystal systems (107, 111, 112, 113) and phospholipid/water systems (114, 115). Considerable controversy has arisen over whether the line-widths and spin-lattice (T_1) and spin-spin (T_2) relaxation times observed in these systems are caused by diffusion of water and lipid molecules through local anisotropic magnetic field gradients (111, 115), by 'magnetic anisotropic effects' (112), or by partially averaged dipolar interactions (113). There was also some doubt as to whether the line-widths and free-induction decays were frequency dependent or not. The position has recently been clarified by Tiddy (116) and Chan et al. (117).

Tiddy has studied neat phase samples of the system sodium caprylate/decanol/D_2O using variable frequency pulse N.M.R. He obtained values of T_{2eff} (the time taken for the decay to reach e^{-1} times the original height) from the free induction decay following a 90° pulse and found no correlation between T_{2eff} and field strength.

T_{2eff} was also measured using the Meiboom-Gill modification (118) of the Carr-Purcell sequence (119) and found to depend on t (the time between successive 180° pulses) being smaller for longer values of t. When T_{2eff} was measured using only the Carr-Purcell sequence no dependence on t was observed. This was interpreted as indicating that the pulse-distance effect was not due to molecular motion or chemical exchange as previously supposed (111). It was suggested that at short values of t the time constant for the decay contains a contribution from $T_{1\rho}$ (the relaxation time in the rotating frame), and is not a pure T_2.

The free induction decay after a 90° pulse was also observed from neat phase samples of the same system, oriented between glass slides, as a function of the angle θ between normal to the slides and

the magnetic field. A maximum value of T_{2eff} was observed at $\theta = 55^{o}$ in agreement with the line-width measurements of Berendsen (108). It was concluded therefore that the free induction decay following a 90° pulse for mesomorphic systems is dominated by dipolar relaxation.

Chan et al. have obtained a non-exponential proton free induction decay from lecithin bilayer dispersed in D_2O, and found that T_{2eff} calculated from the decay is independent of magnetic field strength. They interpret these results as indicating that the N.M.R. spectral line-widths of the lipids in the bilayer arise from slow molecular motion with incomplete averaging of the dipole-dipole interactions. They also recorded the high resolution P.M.R. spectrum at 220 MHz and the Fourier transformed P.M.R. spectrum at 100 MHz of a lecithin bilayer sample. These spectra and the non-exponential free-induction decay lead them to suggest that there is a distribution of transverse relaxation times for the various protons in the bilayers, with an abrupt increase of the transverse relaxation time near the end of the alkyl chains.

Conclusions

The structure of the neat phase as envisaged at present can be summarised as follows.

It is lamellar and smectic with the lipid molecules arranged in equidistant double layers with intervening layers of water. The water molecules are ordered to some extent by hydrogen-bonding to the polar head groups of the lipid molecules, the degree of order being intermediate between that of liquid water and ice. The motion of the alkyl chains consists of restricted rotation about their long axes with a distribution of correlation times along the chain. There is also some evidence for chain diffusion in two dimensions and an abrupt increase in the molecular motion near the end of the chain.

CHAPTER II

NUCLEAR MAGNETIC RESONANCE THEORY

All nuclei with odd mass number possess the property of spin; the spin angular momentum vector, denoted by $\bar{I}\hbar$ is measured in units of $\hbar$, where $\hbar$ is Planck's constant divided by 2π. The value of the spin, I, is an integral multiple of $\frac{1}{2}$. The chemist is mostly concerned with the simplest nucleus, the proton, having spin $\frac{1}{2}$.

The possession of both spin and charge confers on the nucleus a magnetic moment $\bar{\mu}_N$ which is proportional to the magnitude of the spin, that is,

$$\bar{\mu}_N = \gamma_N \hbar \bar{I} \qquad (1)$$

γ_N is the magnetogyric ratio of the nucleus and is measured in rad. $s^{-1}.T^{-1}$.

Quantum theory demands that the allowable nuclear spin states are quantized; the component m_I of the nuclear spin vector in any given direction can only take up one of a set of discrete values which are $+I, (I - 1), \cdots\cdots - I$. For the proton with $I = \frac{1}{2}$, m_I can be either $+\frac{1}{2}$ or $-\frac{1}{2}$. If a steady magnetic field $\bar{B}_o$ is applied to the proton, there is an interaction between the field and the magnetic moment $\bar{\mu}_N$, which may be represented in terms of the Hamiltonian

$$H = -\bar{\mu}_N . \bar{B}_o \qquad (2)$$

If the direction of the magnetic field is defined to be the z direction, the interaction may be written

$$H = -\gamma\hbar B_o Iz \qquad (3)$$

where Iz, the allowed component of the nuclear spin in the z direction, has the value $+\frac{1}{2}$ or $-\frac{1}{2}$.

In order to induce transitions between the resulting two nuclear spin levels, an oscillating magnetic field is applied. Absorption of energy occurs provided the magnetic vector of the oscillating field is

[illegible]

perpendicular to the steady field $\bar{B}_o$ and the frequency of oscillation satisfies the resonance condition,

$$h\nu = \mu \hbar B_o \qquad (4)$$

The oscillating field is equally likely to produce transitions up or down, and absorption of energy from the radiation field can only be detected if there are more nuclear spins in the lower energy level.

In practice a fixed frequency ν is used and the magnetic field swept through resonance to obtain a spectrum in which absorption of energy is plotted as a function of magnetic field strength.

The process which maintains a population difference between the two energy levels is known as spin-lattice relaxation, and is characterised by T_1 (the spin-lattice relaxation time). T_1 is a measure of the time taken for energy to be transferred from the spin system to the lattice, i.e. the other degrees of freedom of the system.

Other processes have the effect of varying the relative energies of the spin levels, rather than their life-times. Such processes are characterised by a relaxation time T_2, often called the spin-spin relaxation time but more satisfactorily the transverse relaxation time.

(I) Broad-line proton magnetic resonance

Molecules in the solid state generally possess very little translational and rotational freedom. This lack of molecular motion has two important consequences. The local magnetic field due to neighbouring dipoles is static causing the nuclear spin system to have a large variety of relative energies giving a short T_2 and a broad resonance absorption line. Also it is difficult for the spin system to lose energy to the lattice and this causes T_1 to be long.

(a) P.M.R. absorption spectra for rigid structures

1. Two identical nuclei

Pake (120) treated the magnetic dipole-dipole interaction between protons occurring in pairs as a perturbation of the energy levels of the protons in the applied field B_o. By a first-order perturbation calculation he found the new energy levels and from these found that the resonance peaks should occur at field strengths given by

$$B_o = B^* \pm {}^3/_2 \mu r_{jk}^{-3} (3 \cos^2 \theta_{jk} - 1) \qquad (5)$$

μ is the proton magnetic moment

r_{jk} is the inter-proton separation

θ_{jk} is the angle between $\bar{B}_o$ and $\bar{r}_{jk}$

The spectrum is therefore expected to consist of two resonance lines equally spaced about the field strength $B^* = h\nu/2\mu$ by an amount ${}^3/_2 \mu r_{jk}^{-3} (3 \cos^2 \theta_{jk} - 1)$.

Pake (120) has determined proton resonance absorption spectra for a single crystal of $CaSO_4.2H_2O$. Since the unit cell contains two types of proton pair with in general different values of θ_{jk}, two pairs of symmetrically disposed resonance lines should be observed. The lines will be broadened by the smaller local magnetic fields of all other neighbouring nuclei. The measured spectra are shown in figure 19. By fitting the observed variation of line displacement to equation (5) the angular disposition of the protons in the unit cell and also r_{jk} were determined.

For a polycrystalline sample the orientation of the dipole pairs is isotropically distributed and the normalised line-shape function for the resonance absorption has been calculated to be (120)

$$f(b) = (6 \sqrt{3} \mu r_{jk}^{-3})^{-1} \left[1 \pm b/({}^3/_2 \mu r_{jk}^{-3}) \right]^{-\frac{1}{2}} \qquad (6)$$

$$b = B_o - B^* \qquad (7)$$

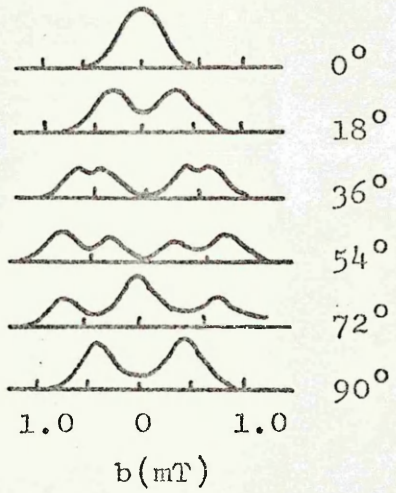

Figure 19

PMR spectra for various directions of the applied field B_o in the (001) plane of a $CaSO_4.2H_2O$ single crystal

The line-shape obtained from equation (6) for polycrystalline $CaSO_4.2H_2O$ is shown as the broken line in figure 20. After taking account

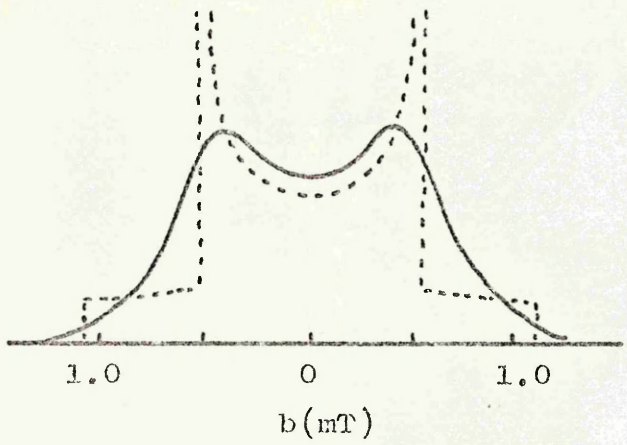

Figure 20

Broken line shows calculated line-shape for the protons in polycrystalline $CaSO_4.2H_2O$, taking into account nearest neighbour interactions. The full line is obtained after taking into account interaction of other neighbours

of broadening by other neighbouring nuclei the full line is obtained. The experimental line-shape obtained (120) is in good agreement with this and from the separation of the two peaks the interproton distance in the water molecules r_{jk} can be calculated, though the accuracy is less than that afforded by a single crystal.

2. More complicated systems

Perturbation analysis has also been carried out to obtain the line-shapes for the interaction of three (121) and four (122-126) identical spin ½ nuclei.

The line-shape for general systems of nuclei cannot be calculated but Van Vleck (127) has shown that the moments of the spectrum can be readily calculated. If the line-shape is described by the function g(b) the nth moment S_n is defined as

$$S_n = \frac{\int_{-\infty}^{+\infty} b^n \cdot g(b)\, db}{\int_{-\infty}^{+\infty} g(b)\, db} \qquad (8)$$

Since g(b) is an even function for magnetic dipolar broadening the odd numbered moments are all zero. For a crystal containing only one species of magnetic nucleus the second moment S is

$$S = {}^3/_2\, I(I+1)\, g^2 \mu_o^{\,2}\, N^{-1} \sum_{j>k} U^2_{jk} \qquad (9)$$

where μ_o is the nuclear magneton, $g\mu_o I$ is the nuclear magnetic moment, N is the number of magnetic nuclei in the system over which the sum is taken, and for a single crystal

$$U_{jk} = (3\cos^2\theta_{jk} - 1)\, r_{jk}^{-3} \qquad (10)$$

Consideration of the symmetry of the system, and other approximations, allow equation (9) to be simplified so that it is of practical use.

For a polycrystalline sample $(3\cos^2\theta_{jk} - 1)^2$ is replaced by its isotropic average ${}^4/_5$ and the second moment using (9) and (10)

[illegible]

[illegible]

[illegible]

becomes

$$S = {}^{6}/_{5}\, I(I + 1)\, g^{2}\mu_{o}^{2}\, N^{-1} \sum_{j>k} r_{jk}^{-6} \qquad (11)$$

(b) Restricted reorientation in solids

The frequency of motion of molecules or atomic groups in solids about one or more axes increases with temperature. Such motion modifies the interaction between neighbouring nuclear magnetic dipoles in the rotating groups and causes a considerable change in the resonance absorption spectrum. The local field at any resonant nucleus is now time-varying and if the variation is sufficiently rapid the time average of the local field must be taken to express the dipole interaction. Since the time average over all permitted pairs can be expected in general to be less than the steady local field for a rigid system, the spectrum may be expected to be altered when the reorientation sets in. Therefore a narrowing of the absorption line with increasing temperature in many solids can be ascribed to increasing molecular motion within the crystal lattice.

The molecular motion can consist of rotation about one or more axes, either free or restricted by potential barriers, quantum-mechanical tunnelling, or molecular diffusion. The resonance line narrows when the reorientation rate is of the order of the line-width in Hz; this frequency is usually about 10^4 to 10^5 Hz.

The effect of molecular motion on line-widths and line-shapes was put on a quantitative basis by Gutowsky and Pake (128).

1. Two identical nuclei

Figure 21 shows an isolated system of two nuclei which are reorienting about some axis at a rate ν much greater than the frequency line-width. $\bar{OP}$ is the vector $\bar{r}_{jk}$ joining the two nuclei j and k and making an angle θ_{jk} with the applied field $\bar{B}_o$; $\bar{ON}$ is the axis of reorientation making an angle θ' with $\bar{B}_o$, and an angle γ_{jk} with $\bar{r}_{jk}$.

[illegible]

[illegible]

[illegible]

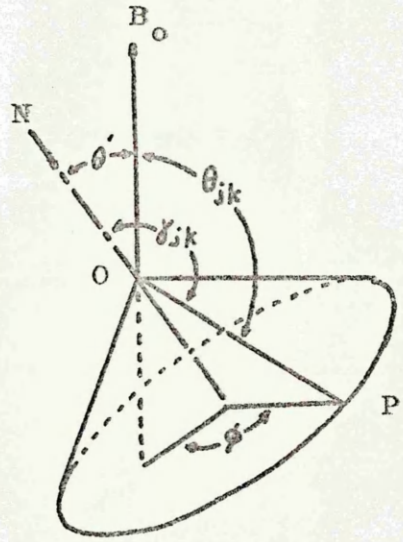

Figure 21
Diagram illustrating the motion of an internuclear vector OP about an axis ON

If reorientation were not taking place, then neglecting the broadening effect of remoter nuclear dipoles, the spectrum consists of two lines given by equations (5) and (7).

$$b = \pm \, {}^{3}/_{2}\mu \, r_{jk}^{-3} \, (3 \cos^2\theta_{jk} - 1) \qquad (12)$$

The reorientation causes θ_{jk} to vary with time as the vector $\bar{OP}$ takes up positions on the conical surface shown in figure 21, and it becomes necessary to take the time average value of $(3 \cos^2 \theta_{jk} - 1)$. The average over all azimuthal angles ϕ in figure 21 is

$$\overline{(3 \cos^2\theta_{jk} - 1)}^{\phi} = \tfrac{1}{2}(3 \cos^2\theta' - 1)(3 \cos^2\gamma_{jk} - 1) \qquad (13)$$

and applies to cases of free rotation, and reorientation over, or tunnelling through, an n-fold periodic potential barrier where $n \geqslant 3$ (128).

The spectrum therefore again consists of two lines given by

$$b = \pm \, {}^{3}/_{4}\mu \, r_{jk}^{-3} (3 \cos^2\theta' - 1)(3 \cos^2\gamma_{jk} - 1) \qquad (14)$$

If the axis of reorientation $\bar{ON}$ is perpendicular to the internuclear

If rotational is more not value, which, then, neglecting the screening effect of remote nodes (figure), the spectrum separation of two lines given by equations (5) and (7),

$$\nu = \pm \sqrt{2\mu}\, r_{jk}^{-3/2} (1 - \cos^2\theta_{jk}) \qquad (10)$$

The rotation angle θ_{jk} varies with time in the vector $\vec{\theta}$ takes up positions on the conical surface shown in figure 2a, and it becomes necessary to take the time average value of $(1 - \cos^2\theta_{jk})$. The average over all azimuthal angles ϕ in figure 2b is

$$(1 - \cos^2\theta_{jk}) = \int_0^{2\pi} (1 - \cos^2\theta) \, d\phi \qquad (11)$$

and applies to cases of free rotation and vibration, vibration transition through, an n-fold degenerate potential barrier where n > 1 (12).

The spectrum therefore again consists of two lines given by

$$\nu = \pm \sqrt{2\mu}\, r_{jk}^{-3/2} (1 - \cos^2\theta) \qquad (12)$$

If the axis of rotation $\vec{\theta}$ is perpendicular to the internuclear

vector $\bar{OP}$, ($\gamma_{jk} = \pi/2$), equation (14) becomes

$$b = \pm\, {}^3/_4 \mu r_{jk}^{-3} (3 \cos^2\theta' - 1) \qquad (15)$$

The dependence of the splitting on the orientation of the system with respect to $\bar{B}_o$ is thus similar in form to that given by equation (12), the axis of reorientation replacing the internuclear vector in specifying the orientation; the maximum splitting however is only half that for a rigid system. Also when $(3 \cos^2\theta' - 1) = 0$ i.e. $\theta' = 54^o\ 44'$ $b = 0$ and the splitting vanishes.

In a polycrystalline solid all values of θ_{jk} and θ' occur, and so if the internuclear vectors of identical isolated pairs in the solid are effectively stationary at low temperature but reorient rapidly at higher temperatures about a perpendicular axis, the absorption line undergoes a transition becoming half as wide and correspondingly more intense at higher temperature.

2. <u>More complicated systems</u>

The perturbation analysis for triangular groups of identical spin $\frac{1}{2}$ nuclei reorienting about any given axis has been carried out by Andrew and Bersohn (121). For reorienting systems containing more than three nuclei Van Vleck's second moment formula (9) is used averaging the terms U_{jk} over whatever motion is occurring.

Consider a single crystal containing a system of molecules or atomic groups each reorienting about one axis only and that the only nuclear dipoles present are those at resonance. The second moment of the spectrum can be divided into an intramolecular part S_1 and an intermolecular part S_2. From (9) S_1 is given by

$$S_1 = {}^3/_2\, I(I + 1) g^2 \mu_o^2\, N^{-1} \sum_{j>k} (\bar{U}_{jk})^2 \qquad (16)$$

where $\bar{U}_{jk}$ is the average of U_{jk} over the motion. For free rotation, or for reorientation over or tunnelling through, an n-fold periodic potential barrier where $n \geqslant 3$ $\bar{U}_{jk}$ is obtained from (10) and (13) giving

$$S_1 = {}^3/8\ I(I+1)g^2\mu_o{}^2N^{-1}(3\cos^2\theta' - 1)^2 \sum_{j>k} (3\cos^2\gamma_{jk} - 1)^2 r_{jk}^{-6} \qquad (17)$$

If the material is polycrystalline there is an isotropic distribution of axes of reorientation, and the factor $(3\cos^2\theta' - 1)^2$ is replaced by its mean value of $^4/5$ giving

$$S_1 = {}^3/10\ I(I+1)g^2\mu_o{}^2\ N^{-1} \sum_{j>k} (3\cos^2\gamma_{jk} - 1)^2\ r_{jk}^{-6} \qquad (18)$$

The reduction of the intermolecular constribution S_2 by molecular motion is more complicated since, in forming $\bar{U}_{jk}$, r_{jk} varies as well as θ_{jk}. Certain special cases have been treated by Andrew (129), and formulae for the general case have been given by Andrew and Eades(130).

Isotropic reorientation of the molecules at a sufficient rate will reduce S_1 to zero, intramolecular local fields being averaged to zero. Local fields which are intermolecular in origin and contribute to S_2 do not average to zero so long as self-diffusion does not alter the centres of mass of the molecules.

3. <u>Variation of line-width with temperature</u>

A line-width transition has been expressed by the relation (128, 130)

$$(\delta\nu)^2 = V^2 + (U^2 - V^2)\ {}^2/_\pi\ \tan^{-1}\alpha\ (\delta\nu/\nu_c) \qquad (19)$$

where $\delta\nu$ is the frequency line-width during the transition, U is the line-width for the rigid lattice, V is the line-width after completion of the narrowing, α is a constant of the order of unity, and $\nu_c = (2\pi\tau_c)^{-1}$ may be regarded as the reorientation frequency. Equation (19) was obtained by making an ad hoc adjustment of the Bloembergen, Purcell, and Pound (131) equation (52) which expresses the width of an absorption line in terms of the Debye correlation time, τ_c. Therefore any results obtained using equation (19) are probably only accurate to an order of magnitude.

Also the variation of ν_c with temperature has been expressed as (128)

$$\nu_c = \nu_o \exp(-E/RT) \qquad (20)$$

a form met in the theory of rate processes. ν_o is a constant and E is analagous to an activation energy for the barrier restricting the appropriate molecular reorientation.

(II) Deuteron magnetic resonance

Besides a magnetic moment the deuteron has an electric quadrupole moment Q which interacts with any electric field gradient at the deuteron site. The magnitude of the interaction is about 100 times greater than the magnetic internuclear interactions between deuterons and surrounding nuclei.

The main contribution to the electric field gradient arises from the chemical bond in which the particular deuteron is involved. Two parameters are required to define the derivatives of the electric field, the field gradient Vzz, and the assymetry parameter $\eta = (Vxx - Vyy)/Vzz$, where Vxx, Vyy, and Vzz are components of the electric field gradient $(\partial^2 V/\partial i^2)$, i = x, y, z, and V is the electrostatic potential.

In the high-field case B_o is selected so that the electric quadrupole interaction energy is small compared to the interaction of the nuclear magnetic moment with the external field, and the N.M.R. experiment is performed in the conventional manner.

In many cases the field gradients have axial symmetry and so $\eta = 0$. The nuclear spin is quantised along $\bar{B}_o$, making some angle ε with the molecular symmetry axis, and under these conditions the effective field gradient along $\bar{B}_o$ is

$$Vzz = \tfrac{1}{2}\, eq\, (3\cos^2\varepsilon - 1) \qquad (21)$$

where eq is a scalar descriptive of the electric environment (132).

[illegible]

[illegible]

[illegible]

The resonance spectrum for each unique deuteron in a solid single crystal consists of two lines at frequencies given by (132)

$$\nu_{m \to m-1} = \nu'_o + \frac{3\, e^2 q\, Q(2m - 1)(3 \cos^2 \varepsilon - 1)}{8I(2I - 1)h} \qquad (22)$$

where ν'_o is the unperturbed resonance frequency $\mu_D B_o/Ih$.

For a polycrystalline sample the spectrum again consists of two lines and the quadrupole coupling constant $|e^2 q\, Q/h|$ (133) can be obtained from the separation between the two maxima. If $\eta = 0$ the separation is $3\, e^2 q\, Q/4h$ (133).

CHAPTER III

EXPERIMENTAL

(I) Materials

(a) Preparation of 1-monoglycerides

Racemic 1-monoglycerides were prepared by Malkin's method (17) but using di-isopropyl ether in the extraction to reduce the loss of monoglyceride into the aqueous layer. The preparation of 1-monooctanoin (MG8) is described in detail and the modifications for the preparation of 1-monoundecanoin (MG11) and 1-mono-olein (MG//18) are given.

1. MG8

Dry HCl was passed into a mixture of 25 g of n-octanoic acid (Koch-Light puriss., $\geqslant$ 99% pure by GLC) and 34 g of isopropylidene glycerol (IPG, additive 'A', Laporte Industries Ltd.) until the solution became cloudy, and then for a further fifteen minutes. The resulting solution was cooled in ice, shaken with 100 ml of ice-cold di-isopropyl ether, and allowed to stand in ice for five minutes. The supernatant liquid was decanted from the glycerol which had settled out, shaken with a further 100 ml of ice-cold di-isopropyl ether, and poured into an ice-cold solution of 17 g of anhydrous calcium chloride in 165 ml of concentrated hydrochloric acid. The solution was shaken for two minutes, 200 ml of ice-cold water added, and poured into a separating funnel. The lower water layer was run off and retained. The ether layer was washed with three 200 ml portions of ice-cold water to remove hydrochloric acid and calcium chloride, and these retained. Each of the four aqueous layers was washed with 100 ml of ice-cold di-isopropyl ether and all the ether layers bulked. The ether was distilled off and the crude monoglyceride crystallised twice from 80 ml of 40/60 petroleum ether at $0^{o}C$. The yield of pure MG8 was 70%. The melting point determined using a heated stage

EXPERIMENTAL

(1) Intermediate

(a) Preparation of 1-vinylcyclohexene

Bromo 1-vinylcyclohexene was prepared by Kohler's method (17) but using di-isopropyl ether in the preparation to reduce the loss of monobromide into the aqueous layer. The preparation of 1-vinylcyclohexene (VCH) is described in detail and the modifications for the preparation of 1-vinylcyclohexene oxide (VCHO) and 1-vinylcyclohexane (VCH\H2) are given.

i. VCHO

Dry KOH was pounded into a mixture of 22 g of n-butanol and (Kodak-light marks), 5 ml pure 5% VCH) and 24 g of isopropylidene glycerol (KIK, mobilize 'A', Imperial Industrial Ltd.) until the solution became cloudy, and then for a further fifteen minutes. The resulting solution was cooled in ice, shaken with 100 ml of ice-cold di-isopropyl ether, and filtered to remove the fine fine minerals. The supernatant liquid was decanted from the inverted round bottom flask, shaken with a further 100 ml of ice-cold di-isopropyl ether, and poured into an ice-cold solution of 11 g of sulphuric acid chloride in 100 ml of concentrated hydrochloric acid. The solution was shaken for two minutes, 200 ml of ice-cold water added, and poured into a separating funnel. The lower water layer was run off and retained. The ether layer was washed with three 50 ml portions of ice-cold water to remove hydrochloric acid and sulphuric acid, and then retained. Half of the ether layer was washed with 100 ml of ice-cold di-isopropyl ether and all the ether layers united. The ether was distilled off on the steam bath, leaving a concentrated solution from 30 ml of ether previous ether or 5%. The yield of pure VCH was 70%. The melting point determined using a Kofler stage

polarising microscope was 38°C (Lit. value 38°C, 17).

The reaction scheme is shown below.

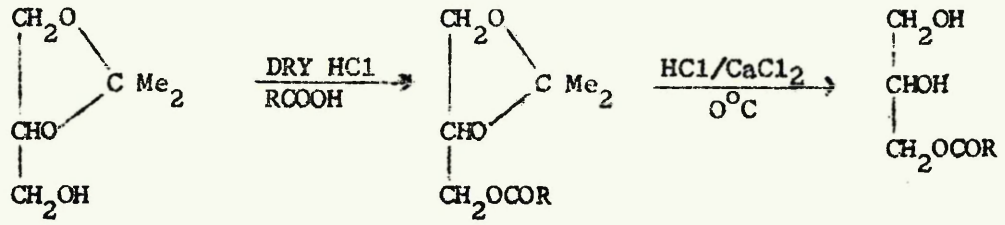

2. MG11

For the preparation of MG11 30 g of IPG and 25 g of n-undecanoic acid (Koch-Light pure, BP. 58) were used. The n-undecanoic acid was found to be ⩾ 99% pure by GLC. The yield of pure MG11 was 75%. The melting point was 56°C (Lit. value 56.5°C, 17).

3. MG//18

For the preparation of MG//18 9 g of IPG and 10 g of oleic acid (Fluka purum ⩾ 96%) were used. After passing in the dry HCl, 80 ml of ice-cold di-isopropyl ether were added and the hydrolysis carried out with an ice-cold solution of 10 g of calcium chloride in 70 ml of concentrated hydrochloric acid. Extractions were carried out as described previously with 50 ml portions of ice-cold water and ice-cold di-isopropyl ether. The crude 1-mono-olein was crystallised twice from 30 ml of 40/60 petroleum ether at 0°C. The yield of pure 1-mono-olein was 60%. The melting point was 35.5°C (Lit. value 35.5°C, 19).

The prepared 1-monoglycerices were stored in desiccators over phosphorus pentoxide in the dark.

(b) Analysis of 1-monoglycerides

Samples of the prepared 1-monoglycerides were analysed for the presence of fatty acid, glycerol and di- and tri-glyceride impurities using thin layer chromatography (T.L.C.).

The TLC analysis was carried out on glass plates 20 cm x 20 cm coated with a 0.25 mm layer of Kieselgel G, which was activated by heating

[illegible]

[illegible]

[illegible]

[illegible]

[illegible]

the plates in an oven at 110°C for thirty minutes. One of these plates was spotted with 200μg of MG8, 200μg of MG11, and 200μg of MG//18 in 40/60 petroleum ether using a micro-syringe. The plate was developed using a solvent system consisting of 106 ml of 40/60 petroleum ether, 47 ml of diethyl ether and 1.5 ml of glacial acetic acid (134). The development time was 45 minutes. The plate was allowed to dry at room temperature and sprayed with a 0.2% solution of 2',7'-dichlorofluorescein in ethanol. The chromatogram was observed under u.v. light of wavelength 350 mμ and consisted of yellow spots on a green background. A diagram of the plate is shown in figure 22. The R_f value for the 1-monoglycerides was 0.14. No other spots which would be impurities could be seen.

A second plate was spotted with 200μg, 400 μg, 600μg and 800μg of MG8 in 40/60 petroleum ether, each containing 5% octanoic acid, to determine where octanoic acid would appear on the chromatogram and also the optimum spot size for development and detection. The plate was developed and observed as described previously and a diagram of it appears in figure 23. The R_f value of octanoic acid was 0.58 and an optimum spot size of 800μg was decided on.

A third plate was spotted with 800μg of MG8 + 5% octanoic acid, 800μg of MG8 + 5% octanoic acid + 5% myristic acid, 800μg of glycerol, and 800μg of MG//18 + 5% oleic acid, dissolved in 40/60 petroleum ether. The plate was developed and observed as described previously and a diagram of it is shown in figure 24.

The glycerol spot was not displaced at all whilst the octanoic acid and myristic acid were separated easily. The R_f values of myristic and oleic acid were both found to be 0.66.

A summary of the observed R_f values is shown in table IV compared to those found using a solvent system containing 70% 40/60 petroleum ether and 30% diethyl ether (135). The higher R_f values found

[illegible]

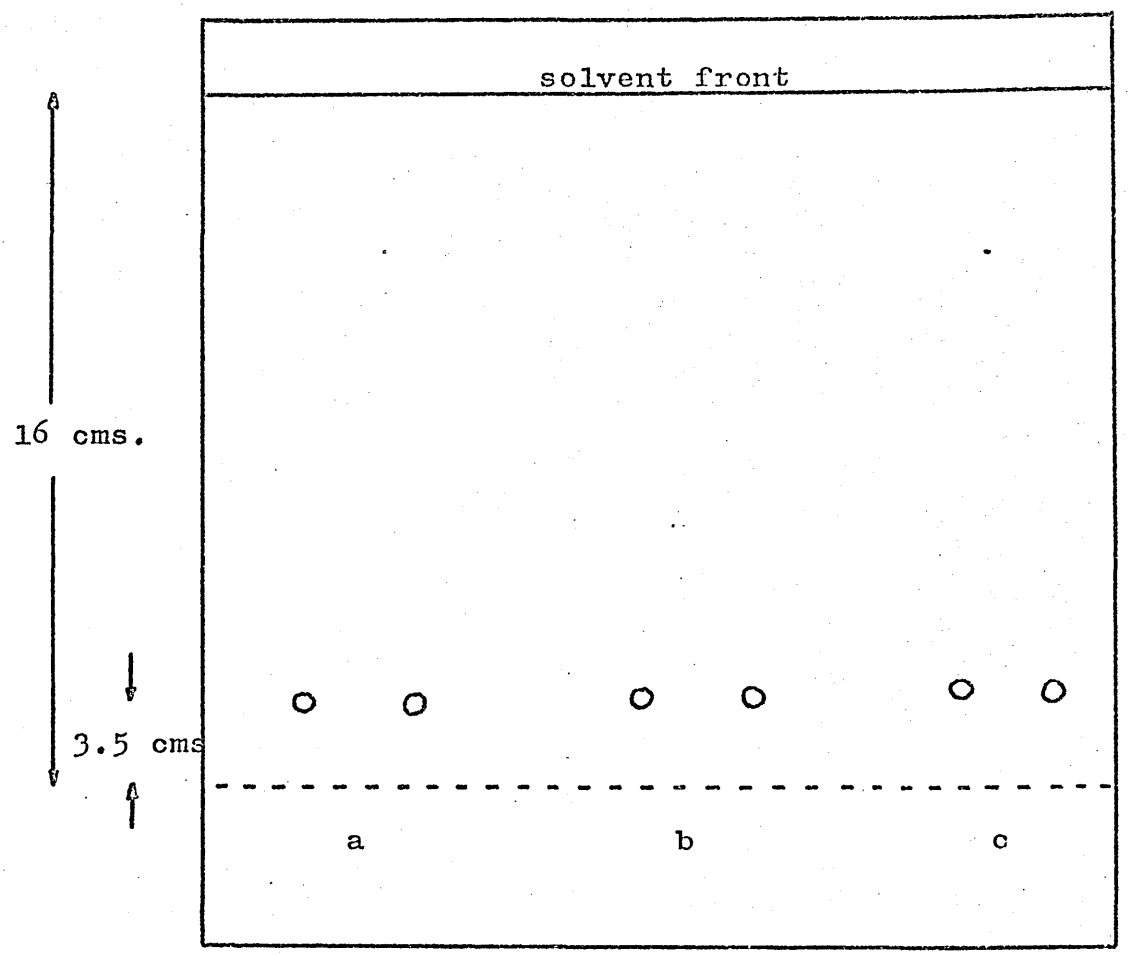

Figure 22

Diagram of TLC plate spotted with 200μg of the following 1-monoglycerides after developing

a. 1-mono-octanoin

b. 1-monoundecanoin

c. 1-mono-olein

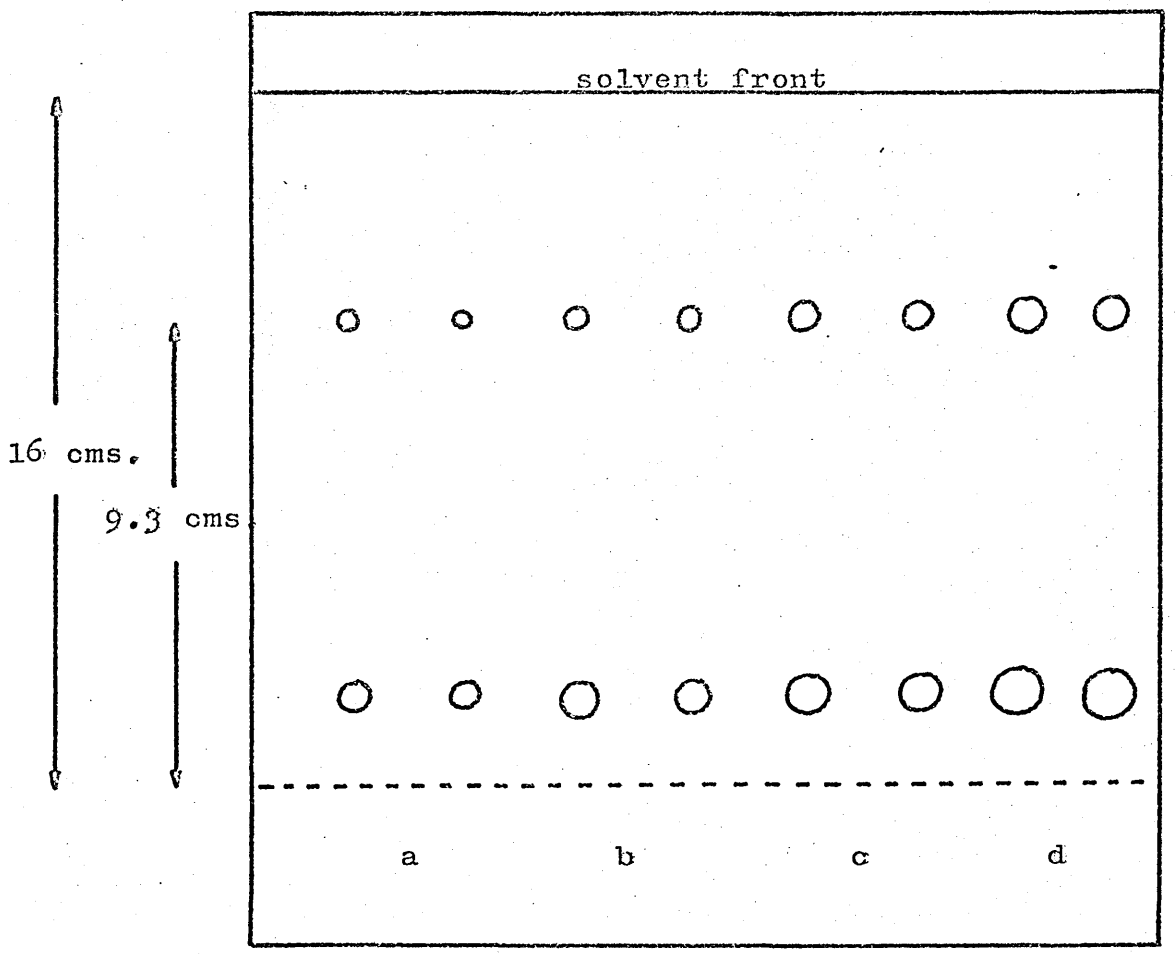

Figure 23

Diagram of TLC plate spotted with following amounts of 1-mono-octanoin+5% octanoic acid after developing.

a. 200μg
b. 400μg
c. 600μg
d. 800μg

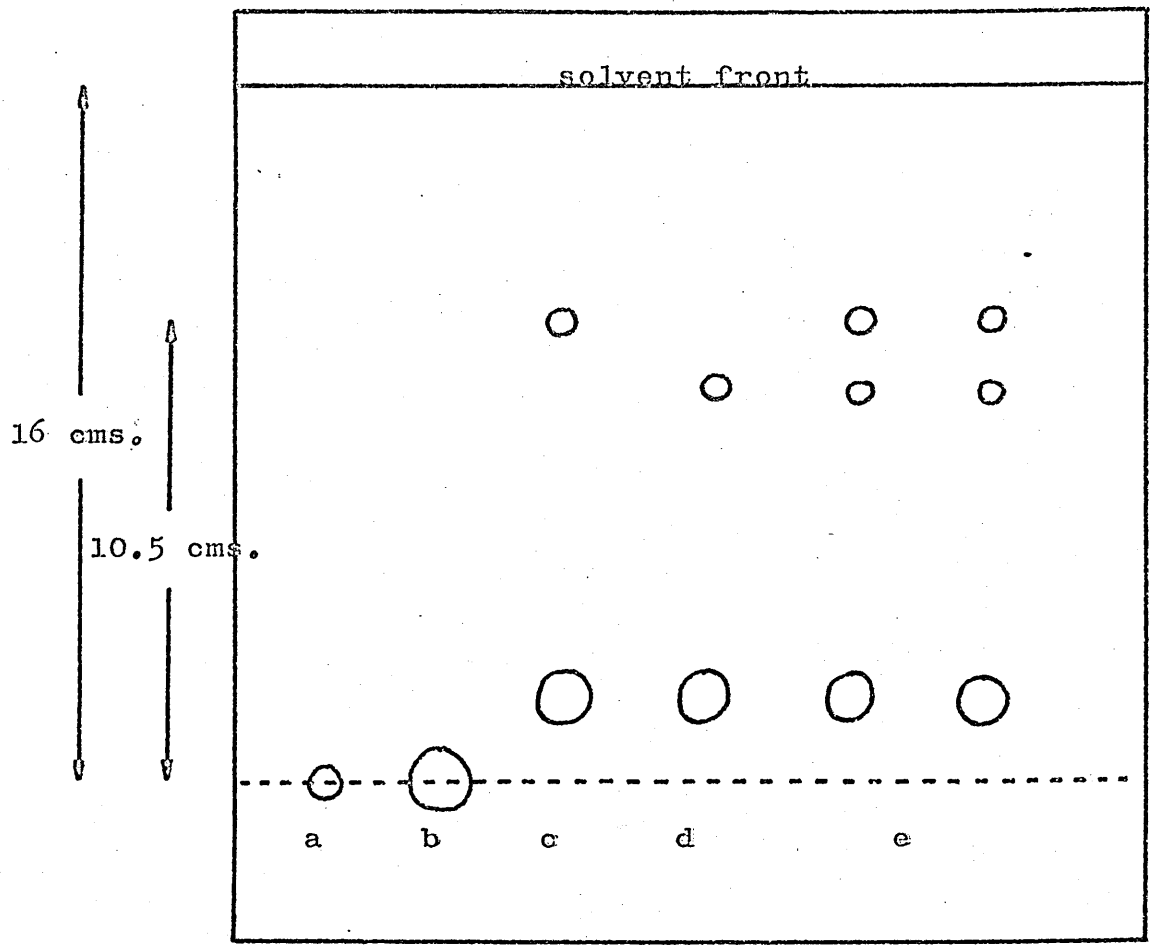

Figure 24

Diagram of TLC plate spotted with the following mixtures after developing.

a. 400μg of glycerol.

b. 800μg of glycerol.

c. 800μg of 1-mono-olein + 5% oleic acid.

d. 800μg of 1-mono-octanoin + 5% octanoic acid.

e. 800μg of 1-mono-octanoin + 5% octanoic acid + 5% myristic acid.

TABLE IV

Solvent System	Component	R_f value
	Glycerol	0
	MG8, MG11, MG//18	0.14
Pet. ether/ether/AcOH		
	Octanoic acid	0.58
68 : 31.5 : 0.5		
	Myristic acid	0.66
	Oleic acid	0.66
	1- and 2-monoglycerides	0 - 0.05
Pet. ether/ether	1,2-diglycerides	0.25
70 : 30	Fatty Acids	0.45
	Triglycerides	0.8

$$R_f \text{ Value} = \frac{\text{distance travelled by sample spot}}{\text{distance travelled by solvent front}}$$

here are due to the higher polarity of the solvent system used.

The R_f values indicate that the presence of di-glyceride, tri-glyceride, glycerol, and fatty acid impurities can be easily detected by the above method of analysis. From the size of the spots on the chromatogram it was established that impurities c.a. 1% could be detected easily. The solvent system used did not separate different 1-monoglycerides but this was considered unnecessary because of the high purity of the fatty acids used.

(c) Additional chemicals

Octylamine (OA, Koch-Light pure $\geqslant$ 97%) was found to be at least 99% pure by titration with N/10 HCl using phenolphthalein as an indicator, and was therefore used without further purification.

The water used was de-ionised and then distilled from alkaline permanganate. It had a conductivity of $< 1\mu$ S. Deuterium oxide (99.7%) was obtained from Koch-Light.

(II) Apparatus and Methods

(a) Construction and calibration of a continuous temperature recorder

The main part of the instrument consists of a highly stable and linear D.C. amplifier, which amplifies the differential output voltage from a pair of copper/constantan thermocouples, one in an ice/water mixture and the other in the sample. The amplified signal is fed to a chart recorder with a full scale deflection (f.s.d.) of 10 mV. The basic range of the instrument is 0-20°C but for measurement of temperatures above 20°C the output voltage from the thermocouples is opposed by a voltage developed across the slider of a helical potentiometer by an internal battery, and the resultant attenuated voltage presented to the input of the amplifier for amplification and recording. The instrument will

[illegible]

[illegible]

[illegible]

therefore record temperatures from 0 - 120°C ± 0.2°C in six 20°C ranges. A circuit diagram of the amplifier and attenuator is shown in figure 25.

The instrument was calibrated after both the amplifier and recorder had been allowed to stabilise for one hour.

With both thermocouples in an ice/water mixture, the helical potentiometer set to zero, and the 1.35 V cell switched out of circuit, the set-zero control of the D.C. amplifier was adjusted so that the pen recorder read zero. The recording thermocouple was placed in a thermostatted bath at 20 ± 0.05°C and VR4 adjusted so that the pen recorder read f.s.d. The basic measuring range was now set at 0 - 20°C.

The 1.35 V cell was now switched into circuit and VR1 adjusted until the voltmeter read 1.1V, establishing a known and reproducible potential difference between points A and B on the circuit diagram. This enabled a highly reproducible potential difference to be set up across the helical potentiometer VR3, which could be varied using VR2.

VR3 was now set to 200 (i.e. one fifth of its total rotation) and VR2 adjusted to bring the recorder reading back to zero. The recording range was now theoretically 20 - 40°C and by further rotation of the helical potentiometer in steps of 200 to increase its resistance and hence the voltage dropped across it, 20°C ranges up to 100 - 120°C can be covered. However because of the non-linearity of the voltage/temperature relationship of the thermocouples the required opposing voltage does not vary linearly with increasing temperature range, and so VR2 and VR4 were finally set to give a convenient range of calibration graphs over the range 0 - 100°C.

The instrument was calibrated using a thermostatted bath as a source of variable temperatures, the temperature being measured with a calibrated thermometer accurate to ±0.05°C. The calibration was checked using the melting or transition points of the following substances.

therefore normal temperatures lower than [illegible] in the [illegible] range.

A circuit diagram of the amplifier and thermostat is given in figure [illegible].

The instrument was calibrated after being in amplifier and thermostat has been allowed to stabilise for one hour.

With zero thermocouple in an ice/water mixture, the [illegible] potentiometer set to zero, and the [illegible] switch set at [illegible], the zero-error control of the [illegible] amplifier was adjusted so that the pen returned zero. The reading thermocouple was placed in a thermostatted bath at [illegible] and the [illegible] adjusted so that the pen reading read [illegible]. The basic measuring range was now set at 0 - 20°C.

The [illegible] cell was then switched into circuit and [illegible] adjusted until the potentiometer read [illegible], representing a known and reproducible thermoelectric difference, between junctions A and B on the circuit diagram. This enabled a slight measurable potential difference to be set up across the heated photomultiplier [illegible], which could be varied under [illegible].

[illegible] was then set to [illegible] (i.e. one fifth of the total resistance) and [illegible] adjusted to bring the recorder reading back to zero. The [illegible] reading was now theoretically 20 - [illegible] and by further reducing the heated potentiometer to a value of [illegible] to increase the sensitivity and hence the voltage obtained across [illegible] range by [illegible] - [illegible] can be achieved. However because of the non-linearity of the voltage/temperature relationship, if the thermocouple is the resistance-producing element, does not vary linearly with increasing temperature range, and so [illegible] and [illegible] was finally set to give a convenient range of calibration angles over the range 0 - [illegible].

The instrument was calibrated using a thermostatted bath as a source of reproducible temperatures, the temperature being measured with a calibrated thermometer to [illegible]. The calibration was checked using the melting or sublimation points of the following substances.

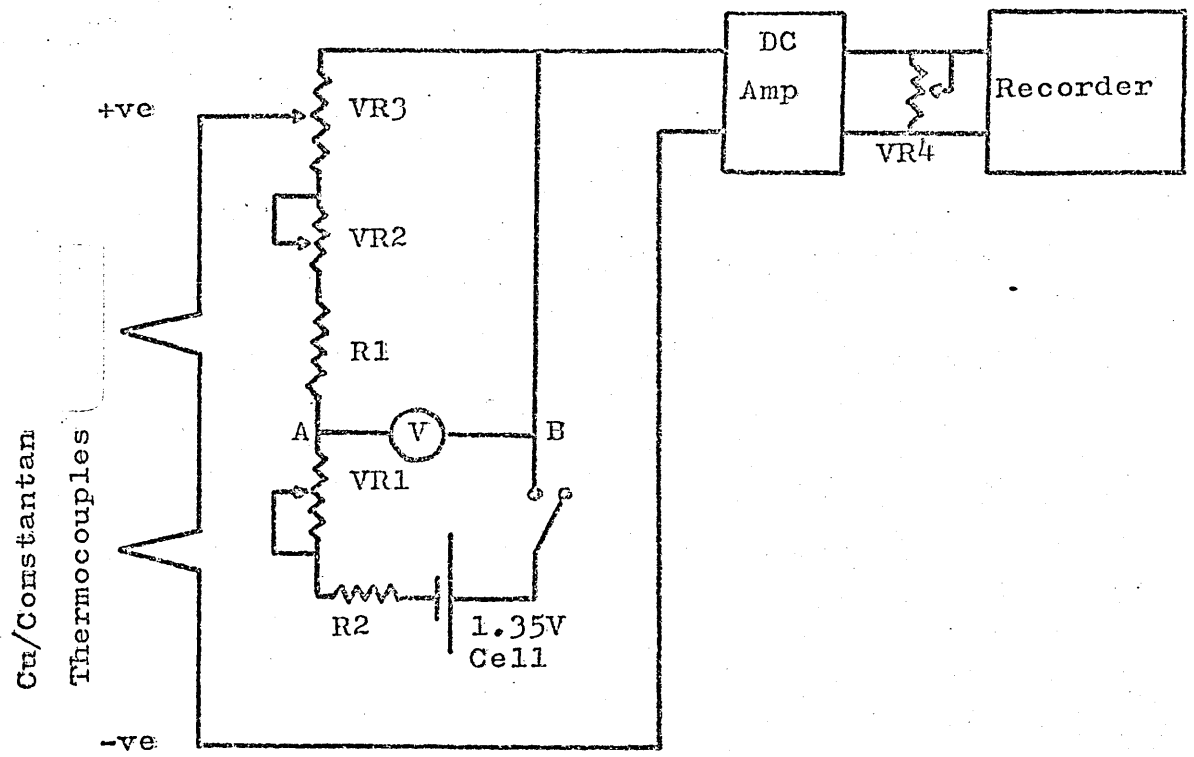

Figure 25

Circuit diagram of temperature recorder.

R1 220k

R2 8.2k

VR1 5k

VR2 50k

VR3 1k Helical

VR4 15 Ω

V 0-3V

C_6H_6	5.5°C
CH_3COOH	16.7°C
$Na_2SO_4.10H_2O$	32.4°C
$NaBr.2H_2O$	50.7°C
$MnCl_2.4H_2O$	58.1°C

(b) Thermal Studies

The MG8, MG11, MG//18, and OA/water samples were made by warming weighed mixtures to the temperature at which they formed isotropic solutions, shaking, and then allowing them to cool.

Samples containing D_2O were made up in a dry box, desiccated with phosphorus pentoxide, under an atmosphere of dry nitrogen.

1. Heating and Cooling Curves

The first investigation of the polymorphism and phase diagrams was carried out using the temperature recorder described previously to record the sample temperature during heating and cooling runs. The insulated container in which the sample was placed during heating and cooling runs is shown in figure 26.

The procedure for the determination of phase transitions shown by a flat or an arrest on the heating or cooling curve was as follows.

Approximately 2 g of the appropriate sample was made up in an 8 mm glass tube and the sample homogenised as described previously. The sample was heated to a temperature approximately 10°C above the phase transition temperature, which was to be determined accurately, and the tube, fitted with a thermocouple and sheath in the sample, placed in the insulated container. The whole assembly was placed in a thermostatted bath approximately 10°C below the transition temperature and allowed to cool.

The temperature of the sample was continuously recorded on the chart recorder, and so a graph of sample temperature against time

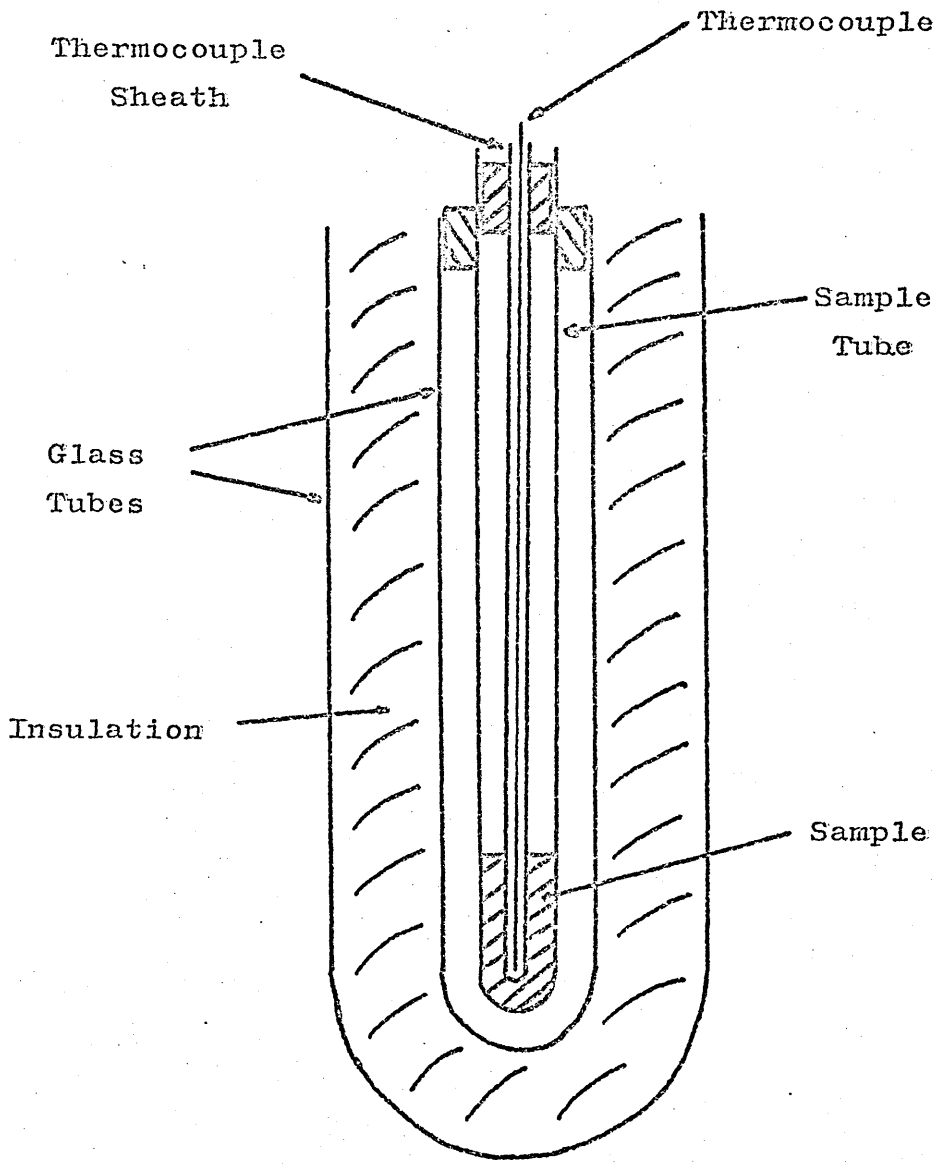

Figure 26
Cross section of insulated sample tube container

was obtained with a flat or an arrest corresponding to the transition temperature.

The transition temperature was also determined from heating runs using a similar technique to that described above and the average of the runs taken to be the true transition temperature.

2. Differential Thermal Analysis and Differential Scanning Calorimetry

Later thermal studies were carried out using a Du Pont 900 differential thermal analyser (D.T.A.) because of its wider temperature range, smaller sample requirements, and accurate and reproducible temperature programming facilities. Because of the supercooling which can occur in these systems it was not possible to determine some transition temperatures on cooling runs. All samples were therefore cooled to -50°C and allowed to warm up at a programmed rate of 3°C/minute to record the thermogram. The transition temperatures were taken to be the peaks of the thermogram (136), as shown in figure 27.

A rubber sleeve over the thermocouple head and the top of the 3 mm bore glass sample tube reduced the risk of water loss during a run.

The points on the phase diagrams are mean values from at least three thermograms.

Some of the transition temperatures were measured with a Du Pont 900 differential scanning calorimeter (D.S.C.) using samples in sealed pans. The transition temperatures were taken to be the extrapolated onset temperatures of the peaks on the thermograms as shown in figure 27.

Both the D.T.A. and D.S.C. were calibrated using the transition temperatures of the compounds given previously and the melting point of ice.

was obtained with a fall or no trend corresponding to the transition temperature.

The transition temperatures were also determined from heating runs using a similar technique to that described above and the average of the runs taken to be the true transition temperature.

2. Differential Thermal Analysis and Differential Scanning Calorimetry

Later thermal studies were carried out using a Du Pont 990 differential thermal analyzer (D.T.A.) because of its wider temperature range, smaller sample requirements, and accurate temperature programming facilities. Because of the supercooling which can occur in these systems it was not possible to determine such transition temperatures on cooling runs. All samples were therefore cooled to -50°C and allowed to warm up at a programmed rate of 5°C/minute to record the thermogram. The transition temperatures were taken to be the peaks of the thermogram (Fig), as shown in Figure 27.

A cooler allows over the thermocouple head and the top of the 3 mm bore glass sample tube reduces the risk of water loss during a run.

The peaks on the above diagrams are mean values from at least three thermograms.

Some of the transition temperatures were measured with a Du Pont 990 differential scanning calorimeter (D.S.C.) using samples in sealed pans. The transition temperatures were taken to be the extrapolated onset temperatures of the peaks on the thermograms as shown in Figure 27.

Both the D.T.A. and D.S.C. were calibrated using the transition temperatures of the compounds given previously and the melting point of ice.

Figure 27.

3. Microscopy

Transition temperatures between -10°C and 60°C were also determined on samples sandwiched between a microscope slide and a cover slip, using a polarising microscope fitted with either a heated or cooled stage.

4. Direct Observation

Some transition temperatures including l.c. melting points and dispersion to two liquid phases were determined by direct observation of samples contained in sealed glass tubes and heated in a stirred glycerol bath. The temperature was measured with a calibrated thermometer.

The agreement between transition temperatures was always at least 1°C.

Figure 17.

3. Discussion

Transition temperatures between -10°C and 10°C were also determined on crystals sandwiched between a microscope slide and a cover slip, using a polarizing microscope fitted with either a heated or cooled stage.

4. Phase Observation

Some transition temperatures including i.e. melting points and discussions to two crystal phases were determined by direct observation of samples contained in sealed pyrex tubes and heated in a stirred glycerol bath. The temperature was measured with a calibrated thermometer.

The supercooled nematic transition temperature was always at least 1°C.

(c) N.M.R. studies

1. Broad-line N.M.R.

Broad-line proton and deuteron resonance measurements were carried out at 60 MHz and 5.8 MHz respectively on samples made up as described previously in 8 mm bore glass tubes, using a JEOL 3H-60 dual purpose spectrometer with variable temperature facilities at both frequencies. A graph of sample temperature against indicated probe temperature was prepared using a calibrated thermocouple covering the range over which measurements were taken. Temperatures are accurate to $\pm 2^{o}C$.

Proton second moments, line-widths, and deuteron quadrupole splittings $\Delta\nu$ (the separation between the maxima in the D.M.R. spectra) were calculated from at least six spectra.

The experimental second moments S_e were calculated by numerical integration using equation 23 derived from equation 8.

$$S_e = {}^1/_3\, C \frac{\sum x^3 y}{\sum xy} \qquad (23)$$

where C is an instrumental calibration constant which relates x measured from the centre of the derivative curve to the field sweep in Tesla and y is the modulus of the amplitude of the derivative curve at each point x. Both x and y were measured in convenient scale units, cm and mm respectively.

2. N.M.R. of oriented samples

Oriented samples were prepared by smearing a thin layer of neat phase onto a piece of microscope cover slip, 22 x 8 mm, (cleaned with chromic acid and distilled water) and pressing a second piece of cover slip gently down onto the l.c. layer to make a sandwich. A stack of fifteen such sandwiches can be fitted into an 8 mm bore N.M.R. sample tube just tightly enough to ensure that the slides are parallel to each other and to the axis of the tube.

[illegible]

[illegible]

[illegible]

[illegible]

[

The sample tube was rotated about its long axis in order to change the setting of the l.c. layers with respect to the magnetic field $\bar{B}_o$, and the value of θ, the angle between the normal to the layers and $\bar{B}_o$ was measurable to $\pm 2^\circ$ of arc. Doublet splittings were calculated from at least four spectra, at each value of θ.

Some of the spectra from oriented samples of each of the systems studied were integrated manually to obtain the absorption line-shape. Gaussian line-shapes were fitted to these experimental line-shapes using a Du Pont 310 curve resolver and the percentages of protons contributing to the different parts of the line-shapes obtained.

3. High-resolution N.M.R.

High resolution N.M.R. measurements were carried out at 60 MHz using a JEOL C-60 HL spectrometer with variable temperature facilities accurate to $\pm 1^\circ$C.

Line-shapes obtained from l.c. samples were compared with Gaussian and Lorenztian line-shapes synthesised using an I.B.M. 1130 computer.

4. Pulse N.M.R.

Pulse N.M.R. measurements on non-oriented samples were carried out at 23°C using a Bruker BKR 201 spectrometer. T_1 and T_2 were measured using $90 - \tau - 90$ and $90 - \tau - 180 - 2\tau - 180 - 2\tau$ pulse sequences respectively. They are accurate to $\pm 5\%$ and $\pm 10\%$ respectively. Signal intensities are accurate to $\pm 5\%$.

Pulse N.M.R. measurements on oriented samples were carried out at 16 MHz using a Bruker D-KR 322S spectrometer. T_1 values were measured using a $90 - \tau - 90$ sequence. The free induction decay of the transverse magnetisation was observed following a 90° pulse and also using the Carr-Purcell sequence (119) and the Meiboom-Gill modification (118) of this sequence.

[illegible]

[illegible]

[illegible]

CHAPTER IV

POLYMORPHISM OF 1-MONOGLYCERIDES

(I) Results

(a) Thermal Studies

When molten samples of the five monoglycerides studied were allowed to cool, phase transitions, observed by DSC, occurred at the temperatures given in table V and figure 28. Typical thermograms are shown in figure 29 and it can be seen that there are no further transitions down to -20°C.

When the same samples were now heated phase transitions were observed at temperatures given in table VI, and the thermograms for MG11 and MG12 are shown in figure 30.

When cooling was stopped after transition A and the samples reheated, phase transitions were observed at the temperatures given in table VII. Typical thermograms observed for MG8 and MG11 are shown in figure 31.

When cooling was stopped after transitions A and B and the samples reheated, transition B was reversed and the transitions given in table VII were again observed with an increase in intensity of transitions F and G for MG8 and MG11, and a decrease in intensity of transition I for MG8. Also transition H for MG8 now occurred at 6°C instead of 13.5°C.

The procedure described in the previous paragraph was repeated except that after transition H a sample of MG8 was cooled down to -20°C. No further transitions were observable, and on reheating transitions I, F and G were observed as would be expected if the sample had not been cooled.

The stability of the phase occurring for MG8 between transitions H and I was investigated by keeping it at 15°C in the

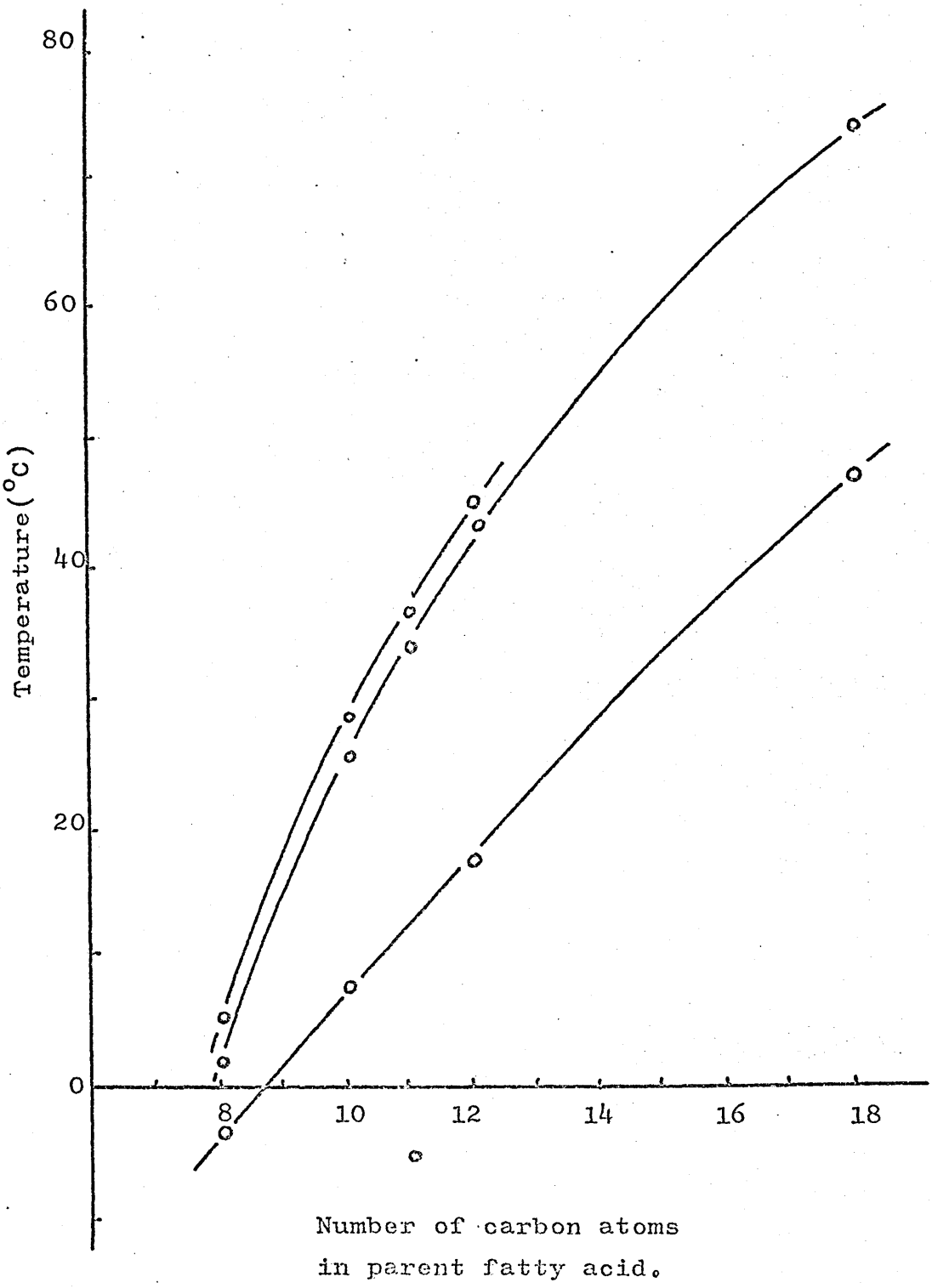

Figure 28
Transition temperatures on cooling from the melt vs. 1-monoglyceride chain length.

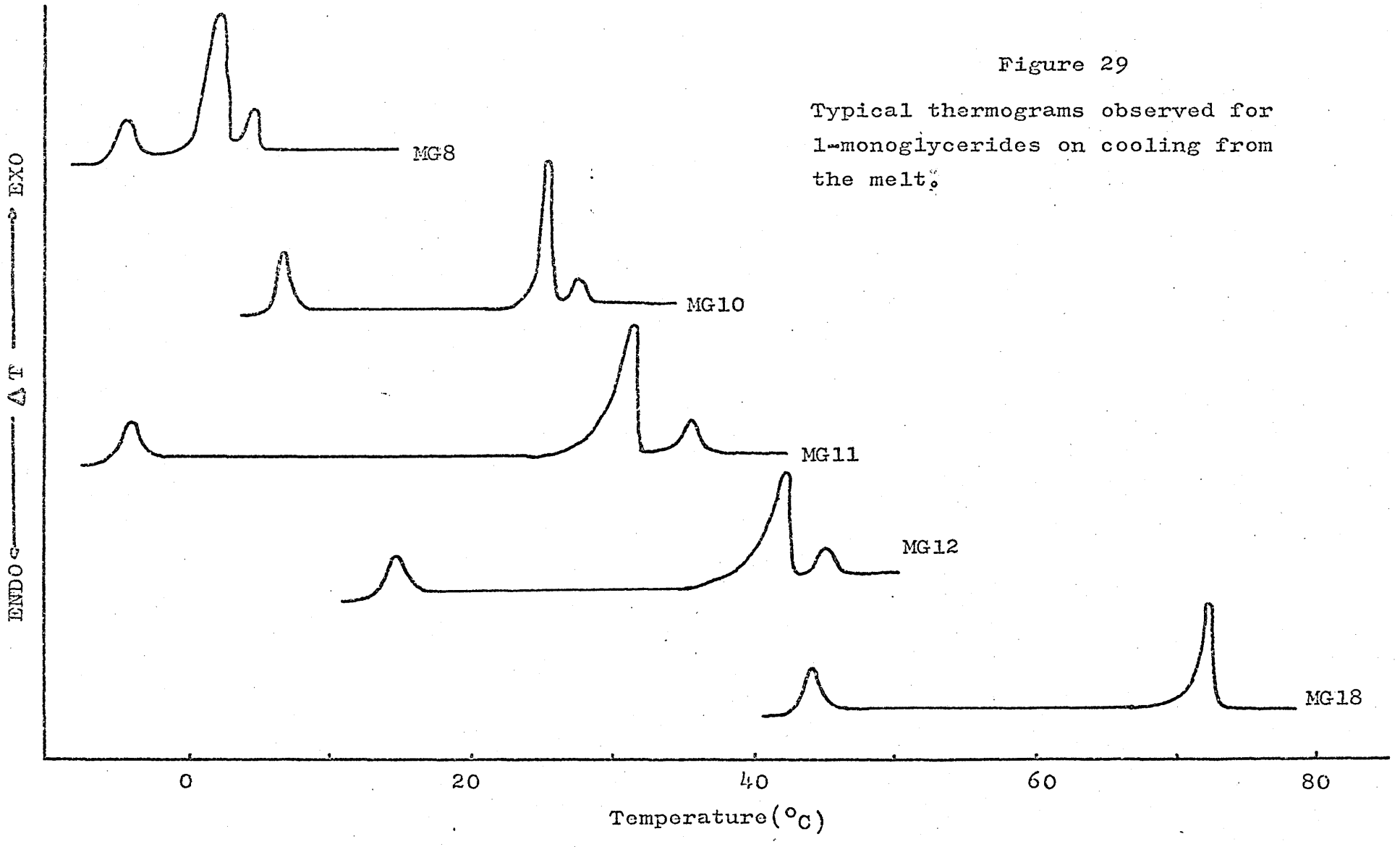

Figure 29

Typical thermograms observed for 1-monoglycerides on cooling from the melt.

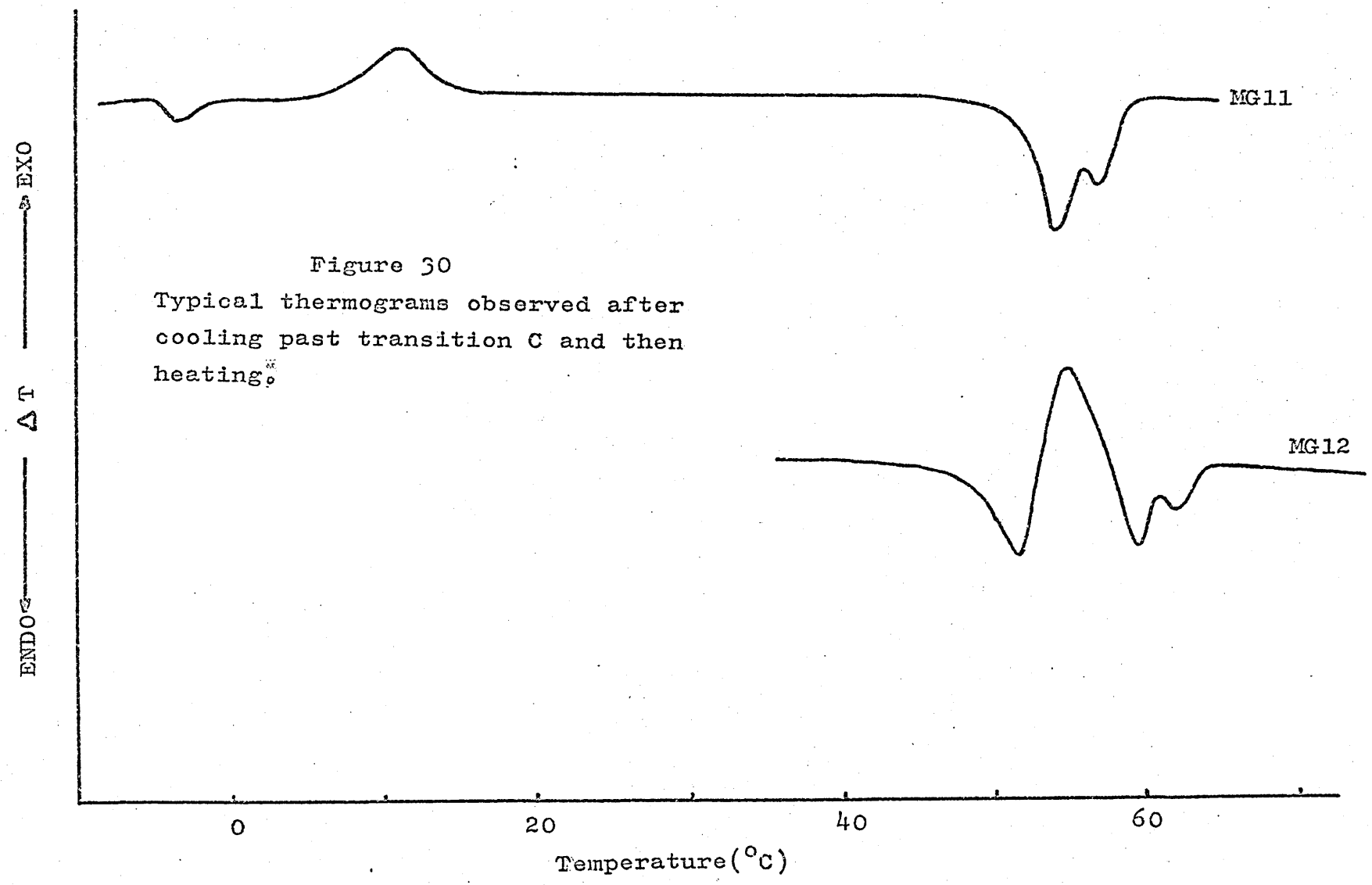

Figure 30
Typical thermograms observed after cooling past transition C and then heating.

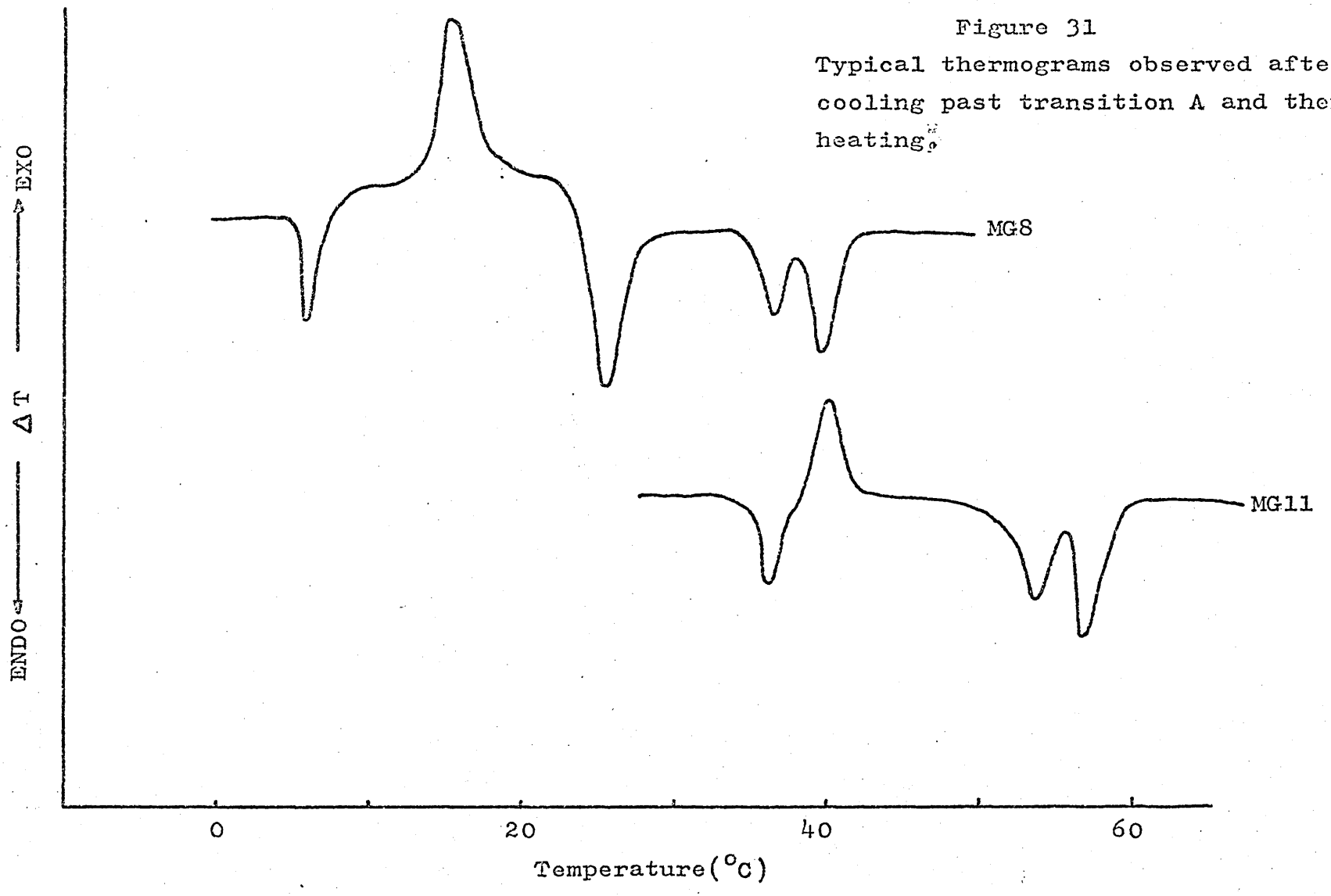

Figure 31
Typical thermograms observed after cooling past transition A and then heating.

differential scanning calorimeter for various lengths of time and observing the phase transitions which occurred on heating. It was found that the phase was only stable for a period of minutes and always changed to the highest melting form.

All the transitions which occur at or above room temperature, except that of MG18 at 47°C, have also been observed using a heated stage polarising microscope.

The first transition which occurred on cooling the molten 1-monoglycerides, except MG18, was the appearance of rings of structure in the liquid. A few degrees lower in temperature the samples assumed a variety of irregular birefringent shapes as described by Malkin (17). This latter transition occurred directly from the melt in the case of MG18.

Samples of MG8 and MG10, observed under the microscope, after being melted and allowed to cool to room temperature, changed slowly to the highest melting form over a period of hours, whilst MG11 and MG12 took several days for the same change to occur. MG18 appeared to be indefinitely stable at room temperature in the form below transition C.

The effect of adding small amounts of D_2O to MG8 on the transition temperatures observed when cooling from the melt, is shown in table VIII and figure 32a. The relative intensity of transition J increased with respect to the intensities of transitions A - C as the D_2O content was increased.

When cooling was stopped after transition A and the samples reheated, transitions now occurred at temperatures given in table IX and figure 32b. When cooling was stopped after transitions A and B and the samples reheated, the effect on transitions F - I was similar to that described previously for anhydrous MG8.

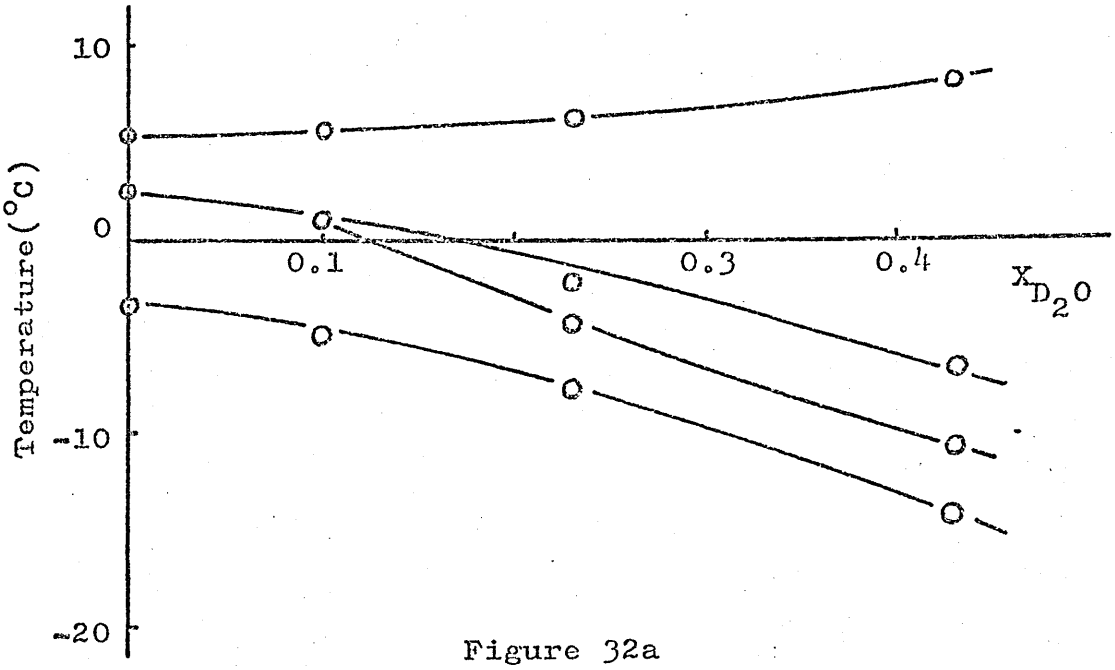

Figure 32a

Transition temperatures observed on cooling from melt for MG8 + various mole fractions of D_2O.

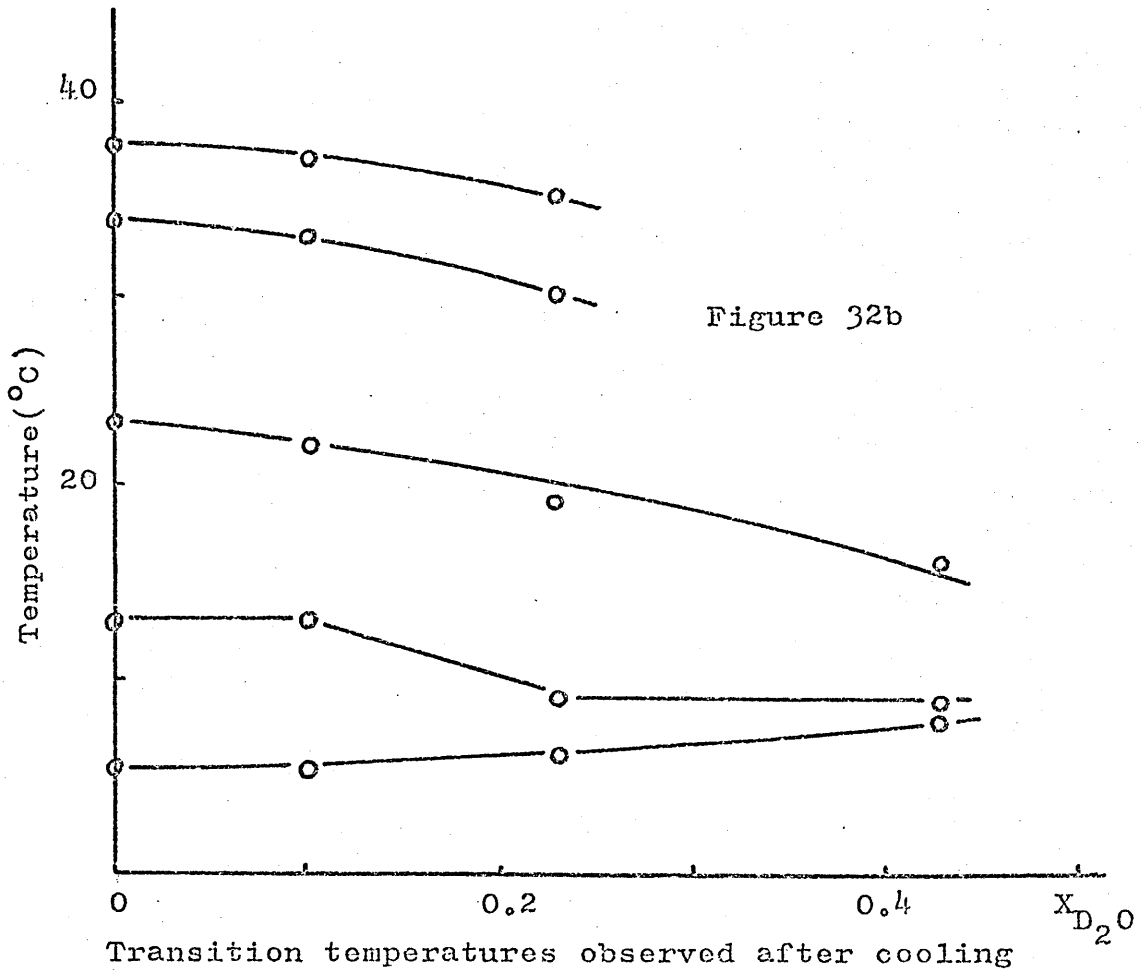

Figure 32b

Transition temperatures observed after cooling past transition A and then heating for MG8 + various mole fractions of D_2O.

(b) PMR Studies

The line-widths and second moments were measured for the highest melting forms of MG8 and MG11 at low temperature, and for the highest melting forms of MG8, MG11, and MG12 at room temperature.

The line-shape for MG8 at low temperature is shown in figure 33, that of MG11 being similar. The line-shapes at room temperature are also similar to those at low temperature except that the narrower line ca. 400μT wide is not resolvable and a weak narrow liquid-like component appears.

Attempts were made to obtain PMR spectra of samples of MG8, MG11, and MG12 between transitions A and B but the life-time of the phase was too short to allow any measurements to be made. A sample of MG8 + 0.23 mole fraction of D_2O was therefore used since it appeared from the thermal studies that addition of D_2O stabilised the required phase to some extent. This sample on cooling from the melt to below transition A appeared to be a cloudy highly viscous liquid. The line-shape observed is shown in figure 34.

Line-widths and second moments were also measured for samples of MG11 and MG12 between transitions B and C. The phases appeared as semi-transparent solids, and both gave similar line-shapes, that of MG11 being shown in figure 35.

Attempts were made to obtain PMR spectra of the forms of MG11 and MG12 below transition C, but due to the poor thermal conductivity of the 1-monoglycerides the outer parts of the samples passed through to the highest melting forms, while the centres were still in the forms between transitions B and C. The PMR spectra obtained confirmed this since they consisted of the line-shapes of the two forms superimposed. The line-widths and second moments of the forms studied are given in tables X and XI.

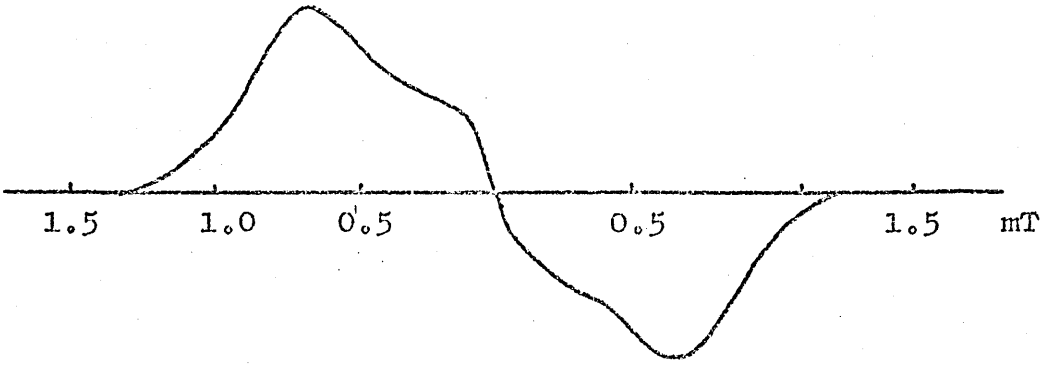

Figure 33

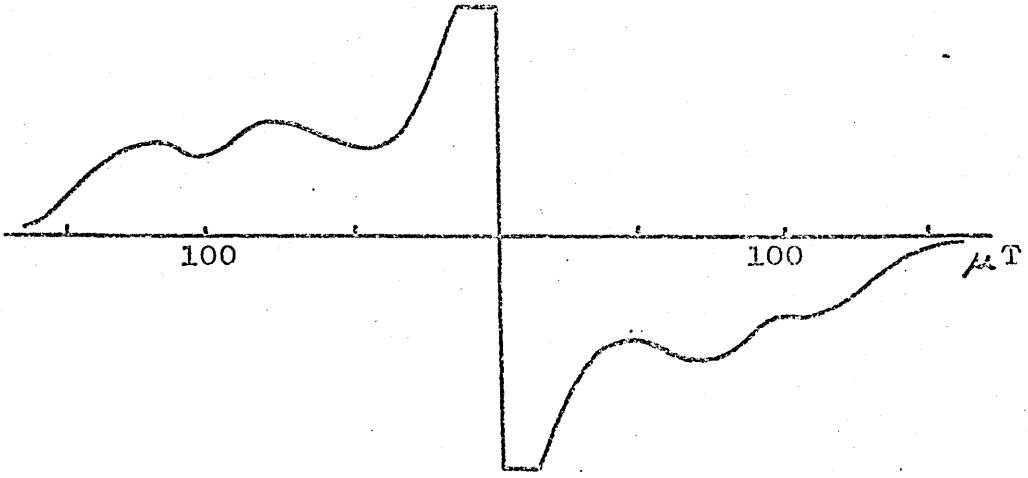

Figure 34

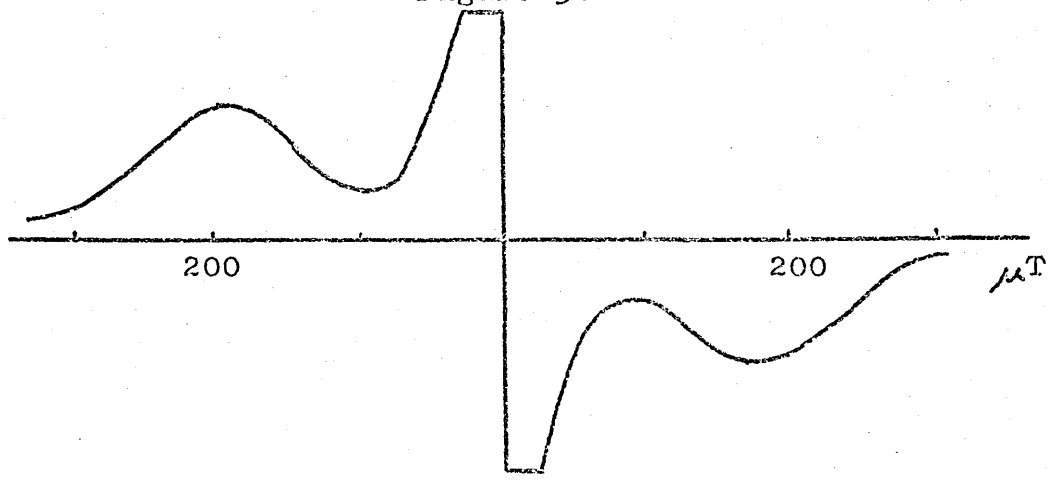

Figure 35

PMR spectra of:-

Figure 33 - MG8 at -58°C.

Figure 34 - l.c. phase of MG8 + 0.23 mole fraction of D_2O at 2°C.

Figure 35 - α'-phase of MG11 at 32°C.

TABLE V

DSC Transition Temperatures - Cooling from the melt.

1-monoglyceride	Temperature (°C)		
	A	B	C
MG8	5.5 (rs)	2.5 (rs)	-3.5
MG10	28.5 (rs)	25.5 (rs)	8
MG11	36.5 (rs)	34 (rs)	-5 (rs)
MG12	45 (rs)	44 (rs)	17.5
MG18		74 (rl)	47 (rl)

All transitions are exothermic.

rs indicates transition is reversible over a short period of time (minutes or sometimes hours).

rl indicates transition is reversible over a long period of time (weeks).

All other transitions are irreversible.

TABLE VI

DSC Transition Temperatures - Heating from -20°C.

1-monoglyceride	Temperature (°C)					
	C	B	D	E	F	G
MG8						38
MG10						53
MG11	-5			0-19(exo)*	52	56
MG12			49	53(exo)	59	62.5
MG18	47	74				

All transitions are endothermic except where stated.

* The temperature at which this transition occurred depended on the lowest temperature to which the MG11 sample was cooled, i.e.

MG11 cooled to (°C)	Transition E Temperature (°C)
-3	19
-10	7
-20	0

TABLE VII

DSC Transition Temperatures - Heating from below transition A.

1-monoglyceride	Temperature (°C)				
	A	H	I	F	G
MG8	5.5	13.5(exo)	23.5	34	38
MG10	28.5				
MG11	36.5	38.5(exo)		52	56
MG12	45				
	B				
MG18	74				

All transitions are endothermic except where stated.

TABLE VIII

DSC Transition Temperatures for MG8 + D_2O - Cooling from the melt.

X_{D_2O}	Temperature (^oC)			
	A	B	J	C
0	5.5	2.5		-3.5
0.1	5.5	1		-5
0.23	6	-2.5	-4.5	-8
0.43	8	-7	-11	-14.5

All transitions are exothermic.

TABLE IX

DSC Transition Temperatures for MG8 + D_2O - Heating from below

Transition A.

X_{D_2O}	Temperature (°C)				
	A	H (exo)	I	F	G
0	5.5	13.5	23.5	34	38
0.1	5.5	13.5	22.5	33	37
0.23	6	9	19	30*	35*
0.43	8	8.5	16		

All transitions are endothermic except where stated.

* These transitions are very weak.

TABLE X

NMR Data - Highest melting form.

1-monoglyceride	Line-width (μT)	Second Moment ($10^4 \mu T^2$)	Temperature (^oC)
MG8	390 ± 20	16.4 ± 0.6	-58
	1260 ± 10		
	1120	13.3 ± 0.5	22
MG11	420 ± 20	18.4 ± 0.4	-65
	1280 ± 10		
	1170	15.5 ± 0.6	22
MG12	1180 ± 10	16.7 ± 0.5	27

TABLE XI

NMR Data - Cooling from the melt.

1-monoglyceride	Line-width (μT)	Second Moment ($10^4 \mu T^2$)	Temperature (^oC)
MG11*	380 ± 10	3.2 ± 0.1	32
MG12*	395 ± 5	5.1 ± 0.05	25
MG8 + 0.23 mole fraction D_2O**	ca. 145		
	ca. 220		2

* Form between transitions B and C

** Form between transitions A and B

(II) Discussion

(a) Complete cooling and heating cycle

The transitions observed on cooling the molten 1-monoglycerides agree to some extent with the work of Malkin (17,21) on MG10-MG18 and Lutton (20) on MG18, but certain additional features have been observed, and it has been possible to confirm some of their suggestions using PMR.

1. At transition A for MG8 and MG10 - MG12 the liquid 1-monoglyceride passes through to a smectic l.c. phase. The ring-like structures observed under the polarising microscope are 'stepped drops' which are formed by many smectic phases under suitable conditions (137). Also the line-widths of 145μT and 220μT observed for this l.c. phase in MG8 + 0.23 mole fraction of D_2O are consistent with the values obtained for the stable l.c. phase of MG8 containing higher mole fractions of D_2O.

Malkin (17) regards an alpha-phase to be formed first from the melt and this is described as 'dark greyish pools which give a strong uniaxial interference figure'. Such a form has been observed but rings of structure were always present as well. It is possible that Malkin was observing the l.c. phase described previously but in a completely oriented state.

2. At transition B the l.c. phase transforms to a solid phase, which Malkin (17) describes as 'aggregates of molecules in all states from vertical rotating to tilted rigid'.

X-ray data, infra-red spectra, and PMR line-widths and second moments have been reported for this solid by Lutton (20), Larsson (14), Chapman (25), and Chapman et al. (26), and from their evidence they consider it to be an alpha-phase in which the alkyl chains are hexagonally packed and rotating about their long axes.

In terms of currently accepted nomenclature this solid cannot correctly be called an alpha-phase, since Larsson (14) and Lutton (20) have reported that the alkyl chains are tilted (but give no angle of tilt), whereas in the alpha-phases of long chain hydrocarbons (31), esters (33), and alcohols (34) the alkyl chains are known to be vertical.

The experimental values of the second moments of MG11 and MG12 in this solid phase are $3.2 \times 10^4 \mu T^2$ and $5.1 \times 10^4 \mu T^2$. The low value of the second moment of MG11 compared to that for MG12 is probably due to the fact that it was obtained at a temperature only 2° below transition B, whereas the second moment of MG12 was obtained at a temperature 20° below transition B.

The experimental values of the second moments can be compared with values derived theoretically, since for a long chain hydrocarbon $C_n H_{2n+2}$ undergoing restricted reorientational motion about the chain axis, sufficient to affect the second moment, the reduced intramolecular contribution to the second moment, as calculated by Andrew, is $\left[6.8 - 11.6/(n + 1)\right] \times 10^4 \mu T^2$ (109). Applying this equation to MG11 and MG12 gives values of $5.8 \times 10^4 \mu T^2$ and $5.9 \times 10^4 \mu T^2$ respectively. For a hydrocarbon the intermolecular broadening is about $2.6 \times 10^4 \mu T^2$ (109) giving totals of $8.4 \times 10^4 \mu T^2$ and $8.5 \times 10^4 \mu T^2$ respectively. Peterlin (138) has also given an equation for calculating the second moment of a non-oriented hydrocarbon in which the alkyl chains are hexagonally packed and rotating about their long axes, $S = \left[7.25 - 16.73/(n + 1)\right] \times 10^4 \mu T^2$, which he claims is more accurate than Andrew's equation. Using this second equation values of $5.85 \times 10^4 \mu T^2$ and $5.95 \times 10^4 \mu T^2$ are obtained for the second moments of MG11 and MG12 respectively, which are closer to the experimental values than the second moments calculated

using Andrew's equation.

If the alkyl chains additionally undergo some lateral and possibly longitudinal motion the contribution of intermolecular broadening to the second moment will be reduced. Also more complex motion of the alkyl chains other than just simple rotation can combine with the above factcrs to reduce the theoretical second moments to values close to those obtained experimentally.

The type of motion required to reduce the theoretical second moments to the experimental values indicates that the solid, which is henceforward termed α', is intermediate between a true alpha-phase and a smectic liquid crystal.

The PMR line-widths and second moments of the highest melting forms of MG8, MG11, and MG12 are similar to those reported by Chapman et al. (26) of MG16 and MG18. The low temperature value of the hydrogen resonance of a 1-monoglyceride is expected to be ca. $25 \times 10^4 \mu T^2$ (26), and the experimental values of ca. $17 \times 10^4 \mu T^2$ therefore indicate that little molecular motion is occurring beyond methyl group rotation.

3. The question of the reversibility of transition C and the nature of the form produced have been subject of a considerable amount of controversy between Malkin (17, 21) and Lutton (20). Lutton studied MG16 and MG18 and stated that at the lowest transition temperature a sub-alpha crystalline form is produced, and the transition is reversible. We have confirmed the reversibility of transition C in the case of MG11 and MG18, and the apparently low value of transition C for MG11 is due to an alternation effect implying greater mobility of the chains in the 1-monoglycerides containing odd-numbered acids. The infrared spectra of a sample of MG18, which had been melted and then cooled below transition C, showed a doublet at 720 cm^{-1}, which

Chapman (25) cites as evidence of a crystalline sub-alpha form.

For the other 1-monoglycerides studied transition C was irreversible and several different types of behaviour have been observed when samples were reheated after cooling past this transition. This is not surprising since the lengths of the alkyl chains of these 1-monoglycerides are in the intermediate range where changes of property occur.

In the case of MG8 and MG10, cooled samples remelted at the B-melting points (transition G), indicating that below transition C the B-form is obtained. We have no evidence from DSC that any intermediate form such as the B' suggested by Malkin (17) occurs under these conditions.

For MG11, on heating past the reversible transition C, a small exotherm (transition E) is observed at a variable temperature, probably determined by the number of seed crystals present and the previous thermal history of the sample. At transition E the B' and B-forms are produced since partial melting now occurs at 52°C and 56°C (transitions F and G respectively). The relative intensities of the two peaks indicate that the lower in temperature the sample is cooled the more B-form is produced at transition E.

The behaviour of MG12 on reheating is more complex than that of any of the other 1-monoglycerides studied. At transition C a solid is formed which melts at 49°C (transition D) and then resolidifies (transition E). The solid produced at transition E is a mixture of the B' and B-forms which melt at 59°C (transition F) and 62.5°C (transition G) respectively. The relative intensities of the two peaks vary from run to run and from sample to sample indicating that the relative amounts of each form produced at transition E are dependent again on the

number and type of seed crystals present and the previous thermal history of the sample.

The solid form of MG12 produced at transition C cannot be a sub-alpha form since it gives only a single infra-red band at 720 cm^{-1} compared to the sub-alpha form of MG18 which gives a doublet in this region. Since its melting point at 49°C is only 5°C above the α' to liquid crystal transition it is possible that the solid is a slightly modified α' form in which the packing of the alkyl chains is more ordered, and consequently their lateral and longitudinal motion reduced.

(b) Partial cooling and heating cycle

In the cases of MG10 and MG12 cooling past only transitions A and B, and then reheating causes the same two transitions to recur.

MG8 and MG11 however, after reheating past transitions A and B, solidify (transition H).

For MG11 the solid produced is a mixture of the B' and B-forms since partial melting now occurs at 52°C (transition F) and 56°C (transition G), similar to that described previously after transition E.

For MG8 an intermediate form is produced with a subsequent change to the B' and B-forms at 23.5°C (transition I) which melt at 34°C (transition F) and 38°C (transition G) respectively. The nature of this intermediate form is discussed in the next section.

(c) The effect of D_2O on the polymorphism of MG8

The addition of small amounts of D_2O to MG8 raises the temperature at which transition A occurs and decreases the temperature at which transition B occurs.

Therefore D_2O is increasing the range of existence and stability of a metastable l.c. phase in which considerable molecular motion is occurring, just as it does for the alpha-forms of aliphatic long chain alcohols (139). This implies that the hydrogen-bonding network involving D_2O and 1-monoclyceride hydroxyl groups is more stable than that involving just hydroxyl groups. Lack of X-ray data on the polar end group region prevents any meaningful structure being assigned to either network.

At transition B the α'-form is produced and D_2O is thrown out of the crystal lattice to subsequently freeze at transition J. Transition C is similar to that occurring in anhydrous MG8.

Addition of D_2O also decreases the temperatures at which transitions F - I occur when heating the l.c. phase from below transition A.

This l.c. phase is metastable with respect to the intermediate solid existing between transitions H and I, which seems to be similar to the 'opaque crystal phase' observed in long chain alcohols (139). At low water contents this opaque phase in alcohol/water systems was found to be a γ-form (140), which is monoclinic with the alkyl chains tilted at approximately 60°. The intermediate solid could be similar in nature to this γ-form. Also at increasing D_2O contents transition I is tending towards Tpen for MG8, and a similar tendency is observed for the transition from alpha to opaque phase in alcohol/water systems.

CHAPTER V

LIPID/WATER SYSTEMS

(I) Results

(a) Phase diagrams

Tpen has been determined for the five 1-monoglycerides studied and the values obtained are given in table XII.

Table XII

1-monoglyceride	Tpen (^{o}C)
MG8	12.5
MG10	30
MG11	36
MG12	41
MG18	65

The phase diagrams of the MG8/D_2O and MG//18/D_2O systems have been determined and are shown in figures 36 and 37. Transition temperatures for the samples studied are given in tables XIII and XIV. The phase diagrams can be compared with those of the MG8/H_2O and MG//18/H_2O systems determined by Larsson (61) and Lutton (59) respectively, shown in figures 38 and 39. The phase diagram for the MG11/D_2O system is shown in figure 40 (92).

The abbreviations used in the phase diagrams are:-

D	Dispersion
F.I.	Fluid isotropic
M	Middle liquid crystal
N	Neat liquid crystal
V.I.	Viscous isotropic

[illegible]

[illegible]

[illegible]

[illegible]

[illegible]

[illegible]

[illegible]	[illegible]
[illegible]	[illegible]
[illegible]	[illegible]
[illegible]	[illegible]
[illegible]	[illegible]
[illegible]	[illegible]

[illegible]

[illegible]

[illegible]

[illegible]	[illegible]
[illegible]	[illegible]
[illegible]	[illegible]
[illegible]	[illegible]
[illegible]	[illegible]

TABLE XIII

Data points for MG8/D_2O phase diagram.

X_{D_2O}	Transition Temperatures (^oC)						
0.22	0.5	11	28	35			
0.31	1.5	11.5	27	32			
0.36	2.5	12	27.5	30			
0.45	3	12		27			
0.5	3	12		25	27.5		
0.55	3.5	12		24	31.5		
0.675	3.5	12.5		18.5	42		
0.73	4	12.5		15.5	44		
0.76	4.5	13		14.5	46		
0.78	4.5	12.5			46.5		
0.83	5	12.5			45		
0.86	5	12.5			43		
0.88	5.5	12.5			38.5		
0.90	5.5	12.5			36.5		53
0.92	5.5	12.5			33.5		37
0.94	5.5	12.5				33.5	
0.96						34	
0.98						34	

TABLE XIV

Data points for MG//18/D_2O phase diagram.

X_{D_2O}	Transition Temperatures (^oC)										
0.15			19.5	34							
0.25			17.5	31							
0.36			16	22	28.5						
0.40			15	19	30.5						
0.47		1.5	14.5	17.5	34						
0.53		2	13	15	38.5						
0.59		2.5	13		46						
0.65		3	13		54						
0.68		3	12.5		54		61				
0.71		3	12		50		69				
0.76		3	12		36		79.5				
0.775		3	12		32		82.5		89	93	
0.82		3	12		27				85.5	97	105
0.85		3.5	12		25.5			80	86	96.5	
0.875		3.5	12		24			59	88	94	
0.90		3.5	12		23.5			40	90		
0.95		4	12			25			90		

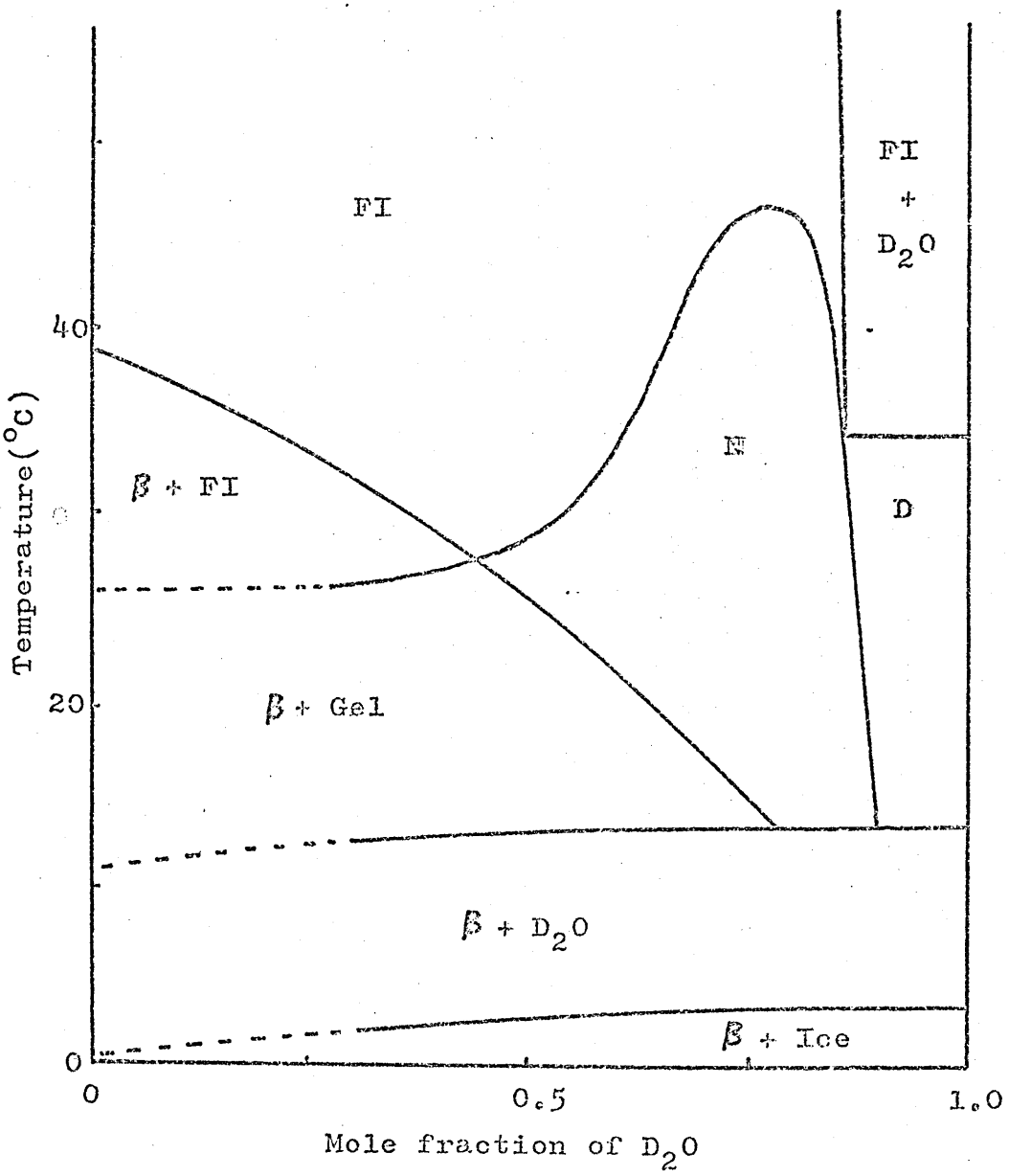

Figure 36

1-mono-octanoin/D_2O phase diagram

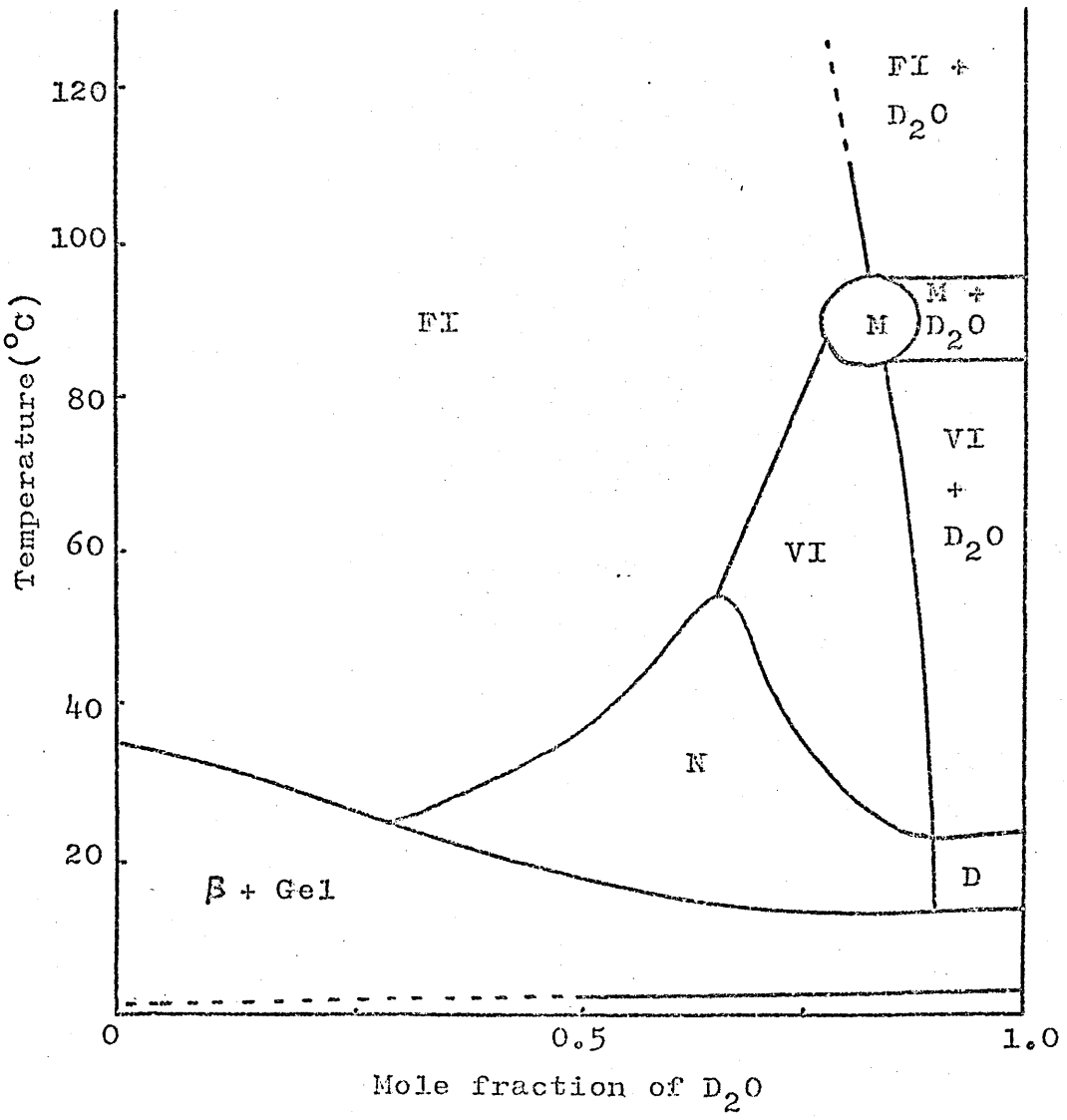

Figure 37

1-mono-olein/D_2O phase diagram

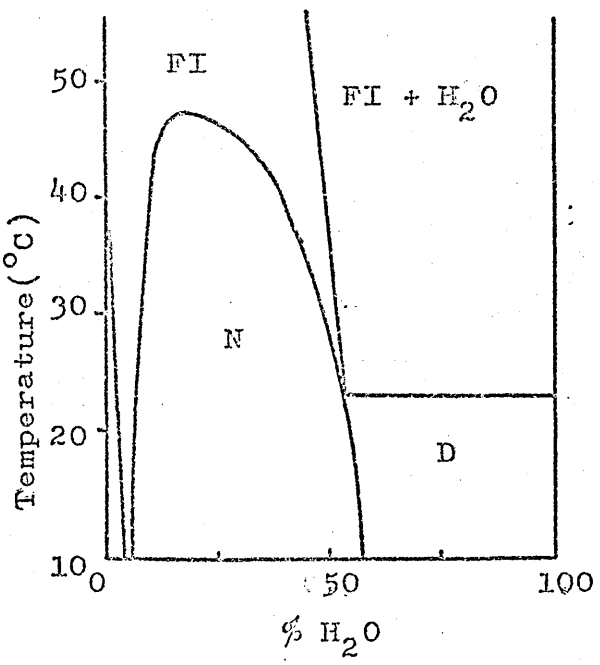

Figure 38

MG8/H_2O phase diagram

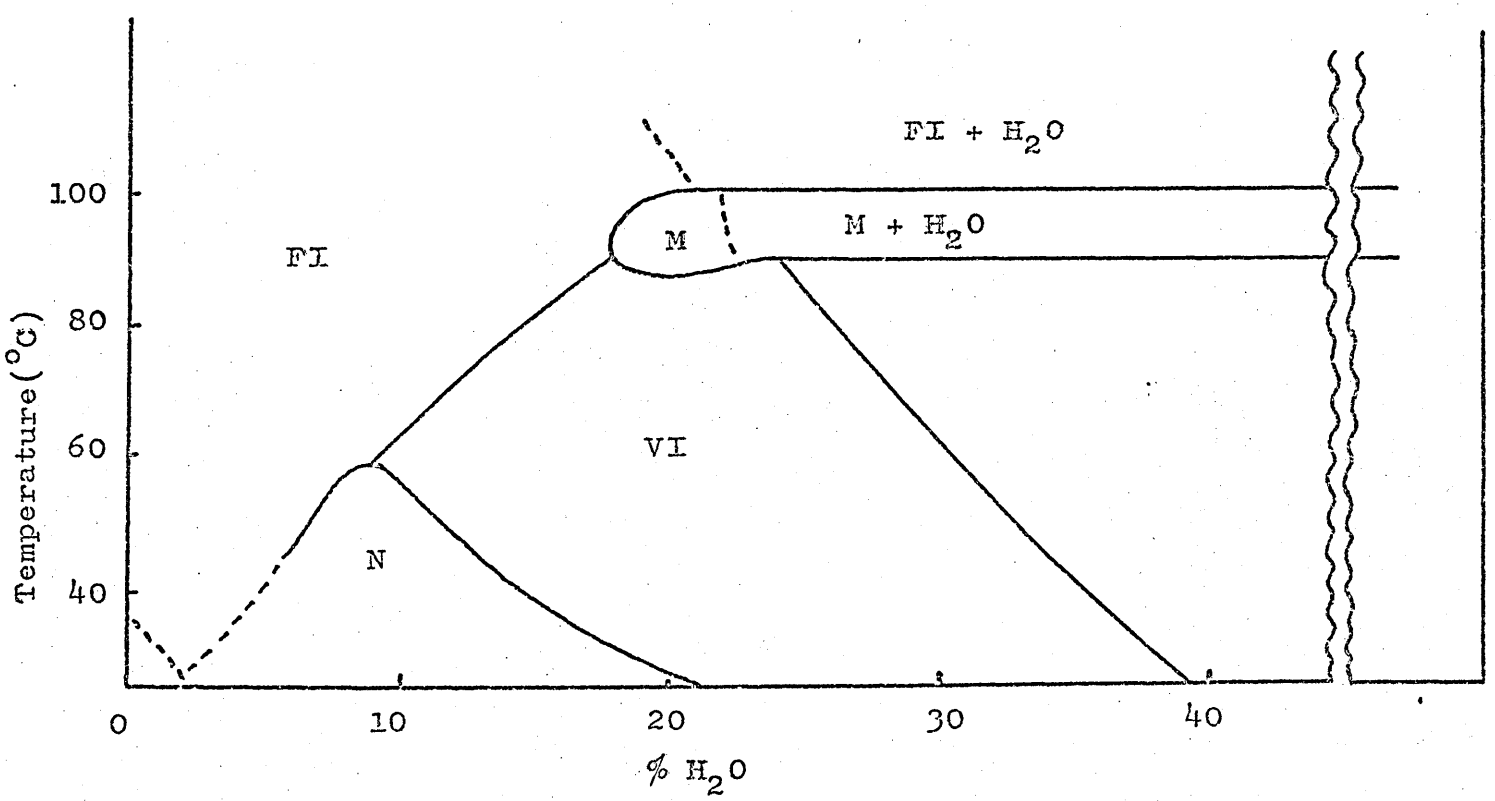

Figure 39

MG//1S/H_2O phase diagram

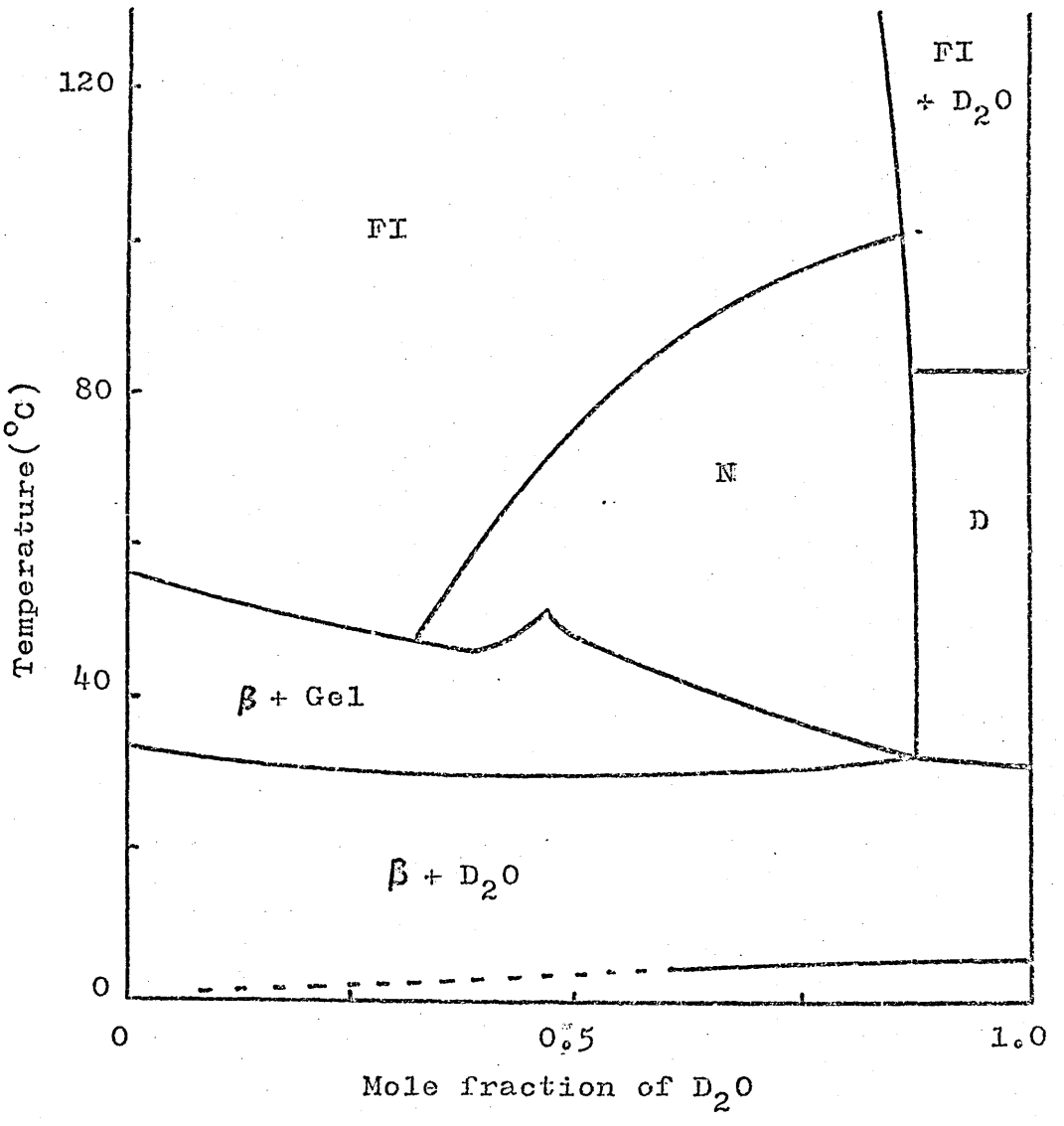

Figure 40

1-monoundecanoin/D_2O phase diagram

TABLE XV

X-ray long spacings for MG8/D_2O neat phase.

X_{D_2O}	d(Å)
0.66	27.1 ± 0.6
0.80	30.1 ± 0.7
0.89	37.6 ± 1.1

X-ray long spacings for OA/D_2O neat phase.

X_{D_2O}	d(Å)
0.80	29.7 ± 0.7
0.85	33.9 ± 0.9
0.92	44.7 ± 1.6

(b) X-ray studies

The variation of d with D_2O content is given in table XV for the neat l.c. phases of the systems MG8/D_2O and OA/D_2O.

L.c. samples of MG8/D_2O and OA/D_2O gave diffuse side-spacings of ca. 4.5Å which did not vary significantly with water content.

(c) NMR of non-oriented systems

1. 1-mono-octanoin/H_2O and D_2O

The broad-line PMR spectra at -58°C of MG8 containing 0.55 and 0.90 mole fractions of D_2O are shown in figures 41 and 42. The line-widths of the broad and narrow components in figure 42 are 1140μT and 390μT respectively. Second moment values at -58°C are given in table XVI.

Table XVI

MG8 + X_{D_2O}	Second Moment ($10^4 \mu T^2$)
0	16.4 ± 0.6
0.55	16.5 ± 0.3
0.90	14.8 ± 0.4

Figure 43 shows the PMR line-shape for MG8 + 0.55 mole fraction of D_2O at 5°C and figure 44 the PMR line-shape for MG8 + 0.90 mole fraction of D_2O in the neat l.c. phase at 26°C.

The broad-line PMR spectra of the neat l.c. phases of MG8 containing 0.66, 0.80, and 0.89 mole fractions of D_2O have been determined at 23°C and the line-widths and second moments are given in table XVII.

The variations of the PMR line-widths and second moment with temperature have been determined for MG8 + 0.80 mole fraction of D_2O and are given in table XVIII. Above room temperature the outer line, ca. 200μT wide, was very weak

[illegible]

[illegible]

[illegible]

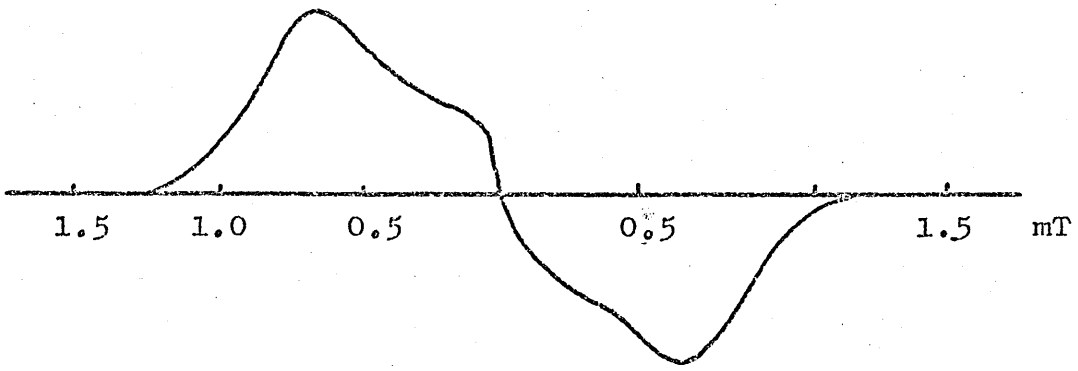

Figure 41

PMR spectrum of MG8 + 0.55 mole fraction of D_2O at -58°C.

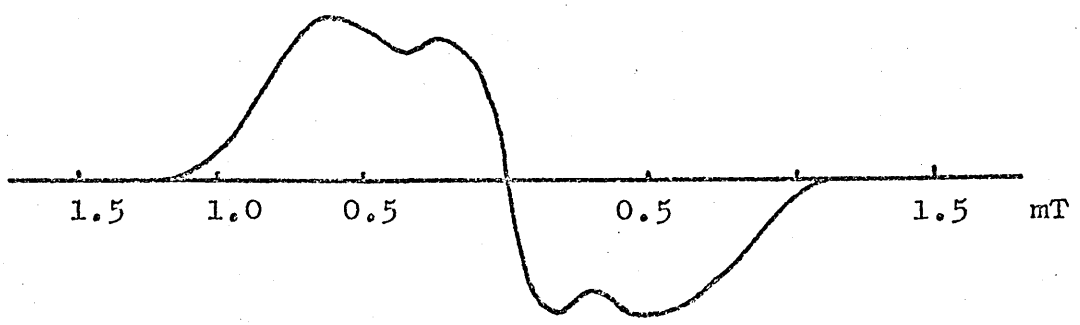

Figure 42

PMR spectrum of MG8 + 0.9 mole fraction of D_2O at -58°C.

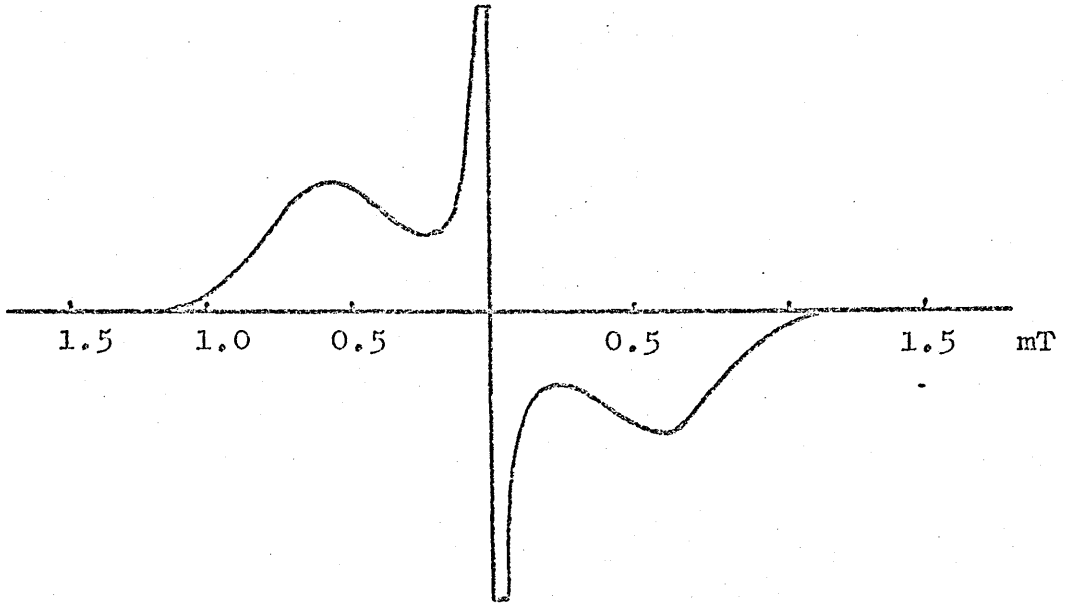

Figure 43

PMR spectrum of MG8 + 0.55 mole fraction of D_2O at 5°C

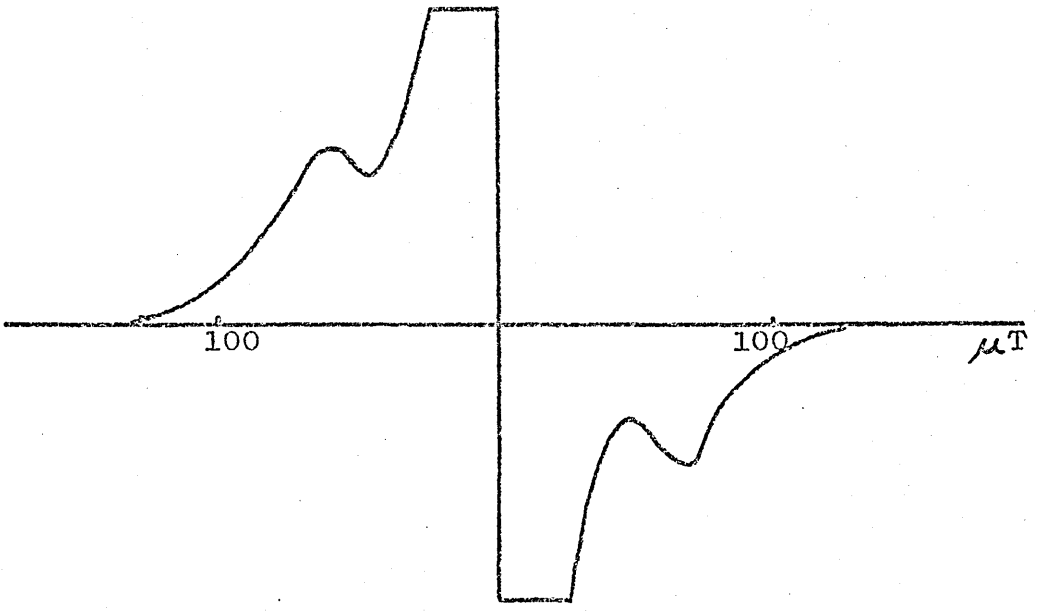

Figure 44

PMR spectrum of MG8 + 0.9 mole fraction of D_2O neat phase at 26°C

Table XVII

PMR line-widths and second moments for MG8/D_2O neat phase at 23°C.

X_{D_2O}	Line-width (μT)	Second Moment ($10^4 \mu T^2$)
0.66	146 ± 2 ca. 200	0.25 ± 0.01
0.80	141 ± 5 ca. 200	0.23 ± 0.01
0.89	125 ± 5 ca. 180	0.19 ± 0.01

Table XVIII

PMR line-widths and second moments for MG8 + 0.80 mole fraction of D_2O neat phase at various temperatures.

Temperature (^oC)	Line-width (μT)	Second Moment ($10^4 \mu T^2$)
2	172 ± 6 ca. 220	0.26 ± 0.01
10	161 ± 5 ca. 200	0.24 ± 0.01
23	141 ± 5 ca. 200	0.23 ± 0.01
27	137 ± 3	0.23 ± 0.01
33	126 ± 3	0.225 ± 0.005
37	121 ± 3	0.215 ± 0.005
41	118 ± 3	0.21 ± 0.005

and could not be measured. The narrow line in the spectra had a width of ca. 13μT which did not vary appreciably with temperature or composition over the range described.

DMR spectra were obtained of neat l.c. samples of MG8 containing various mole fractions of D_2O, and a typical line-shape, that from MG8 + 0.73 mole fraction of D_2O at 22°C, is shown in figure 45. The frequency separation in Hz ($\Delta\nu$) between the two principal peaks as a function of X_{D_2O} is given in table XIX and figure 46. For a given composition $\Delta\nu$ was found to be independent of temperature. The widths of the component lines were ca. 160 ± 20 Hz at 22°C, and they broadened slightly with increasing temperature. For samples containing greater than 0.92 mole fraction of D_2O in the dispersion region an additional line with a width of 50 ± 5Hz, appeared in the centre of the doublet. For samples containing 0.90 and 0.92 mole fraction of D_2O which are in the transition region between neat l.c. phase and dispersion a typical line-shape is shown in figure 47. The ratio of outer peak separation to inner peak separation is between 1.7 and 1.9.

High resolution PMR spectra of MG8/H_2O neat l.c. samples at 23°C were not reproducible but showed similarities to the 'powder patterns' observed in deuteron resonance spectra. The spectra usually consisted of two or three lines with widths between 20 and 100 Hz, the separation between the outermost lines being several hundred Hz. The spectra were centred on ca. 5ppm. and the line-widths and separation between the outermost peaks decreased as the mole fraction of water increased from 0.66 to 0.90.

Relaxation times have been determined for MG8 neat l.c. samples containing various mole fractions of H_2O or D_2O, the values obtained being given in table XX. The values listed

Table XIX

Quadrupole splittings for MG8/D_2O neat phase and dispersion at 23°C.

X_{D_2O}	$\Delta\nu$ (kHz)
0.55	3.97
0.66	3.14
0.73	2.24
0.79	1.92
0.82	1.60
0.88	0.94
0.90	0.78
0.92	0.59
0.95	0.58

Error in measurement of $\Delta\nu$ is $\pm$ 2%.

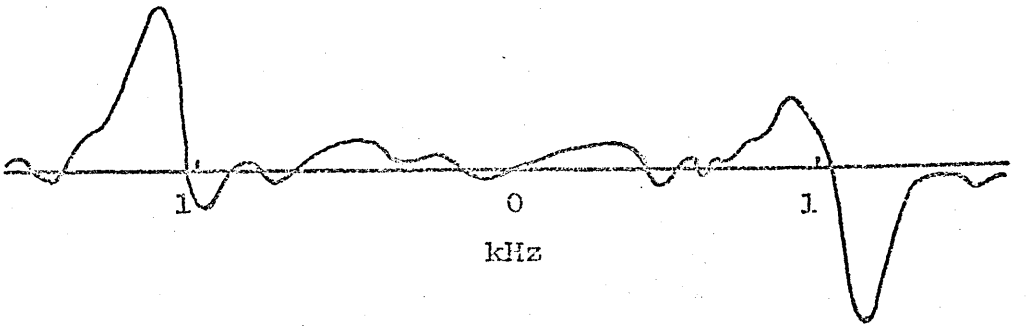

Figure 45

DMR spectrum of MG8 + 0.73 mole fraction of D_2O at 22°C

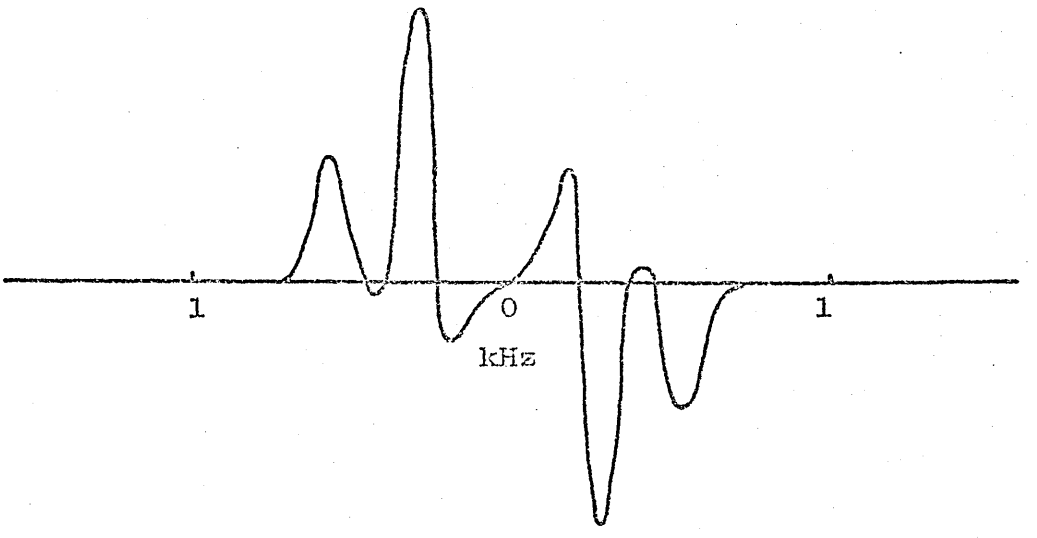

Figure 47

DMR spectrum of MG8 + 0.92 mole fraction of D_2O at 22°C

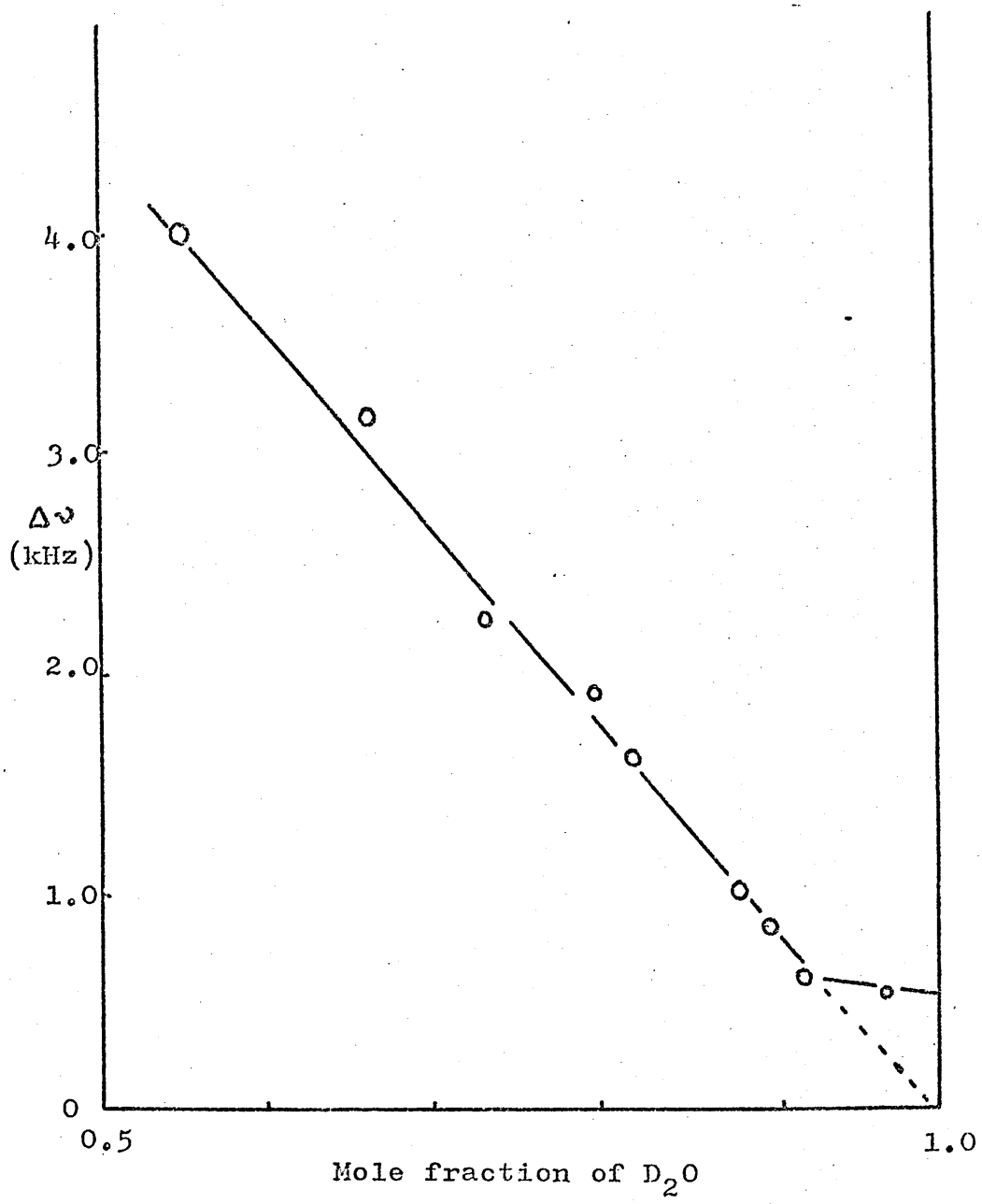

Figure 46

$\Delta\nu$ vs. X_{D_2O} for neat phase and dispersion of MG8/D_2O

Table XX

Relaxation times for MG8/H_2O neat phase at 24°C.

X_{H_2O}	T_2(fast)(μs)	T_2(med.)(ms)	T_2(slow)(s)	T_1 (s)
0.66	52 (34%)	4.6 (52%)	0.044 (14%)	0.29
0.80	54.6 (32%)	5.6 (50%)	0.113 (18%)	0.46
0.90	62 (22%)	5.1 (44%)	0.339 (34%)	0.67
0.80 (D_2O)	69 (50%)	3.9 (50%)	-	0.357

Figures in brackets refer to signal intensities (± 5%).

Accuracy of T_2(fast) and T_2(med.) is ± 20%.

Accuracy of T_2(slow) is ± 10%. and T_1 better than ± 5%.

were determined at τ = 40μs, and at τ = 80μs and 200μs the intensity of T_2 (fast) increases and that of T_2 (medium) decreases. A similar type of pulse distance dependence was observed for the decay of the water signal.

2. <u>1-monundecanoin/H_2O and D_2O</u>

PMR line-widths and second moments have been determined at 27°C for MG11/D_2O neat l.c. samples containing three different mole fractions of D_2O. The results are shown in table XXI and in the spectra there was also a narrow line of width ca. 10μT which did not vary significantly with composition.

A solid sample of MG11 + 0.43 mole fraction of D_2O at 25°C gave a line of width 1180 ± 10μT and in the l.c. phase at 45°C gave lines of widths 100 ± 4μT and 175 ± 3μT.

DMR spectra have been obtained at 25°C for MG11 containing various mole fractions of D_2O. The variation of $\Delta\nu$ with mole fraction of D_2O is given in table XXII and figure 48. The overall line-shapes observed were similar to those described previously for MG8/D_2O samples.

For a given sample $\Delta\nu$ showed no change with temperature over the range 25°C to 65°C. The width of the component lines at 25°C was ca. 200 Hz and slight broadening occurred with increasing temperature.

In the dispersion region above 0.86 mole fraction of D_2O an additional central line of width ca. 50 Hz appeared in the DMR spectra.

3. <u>1-mono-olein/H_2O</u>

Three neat l.c. samples of MG//18 containing 0.45, 0.66, and 0.77 mole fractions of water have been studied. The PMR spectra of the samples at 25°C consisted of a narrow line of

Table XXI

PMR line-widths and second moments for MG11/D_2O neat phase at 27°C.

X_{D_2O}	Line-width (μT)	Second Moment ($10^4 \mu T^2$)
0.57	158 ± 3 260 ± 10	0.54 ± 0.03
0.70	154 ± 3 240 ± 10	0.47 ± 0.03
0.85	146 ± 3 226 ± 5	0.41 ± 0.03

Table XXII

Quadrupole splittings for MG11/D_2O neat phase and dispersion at 25°C.

X_{D_2O}	$\Delta\nu$ (kHz)
0.7	2.1
0.804	1.48
0.85	1.09
0.90	0.98
0.95	0.97

Error in measurement of $\Delta\nu$ is ± 2%.

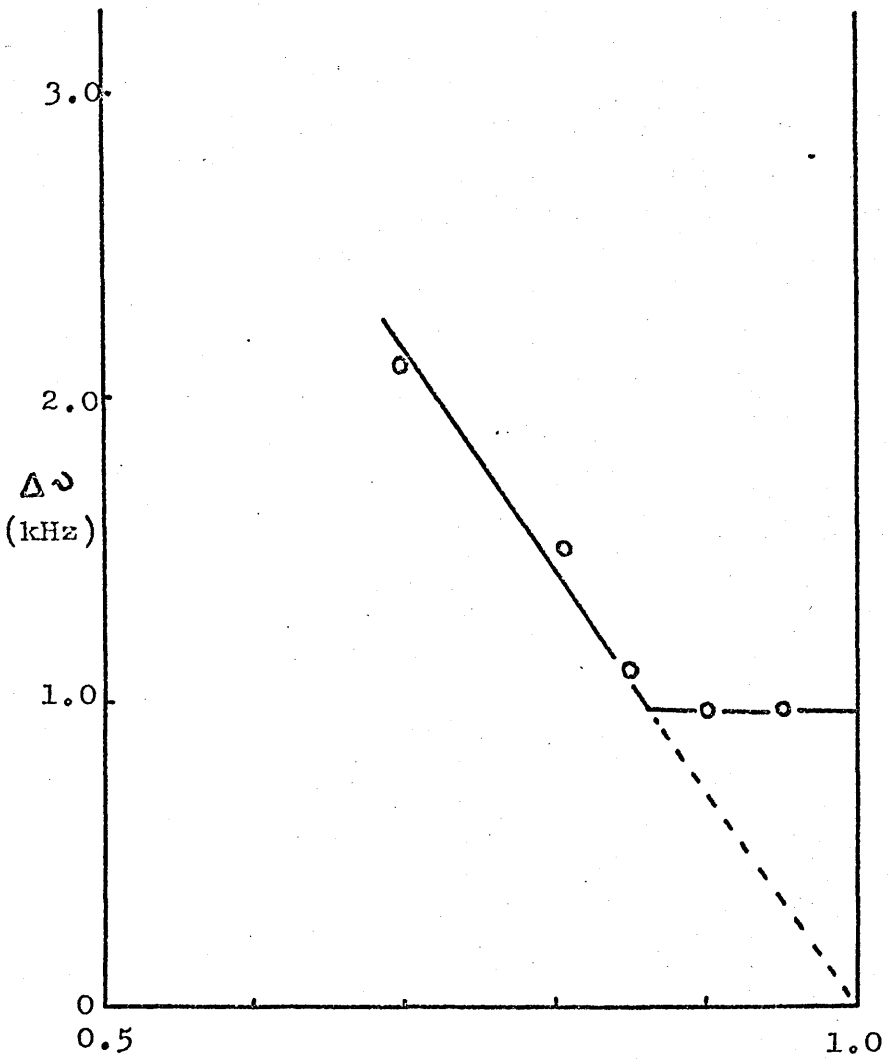

Figure 48

$\Delta\nu$ vs. X_{D_2O} for neat phase and dispersion of MG11/D_2O

width ca. 3μT and wider lines of widths 94 $\pm$ 5, 110 $\pm$ 3, and 120 $\pm$ 5 for the three different mole fractions of water.

When the sample containing 0.77 mole fraction of water was heated up to 55°C into the viscous isotropic region the broad line disappeared leaving two principal narrow lines chemically shifted by about 3ppm.

4. <u>Octylamine/H_2O and D_2O</u>

PMR spectra have been obtained at 0°C and 25°C from neat l.c. samples of OA containing three different mole fractions of D_2O. The line-widths and second moments observed are given in table XXIII. In all spectra there was also a narrow line of width ca. 5μT. The variation of the line-widths with temperature for OA + 0.835 mole fraction of D_2O is given in table XXIV and figure 49.

A solid sample of OA + 0.843 mole fraction of D_2O at -35°C gave line-widths of 385 $\pm$ 5μT and 1230 $\pm$ 20μT whilst a sample of anhydrous octylamine, with the amine protons replaced by deuterons, at the same temperature gave a line of width 1150 $\pm$ 10μT.

A sample of OA + 0.80 mole fraction of D_2O neat phase at 23°C gave a similar DMR spectrum to those described previously for MG8/D_2O and MG11/D_2O, $\Delta\nu$ in this case being 6.76 kHz.

High resolution PMR spectra from OA/H_2O neat phase samples at 23°C were much more reproducible than the corresponding spectra obtained from MG8/H_2O samples described previously. The spectra always consisted of a single peak at ca. 4.2 ppm. the line-width decreasing with increasing water content from 40 Hz at X_{H_2O} = 0.75 to 25 Hz at X_{H_2O} = 0.92.

Relaxation times have been determined for neat l.c. samples of OA containing various mole fractions of H_2O and

Table XXIII

Line-widths and second moments for OA/D_2O neat phase.

Temperature 25°C

X_{D_2O}	Line-width (μT)	Second Moment ($10^4 \mu T^2$)
0.784	94 ± 2	0.28 ± 0.005
	214 ± 2	
0.843	87 ± 3	0.27 ± 0.005
	212 ± 2	
0.916	77 ± 2	0.255 ± 0.005
	198 ± 2	

Temperature 0°C

X_{D_2O}	Line-width (μT)	Second Moment ($10^4 \mu T^2$)
0.784	136 ± 2	0.53 ± 0.01
	280 ± 5	
0.843	125 ± 3	0.49 ± 0.02
	260 ± 3	
0.916	110 ± 3	0.47 ± 0.02
	248 ± 3	

Table XXIV

Line-widths for OA + 0.835 mole fraction of D_2O neat phase at various temperatures.

Temperature (°C)	Line-width (μT)
-28	165
	310
-22	160
	300
-16	150
	288
-10	143
	278
-5	135
	270
0	125
	263
6	120
	250
10	118
	246
15	115
	232
23	100
	213
30	70
	192

Average error in measurement is ± 3μT.

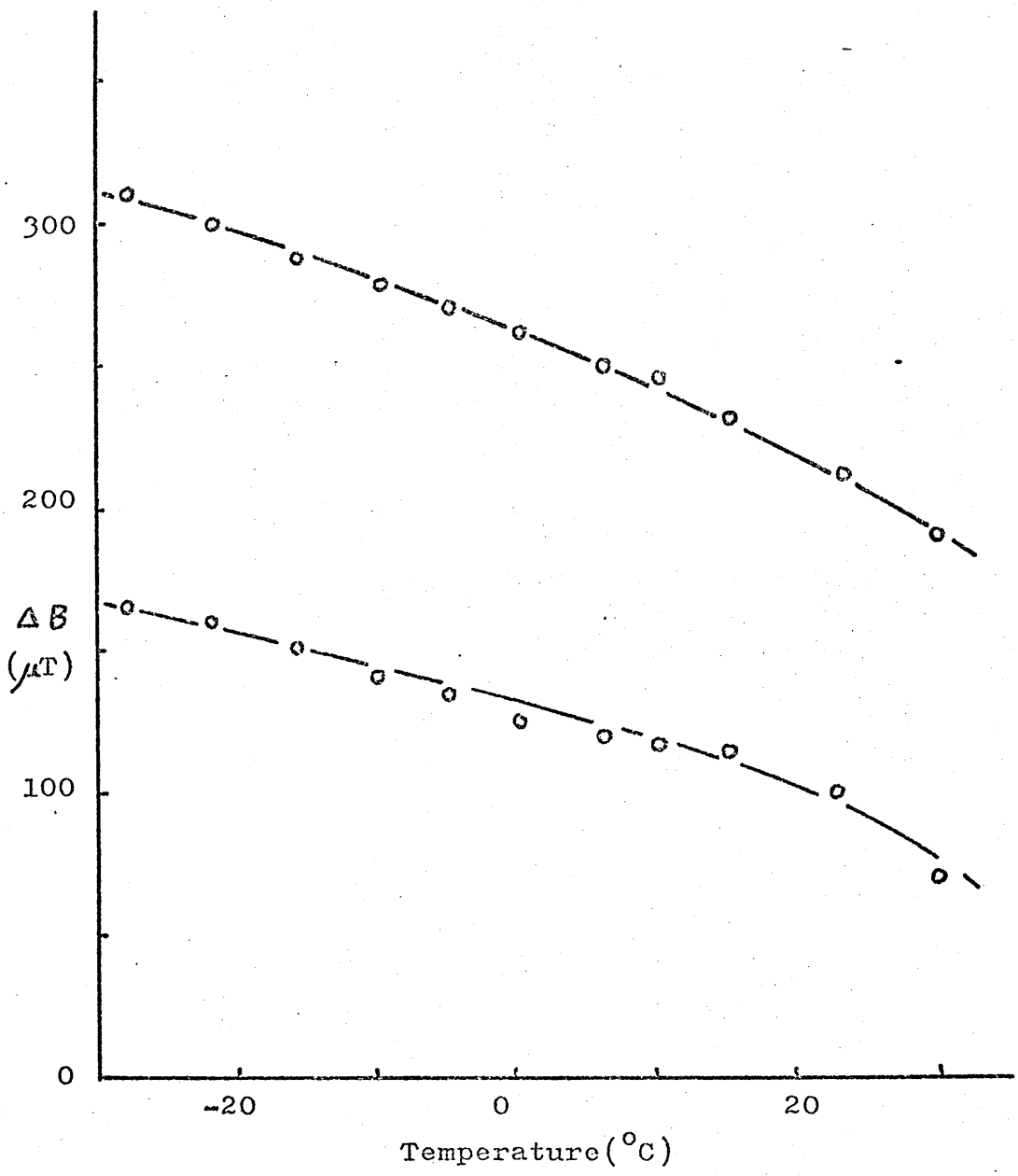

Figure 49

Line-widths vs. temperature for OA + 0.835 mole fraction of D_2O neat phase.

Table XXV

Relaxation times for OA/H_2O neat phase at 23°C.

X_{H_2O}	T_2(fast)(μs)	T_2(med.)(ms)	T_2(slow)(s)	T_1 (s)
0.8	111 (22%)	10 (58%)	0.15 (22%)	1.04
0.85	103 (24%)	8 (40%)	0.17 (24%)	1.16
0.915	90 (20%)	10.8 (32%)	0.19 (46%)	1.4
0.85 (D_2O)	126 (40%)	10 (47%)	not measurable (ca. 13%)	1.17

Figures in brackets are intensity values (± 5%).

T_2(fast)is accurate to ± 20%.

T_2(med.), T_2(slow), and T_1 are accurate to ± 10%.

D_2O, the values obtained being given in table XXV. T_2 (fast) and T_2 (medium) showed the same type of 'pulse distance dependence' that was observed for the MG8/H_2O and D_2O neat l.c. samples. This type of behaviour was also observed for the decay of the water signal.

(d) NMR of oriented systems

1. 1-mono-octanoin/H_2O and D_2O

Measurements were first made on an oriented neat l.c. sample of MG8 + 0.8 mole fraction of H_2O at 23°C. At small modulation widths a doublet was observed with a splitting (δB) from centre to centre of 22.6μT at $\theta = 0°$ and some evidence of a very weak central line as shown in figure 50a. When the modulation was increased a second doublet was observed for which δB (peak-to-peak) was 3'7μT as shown in figure 50b.

Both these doublets varied in splitting as θ was varied from 0° to 180° according to a $K(3\cos^2\theta - 1)$ relationship where K is the value of δB when $\theta = 90°$ for each pair. Experimental values for the sample MG8 + 0.66 mole fraction of H_2O are compared with calculated values in tables XXVI and XXVII, and the results shown in figures 51 and 52. The average chemical shift of the inner doublet centre was 3 ppm to low field of the outer doublet centre.

At $\theta = 55°$ only a narrow line of width ca. 5μT was observed but within $\pm$ 10° of this angle an additional peak, whose position was angularly dependent, appeared on the high field side of the spectrum as shown in figure 53. When this peak appeared the high field component of the outer doublet was always smaller than that at low field. However no complementary peak could be resolved on the low field side of the spectrum at any angle.

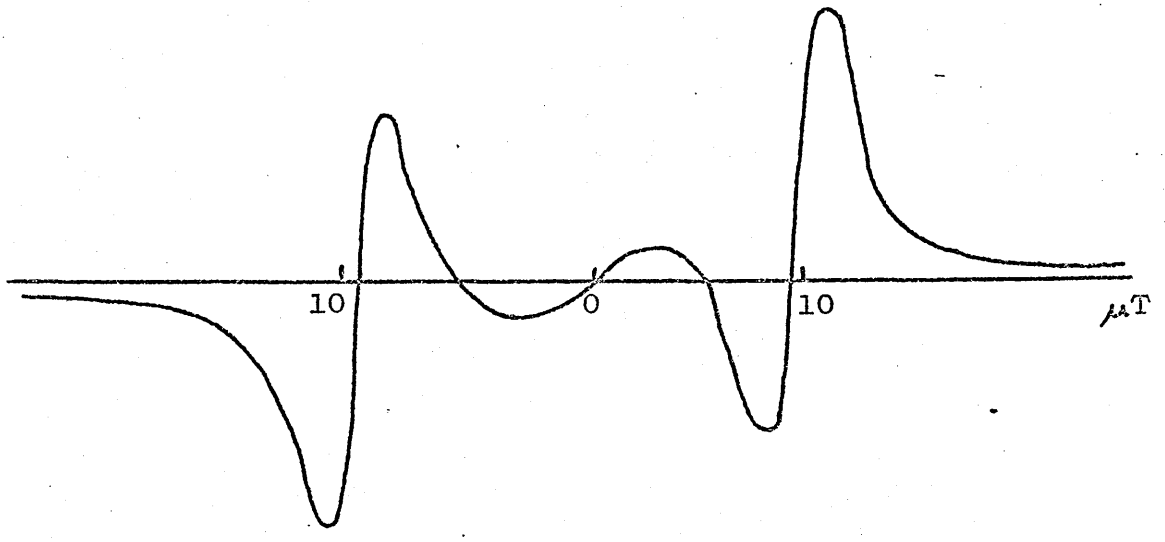

a

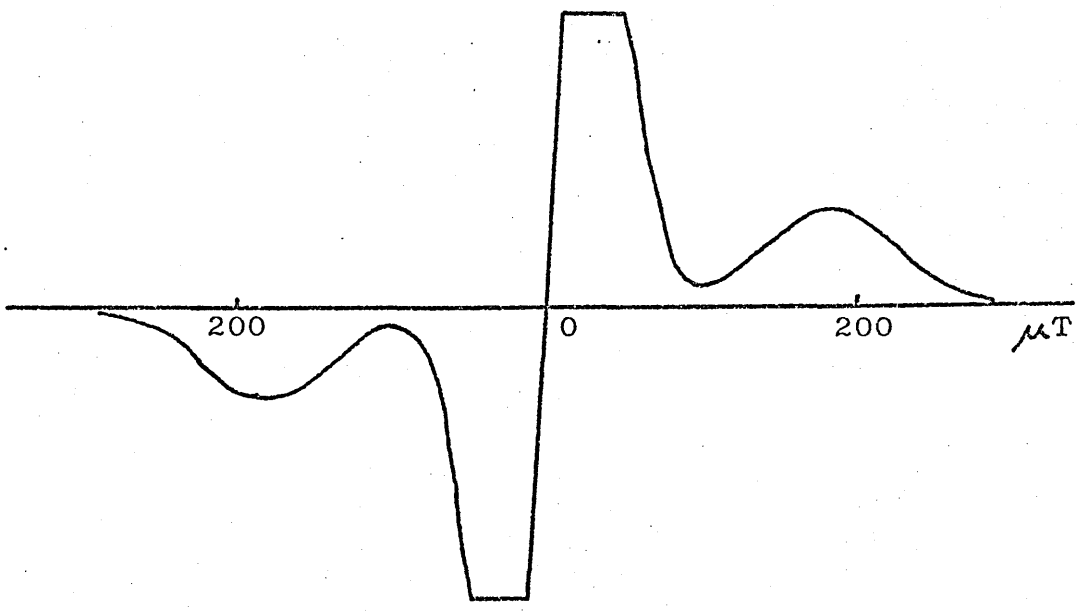

b

Figure 50

PMR spectra of oriented MG8 + o.8 mole fraction of H_2O neat phase at $\theta = 0^{o}$.

(a) inner doublet

(b) outer doublet

Table XXVI

PMR splitting for inner doublet of oriented MG8 + 0.66 mole fraction of H_2O neat phase as a function of θ at 23°C.

θ (degrees)	δB (experimental, μT)	δB (calculated, μT)
0	38.3	38.2
10	36.6	36.6
20	33.0	31.5
30	24.8	23.8
40	14.0	14.5
70	10.8	12.2
80	16.6	17.3
90	19.0	19.1
100	16.5	17.3
110	11.4	12.2
140	13.6	14.5
150	23.5	23.8
160	30.5	31.5
170	36.9	36.9
180	38.0	38.2

δB (calculated) values were obtained from δB (calculated) $= 19.1\ (3 \cos^2\theta - 1)$.

[illegible]

[illegible]

[illegible]	[illegible]	[illegible]
[illegible]	[illegible]	[illegible]
[illegible]	[illegible]	[illegible]
[illegible]	[illegible]	[illegible]
[illegible]	[illegible]	[illegible]
[illegible]	[illegible]	[illegible]
[illegible]	[illegible]	[illegible]
[illegible]	[illegible]	[illegible]
[illegible]	[illegible]	[illegible]
[illegible]	[illegible]	[illegible]
[illegible]	[illegible]	[illegible]
[illegible]	[illegible]	[illegible]
[illegible]	[illegible]	[illegible]
[illegible]	[illegible]	[illegible]
[illegible]	[illegible]	[illegible]
[illegible]	[illegible]	[illegible]
[illegible]	[illegible]	[illegible]
[illegible]	[illegible]	[illegible]

[illegible]

Table XXVII

PMR splitting for outer doublet of oriented MG8 + 0.66 mole fraction of H_2O neat phase as a function of θ at 23°C.

θ (degrees)	δB (experimental, μT)	δB (calculated, μT)
0	370	372
10	360	355
20	310	307
30	245	233
40	131	141
60	48	47
70	120	120
90	184	186
110	123	120
120	49	47
140	133	141
150	240	233
160	320	307
170	360	355
180	376	372

δB (calculated) values were obtained from δB (calculated) $= 186\ (3\cos^2\theta - 1)$.

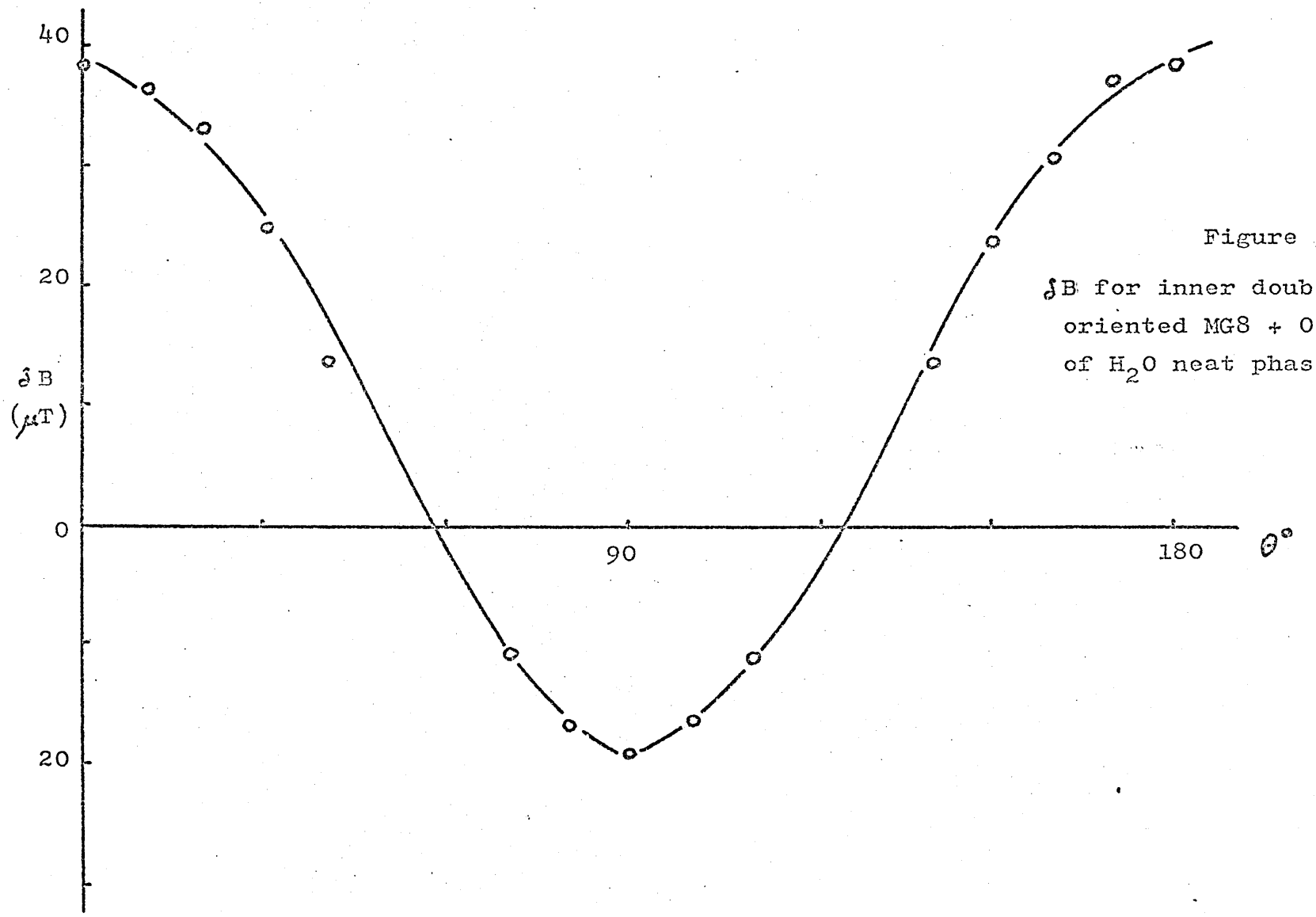

Figure 51

δB for inner doublet vs. θ for oriented MG8 + 0.66 mole fractio of H_2O neat phase

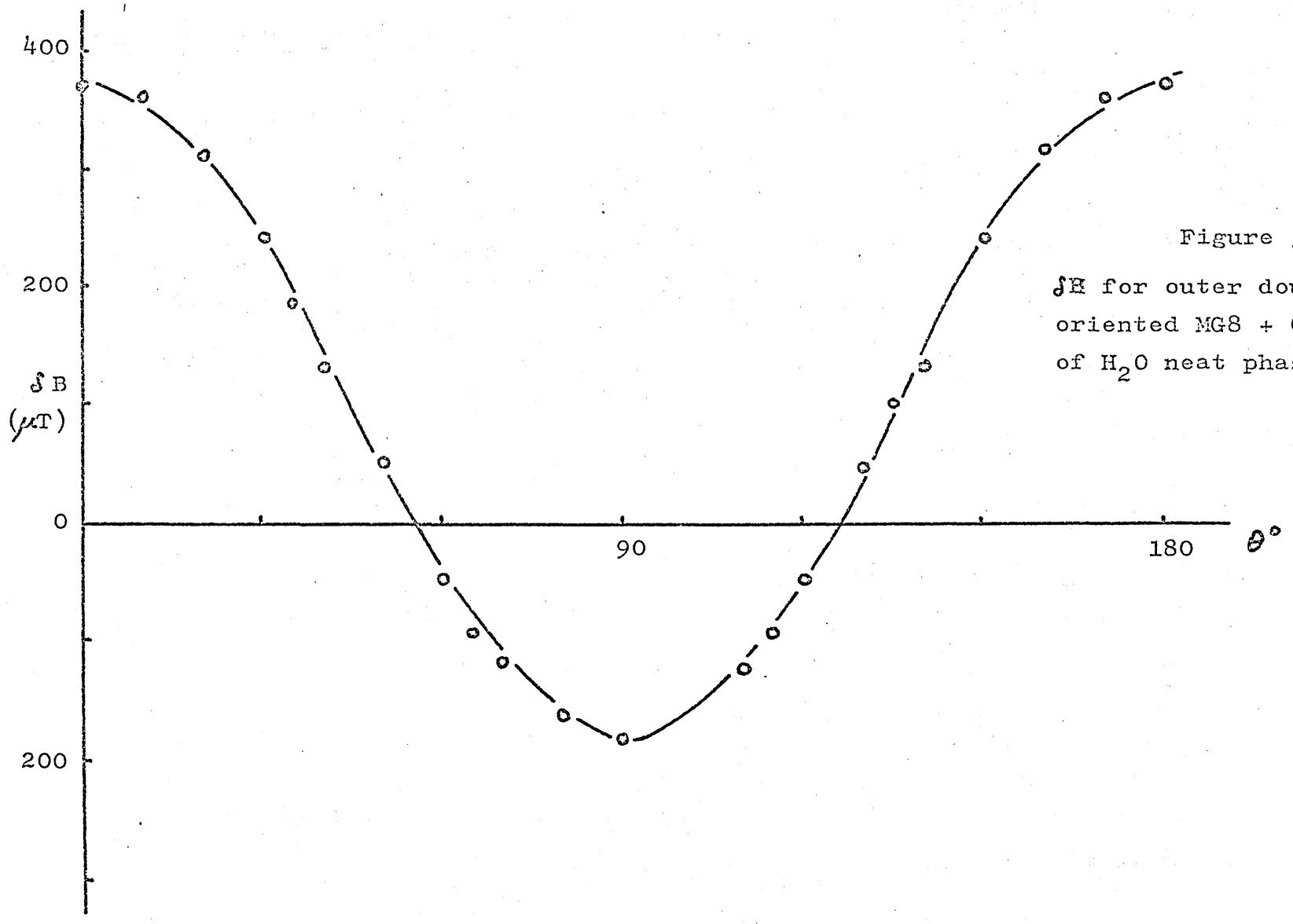

Figure 52

δB for outer doublet vs. θ for oriented MG8 + 0.66 mole fract of H_2O neat phase

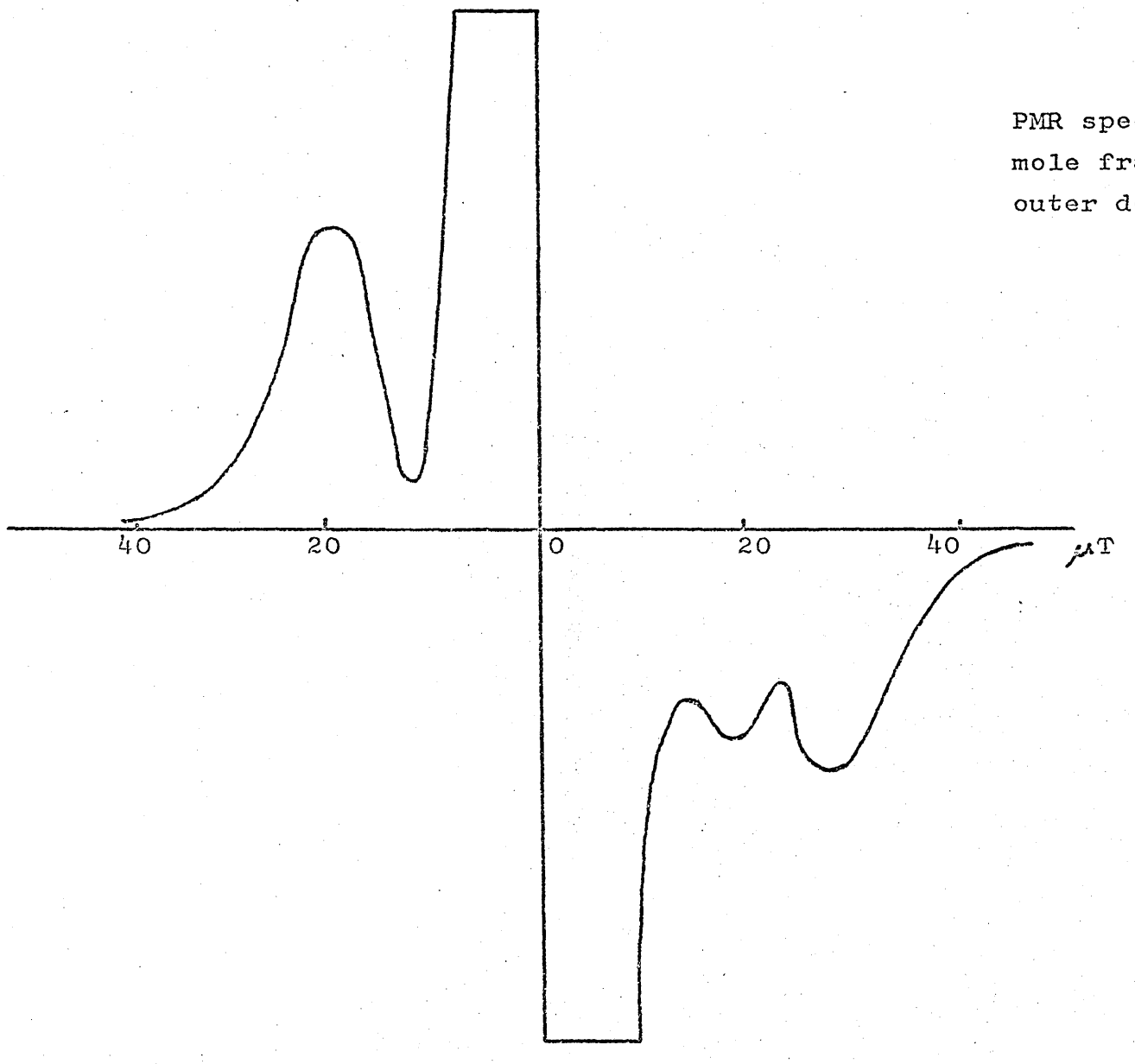

Figure 53

PMR spectrum from oriented MG8 + 0.8 mole fraction of H_2O neat phase showing outer doublet + high field line at $\theta = 50^{\circ}$

The values of δB at $\theta = 0^{\circ}$ for both doublets were measured for a number of different compositions within the neat l.c. region and are given in tables XXVIII and XXIX.

The additional peak on the high field side was assumed to be one component of a middle doublet whose other component was superimposed on the low field component of the outer doublet. Approximate splittings at $\theta = 0^{\circ}$ and a temperature of $16^{\circ}C$ were calculated for this middle doublet by multiplying the splittings at 50° by the appropriate factor $(3 \cos^2 0^{\circ} - 1)/(3 \cos^2 50^{\circ} - 1) = 8$, and are given in table XXX.

Table XXX

X_{H_2O}	δB (μT, $\theta = 0^{\circ}$)
0.66	310
0.75	340
0.80	330

The error in measuring δB for the middle doublet is probably ca. $\pm 20 \mu T$.

For samples made up using D_2O and MG8, deuterated at the hydroxyl groups, the inner doublet was not observed whilst the values of the middle and outer doublets remained as before.

An oriented sample made up with just water sandwiched between the glass slides gave only a single narrow line at all values of θ and modulation width.

Figure 54 shows that δB at $\theta = 0^{\circ}$ for the inner doublet decreased linearly with increasing mole fraction of water, X_{H_2O}, over an appreciable concentration range and the extrapolated linear portion of the curve cuts the mole

Table XXVIII

PMR splitting for inner doublet of oriented MG8/H_2O neat phase at $\theta = 0^{\circ}$ and $23^{\circ}C$.

X_{H_2O}	δB (μT)
0.66	38.3
0.75	28.8
0.80	22.6
0.86	16.3
0.89	8.8

Measurements of δB accurate to $\pm$ 0.5μT.

Table XXIX

PMR splitting for outer doublet of oriented MG8/H_2O neat phase at $\theta = 0^{\circ}$ and $16^{\circ}C$.

X_{H_2O}	δB (μT)
0.67	393
0.75	395
0.80	390
0.86	383
0.90	388

Measurement of δB accurate to $\pm 5 \mu T$.

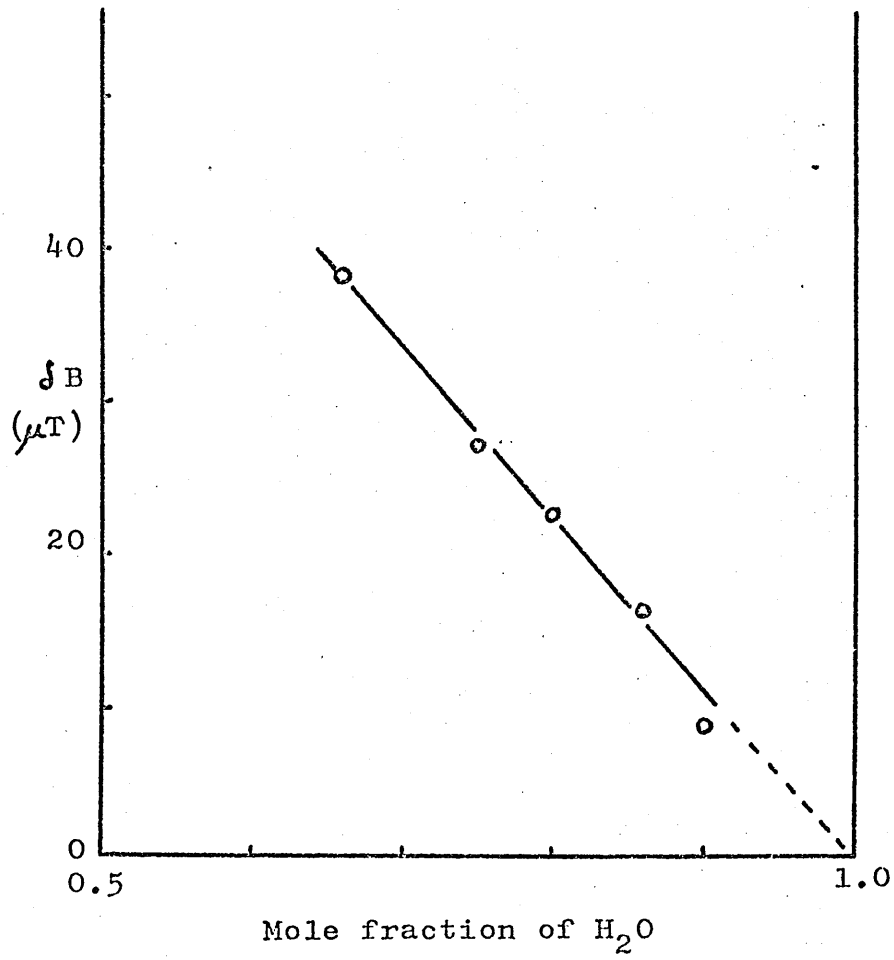

Figure 54

δB vs. X_{H_2O} for inner doublet from oriented MG8/H_2O neat phase at $\theta = 0^\circ$

fraction axis at the composition of pure water.

For the outer doublet δB at $\theta = 0^{\circ}$ also varies with X_{H_2O} but the variation is only slightly greater than the experimental error.

The effect of temperature on these spectra was investigated for a sample of MG8 containing 0.8 mole fraction of H_2O. Figure 55 and tables XXXI and XXXII show that δB at $\theta = 0^{\circ}$ for the inner doublet is virtually independent of temperature, whilst for the outer doublet δB at $\theta = 0^{\circ}$ decreases with increasing temperature. Although δB at $\theta = 0^{\circ}$ is independent of temperature for the inner doublet, the value of ΔB, the line-width of the doublet components, decreased with decreasing temperature from 7.6μT at 37°C to 4.1μT at -27°C where the l.c. phase is metastable.

When the temperature was reduced below -27°C the sample became solid and the doublets disappeared. On raising the temperature again, first a narrow water line appeared around 0°C and then the three doublets reappeared above 12°C, the penetration temperature for MG8. The values of δB for the three doublets at corresponding temperatures on the cooling and heating runs were the same.

No additional lines appeared in the PMR spectrum with increasing temperature until the l.c. melting point was reached when all three doublets disappeared leaving a three line high resolution PMR spectrum. The two outer lines were both chemically shifted 2.5 ppm from the centre line and the line to high field was the most intense whilst the line to the low field was weakest.

The decay of transverse magnetisation following a 2μs 90° pulse has also been observed for an oriented neat l.c. sample of MG8 + 0.8 mole fraction of H_2O at 25°C and $\theta = 0^{\circ}$,

Table XXXI

PMR splitting for inner doublet of oriented MG8 + 0.8 mole fraction of H_2O neat phase at $\theta = 0^\circ$ and various temperatures.

Temperature ($^\circ$C)	δB (μT)
-27	20.5
-16	21.0
0	21.5
8	22.6
23	22.6
31	22.0
37	22.8
18 (after sample had been solid at -30°)	22.6

Table XXXII

PMR splitting for outer doublet of oriented MG8 + 0.8 mole fraction of H_2O neat phase at $\theta = 0^{\circ}$ and various temperatures.

Temperature ($^{\circ}C$)	δB (μT)
-15	465
-5	448
2.5	430
14	405
21	385
28	365
31	348
37	332

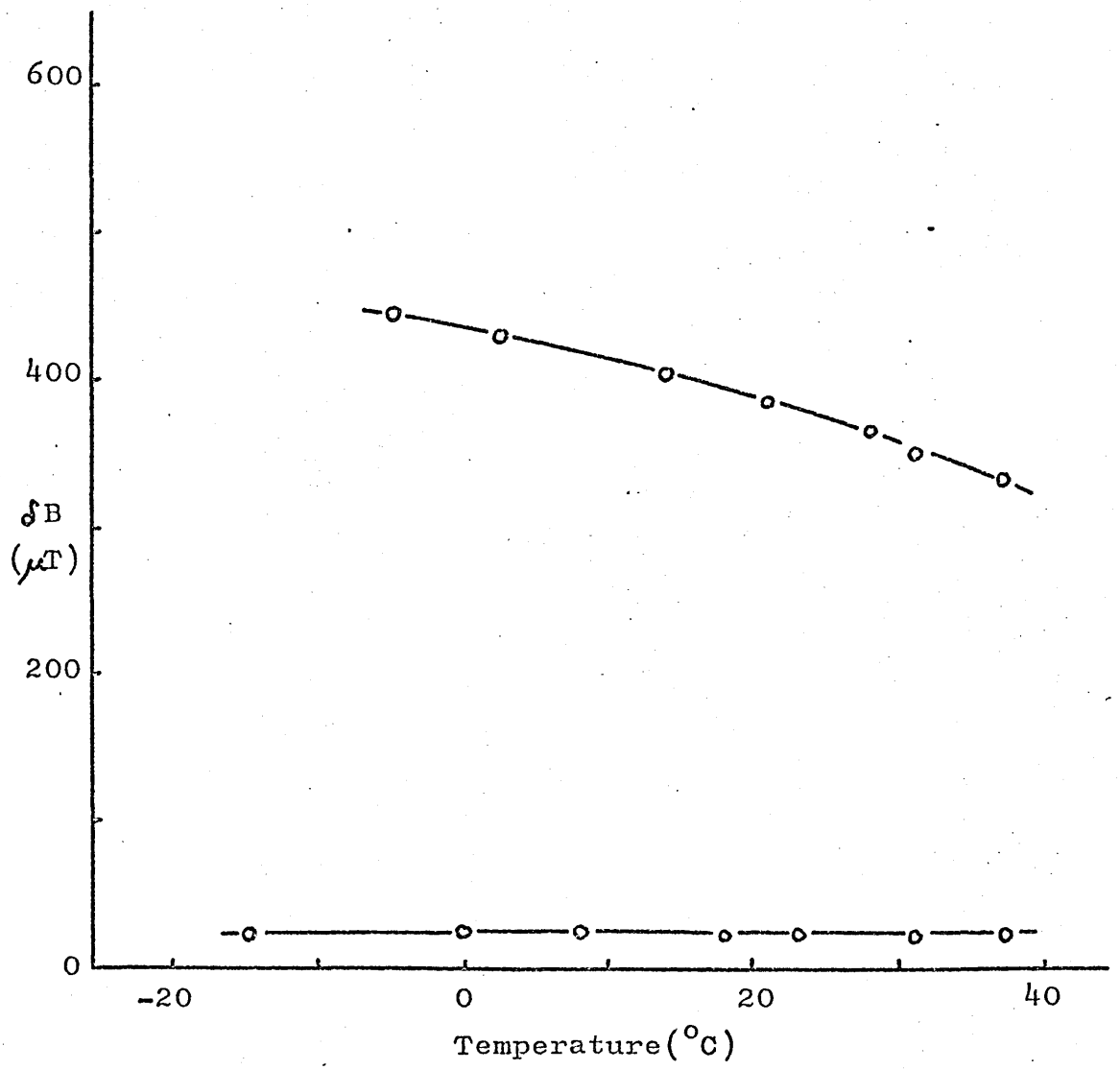

Figure 55

Variation of δB for inner and outer doublets with temperature for oriented MG8 + 0.8 mole fraction of H_2O neat phase at $\theta = 0^\circ$

55°, and 90°. The observed decays are shown in figure 56 and the peak to peak separations from the modulated decays are given in table XXXIII.

Table XXXIII

θ (degrees)	Separation (ms)
0	ca. 0.1 and 0.17
90	ca. 0.2 and 0.35

The decays were also observed using a Carr-Purcell sequence and found to be similar to those described previously with no significant dependence on τ. When the Meiboom-Gill modification of the Carr-Purcell sequence was used the time constant for the decay depended on τ and this indicated that the time constant contained a contribution from $T_{1\rho}$ which was largest at short values of τ.

T_1 was obtained using a 90° saturating pulse and measuring the amplitude of the free induction decay after a second 90° pulse as a function of the spacing between the two pulses. A single exponential decay was observed at all angles and the values of T_1 at $\theta = 0^{\circ}$ and 55° were 0.3s and 0.4s respectively.

2. <u>1-monoundecanoin/H_2O and D_2O</u>

All oriented samples of MG11/water neat phase between glass slides were contained in the NMR tubes between PTFE plugs to prevent loss of water occurring at temperatures significantly higher than room temperature.

PMR spectra have been obtained for these oriented neat phase samples of MG11 containing various mole fractions of

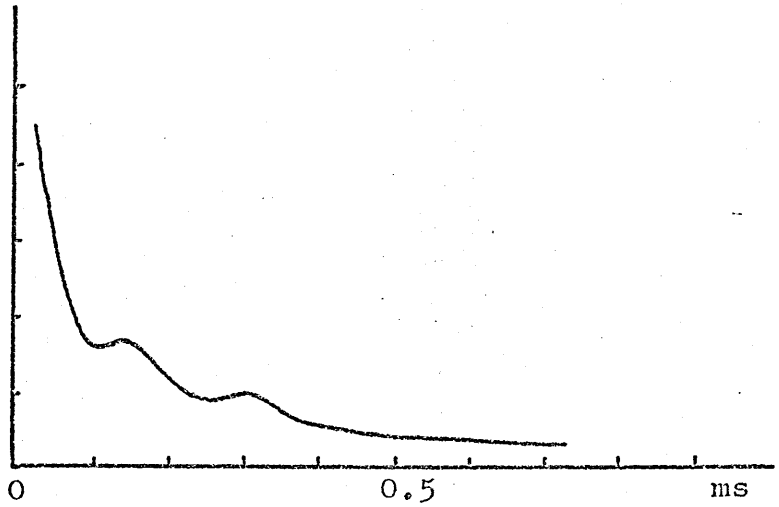

(a)

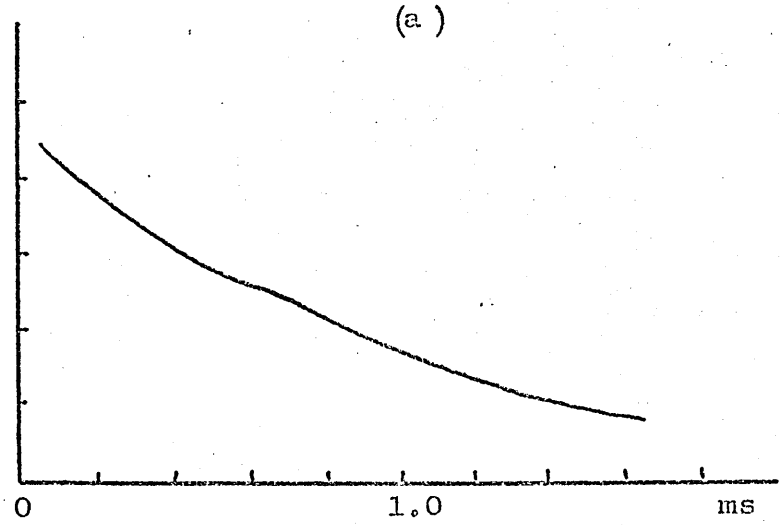

(b)

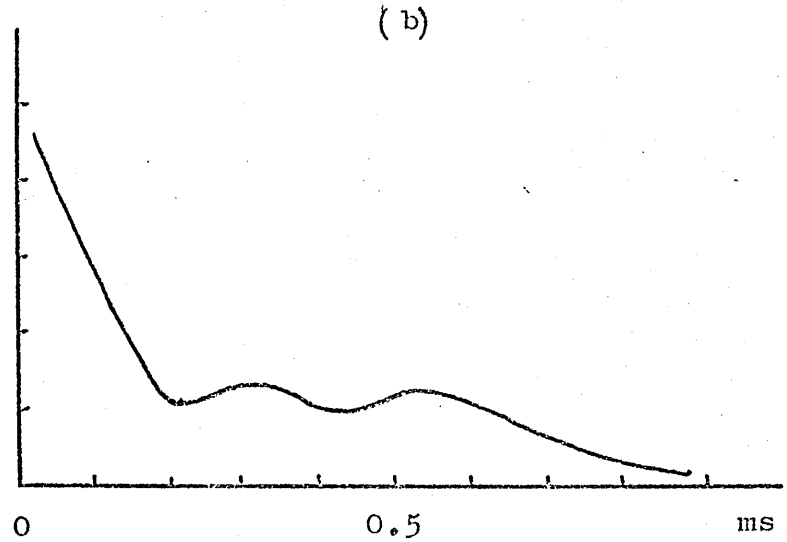

(c)

Figure 56

Decay of transverse magnetisation observed from oriented MG8 + 0.8 mole fraction of H_2O neat phase

(a) $\theta = 0^\circ$

(b) $\theta = 55^\circ$

(c) $\theta = 90^\circ$

water and three doublets have been observed whose splittings have the same angular dependence as described previously. The variation of $\int B$ values with X_{H_2O} for $\theta = 0^\circ$ are given in tables XXXIV and XXXV and figures 57 and 58. The inner doublet was again absent in the spectra of samples made up using D_2O and MG11 deuterated at the hydroxyl groups. The middle and outer doublets were clearly resolvable at $\theta = 0^\circ$ as shown in figure 59, but at angles between 40° and 70° the two doublet components on the low field side coalesced to give a single peak whose intensity was greater than either of the two upfield doublet components which were still resolvable. The resultant spectra were similar to those observed for oriented samples of MG8/H_2O neat phase also at angles between 40° and 70°.

In addition to the three doublets, in all spectra there was also a narrow line slightly upfield of the centre of the inner doublet. The width of this line at 45°C was ca. 8μT while the width of the component lines of the inner doublet was ca. 5μT. These component lines became narrower at lower temperatures and broader at higher temperatures.

The splitting of the inner doublet was invariant with temperature over the range 0 - 60°C. The variation of the splittings of the two other doublets with temperature for four different compositions is given in tables XXXVI - XXXIX and figures 60 - 63. At the neat l.c. melting points the doublets disappeared leaving a three line spectrum similar to that described for MG8/H_2O samples.

The derivative spectra at 21°C of the middle and outer doublets for oriented neat l.c. samples of MG11 containing different mole fractions of H_2O were integrated manually and

Table XXXIV

PMR splitting for inner doublet of oriented MG11/H_2O neat phase at $\theta = 0^{\circ}$ and $45^{\circ}C$.

X_{H_2O}	δB (μT)
0.51	58.0
0.58	49.0
0.64	42.5
0.72	33.0
0.80	22.5
0.85	18.5

Measurement of δB accurate to $\pm$ 0.5μT.

Table XXXV

PMR splittings for middle and outer doublets of oriented MG11/H_2O neat phase at $\theta = 0^\circ$ and $45^\circ C$.

X_{H_2O}	δB (μT)
0.43	233
	344
0.51	254
	365
0.58	260
	380
0.64	274
	410
0.72	291
	430
0.80	311
	440
0.85	319
	453

Measurement of δB accurate to $\pm$ 5μT.

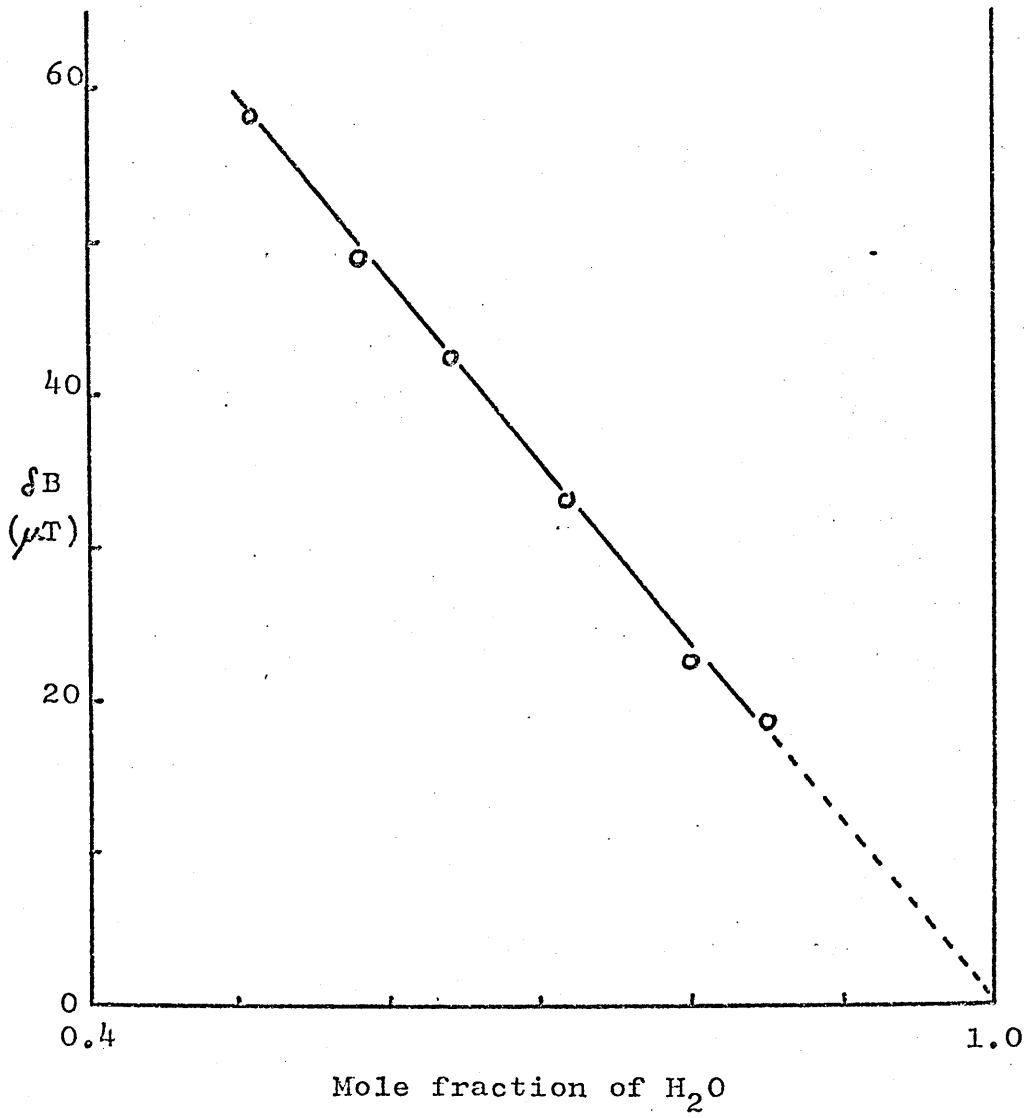

Figure 57

δB vs. X_{H_2O} for inner doublet from oriented MG11/H_2O neat phase at $\theta = 0^\circ$

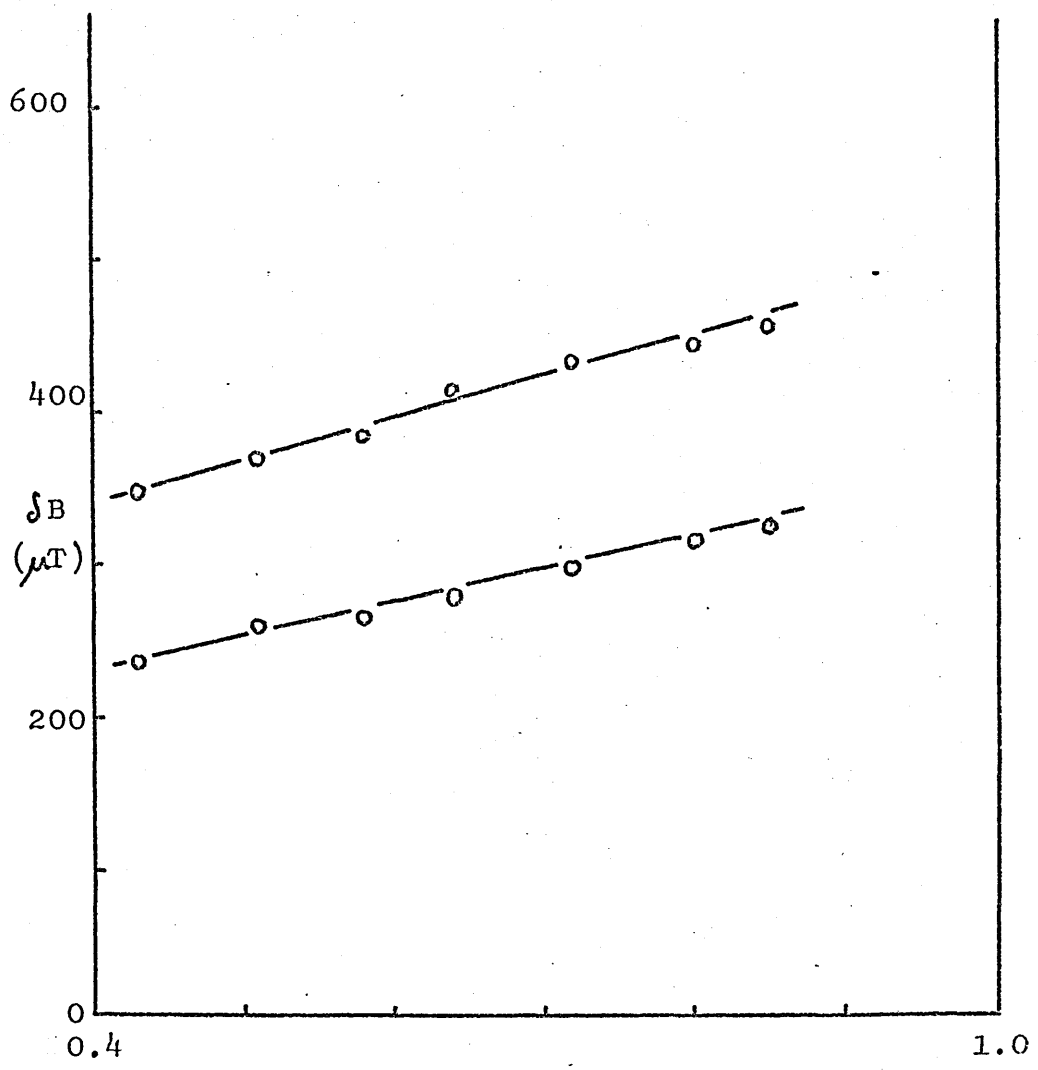

Figure 58

δB vs. X_{H_2O} for middle and outer doublets from oriented MG11/H_2O neat phase at $\theta = 0^o$

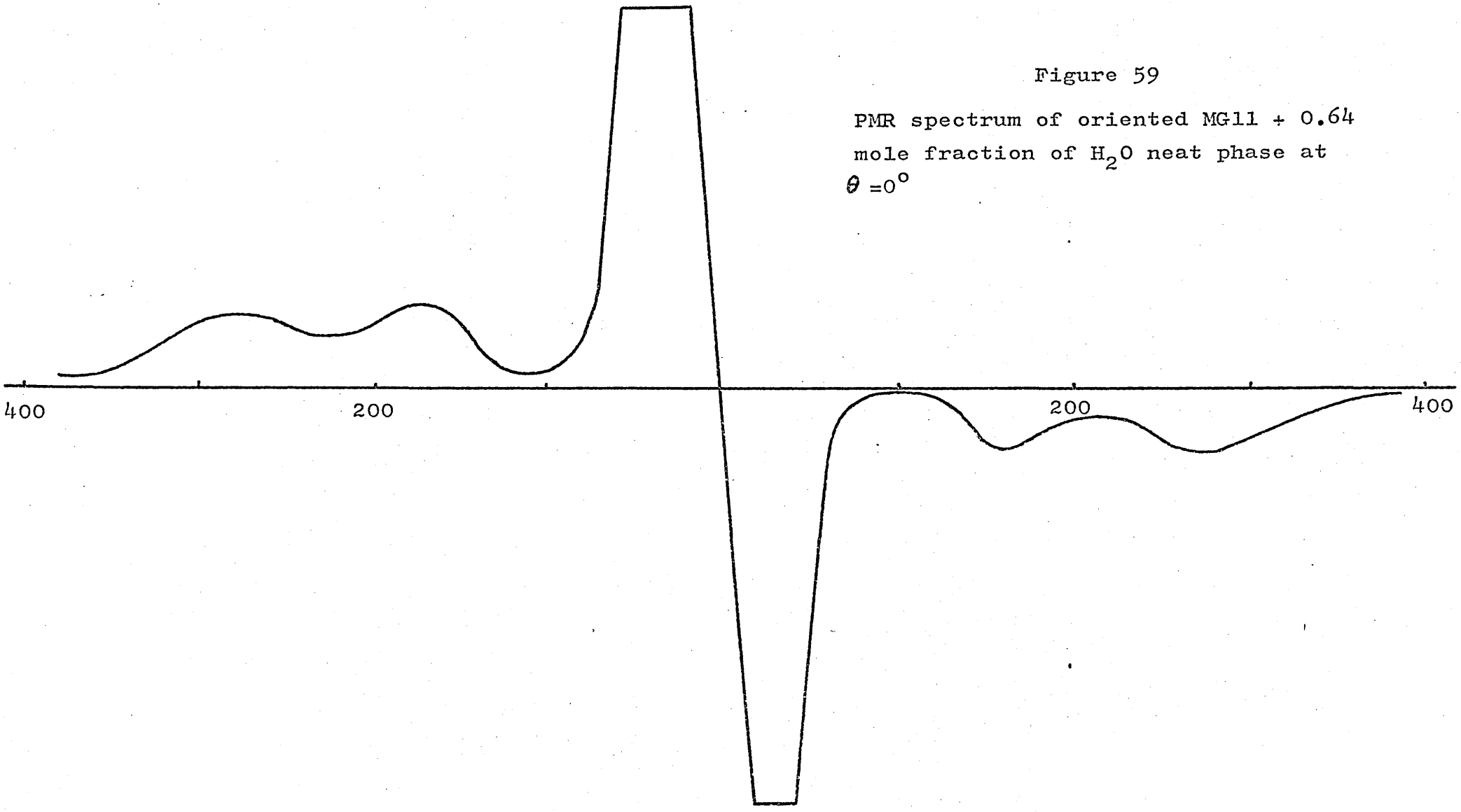

Figure 59

PMR spectrum of oriented MG11 + 0.64 mole fraction of H_2O neat phase at $\theta = 0^{\circ}$

Table XXXVI

PMR splittings for middle and outer doublets of oriented MG11 + 0.64 mole fraction of H_2O at $\theta = 0^o$ and various temperatures.

Temperature (^oC)	δB (μT)
21	378
	652
23	375
	625
30	343
	560
37	323
	515
45	274
	410
55	244
	340
62	220
	282

Table XXXVII

PMR splittings for middle and outer doublets of oriented MG11 + 0.72 mole fraction of H_2O neat phase at $\theta = 0^\circ$ and various temperatures.

Temperature ($^\circ$C)	δB (μT)
22	369
	632
29	342
	575
35	328
	527
40	312
	481
45	291
	430
50	278
	385
56	250
	340
65	208
	260

Table XXXVIII

PMR splittings for middle and outer doublets of oriented MG11 + 0.80 mole fraction of H_2O neat phase at $\theta = 0^\circ$ and various temperatures.

Temperature ($^\circ$C)	δB (μT)
21	370
	579
27	350
	540
32	340
	510
37	325
	480
45	311
	440
55	273
	378
65	245
	322

Table XXXIX

PMR splittings for middle and outer doublets of oriented MG11 + 0.85 mole fraction of H_2O at $\theta = 0^\circ$ and various temperatures.

Temperature ($^\circ$C)	δB (μT)
24	343
	538
29	340
	518
35	332
	490
40	323
	476
45	319
	453
50	305
	437
54	301
	421
60	285
	395
65	280
	371
75	262
	335

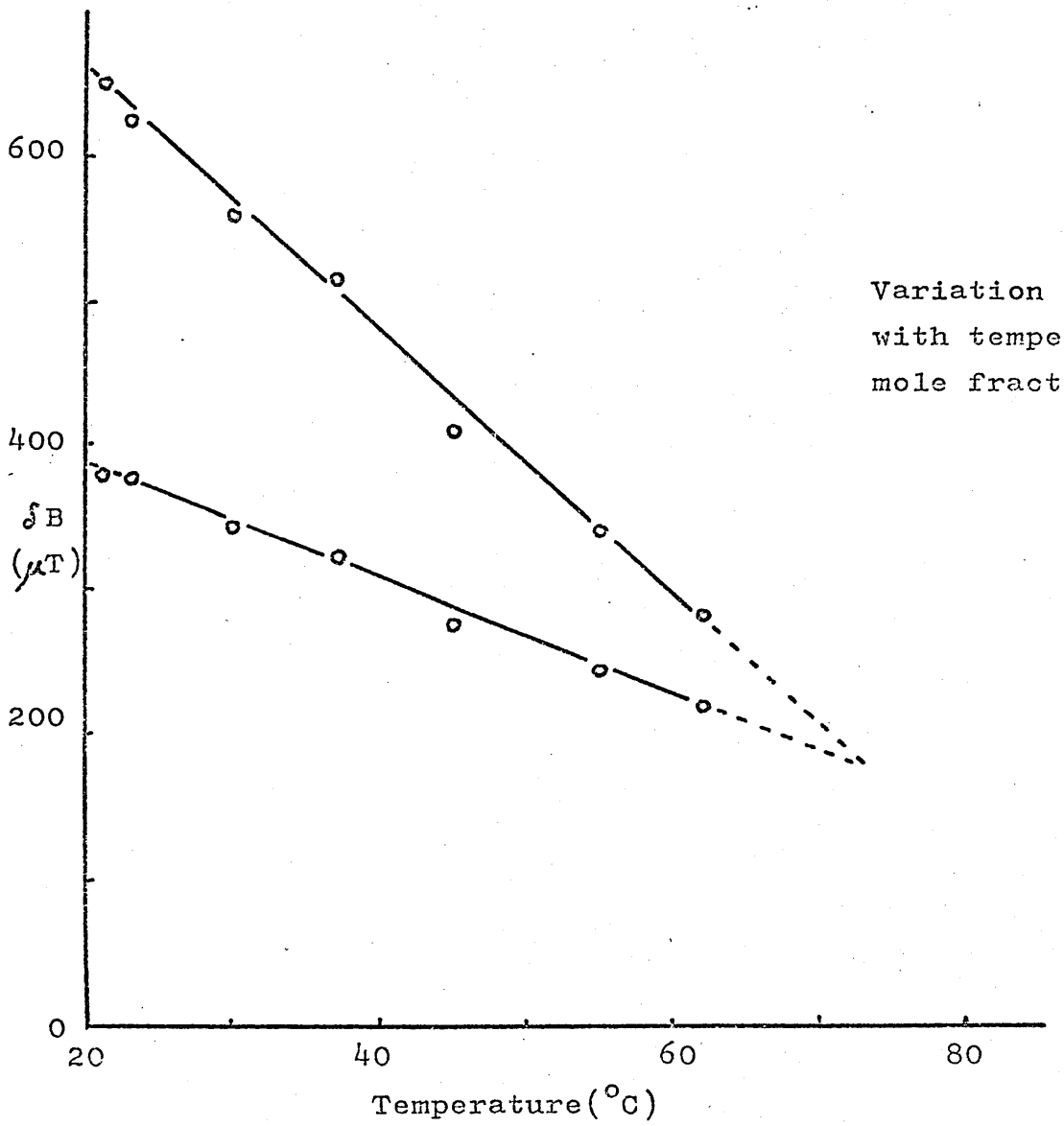

Figure 60

Variation of δB for middle and outer doublets with temperature for oriented MG11 + 0.64 mole fraction of H_2O neat phase at $\theta = 0^\circ$

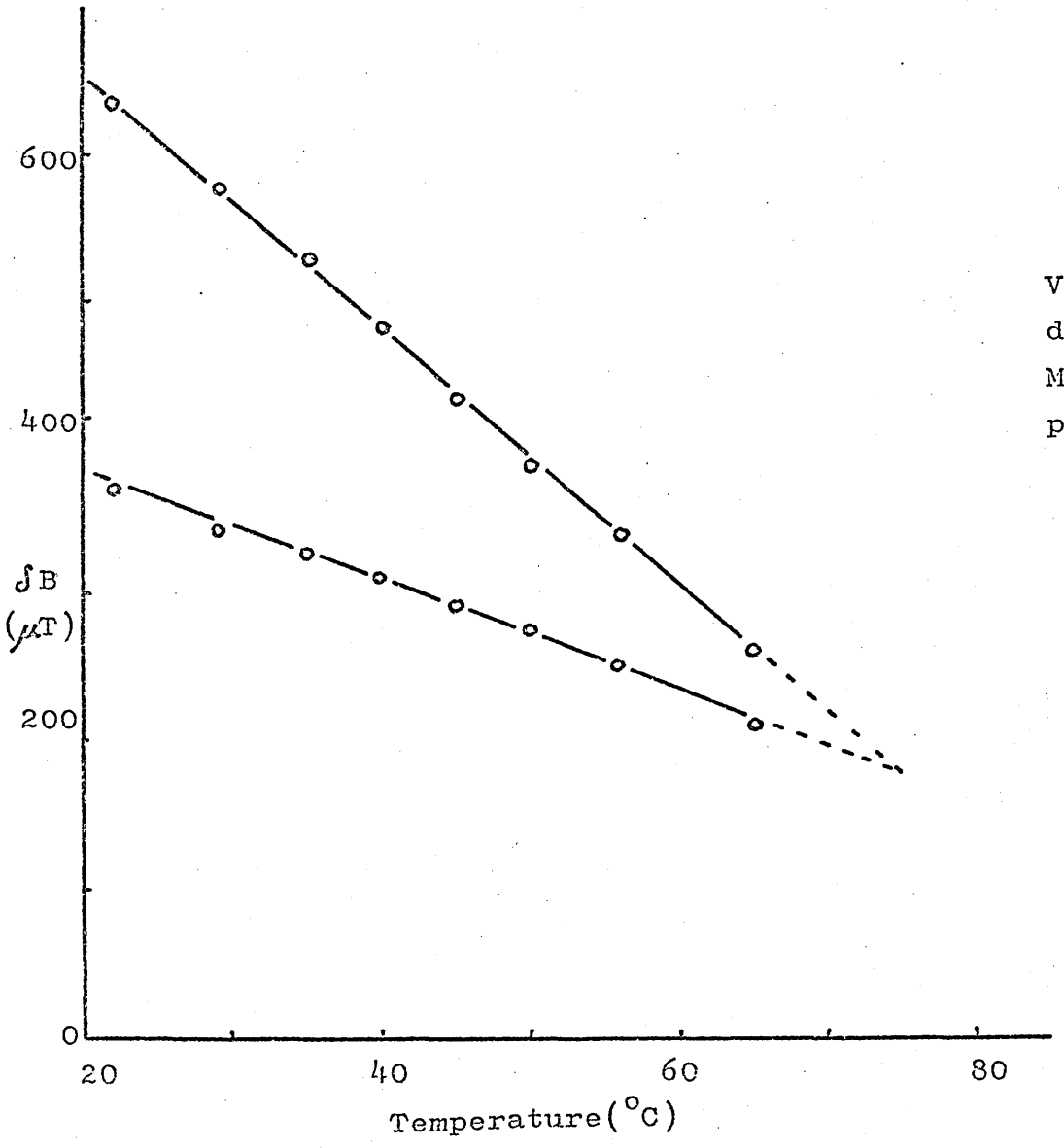

Figure 61

Variation of δB for middle and outer doublets with temperature for oriented MG11 + 0.72 mole fraction of H_2O neat phase at $\theta = 0^{\circ}$

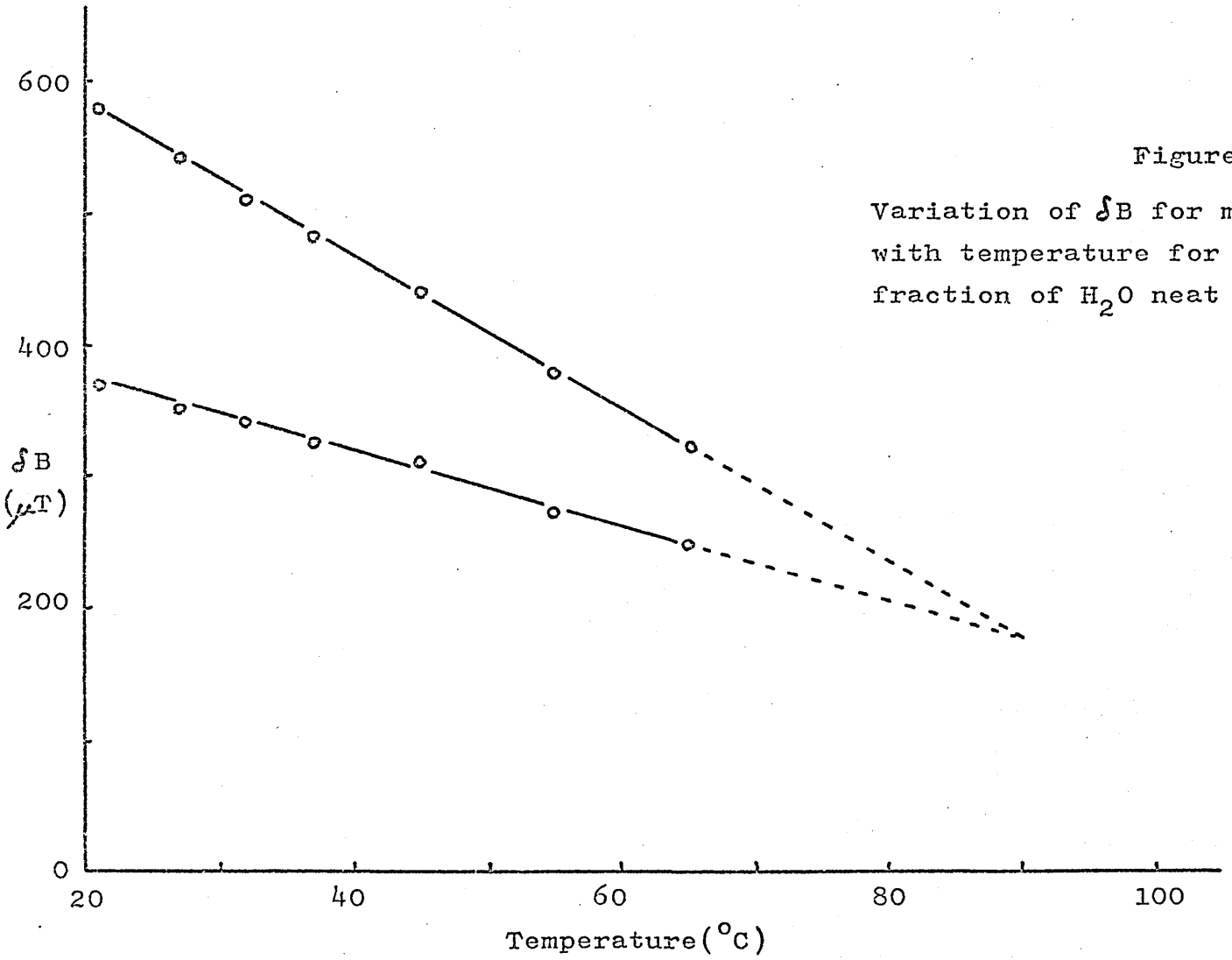

Figure 62

Variation of δB for middle and outer doublets with temperature for oriented MG11 + 0.8 mole fraction of H_2O neat phase at $\theta = 0^\circ$

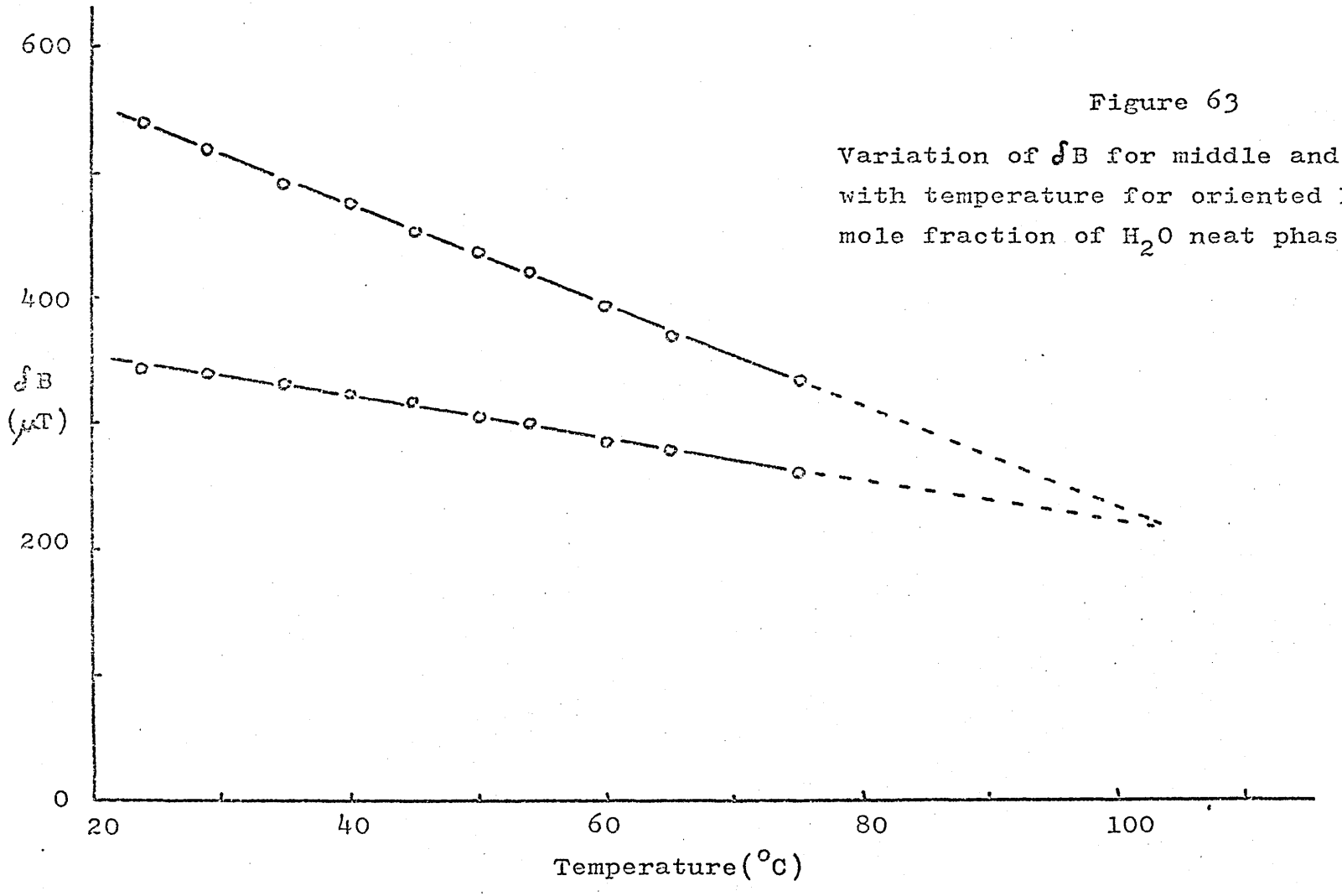

Figure 63

Variation of δB for middle and outer doublets with temperature for oriented MG11 + 0.85 mole fraction of H_2O neat phase at $\theta = 0^\circ$

two pairs of Gaussian lines symmetrical about the centre fitted to the line-shape obtained. Figure 64 shows the result for MG11 + 0.80 mole fraction of H_2O. The percentage of protons contributing to the outer doublet varied between 25% and 50%, there being no significant correlation between percentage and l.c. composition. This range of values is due to the fact that several different sets of two pairs of Gaussian lines would fit the derived line-shape reasonably well depending on the width and intensity given to each pair, whilst keeping the centre-to-centre splittings for each doublet within a range of values consistent with the experimental line-shape.

3. <u>1-mono-olein/H_2O</u>

PMR spectra of oriented neat l.c. samples of MG//18/H_2O at 25°C consisted of three doublets, whose angular dependence was similar to that described previously, and a very weak central line. The doublet splittings at $\theta = 0°$ and a temperature of 25°C for three different mole fractions of H_2O are given in table XL.

Table XL

MG//18 + X_{H_2O}	δB (μT)		
0.45	30.5	82	260
0.66	25	100	297
0.77	20.5	124	363

δB for the inner doublet was independent of temperature over the range 10 - 50°C, the only change being a broadening of the component lines with increasing temperature. The variation of the δB values for the middle and outer doublets with temperature for samples containing 0.66 and 0.77 mole

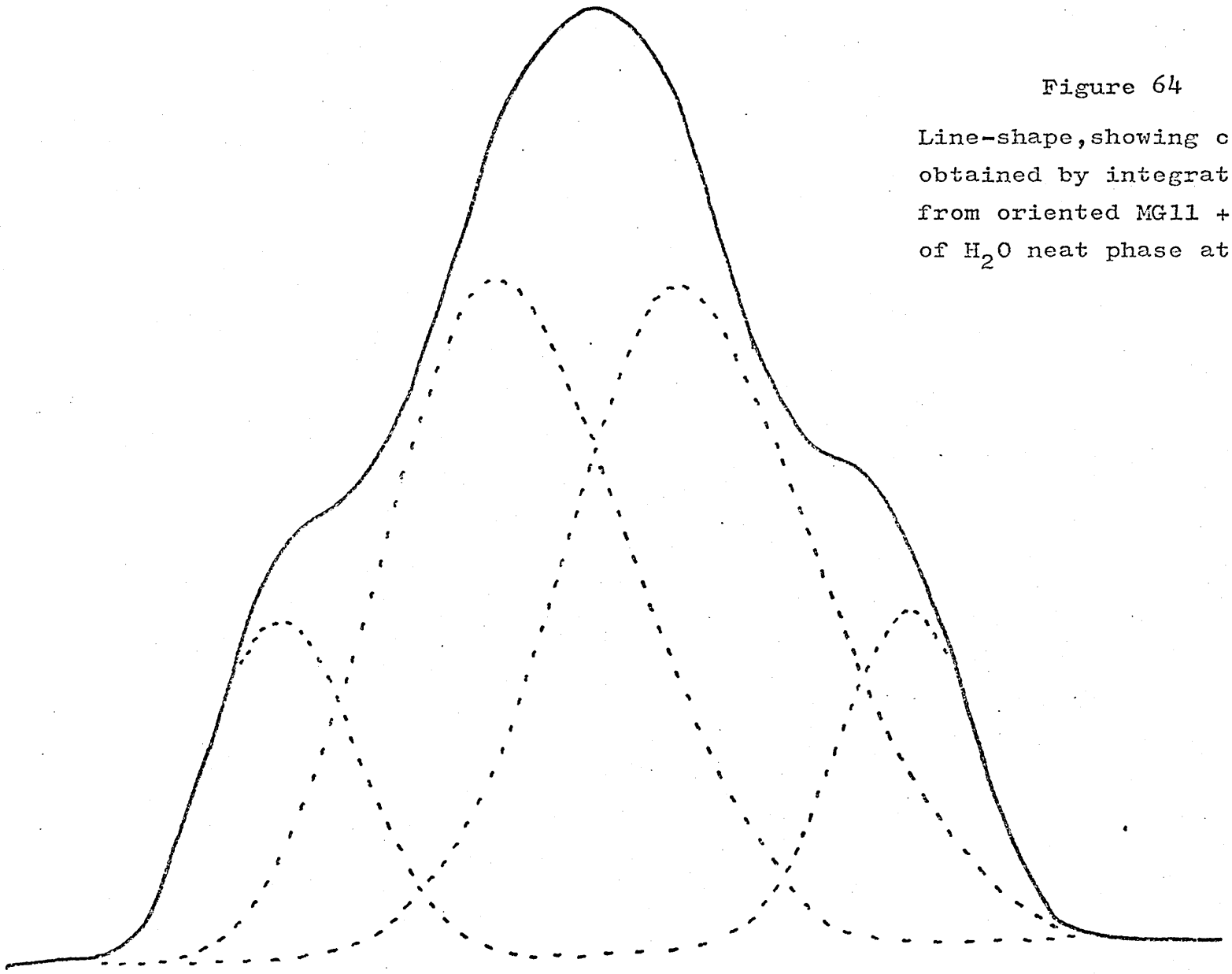

Figure 64

Line-shape, showing component doublets, obtained by integrating PMR spectrum from oriented MG11 + 0.8 mole fraction of H_2O neat phase at $\theta = 0^\circ$

fractions of H_2O is shown in tables XLI and XLII.

When an oriented sample of MG//18 + 0.77 mole fraction of H_2O was heated to 55°C into the viscous isotropic region all three doublets disappeared leaving only two narrow high resolution lines chemically shifted by about 2.5 ppm. Altering the angle θ had no effect on this spectrum. When the sample was allowed to cool back into the l.c. region all three doublets reappeared with splittings identical to those recorded previously.

4. <u>Octylamine/H_2O and D_2O</u>

The PMR spectra of oriented neat l.c. samples of OA containing H_2O or D_2O consisted of two doublets and a central line with high resolution structure. The doublets had a similar angular dependence to that described previously, and the values of δB at $\theta = 0°$ and a temperature of 20°C for three different mole fractions of H_2O are given in table XLIII

Table XLIII

OA + X_{H_2O}	δB (μT)	
0.8	240	540
0.85	236	540
0.92	225	520

Accuracy of measurement of $\delta B \pm 5\mu T$.

Table XLI

PMR splittings for middle and outer doublets of oriented MG//18 + 0.66 mole fraction of H_2O neat phase at $\theta = 0^\circ$ and various temperatures.

Temperature ($^\circ$C)	δB (μT)
10	145
	370
25	100
	297
43	not measurable
	190

Table XLII

PMR splittings for middle and outer doublets of oriented MG//18 + 0.77 mole fraction of H_2O at $\theta = 0^\circ$ and various temperatures.

Temperature ($^\circ$C)	δ B (μT)
10	235
	475
25	124
	363
33	66
	225

The variation of the splittings with temperature for OA + 0.85 mole fraction of H_2O is given in table XLIV and figure 65.

Derivative spectra of oriented neat l.c. samples of OA containing 0.8, 0.85, and 0.92 mole fractions of H_2O at various temperatures were integrated manually and curve fitting carried out as before. The same difficulties were experienced as described for MG11/H_2O spectra and the percentage of protons contributing to the outer doublet was found to vary between 40% and 60% correlating very little with mole fraction of H_2O or temperature.

The decay of transverse magnetisation has also been observed for an oriented neat l.c. sample of OA + 0.85 mole fraction of H_2O at a temperature of 25°C and $\theta = 0°$, 55°, and 90° as described previously for MG8/H_2O samples. The observed decays are shown in figure 66.and the peak to peak separations from the modulated decays are given in table XLV.

Table XLV

θ (degrees)	Separation (ms)
0	ca. 0.1
90	ca. 0.2

Table XLIV

PMR splittings for middle and outer doublets of oriented OA + 0.85 mole fraction of H_2O neat phase at $\theta = 0^\circ$ and various temperatures.

Temperature ($^\circ$C)	δB (μT)
-20	400
	725
-15	380
	700
-10	360
	680
-3	325
	645
4	310
	610
10	270
	580
16	260
	560
20	236
	540
25	230
	520
30	200
	490

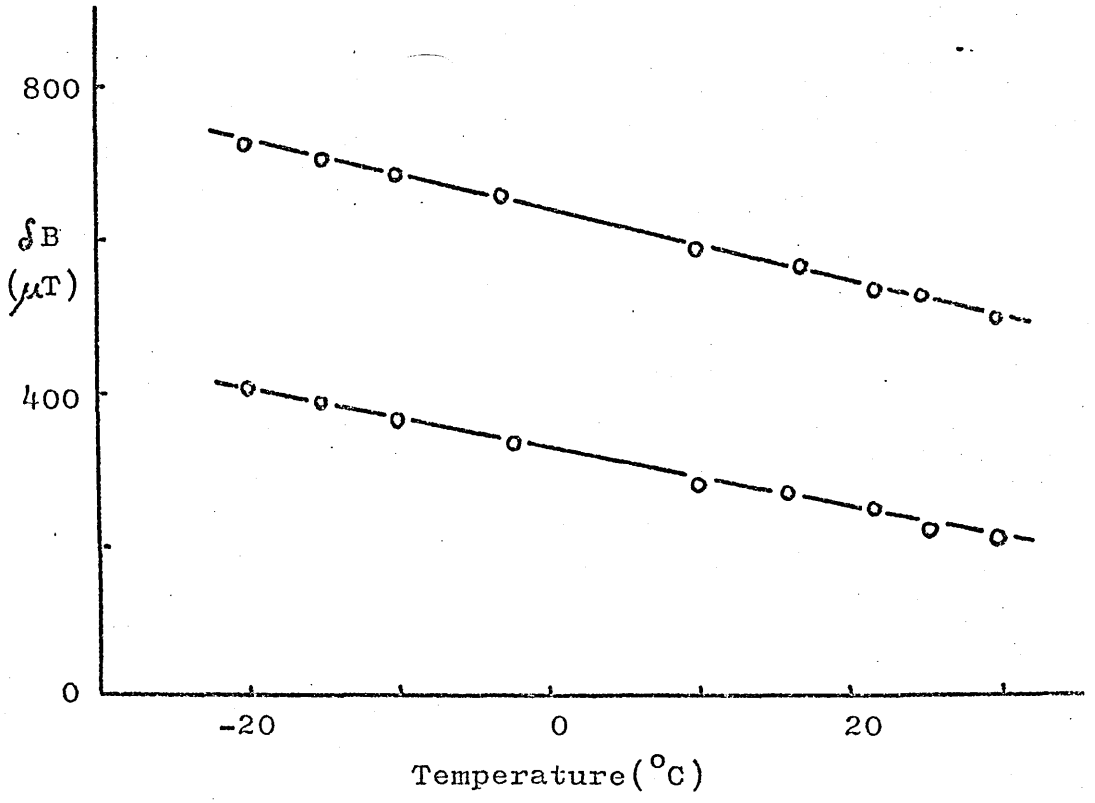

Figure 65

Variation of δB for middle and outer doublets with temperature for oriented OA + 0.85 mole fraction of H_2O neat phase at $\theta = 0^\circ$

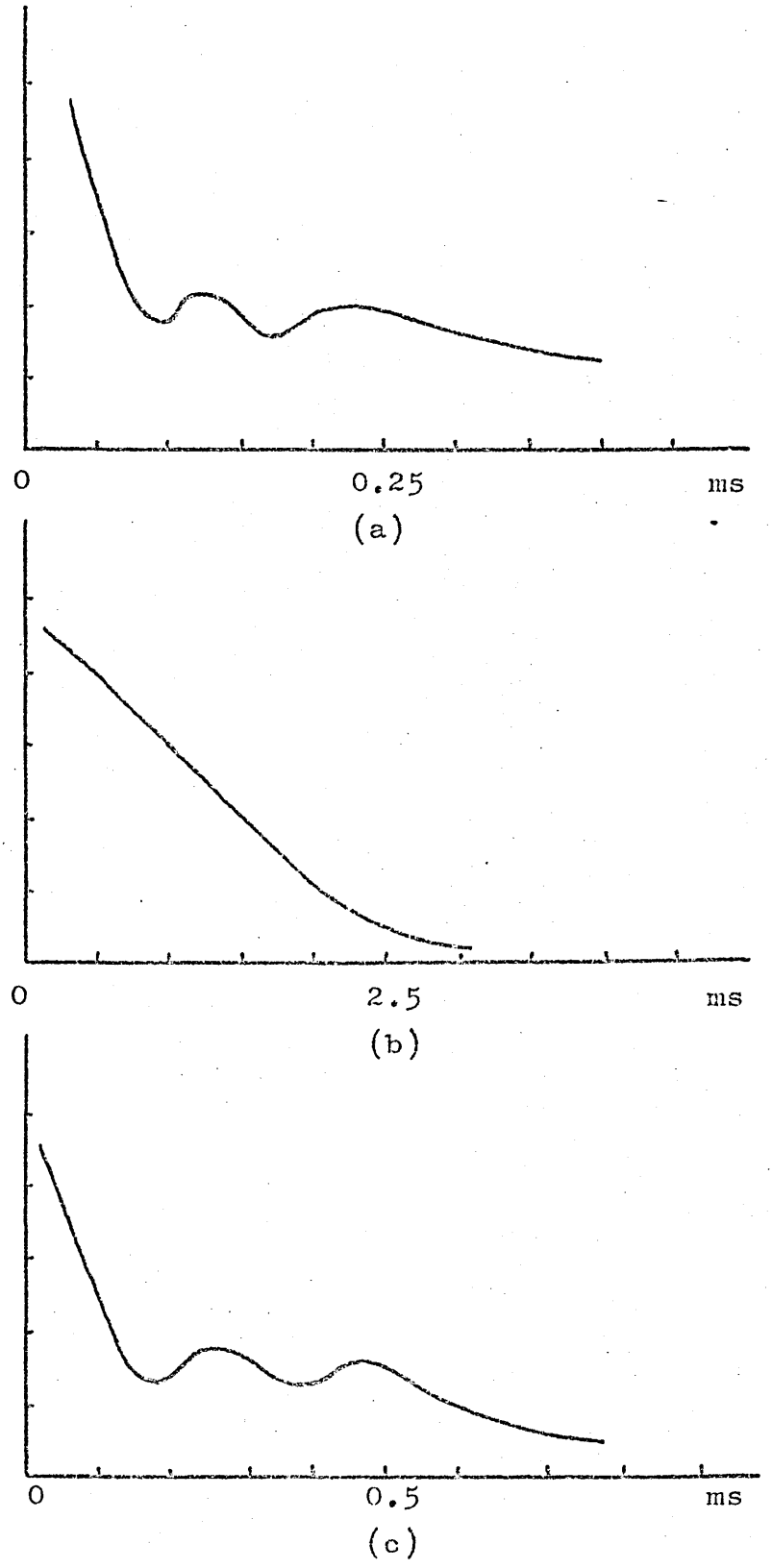

Figure 66

Decay of transverse magnetisation observed from oriented OA + 0.85 mole fraction of H_2O neat phase

(a) $\theta = 0^{\circ}$

(b) $\theta = 55^{\circ}$

(c) $\theta = 90^{\circ}$

(e) Effect of dissolved ionic salts on stability of MG8/H_2O neat phase and molecular motion in water layer

The systems studied, their neat l.c. melting points, and the pH of the solutions used are given in table XLVI.

The middle and outer doublets of the broad-line PMR spectra at 22°C of oriented neat l.c. samples with the compositions given in table XLVI were unaffected. The effects on the inner doublet for each system are given below.

1. MG8 + 0.8 mole fraction of M/100 HCl

No inner doublet was observed, there being only a narrow line of width 3μT which did not vary with θ. The effect was also detectable in the high resolution spectrum which for a non-oriented sample of MG8 + 0.80 mole fraction of H_2O at 23°C consisted of a two or three line 'powder pattern' as described previously. When M/100 HCl was used to make up the sample only a single line of width 11 Hz was observed at 5ppm.

2. MG8 + 0.8 mole fraction of M/100 NaOH

The splitting of the inner doublet was 21.6μT at θ = 0°, and there was no centre line present. Each doublet component appeared to consist of two lines which were ca. 3.5μT apart.

When the temperature was raised to 34°C a line-shape which had two components ca. 4μT apart appeared in the centre of the doublet. Altering θ had no effect on this central line-shape except for the normal increase in intensity when θ = 55°.

At the l.c. melting point the doublets vanished leaving a three line high resolution spectrum with about 2.5 ppm between each component. The weakest line occurred at the

Table XLVI

Data for neat phases of MG8 + various ionic solutions.

System	Transition Temperature N-FI (°C)	pH of ionic solution
MG8 + 0.8 mole fraction of H_2O	48	5.2
0.8 mole fraction of M/100 HCl	32	2.15
0.8 mole fraction of M/100 NaOH	42	11.6
0.8 mole fraction of M/10 NaOH	38	12.2
0.8 mole fraction of M/100 NaCl	37	6.9
0.8 mole fraction of M/100 NaH_2PO_4 and M/100 Na_2HPO_4	36	7.0

lowest field strength and the most intense line at the highest field strength.

High resolution PMR spectra were obtained from several different non-oriented l.c. samples of MG8 + 0.8 mole fraction of M/100 NaOH, which had been allowed to cool slowly from the isotropic liquid state. These spectra were not reproducible and in several cases the line-shape observed consisted of two broad overlapping peaks 1.5 - 2.5 ppm (2 - 3.5μT) apart. On other occasions a broad line-shape several ppm wide with a single peak was observed.

3. <u>MG8 + 0.8 mole fraction of M/10 NaOH</u>

The splitting of the inner doublet at $\theta = 0^{\circ}$ was 19μT and no central line was present. With increasing temperature a narrow central line appeared and grew in intensity, while the doublet components broadened and became weaker. At the l.c. melting point the doublets vanished leaving a three line high resolution spectrum similar to that described previously.

4. <u>MG8 + 0.8 mole fraction of M/100 NaCl</u>

The splitting of the inner doublet at $\theta = 0^{\circ}$ was 21μT and no central line was present. Also no central line appeared until the l.c. melting point was reached when the doublets vanished and the three line high resolution spectrum described previously appeared.

5. <u>MG8 + 0.8 mole fraction of M/100 Na_2HPO_4/NaH_2PO_4</u>

The peak to peak splitting of the inner doublet was 23.5μT. The estimated centre to centre splitting was about 15μT. It was impossible to measure accurately because of the presence of a central line of width 4μT with an intensity slightly greater than that of the doublet components.

With increasing temperature this central line increased in intensity while the doublet components became weaker and broader. At the l.c. melting point the doublets vanished leaving the three line high resolution spectrum described previously.

(II) Discussion

(a) Phase diagrams

1. In figure 67 T_{pen} for the B-form is shown as a function of alkyl chain length for the five 1-monoglycerides studied and MG14 (5). T_{pen} does not appear to alternate or correlate with any transition in the anhydrous 1-monoglycerides. However in the cases of MG8 and MG11 T_{pen} correlates well with the lowest temperature at which the l.c. phase is stable as shown by the phase diagrams (figures 36 and 40).

Since water is observed to penetrate along the edges of the crystals this indicates that penetration is occurring between layers of polar groups.

T_{pen} seems likely to be that temperature at which thermal motion of the 1-monoglycerides is great enough to cause a breakdown of the hydrogen-bonding system between the hydroxyl groups in the crystal lattice, and the subsequent incorporation of water into a new and more stable hydrogen-bonding system. At the same time the thermal motion has reduced the Van der Waals' bonding between the alkyl chains so as to allow them to move laterally and longitudinally to expand the crystal lattice for water to be incorporated.

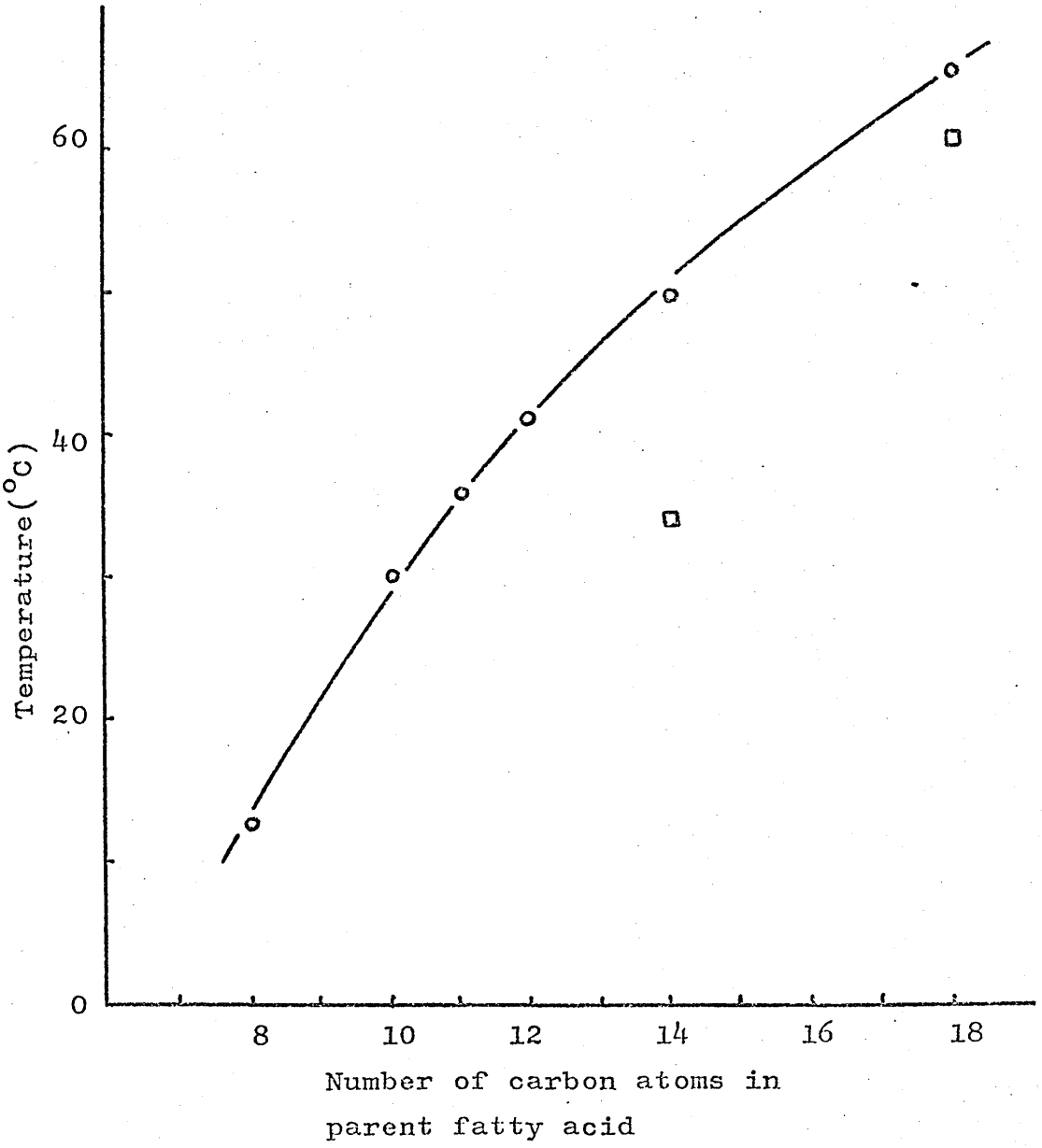

Figure 67

T_{pen} for β (o) and α'-forms (□) vs. 1-monoglyceride chain length

Lawrence has also determined T_{pen} values for the penetration of water into the α' phases of two 1-monoglycerides (5) and these are also shown in figure 67.

In the α' phase the alkyl chains are rotating about their long axes and therefore the spacing between adjacent alkyl chains will be greater than in the B-form. Therefore the hydrogen-bonding system between the hydroxyl groups will be more open and less stable allowing penetration of water to occur at a lower temperature.

2. The main features of the MG8/D_2O phase diagram are similar to those of the MG8/H_2O phase diagram as determined by Larsson (61) down to 10°C. However the deeply plunging eutectic below 10°C shown in Larsson's phase diagram at 0.39 mole fraction of H_2O was not observed but a much shallower eutectic at 28°C and 0.45 mole fraction of D_2O.

A sample was made up with the composition MG8 + 0.39 mole fraction of H_2O and was found to be a highly viscous but isotropic fluid when allowed to cool after being homogenised. It was kept in this state in a sealed tube at room temperature for six months and so was presumed to be indefinitely stable. The sample was then frozen in liquid nitrogen and the solid formed was allowed to warm back up to room temperature. This solid remained unchanged at room temperature for six months. However when melted at 29°C and allowed to cool back to room temperature it again remained in the fluid isotropic state indefinitely. It is concluded that at room temperature the sample remains in a metastable fluid isotropic phase because its high viscosity reduces the rate at which the system can crystallise. Therefore the

correct phase behaviour for samples in this region of the phase diagram is that shown in the MG8/D_2O phase diagram in figure 36 rather than Larsson's MG8/H_2O phase diagram in figure 38.

3. The changes occurring during a heating run on samples of MG8 with a low D_2O content are firstly the melting of D_2O ice between 0^oC and 5^oC, and then the penetration of the liquid D_2O into the B crystals at temperatures between 11^oC and 12.5^oC to give a gel phase and B crystals. This gel phase melts at 28^oC to give samples consisting of B crystals and fluid isotropic liquid. Samples finally become completely fluid isotropic at a temperature which decreases with increasing D_2O content down to the shallow eutectic at 28^oC and 0.45 mole fraction of D_2O. Above 0.45 mole fraction of D_2O the gel phase transforms to l.c. phase N at a temperature which decreases from 28^oC to 12.5^oC at 0.8 mole fraction of D_2O. There is no indication in the boundary between l.c. phase and gel of the formation of a monohydrate. This is probably because the MG8 alkyl chains are shorter than required for providing lateral bonds between adjacent molecules sufficient to form stable hydrated crystals as does MG11. Broad-line PMR spectra show that no significant extra motion of the alkyl chains is occurring in the gel phase compared to the anhydrous B crystals.

4. At higher D_2O contents the B crystals + D_2O transform directly at T_{pen} to l.c. phase N without forming an intermediate gel phase. The composition at which this first takes place, 0.8 mole fraction of D_2O, is also that at which l.c. phase N has its maximum melting point, and perhaps

indicates that an MG8. $4D_2O$ aggregate is particularly stable, although there is no evidence from the phase studies of a solid tetrahydrate.

5. For samples containing more than 0.92 mole fraction of D_2O, at T_{pen}, a dispersion is formed. Larsson (61) concluded from X-ray diffraction and optical microscopy studies that the structure of this dispersion consists of concentric bimolecular shells of 1-monoglyceride molecules alternating with water shells.

At 33°C the dispersion becomes two isotropic liquids, one being fluid isotropic and the other D_2O. The phase boundary between fluid isotropic and fluid isotropic + D_2O rises almost vertically from the composition MG8 + 0.92 mole fraction of D_2O. A sample containing 0.90 mole fraction of D_2O became two phase at 53°C whilst a sample containing 0.88 mole fraction of D_2O was still one-phase at 130°C.

6. The MG11/D_2O system has similar phases to the MG8/D_2O system but these exist at higher temperatures because of the longer alkyl chain.

The l.c. region shows no well defined upper node as in the MG8/D_2O system but only a maximum melting point at MG11 + 0.85 mole fraction of D_2O.

There is a small peak in the phase boundary between the gel and l.c. regions at MG11 + 0.5 mole fraction of D_2O suggesting the presence of a monohydrate.

7. The MG//18/D_2O phase diagram is similar to that of MG//18/H_2O determined by Lutton (59) down to 25°C. Penetration of D_2O into the MG//18 crystal lattice occurs at temperatures between 12.5°C and 20°C forming a gel phase + B crystals.

With increasing D_2O content this gel phase + B crystals pass through to a fluid isotropic phase at decreasing temperatures until at ca. 0.35 mole fraction of D_2O an l.c. phase is formed which exists up to 0.92 mole fraction of D_2O. The l.c. phase has a maximum melting point at the composition MG//18 + 0.67 mole fraction of D_2O i.e. MG//18. $2D_2O$, and although the upper node is clearly defined at this composition it is difficult to attach any special significance to the possible role of an MG//18. $2D_2O$ aggregate in the structure of the l.c. phase.

For mole fractions of D_2O between 0.67 and 0.92, at higher temperatures the l.c. phase changes to an optically isotropic and highly viscous phase, which has been classed as cubic by Luzzati et al. on the basis of X-ray diffraction studies (82).

The MG//18/D_2O system shows a region of middle l.c. phase existing between 0.77 and 0.87 mole fraction of D_2O and 85°C and 97°C. Larsson (61) has shown using X-ray diffraction studies that the middle phase in the MG22/H_2O system has a structure consisting of infinite hexagonally packed arrays of water cylinders surrounded by 1-monoglyceride molecules with their polar groups in contact with the water cylinders.

For MG//18/D_2O samples containing more than 0.92 mole fraction of D_2O, at T_{pen}, a dispersion is formed as in the MG8/D_2O and MG11/D_2O systems. With increasing temperature the samples then change to viscous isotropic + D_2O at 25°C, middle + D_2O at 90°C and fluid isotropic + D_2O at 97°C.

(b) Liquid crystalline phases

The structure of the neat l.c. phase N in 1-monoglyceride /water systems was shown to be lamellar by Larsson (61) and Reiss-Husson (80) using X-ray diffraction.

On the basis of microscope observations Ralston et al. (53) originally assigned the l.c. phase N in the OA/H_2O system a nematic structure but X-ray diffraction studies by Friberg and Mandell (141), and Ekwall et al. (142) have shown the structure to be lamellar and the results given in table XV agree with this.

1. Structure of the water layer

1. The long spacings obtained from the MG8/D_2O neat phase can be compared with the values obtained by Larsson (61) shown in table XLVII. The thickness of the water layer, d_w, can be calculated from these values, $d_w = d_1 - d$, and d_w is also shown as a function of mole fraction of water in table XLVII and figure 68.

Table XLVII

Neat phase of MG8/H_2O at 25°C.

X_{H_2O}	d(Å)	d_1(Å)	d_w(Å)
0.39	26.5	24.2	2.3
0.57	27.1	24.2	2.9
0.75	29.5	23.4	6.1
0.84	32.9	22.7	10.2
0.89	38.5	22.6	15.9
0.92	45.5	22.0	23.5

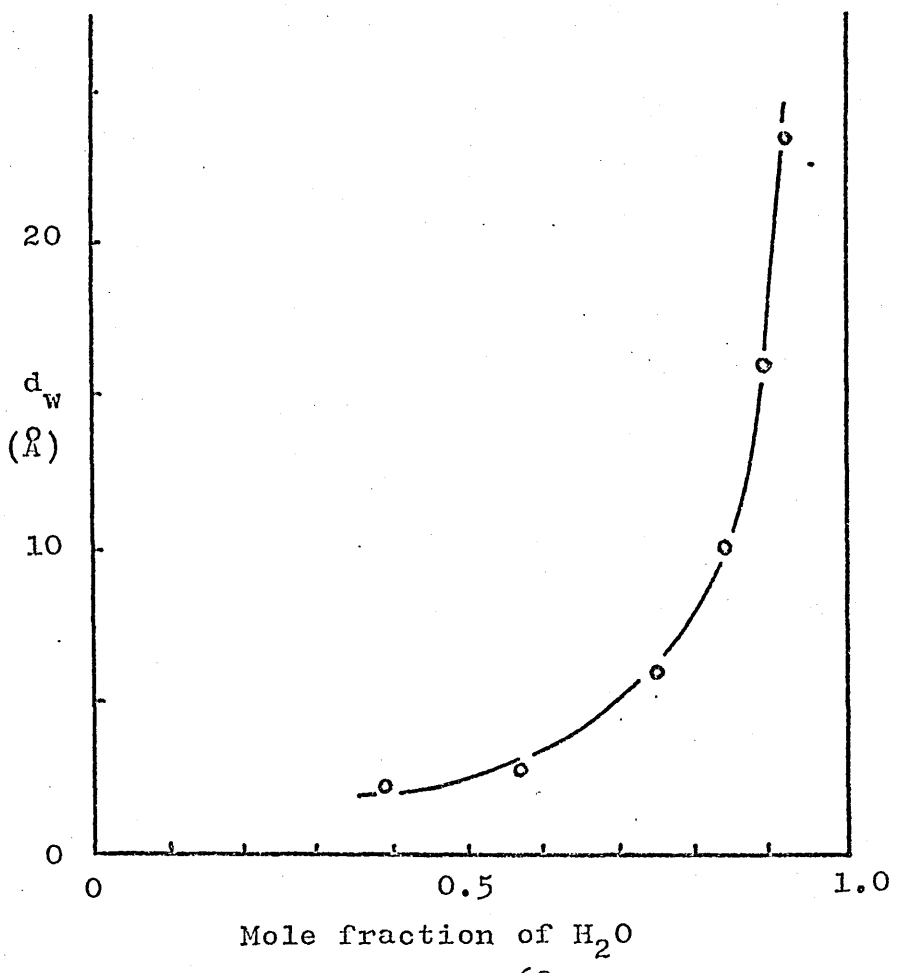

Figure 68

Thickness of water layer (d_w) vs. X_{H_2O} for MG8/H_2O neat phase

If we consider a mole fraction of water of 0.8 d_w is 7.8 Å (from figure 68) for an MG8 : H_2O ratio of 1 : 4. Making the assumption that the water exists in an ice-type lattice a d_w of 7.8 Å corresponds to a layer of 4 water molecules in thickness. This figure is in agreement with the total number of water molecules per MG8 molecule at this composition, which seems to indicate that MG8 molecules on opposite sides of the water layer are joined by chains of water molecules, with one chain between two hydroxyl groups. This model suggests that only slight penetration of water is occurring into or around the glyceryl residue and so the carbonyl group of MG8 is playing only a small part in the hydrogen-bonding network.

2. Now considering the neat phase in the OA/H_2O system, if we assume that OA molecules on opposite sides of the water layer are linked by chains of water molecules with two chains between two amine groups, and also that the water structure is similar to that in the MG8/H_2O system, using figure 68 we find that at mole fractions of water of 0.8, 0.85, and 0.92 d_w is 7.8, 10.8, and 23.5Å respectively. Now using the long spacing data in table XV we obtain values for half the thickness of the lipid layer of 21.9, 23.1, and 21.2 Å respectively. These values are very close to the length of an octylamine molecule with an extended alkyl chain, which is 22 Å, suggesting that in the OA/H_2O neat phase the alkyl chains are extended and are not tilted significantly.

3. CW PMR, DMR, and pulse NMR have been used previously to obtain information on the structure of the water in lyotropic l.c. systems (55, 60, 64, 100, 102-107, 110-112, 143, 144, 187), mineral and clay/water systems (145-152), and other systems of biological importance (153-160).

The results have been explained using the following model systems for the water structure.

1) 'Ordered' and 'free' water molecules with fast or slow exchange occurring between the two (143).

2) A similar model to 1) but also allowing for exchange between water protons or deuterons and protons or deuterons covalently bonded to the lipid molecules in the lamellae. This model will only be significant for lipid molecules with end groups containing exchangeable protons such as NH_2, OH, COOH, etc. (143).

3) Chains of water molecules, with rotation of the chains occurring only around one axis, while the water molecules in each chain reorient anisotropically (153).

4) Water molecules undergoing rapid diffusional and rotational motions which deviate slightly from spherical symmetry (145). This deviation is caused by spatial restrictions being applied to the water molecules due to the overall structure of the system.

5) A slightly distorted lattice of water molecules tetrahedrally oriented in which one of the tetrahedral positions has a population which is different from the other three (152,160), i.e. a tetrahedral lattice of water molecules undergoing anisotropic reorientation. This model would seem to be one particular case of model 4) with the spatial restrictions producing a tetrahedral lattice.

4. All of the above models require the water molecules to undergo anisotropic motion or be ordered in some way, and a general method of characterising partially oriented systems was developed by Saupe (161) and extended by Buckingham and McLauchlan (162).

The probability $P(\alpha, \phi)$ that the constraint is at the spherical polar angles α, ϕ relative to the cartesian axes 1,2,3 fixed in the molecule may be written as a series of spherical harmonics:

$$P(\alpha,\phi) = \sum_{l,m} a_{lm} Y_{l,m}(\alpha,\phi)$$

$$= (4\pi)^{-1} \Big\{ 1 + \big[3S_3 \cos\alpha + 3S_1 \sin\alpha \cos\phi + 3S_2 \sin\alpha \sin\phi \big] + \big[5/2\, S_{33} (3\cos^2\alpha - 1) + 5/2 (S_{11} - S_{22}) \sin^2\alpha \cos 2\phi + 10 S_{12} \sin^2\alpha \sin\phi \cos\phi + 10 S_{23} \cos\alpha \sin\alpha \sin\phi + 10 S_{31} \cos\alpha \sin\alpha \cos\phi \big] + \ldots\ldots \Big\} \qquad (24)$$

where

$$S_3 = \overline{\cos\alpha}$$

$$S_1 = \overline{\sin\alpha \cos\phi}$$

$$S_2 = \overline{\sin\alpha \sin\phi}$$

$$S_{33} = \tfrac{1}{2} (3\, \overline{\cos^2\alpha} - 1)$$

$$S_{11} = \tfrac{1}{2} (3\, \overline{\sin^2\alpha \cos^2\phi} - 1)$$

$$S_{22} = \tfrac{1}{2} (3\, \overline{\sin^2\alpha \sin^2\phi} - 1)$$

$$S_{12} = 3/2\, \overline{\sin^2\alpha \sin\phi \cos\phi}$$

$$S_{23} = 3/2\, \overline{\cos\alpha \sin\alpha \sin\phi}$$

$$S_{31} = 3/2\, \overline{\cos\alpha \sin\alpha \cos\phi}$$

The S - coefficients have the following limits

$$-1 \leq S_1, S_2, S_3 \leq 1$$

$$-\tfrac{1}{2} \leq S_{11}, S_{22}, S_{33} \leq 1$$

$$-\tfrac{3}{4} \leq S_{12}, S_{23}, S_{31} \leq \tfrac{3}{4}$$

Only five of the S_{ij} coefficients are independent since

$S_{11} + S_{22} + S_{33} = 0$

In the case of a water molecule with C_{2v} symmetry and the cartesian axes fixed as shown in figure 69 only S_{11}, S_{22} and S_{33} are non-vanishing coefficients.

5. The proton-proton splitting in partially oriented water is given by (162)

$$\delta B = 3/2\ P_2\ (\cos\Omega)\ L^{(HH)}\ S_{22} \qquad (25)$$

$$= \left| \tfrac{3}{4}\ (3\cos^2\Omega - 1)\ L^{(HH)}\ S_{22} \right| \qquad (26)$$

where Ω is the angle between the constraint and the magnetic field $\bar{B}_o$, and $L^{(HH)} = \hbar\gamma^2/\pi r^3 = 60.8$ kHz for H_2O.

In the case of the D_2O molecule if the electric field gradient is axially symmetric and its principal tensor component is directed along the O - D bond, the quadrupolar splitting given by equation (22) can be rewritten in terms of S - coefficients as :-

$$\Delta\nu = \left| \frac{3}{2h}\ e^2 q\ Q \left[S_{11}\left(\frac{3}{2}\cos^2 B - \frac{1}{2}\right) + \frac{1}{2}(S_{22} - S_{33}) \sin^2 B \right] \left\langle \frac{3}{2}\cos^2\Omega - \frac{1}{2} \right\rangle \right. \qquad (27)$$

where B is half the D-O-D angle.

In a randomly oriented phase a powder pattern is observed, separation between the absorption maxima being given by:-

$$\Delta\nu = \left| \frac{3\ e^2 q\ Q}{4h} \cdot S \right| \qquad (28)$$

$$\text{where } S = \left[S_{11}\ \frac{3}{2}\left(\cos^2 B - \frac{1}{2}\right) + \frac{1}{2}\left(S_{22} - S_{33}\right)\sin^2 B \right] \qquad (29)$$

Accurate experimental values of the quadrupole coupling constant, e^2qQ/h (henceforth denoted by E_Q) and the

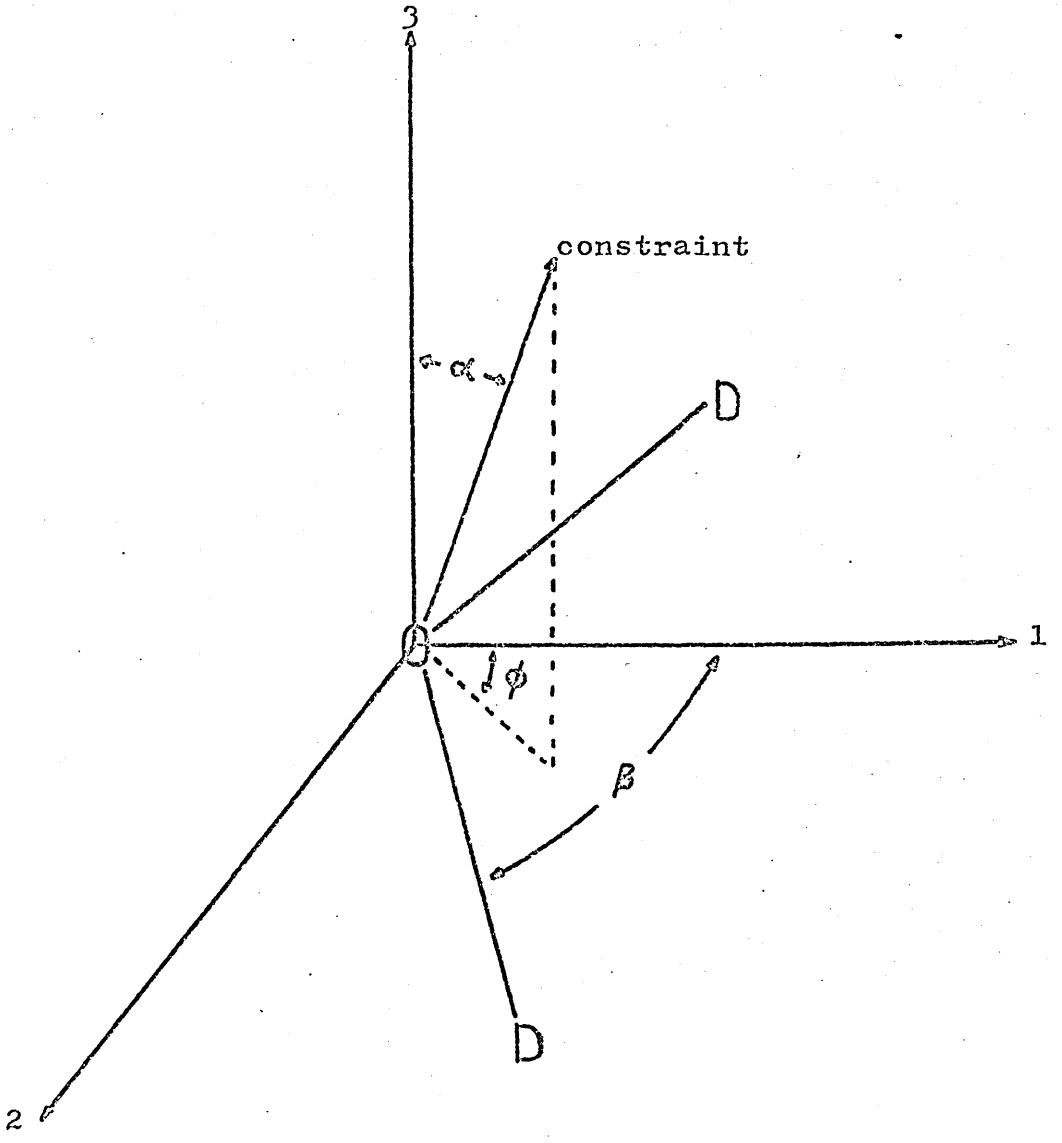

Figure 69

Choice of axes in the coordinate system fixed to the D_2O molecule

asymmetry parameter, η , in D_2O are only known for the solid and gaseous states. The value of E_Q is 215 kHz (163) (mean value) and 305 kHz (164,165) in the solid and gaseous states respectively: the corresponding η values are 0.100 (163) and 0.115 (164) respectively. It is reasonable to assume that, in the liquid state, both E_Q and η are intermediate between the values in solid and gaseous D_2O and closer to the values in the solid state.

The asymmetry of the EFG has not been considered in equations (27) and (28) and no theoretical treatment of the notional averaging of an asymmetric EFG has been reported in the literature. However the observed spectra show a line-shape characteristic of a symmetric EFG since the separation between the outer shoulders of the absorption line is within experimental error exactly twice the separation between the maxima. We can therefore assume that the average EFG is nearly symmetric and consequently equation (28) is applicable although the definition of S is only approximate. Changes in $\Delta\nu$ cannot be unambiguously related to a change in S since E_Q may vary also. The value of E_Q could be influenced by variations in the degree of hydrogen bonding. However the difference in the value of E_Q between solid and gaseous D_2O is ca. 50% and we therefore assume that the relatively small variations in the degree of hydrogen-bonding present in the systems investigated do not markedly influence the value of E_Q.

6. The effect of chemical exchange on an NMR line-shape in the presence of quadrupole coupling has not yet been given any detailed theoretical treatment. However on the basis of the general principles of NMR it is possible to make some qualitative statements. Let us assume that deuterons are

exchanging between chemically distinguishable sites, 1,2, 3 ····· , which in the absence of exchange exhibit the quadrupolar splittings $\Delta\nu_i$, i = 1,2,3 ····· . If the life-times of the deuterons in the individual sites are much longer than the inverse of the differences in quadrupolar splittings, i.e. $1/|(\Delta\nu_i - \Delta\nu_j)|$, separate resonance signals will be observed from the deuterons in the various sites. If, on the other hand, the life-times are much shorter than $1/|(\Delta\nu_i - \Delta\nu_j)|$, only an average resonance signal will be observed for which the quadrupolar splitting is given by

$$\Delta\nu = \sum_i x_i \Delta\nu_i \qquad (30)$$

where x_i is the fraction of deuterons situated in site i. For the intermediate case, i.e. when the life-times and the values of $1/|(\Delta\nu_i - \Delta\nu_j)|$ are of the same order of magnitude, a more complicated line-shape may be expected.

7. The quadrupolar splittings observed in this work originate from an anisotropic orientation of the EFGs felt by the water deuterons. This can be caused (a) by partial orientation of D_2O molecules or (b) by covalent bonding of deuterons to lipid molecules in the lamellae. The molecular interaction giving rise to the partial orientation will be hydrogen bonding to the polar end groups of the lipid molecules.

A change in the quadrupolar splitting can arise from both a change in the length of time any water molecule spends in association with a lipid molecule and from an altered degree of orientation of the lipid molecules. According to the commonly accepted picture of the organisation of lamellar mesophases the orientation of the lipid molecules must be

highly anisotropic, and thus any relative change in their degree of orientation is expected to be small. This is shown to be a valid conclusion in section 2. We therefore conclude that the variations in the S coefficients observed on changing the composition of the hydrophilic part of the system are to a large extent caused by a change in the time-scale of the lipid/water interaction.

8. Drakenberg (143) has discussed his quadrupolar splitting results from lyotropic l.c. systems on the basis of models 1) and 2) with rapid exchange occurring between 'ordered' and 'free' water. We however consider it unnecessary to talk in terms of two types of water and prefer instead model 4) in which all the water molecules are equivalent and have a certain degree of partial orientation due to the fact that they all spend a fraction of their time at the lipid/water interface. If we assume that the observed quadrupolar splitting $\Delta\nu$ is directly proportional to the degree of partial orientation, D, and also that D is directly proportional to the mole fraction of lipid molecules, x_1, we can write :-

$$\Delta\nu = k_1 D = k_2 x_1 = k_2(1-x_{D_2O}) \qquad (31)$$

where k_1 and k_2 are constants, independent of compostion. Therefore equation (31) indicates that the quadrupolar splitting due to partial orientation of water molecules will decrease approximately linearly with increasing mole fraction of D_2O.

This behaviour has been found experimentally in the MG8/D_2O and MG11/D_2O systems and therefore the above model for the water region of the l.c. phase would seem to be appropriate in the case of these two systems. The model

assumes that exchange between 1-monoglyceride hydroxyl protons and water deuterons is slow or does not occur at all. This assumption is probably valid for 1-monoglyceride/water systems since the water resonance in the high resolution PMR spectrum of a sample of MG8 + 0.8 mole fraction of H_2O in the fluid isotropic phase consisted of several overlapping lines of total width ca. 30 Hz. Also the fact that the high resolution PMR spectrum of the l.c. phase of MG8/H_2O shows the characteristics of a powder pattern, with a total overall width of ca. 600Hz, caused by dipolar splitting, indicates that the rate of any exchange which might be occurring is less than ca. 1kHz. When M/100 HCl instead of water was used to prepare the l.c. phase only a narrow line was observed for the water resonance from both ordered and non-ordered samples, indicating that the increased rate of exchange caused by the presence of H_3O^+ was collapsing the water doublet. The above discussion means that an earlier explanation of the quadrupolar splittings observed from MG8/D_2O l.c. phases is probably wrong (64) since it required rapid exchange to occur between water deuterons and deuterons covalently bonded to MG8 molecules.

In the case of slow exchange we would also expect to observe an additional large quadrupolar splitting from 1-monoglyceride hydroxyl deuterons. However in the MG8/D_2O and MG11/D_2O systems this has not been observed and we agree with Drakenberg (143), who has also been unable to observe it in the systems which he studied, that this is probably due to its low intensity.

The quadrupolar splittings observed for the systems MG8/D_2O and MG11/D_2O were independent of temperature over the range of existence of the l.c. phase. The only ways in which

the quadrupolar splitting could become temperature dependent is if either the time-scale of the lipid/water interaction or the partial orientation of the lipid molecules was changing with temperature. The former is unlikely since the ratio of the time spent by a water moleule at the lipid/water interface to the time it spends surrounded by other water molecules should be independent of temperature. In the case of the latter even though measurable changes do occur in the partial orientation of the chains of the lipid molecules with temperature (see section 2) the small partial orientation passed on to the water molecules, which are associated with the end groups, will not change significantly.

In figures 46 and 48 the slopes of the graphs of $\Delta\nu$ against mole fraction of D_2O are - 8.4 kHz/ mole fraction and - 7.3 k Hz/mole fraction for the MG8/D_2O and MG11/D_2O systems respectively. The larger slope for the MG8/D_2O system, reflecting a faster decrease in partial orientation of the water molecules with increasing D_2O content compared to the MG11/D_2O system, is probably due to the fact that slight changes in the partial orientation of the 1-monoglyceride molecules due to increasing D_2O content will be greater for MG8 than MG11 because of its shorter alkyl chain.

9. We now consider how deuteron exchange between water and lipid molecules can affect the observed quadrupolar splittings. The previously discussed model has to be modified to include the chemically distinguishable deuteron sites on the end groups of the lipid molecules. In the case of slow deuteron exchange separate resonance signals may be observed from the different types of deuterons. If, on the other hand,

the deuterons are exchanging rapidly between water and lipid molecules an average quadrupolar splitting will be observed (c.f. equation 30), which is given by :

$$\Delta\nu = x_w \Delta\nu_w + \sum_i x_{li} \Delta\nu_{li} \qquad (32)$$

where x_w is the mole fraction of water deuterons and x_{li} is the mole fraction corresponding to the ith site of exchangeable lipid deuterons. $\Delta\nu_w$ and $\Delta\nu_{li}$ are the respective quadrupolar splittings in the absence of exchange. Using equation (31) and assuming that x_{li} is proportional to the mole fraction of lipid molecules we can write equation (32) as:

$$\Delta\nu = x_w k_2 (1 - x_{D_2O}) + (1 - x_{D_2O}) \sum_i k_i' \Delta\nu_{li} \qquad (33)$$

This equation also predicts a linear decrease of $\Delta\nu$ with increasing mole fraction of D_2O but the slope and intercept will be different from those in equation (31).

The above model in which rapid deuteron exchange is occurring between water and lipid molecules is probably applicable to the OA/D_2O l.c. phase. Firstly the presence of only a single narrow line of width ca. 30 Hz at 4.2 ppm in the high resolution PMR spectrum of the neat phase supports the assumption that rapid chemical exchange is occurring between water protons at 4.8 ppm and amine protons at 0.8 ppm. Since the line is narrow the exchange rate must be much faster than $2\pi\Delta\delta$ (where $\Delta\delta$ is the chemical shift difference between the two types of protons) i.e. 1.5 kHz. Secondly rapid chemical exchange faster than ca. 1kHz would tend to collapse any doublet due to dipole-dipole interactions and none is observable experimentally in the PMR spectra of ordered samples.

The value of 6.76 kHz for the quadrupolar splitting

observed from an OA + 0.8 mole fraction of D_2O sample is larger than the values from MG8/D_2O and MG11/D_2O samples of similar compositions. This is a result of the contribution to the overall splitting from deuterons on the amine groups of the OA molecules which are appreciably more ordered than those on water molecules.

10. Using equation (29) and the fact that $S_{11} + S_{22} + S_{33} = 0$ we can write:-

$$S = S_{11} \cos^2 B + S_{22} \sin^2 B \qquad (34)$$

for the D_2O molecule $B = 52^\circ 16'$ and so

$$S = 0.375\, S_{11} + 0.625\, S_{22} \qquad (35)$$

Inserting appropriate values of the inner doublet splitting and quadrupolar splitting in equations (26) and (28) respectively, S_{22} and S can be calculated. Then using these values, equation (35) and the fact that $S_{11} + S_{22} + S_{33} = 0$, S_{11} and S_{22} can be calculated. Because only the moduli of S_{22} and S appear in equations (26) and (28) their sign is unknown and so only sets of possible S - coefficients can be calculated using the positive and negative values of S and S_{22}. The possible sets of calculated S coefficients for MG8 + 0.66 mole fraction of water and MG11 + 0.66 mole fraction of water are shown in tables XLVII and XLVIII. Similar sets of S-coefficients for OA + 0.8 mole fraction of water are shown in table XLIX. The rapid exchange process which gives the increased value of S for the OA/D_2O l.c. phase causes the collapse of any doublet due to dipole-dipole interactions and so S_{22} is zero.

Table XLVII

Calculated possible sets of S - coefficients for MG8 + 0.66 mole fraction of water.

S	S_{11}	S_{22}	S_{33}
0.02	0.022	0.018	-0.04
0.02	0.082	-0.018	-0.064
-0.02	-0.082	0.018	0.064
-0.02	-0.022	-0.018	0.04

Table XLVIII

Calculated possible sets of S - coefficients for MG11 + 0.66 mole fraction of water.

S	S_{11}	S_{22}	S_{33}
0.015	0.008	0.019	-0.027
0.015	0.071	-0.019	-0.052
-0.015	-0.071	0.019	0.052
-0.015	-0.008	-0.019	0.027

Table XLIX

Calculated possible sets of S - coefficients for OA + 0.8 mole fraction of water.

S	S_{11}	S_{22}	S_{33}
0.042	0.11	0	-0.11
-0.042	-0.11	0	+0.11

The S_{22} value for MG//18 + 0.66 mole fraction of H_2O is $\pm$ 0.012 which is approximately 50% lower than the values for corresponding MG8 and MG11 samples. This indicates a lower degree of order for the MG//18 molecules, which are causing the partial orientation of the water molecules, compared to MG8 and MG11. This might be expected because of the disruptive effect of the double bond, with a cis configuration, in the centre of the MG//18 alkyl chain.

δB values and hence S_{22} values for the water in biological systems, and mineral and clay/water systems are ca. three to four times greater than those described above. This reflects the larger partial orientation of the water molecules in these systems due to the increased number of hydrogen-bonding sites on large biological molecules and clay and mineral lattices.

Variations of the S - coefficients may be due to changes in either degree of orientation or direction of preferred orientation. The former causes the variation of S - coefficients with mole fraction of water while the latter controls the maximum possible S - coefficient values.

The linear decrease of δB, and hence S_{22}, with increasing mole fraction of D_2O for the l.c. phases in the MG8, MG11 and MG//18/H_2O systems can be explained in a similar way to that used previously for the similar behaviour of $\Delta\nu$ (see equation 31).

The two possible modes of hydrogen-bonding between water molecules and 1-monoglyceride hydroxyl groups are shown in figure 70. Figure 70a corresponds to hydrogen bonding between a proton on the water molecule and a lone pair on the hydroxyl oxygen atom (mode a), and figure 70b to hydrogen-bonding between a lone pair on the water oxygen atom and the proton of a hydroxyl group (mode b). The S - coefficients calculated for the two modes using equation (24) are given in table L.

Table L

	S	S_{11}	S_{22}	S_{33}
Mode a	0.3	0.062	0.44	-0.5
Mode b	-0.23	-0.333	-0.17	0.5
Average of mode a and b	0.034	-0.14	0.14	0

It is likely that both modes will be equally probable and therefore the average values of the S - coefficients for the two modes are also given in table L. Rotation of the water molecule about the hydrogen bond does not alter the values of the S - coefficients.

The next simplest motion of the water molecules is rotation about an axis bisecting the H-O-H angle which will periodically interchange the proton which is bonded to

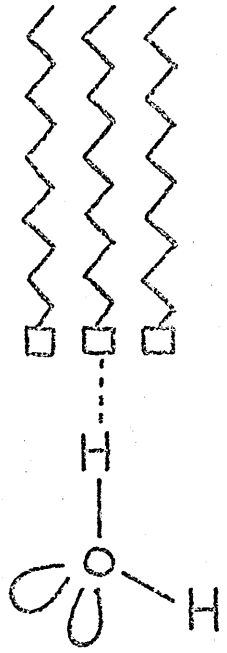

(a)

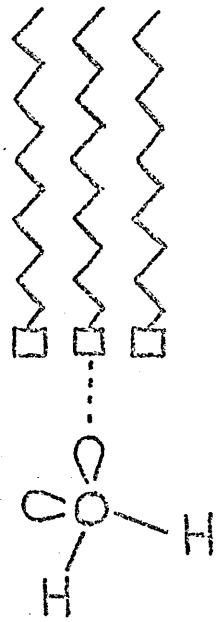

(b)

Figure 70

Possible hydrogen-bonding modes of H_2O molecule to polar lipid end group

the 1-monoglyceride hydroxyl group in case a, or the lone pair of the oxygen atom which is bonded to the 1-monoglyceride hydroxyl group in case b. New S - coefficients can be calculated for the two hydrogen bonding modes taking account of this rotation (mode a′ and mode b′) and these and their averages are shown in table LI.

Table LI

	S	S_{11}	S_{22}	S_{33}
Mode a′	0.11	-0.07	0.22	-0.15
Mode b′	0.11	-0.13	0.25	-0.12
Average of mode a′ and mode b′	0.11	-0.1	0.23	-0.14

Comparison of the calculated S - coefficients in tables L and LI with the experimental S - coefficients in tables XLVII and XLVIII shows that the molecular motion associated with the model water structure described above is too simple to explain the observed values. However the calculated S - coefficients are approaching the values of the experimental ones and a more complex model for the motion of the water molecules involving rotation about more axes and allowing for the effects of diffusion, although virtually impossible to analyse mathematically, would probably lead to S - coefficients comparable to those observed experimentally.

2. Structure of the lipid layer

1. It has been well established that the neat l.c. phase has a bilayer structure. The next step towards a complete understanding of the structure of the lipid region of the bilayer is to determine the molecular motion which the alkyl chains of the lipid molecules undergo. This molecular motion can be divided into two parts a) any motion which does not alter the position of the molecular axis e.g. rotation and b) any motion which alters the position of the molecular axis e.g. diffusion. Considering a) first, two basic models have been put forward for the reorientational motion of individual chains in l.c. systems.

1) The Porod-Kratky model (99) involving free rotation about each carbon-carbon bond, the angle between adjacent carbon-carbon bonds being an adjustable parameter. This leads to an exponential decrease in degree of order along the alkyl chain away from the head group and hence a continuous increase in amplitude of molecular motion.

2) A model put forward by Charvolin and Rigny (166) and Hubbell and McConnell (167) of rapidly interconverting isomeric states of a polymethylene chain involving gauche-trans isomerism. The model predicts that the first few methylene groups (ca. 5-6) away from the head group behave as a rigid rod with rapidly increasing possibilities for gauche configurations at larger distances from the head group. In both models rotation of the alkyl chain as a whole about its long axis is assumed to occur.

It has been shown that the Porod-Kratky model is a poor representation of the physical properties of polymethylene polymers (168) and it seems likely that the same limitations

will apply to its use as a model for the motion of the alkyl chains in a lipid bilayer. Moreover Chan et al. (117) have studied dispersions of lecithin bilayers in D_2O using CW and pulse NMR and found both a narrow and a broad resonance from methylene protons. They therefore concluded that 'the end of the hydrocarbon chain is significantly more mobile than the rest of the chain'. This conclusion supports model 2).

Now considering motions of type b) Charvolin and Rigny (166) have studied the neat phase of potassium laurate/D_2O using pulse NMR and obtained a value of ca. 10^{-6}s for the correlation time for the two-dimensional diffusion of laurate molecules in the plane of the bilayer. Also Kornberg and McConnell (169) by measuring the broadening of NMR lines caused by small amounts of spin-labelled phospholipids have found the molecular frequency of the translation step for lateral diffusion of phospholipid molecules in a vesicle membrane, which has a bilayer structure, to be much greater than 3kHz at $0^{o}C$.

The NMR results obtained in this work will now be discussed in terms of the molecular motions described above. They will also be used to provide substantial evidence for the appropriateness of model 2) in describing the alkyl chain motions of the lipid molecules in the systems studied.

2. Non-ordered l.c. samples of MG8, MG11 and OA/water give PMR spectra with two broad and one narrow components. Similar l.c. samples of MG//18/water give PMR spectra with only one broad component and one narrow one. There are two possible models to explain the occurrence of two broad lines. The first model involves the presence in the bilayer of two

sites for the lipid molecules to occupy with two different types of molecular motion of the alkyl chains. Alternatively all the lipid molecules may occupy identical sites but there may be two different types of motion along each alkyl chain.

The difference in half-widths between the two broad lines is ca. 1-2 kHz and therefore any exchange of lipid molecules between two possible sites faster than ca. 2kHz will lead to only one averaged resonance line of intermediate width being observable. Since exchange of lipid molecules occurs at a rate of at least 3kHz according to Kornberg and McConnell (169) the two broad lines cannot be due to two types of alkyl chain on different sites as was proposed in the first model. The second model assumes that all the lipid molecules are equivalent and so site exchange or lateral diffusion of lipid molecules at any rate will not affect the possibility of two types of motion along the alkyl chain.

Taking the OA/water neat phase first we would expect the broader line of width ca. 210μT (table XXIII) to originate from the methylene protons near to the hydrogen bonded NH_2 group, with the other line of width ca. 90μT originating from methylene protons at the end of the alkyl chain. The end methyl group and water protons give the narrow central line.

MG8/water neat phase also gives a line ca. 200μT wide (table XVII) which probably originates from the first few methylene protons after the carboxyl group. In the case of MG11/water neat phase the line-width is ca. 240μT (table XXI) indicating the reduced molecular motion of these methylene protons which one would expect to occur for a longer alkyl

chain.

The line of width ca. 150μT from MG8 and MG11/water neat phases is assumed to be due to the end methylene protons but probably also contains a contribution from the protons of the glyceryl residue. Since this residue will be somewhat restricted in its motion due to hydrogen bonding to the water layer the line-width is greater than that of the corresponding line for the OA/water neat phase.

The occurrence of only a single broad line ca. 110μT wide from the MG//18/water neat phase is probably due to the disruptive effect of the cis configuration around the double bond allowing greater freedom of motion of all the methylene protons along the alkyl chain and also the protons of the glyceryl residue so that the line-widths are virtually equivalent.

The line-widths and second moments ($0.2 - 0.5 \times 10^4 \mu T^2$) of all the neat phases are only ca. $\frac{1}{3} - \frac{1}{2}$ and 1/10 respectively of those of the α' - phases of anhydrous 1-monoglycerides. This is a reflection of the increased motion of the terminal methylene groups of the alkyl chains and also the increased rate of diffusion in the neat phase compared to the α'- phase.

3. The line-widths of MG8 and OA/water neat phases at room temperature decrease slightly with increasing water content. A similar decrease is also observed for the MG11/water neat phase at room temperature where the neat phase is metastable. Measurements were not carried out above 40°C where the neat phase would be stable since the probable loss of water from the samples would invalidate the results. MG//18/water neat phase shows a slight increase of line-width with increasing

water content at room temperature. The slight decrease in line-widths for the first three systems can be explained by the reasonable assumption that a slight increase in molecular motion of the alkyl chain occurs with increasing water content at room temperature. The slight increase in line-width for the MG//18/water neat phase is possibly associated with an increasing interaction between the alkyl chains which eventually leads to formation of the viscous isotropic phase at higher water contents. In the other three systems increase of water content leads to the formation of a dispersion.

4. The effect of increasing temperature on the line-widths from the neat phases of all four systems studied is very similar causing a relatively linear decrease of line-width with increasing temperature. The decrease in line-width with temperature for the broader line from samples containing ca. 0.8 mole fraction of water is $-2\mu T/^{\circ}C$, while for the other line the figure is $-1.5\mu T/^{\circ}C$. The larger negative slope for the broader line indicates that the motions of the two parts of the alkyl chain are becoming increasingly similar with increasing temperature.

5. Relaxation time measurements on the neat phases of the OA/water and MG8/water systems give three different T_2 values. The shortest T_2 observed, ca. $100\mu s$, corresponds to a line-width of ca. $100\mu T$(line-width $= 1/\sqrt{2\pi}\, T_2$). The agreement between line-widths calculated from T_2 values and those measured from PMR spectra is very good. For samples of MG8 and OA both containing 0.8 mole fraction of water the measured line-widths were $150\mu T$ and $90\mu T$ while those calculated from T_2 values were $155\mu T$ and $84\mu T$. This close agreement indicates that the widths of the broad-lines are

due solely to dipolar interactions and are not due to broadening by internal magnetic field gradients or diffusion through such gradients as thought previously (111,112,115). No shorter T_2 value corresponding to the broader line of width ca. 200 - 240μT was observable. This is probably because in the fast decay region part of the signal can be lost in the apparatus recovery time.

If we assume that the methyl protons and water protons are responsible for T_2(med.) and T_2(slow) respectively we can calculate the total number of protons responsible for all three T_2 values. Therefore for a particular sample composition we can calculate the number of protons contributing to the broader line. The way in which this is carried out is shown in appendix 1. For the MG8/water neat phase we can say that the protons of five methylene groups are contributing to the broader line and the protons of one methylene group and the glyceryl residue to the second broad line. For the OA/water neat phase we can say that the protons of ca. 4 methylene groups are contributing to the broader line and ca. 3 methylene groups to the second broad line.

Only one T_1 value was observed for all samples in each system studied indicating that spin diffusion is occurring making T_1 uniform over the whole system. We agree with Charvolin and Rigny (166) that the motion acting as an energy sink for the system probably consists of the internal isomeric rotations about the carbon-carbon bonds of the most 'liquid-like' part of the alkyl chain.

6. Further evidence for the occurrence of two distinguishable types of molecular motion are provided by

the PMR spectra from oriented neat phase samples of all four systems. The middle and outer doublets in these spectra originate from the dipole-dipole interaction of methylene group protons making up the alkyl chain and probably also the glyceryl residue. The way in which the magnitudes of the doublet splittings vary from system to system is very similar to the way in which the widths of the two broad lines vary. This indicates that the origins of the two doublets are the same as the origins of the two broad lines, i.e. the outer doublet originates from methylene protons close to the hydrogen bonded head group while the middle doublet originates from methylene protons near the end of the alkyl chain and also probably on the glyceryl residue.

The splittings of the two doublets from an oriented MG8/water neat phase are very similar indicating only a slight difference in the motion of the protons producing them. This is because as the alkyl chain is short there is unlikely to be a large distribution of motion along its length and so the majority of the methylene protons along the chain contribute to the outer doublet with apparently the protons of the methylene group adjacent to the terminal methyl group and the glyceryl residue protons giving the middle doublet. If the main contribution to the middle doublet originates from the protons of the glyceryl residue we would expect the middle doublet components to be slightly chemically shifted with respect to those of the outer doublet. This would lead to the downfield components of the two doublets overlapping while the upfield components would be separated more and this has been observed experimentally.

OA has a chain length similar to MG8 but now the middle and outer doublets from oriented OA/water neat phase are clearly distinguishable. The amine head group of OA is much smaller than the glyceryl residue head group of MG8 and therefore this might be expected to lead to better packing of the first few OA methylene groups with reduced molecular motion giving the wider outer doublet observed experimentally. Relaxation data given previously have indicated that protons from the first four methylene groups, i.e. 57% of the total methylene group protons, contribute to the outer doublet from oriented OA/water neat phase. This compares reasonably well with a value of 50 ± 10% calculated using curve fitting to integrated doublet spectra.

The middle and outer doublets from oriented MG11/water neat phase are clearly defined indicating the smaller relative contribution to the inner doublet of the glyceryl residue protons for the longer alkyl chain. If we assume that the protons of the first five methylene groups give the outer doublet, as was calculated earlier for MG8 from relaxation data, we find that this constitutes 43% of the methylene group and glyceryl residue protons. This compares reasonably well with a value of 40 ± 10% calculated using curve fitting to the integrated doublet spectra.

The middle doublet splitting from MG//18/water neat phase is significantly smaller than those observed from the other three systems. This indicates a much larger degree of motion for a part of the alkyl chain almost certainly that between the double bond and the terminal methyl group, with the cis configuration around the double bond being responsible

for the increase in freedom of motion. Since the outer doublet splitting in this case is almost the same as the inner doublet splitting for MG11/water neat phase we consider that the protons of the glyceryl residue and the remaining methylene protons are giving the outer doublet corresponding to the 110μT wide line from non-oriented samples. No line from non-oriented samples corresponding to the methylene protons at the end of the alkyl chain was observable because of its possible low intensity and the difficulty of separating it between the broad and narrow lines.

There is only a slight suggestion of a narrow central line in the spectra of oriented MG8/water and MG//18/water neat phases. This line is slightly more pronounced in spectra from MG11/water neat phases but this is possibly due to the greater difficulty in achieving a well-oriented sample since the smearing must be carried out at 45°C. A narrow central line would be expected from the 1-monoglyceride/water systems in view of the high degree of rotational freedom of methyl groups at these temperatures. It has been established by deuteration that methyl protons in nematic 4,4' - azoxy dianisole do give rise to a central single line (170) but Lippmann and Weber (171) noticed that in the nematic phases of the 4,4' - azoxydi-n-alkyloxybenzene series a middle peak was obtained for even chain lengths only. This alternation in behaviour of the methyl group may be connected with our inability to observe its resonance in our systems but further investigation is required to explain either occurrence.

7. Change in water content has only a slight effect on the splittings of the middle and outer doublets from

OA/water and MG8/water neat phases, the slight decrease being virtually within experimental error. However the middle and outer doublet splittings increase significantly for the MG//18/water neat phase with increasing water content. A similar significant increase is also observed for the MG11/water neat phase but only above ca. 40°C when the neat phase becomes stable as shown in figure 71 which is a superimposition of figures 60-63. This correlates with the fact that the maximum melting point of the neat phase is higher for these last two systems, being highest for the MG11/water neat phase which shows the largest increase in splittings. Therefore the motion of the alkyl chains of the short chain lipids appears to be independent of water content, while for the longer chain lipids the motion seems to decrease with increasing water content. It is possible that with increasing water content penetration of water into the region around the carboxyl group occurs, and therefore this additional hydrogen bonding reduces the motion of the alkyl chains to such an extent that additional Van der Waals' interaction occurs which is only significant for MG11 and MG//18 with their longer chains. This apparently significant increase in the Van der Waals' interaction between chains $\geqslant$ ca. eight carbon atoms is also probably responsible for the fact that only even membered alcohols with chain lengths $\geqslant$ C10 have been observed to form α-phases, the stability of which is very dependent on the water content (139).

8. The slopes for the changes of middle and outer doublet splittings with temperature for the systems studied are given in table L11. It is apparent that the slope for the outer doublet splitting is the greater, as would be

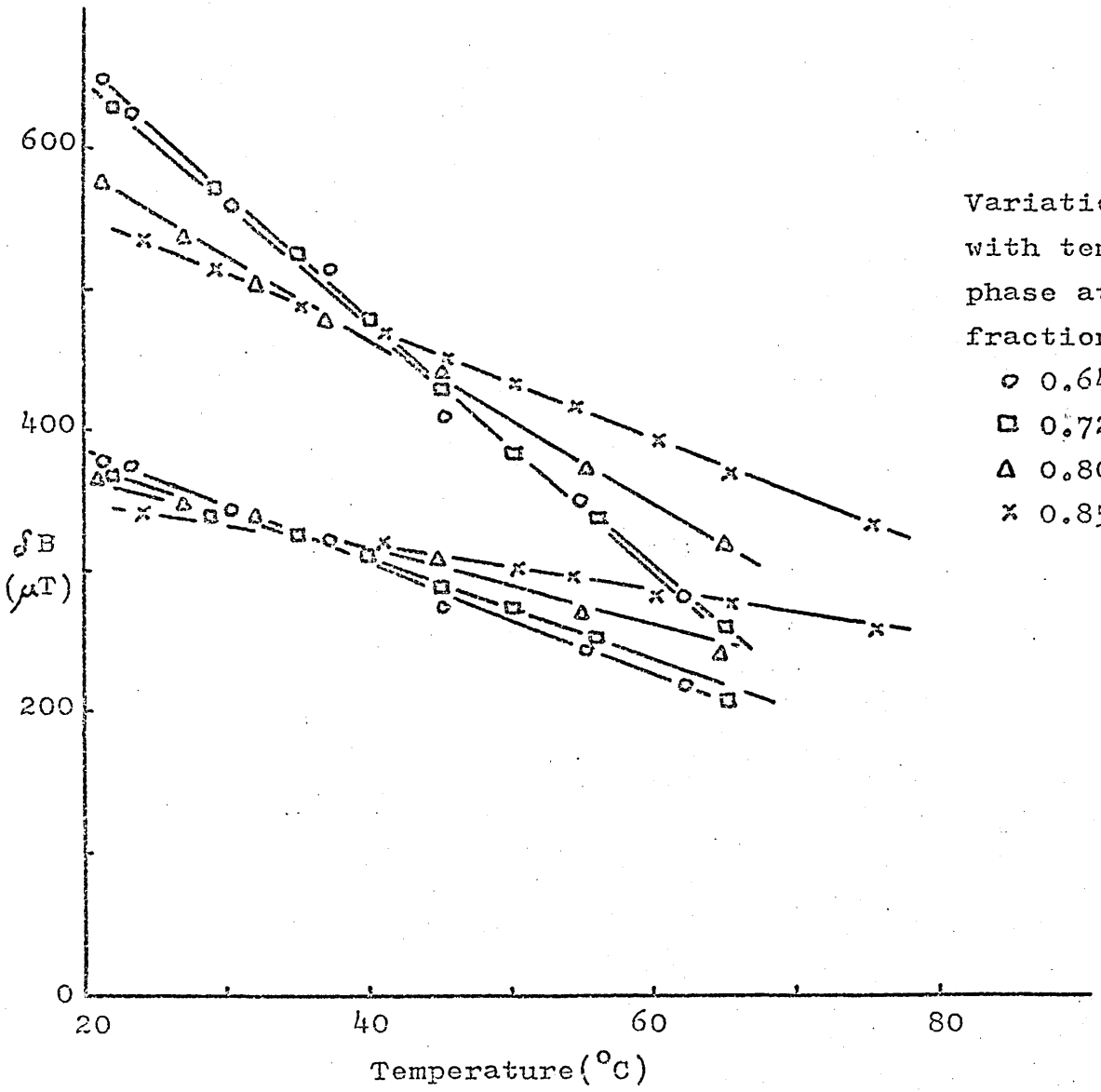

Figure 71

Variation of δB for middle and outer doublets with temperature for oriented MG11/H_2O neat phase at $\theta = 0^\circ$ containing the following mole fractions of H_2O

- ○ 0.64
- □ 0.72
- △ 0.80
- × 0.85

Table LII

		X_{H_2O}	Slope ($\mu T/^{o}C$) Middle doublet	Outer doublet
MG8	+	0.8	-	-2.6
MG11	+	0.64	-4.0	-9.0
MG11	+	0.72	-3.8	-8.7
MG11	+	0.80	-2.8	-5.8
MG11	+	0.85	-1.6	-4.0
MG//18	+	0.66	-3.0	-5.5
OA	+	0.85	-4.0	-4.7

expected, since the increasing temperature will tend to equalise the motions of the two parts of the chain. In the case of the MG11/water system it appears from extrapolation of the experimental lines as shown in figures 60-63 that at the temperature at which the motion of the chains becomes uniform the neat phase breaks down. For the other three systems there is still a measurable difference in the motion of the two parts of the chain when the neat phase breaks down. The stability of the neat phase will probably be controlled by the combination of the hydrogen bonding between the lipid end groups and the water layer, and the Van der Waals' interaction between the alkyl chains. The longer the chain the greater the interaction will be and therefore the MG11/water neat phase should be able to tolerate a much greater degree of motion of the alkyl chains before it breaks down than the neat phases of the shorter chain length lipids. The cis configuration around the double bond of MG//18 seems to reduce the Van der Waals' interaction between MG//18 chains to a level similar to that of MG8 chains on the basis of the similarity of the maximum neat phase melting points.

Values of E, the activation energy for the outer doublet narrowing motions, can be calculated using equations 19 and 20 and the δB/temperature data for the MG11/water and OA/water neat phases in tables XXXVI-XXXIX and XLIV respectively. If we take U = 740μT the splitting for methylene protons undergoing restricted rotation about an axis parallel to $\bar{B}_o$ with the interproton vector making an angle of 90° with the axis of rotation, and V=0, we obtain a value for E of ca. 30kJ mole^{-1}. In obtaining this figure we are assuming

that equations 19 and 20 are applicable to dipolar splittings as well as line-widths which is not unreasonable since a broad line is composed of many overlapping dipolar splittings. The value of E is probably only accurate to about an order of magnitude but is relatively close to the value which has been obtained from the approximate treatment of a hindered rotor (172).

Using the δB/temperature data on the inner doublets from the OA/water and MG11/water neat phases we now obtain a value for E of ca. 10kJ $mole^{-1}$. Therefore the potential barrier restricting the motion of the end of the alkyl chain is significantly smaller than that for the part of the chain nearest the head group. This suggests that the motion of this end of the chain can be circumscribed by a cone-shaped figure whose apex occurs at some point along the chain. The proposed total chain motion is shown in figure 72.

9. Using the fact that the proton-proton distance in a methylene group is 1.7862 Å we can calculate a value for L^{HH} of 42kHz for the dipole-dipole interaction associated with methylene group protons. Putting this figure into equation 26 leads to the expression $S_{22} = \delta B/63$ (where δB is in kHz) for the methylene groups. Using this expression we can calculate S_{22} values for the different parts of the alkyl chains in the four systems studied and these are given in table LIII.

An alkyl chain undergoing simple rotation about its long axis would give an S_{22} value of 0.5. Samples of MG11 + 0.64 mole fraction of water and OA + 0.85 mole fraction of water at 21°C and -20°C respectively, where the neat phase is metastable give S_{22} values, calculated

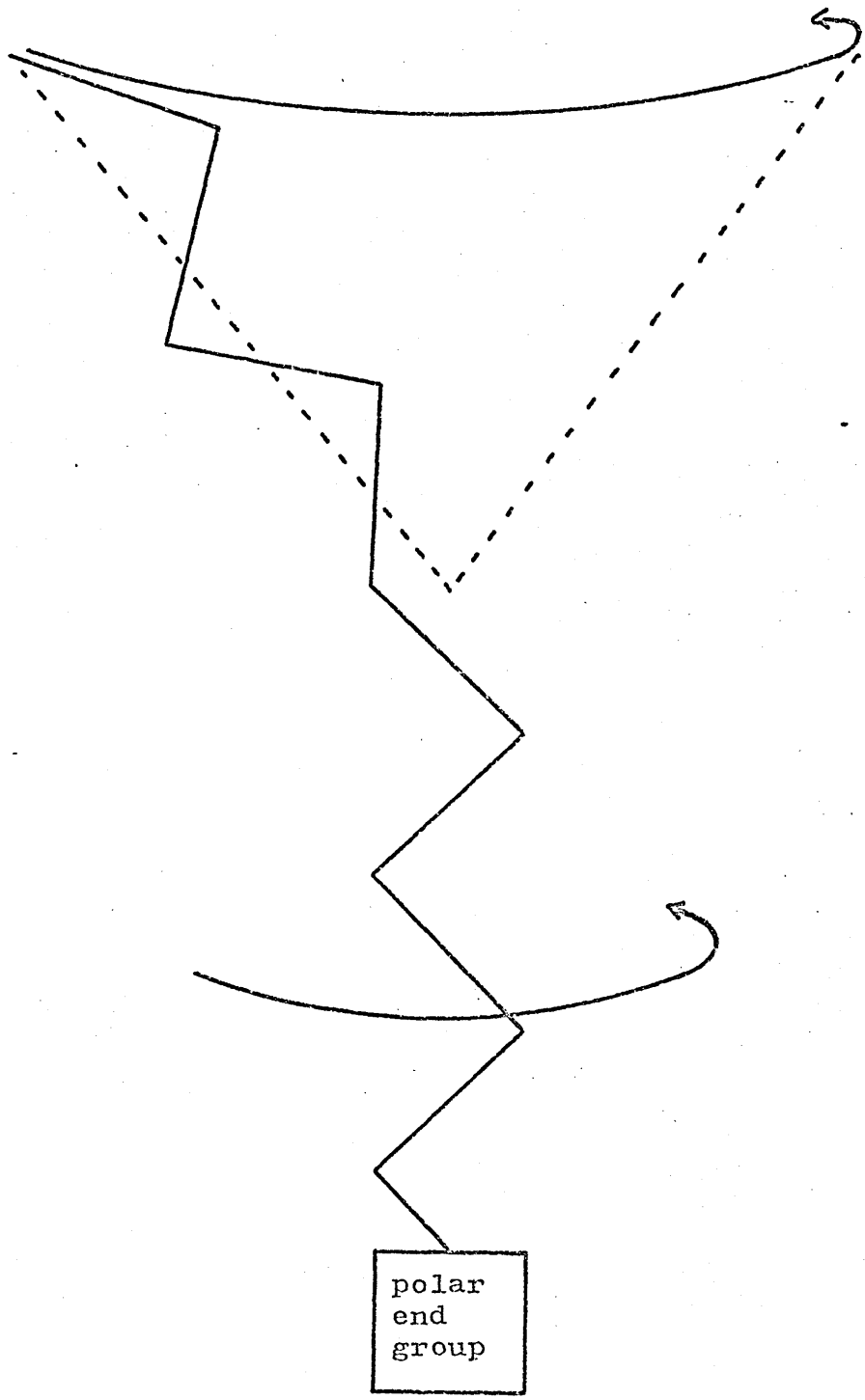

Figure 72

Diagram illustrating possible alkyl chain motion in bilayer

Table LIII

Calculated S_{22} values for middle and outer doublets of four different systems at 20°C.

		X_{H_2O}	S_{22} Value Middle	S_{22} Value Outer
MG8	+	0.8	0.21	0.26
MG11	+	0.8	0.25	0.39
MG//18	+	0.77	0.09	0.26
OA	+	0.8	0.16	0.37

from the outer doublet splittings, of 0.44 and 0.49 respectively. Therefore in the neat phase at low temperatures the part of the alkyl chain near the head group for MG11 and OA is undergoing virtually simple rotation. The highest comparable S_{22} values observed for MG8 + 0.8 mole fraction of water and MG//18 + 0.77 mole fraction of water were 0.32 and 0.31 at -15°C and 10°C respectively. The MG8/water sample became solid at this temperature but it is probably possible to cool the MG//18/water sample further to obtain higher values of S_{22}.

Lippmann and Weber (171) have obtained a maximum dipole splitting of 700μT for a magnetically oriented smectic mesophase of 4,4′ - azoxydi(n-heptyloxybenzene), giving an S_{22} value of 0.48. Our smaller S_{22} values in the stable neat phase regions and their negative temperature coefficients are more in line with the behaviour of nematic mesophases (171, 173-175) than that of 4,4′ - azoxydi(n-heptyloxybenzene) in which S_{22} is independent of temperature. A greater restriction to molecular motion might be expected in 4,4′ - azoxydi(n-heptyloxybenzene) since the molecule is effectively twice as long as any of our straight chain lipids. When the temperature is high enough (92°C) for this motion to affect the value of δB the molecules have by then acquired freedom of motion in a direction parallel to their long axes and transform to a nematic phase.

10. In the OA/water system we know that exchange is occurring between water protons and amine protons. Therefore making some assumptions it is possible to calculate a degree of order for the amine protons and hence the amine group,

and attempt to relate this to the degree of order of the alkyl chain.

If we assume firstly that the quadrupolar splitting from D_2O molecules in the OA + 0.8 mole fraction of D_2O neat phase in the absence of exchange would be similar to that from the MG8 + 0.8 mole fraction of D_2O neat phase, in which exchange does not affect the splitting, i.e. 1.75kHz, we can write for the overall splitting of 6.76kHz from the OA/D_2O neat phase:-

$$6.76 = 1.75 \times 0.8 + 0.2\ \Delta\nu_{ND_2}$$

where $\Delta\nu_{ND_2}$ is the quadrupolar splitting of the amine deuterons. This gives a value for $\Delta\nu_{ND_2}$ of 26.8kHz. Since the magnitudes of the quadrupole coupling constants for deuterons attached to oxygen or nitrogen are similar (163,176) we can use the value of $\Delta\nu_{ND_2}$ in equation (28) to obtain a value of S of 0.17 for the amine deuterons and hence the amine group. The values of S and S_{22} for the water molecules are very similar (tables XLVII and XLVIII) and it seems reasonable to assume therefore that S_{22} for the amine group is 0.17. It can be seen in table LIII that the appropriate S_{22} value for the methylene protons near to the amine group in the oriented neat phase is 0.37 which is approximately double the value we have calculated above from DMR spectra of the non-oriented neat phase. Since the dipolar and quadrupolar splittings from the same protons or deuterons are always twice as great in oriented as in non-oriented systems this suggests that the assumptions made are reasonable, and therefore that the motion of the amine group

in OA/water neat phases is very similar to that of the more rigid part of the alkyl chain. Therefore similar degrees of order have been obtained for a part of the alkyl chain from quadrupolar splitting of deuterons in the water layer and dipolar splittings of methylene protons in the hydrocarbon layer.

CHAPTER VI

HIGH RESOLUTION PMR OF 1-MONOGLYCERIDES

(I) Results and Discussion

1. High resolution PMR spectra have been obtained at 60 MHz and 25°C for MG8 and MG11 dissolved in carbon tetrachloride. The spectra were very similar, that of MG11 being shown in figure 73 and the band assignments given in table LIV. These are substantially in agreement with the assignments and chemical shift values reported previously by Chapman (42) and Hopkins (43).

The high resolution PMR spectrum has been observed at 220 MHz for MG8 dissolved in deuterated dimethyl sulphoxide (d_6-DMSO). The spectrum is similar to the 60 MHz spectrum of MG11 in CCl_4 up to 3.2 ppm but beyond this the higher operating frequency allows the hydroxyl and glyceryl residue protons and their splitting patterns to be resolved.

5 x expansions of the spectrum between 3.2 and 4.2 ppm, and 4.2 and 5.2 ppm are shown in figures 74 and 75. The bands are assigned in table LV.

2. The resonances at 4.6 ppm and 4.85 ppm have been assigned to primary and secondary hydroxyl protons respectively on the basis of their spin-spin coupling patterns involving the methylene and methine protons. $J_{HCOH'}$ which is known to be positive (177), is 5.5 Hz for the coupling between the primary hydroxyl proton and the methylene protons, and 4.8 Hz for the coupling between the secondary hydroxyl proton and the methine proton. J_{HCOH}

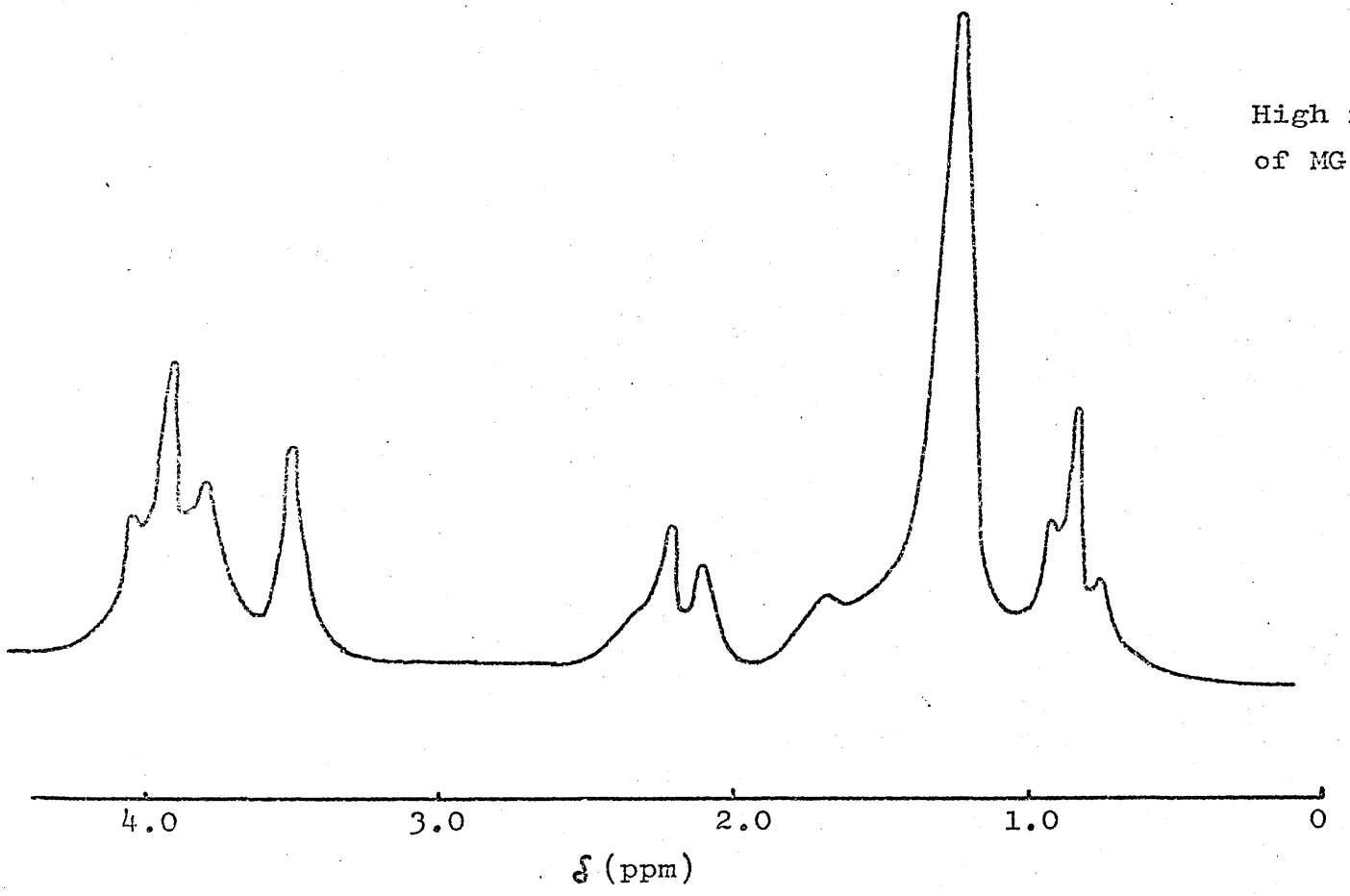

Figure 73

High resolution PMR spectrum of MG11 in CCl_4

Table LIV

Band assignments for high resolution PMR spectrum of MG11 in CCl_4.

δ (ppm)	Group
0.9	$\underline{CH_3}CH_2$
1.3	$(\underline{CH_2})_6$
2.32	$\underline{CH_2}CO$
3.57	$\underline{CH_2}OH$
3.85	$\underline{CH}OH$
3.97	$\underline{OH}$
4.04	$\underline{CH_2}OCO$
4.1	$\underline{OH}$

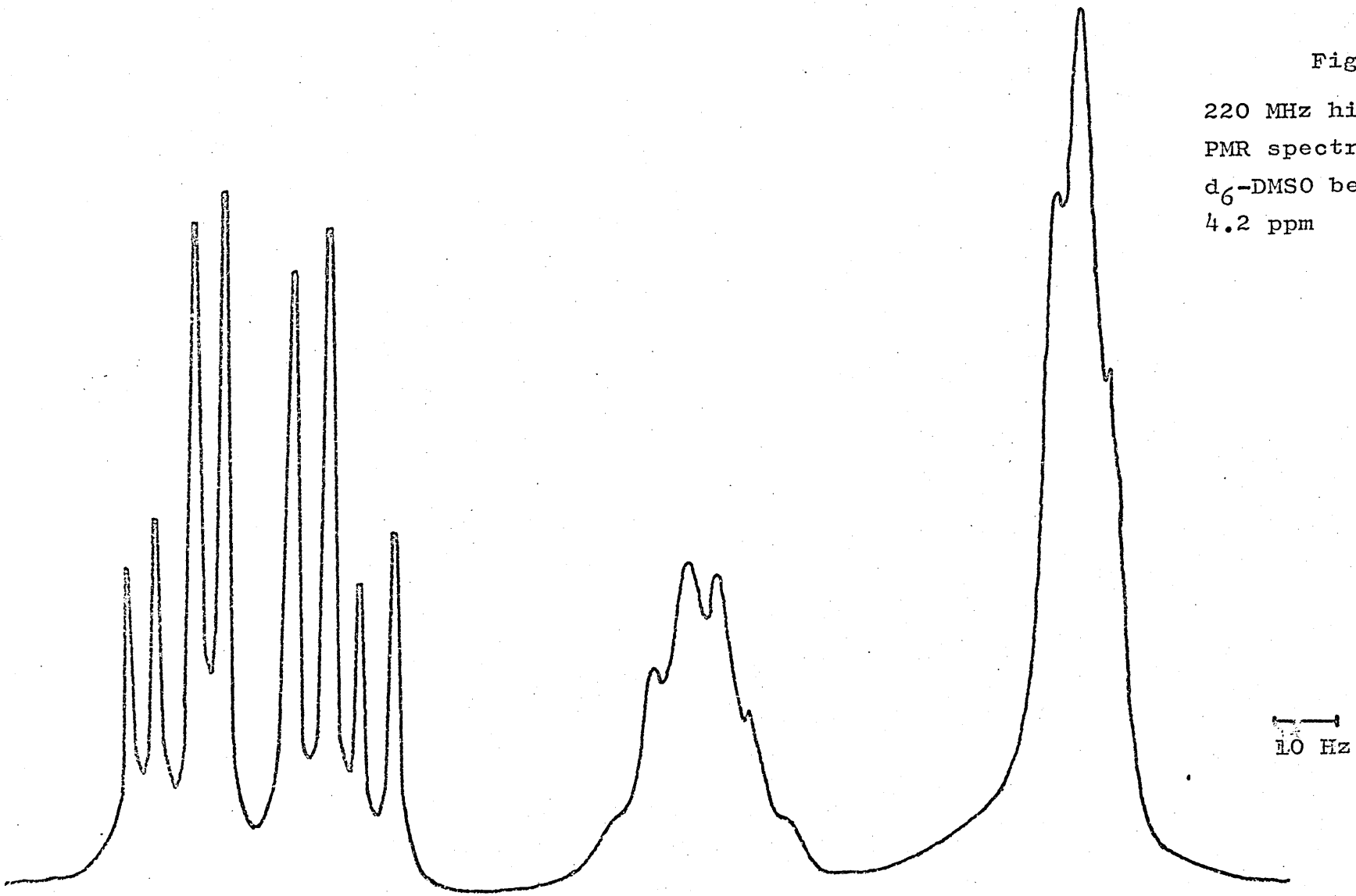

Figure 74

220 MHz high resolution PMR spectrum of MG8 in d_6-DMSO between 3.2 and 4.2 ppm

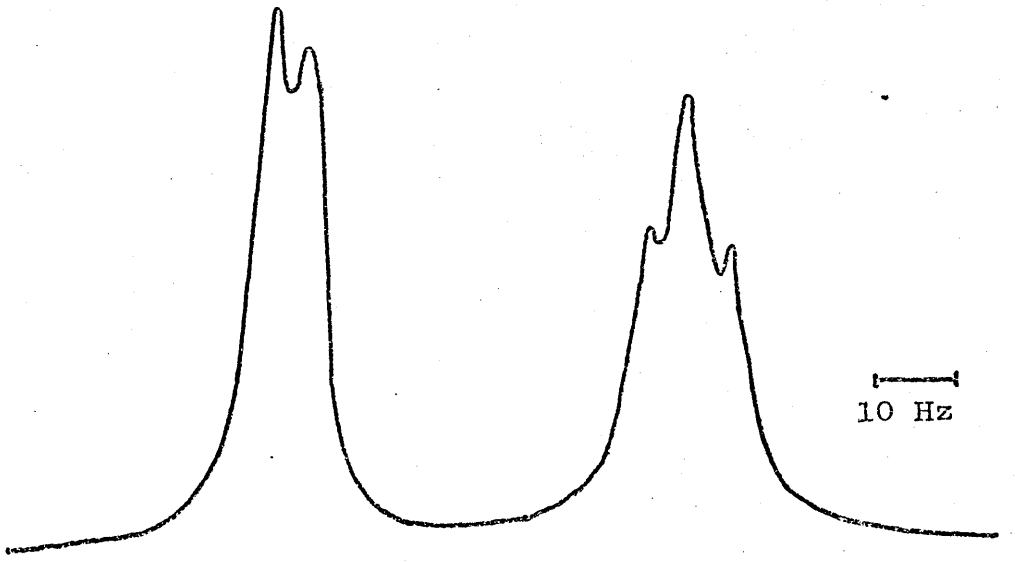

Figure 75

220 MHz high resolution PMR spectrum of MG8 in d_6-DMSO between 4.2 and 5.2 ppm

Table LV

Band assignments for 220 MHz high resolution PMR spectrum of MG8 in d_6-DMSO.

Chemical Shift (ppm)	Type	Group
0.9	triplet	$\underline{CH_3}CH_2$
1.3	singlet	$(\underline{CH_2})_4$
1.55	triplet	$\underline{CH_2}CH_2CO$
2.3	triplet	$\underline{CH_2}CO$
3.4	triplet	$\underline{CH_2}OH$
3.7	sextet	$\underline{CH}$
4.0	octet	$\underline{CH_2}OCO$
4.6	triplet	$CH_2\underline{OH}$
4.85	doublet	$CH\underline{OH}$

values for simple unsubstituted primary and secondary alchols have been found to be 5.1 Hz and ca. 4.5 Hz respectively (178,179). It has also been found that electronegative substituents on the β carbon atom increases J_{HCOH} values (180), which explains our higher observed values, the substituents being in one case OH and in the other OH and $CH_3(CH_2)_6COO$.

Chapman and King (181) have found the primary and secondary hydroxyl proton chemical shifts of propane-1,2-diol in d_6-DMSO to be 4.45 ppm and 4.38 ppm respectively. However in the case of MG8 the secondary hydroxyl proton resonates downfield of the primary hydroxyl proton which itself is only slightly chemically shifted (0.15 ppm downfield) from the propane-1,2-diol primary hydroxyl proton resonance. It has also been found that the chemical shifts of the two MG8 hydroxyl proton resonances are virtually invariant with concentration over the range 1.5 - 15% w/v for solutions of MG8 in d_6-DMSO, the shifts being 1Hz downfield. Furthermore in the infra-red spectrum of MG8 in d_6-DMSO the band due to the carbonyl group is a doublet at 1731.6 cm^{-1} and 1739 cm^{-1}, the former band being from a hydrogen-bonded carbonyl group and the latter a non hydrogen-bonded carbonyl group. There was no significant change in wavelength or intensity of the bands over the range 1.5 - 15% w/v of MG8 in d_6-DMSO.

The above results suggest that the OH groups are predominantly involved in either intramolecular hydrogen bonds (182) or some form of hydrogen bonding to DMSO (177-181).

There are several possible intramolecular hydrogen bonded structures and it is obvious from the above infra-red work that the carbonyl group must be involved to a significant extent. Some of the possible structures are shown in figure 76 and there

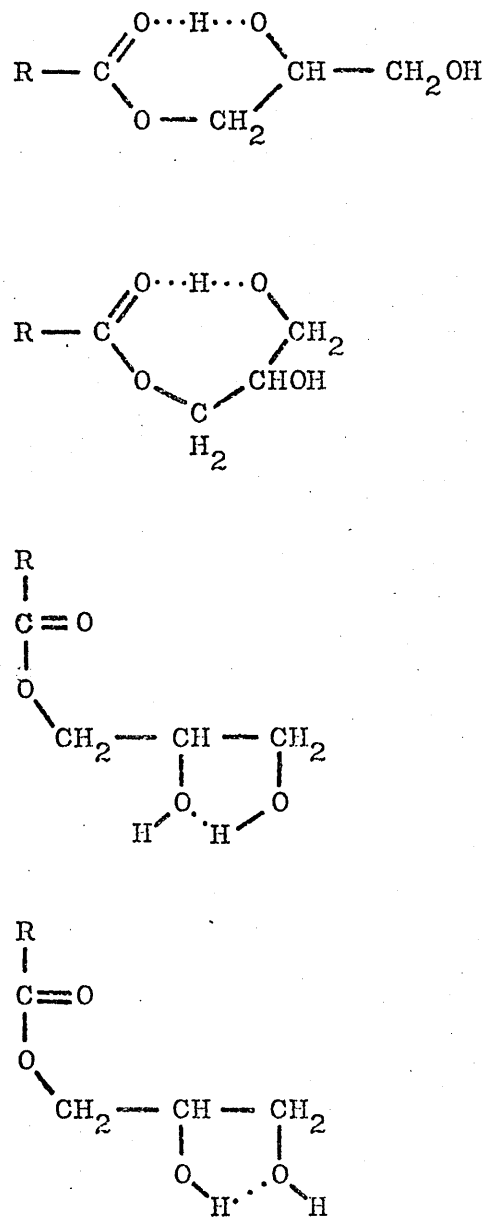

R is $CH_3(CH_2)_6$

Figure 76

Possible intramolecularly hydrogen-bonded structures of 1-mono-octanoin in solution

are also some structures which will involve the alkoxy oxygen. Some attempt to estimate the predominating forms is being made by extended IR and NMR studies.

3. To simplify the discussion of the spin-spin splitting pattern from the protons of the glyceryl residue we can regard the MG8 molecule as a substituted ethane CH_2U-CHVW, where U is $CH_3(CH_2)_6COO$, V is OH and W is CH_2OH. The three protons of the substituted ethane form an approximate ABX system which has been analysed using the method described by Abraham (183). The geminal protons of the CH_2U- group give the octet at 4.0 ppm with values of δ_{AB} and J_{AB} of 25.75 Hz and -11 Hz respectively. J_{AX} and J_{BX} have been found to be 4.45 Hz and 6.55 Hz respectively. Similar J_{AB} values have been reported for compounds containing methylene groups adjacent to one oxygen atom (184,185).

Because of the number of possible intramolecularly hydrogen-bonded structures and the unknown effect of the three electro-negative substituents U,V and W it was decided that any attempt to use the J_{AX} and J_{BX} values in the Karplus equation (186) to calculate dihedral angles to obtain the conformation of the glyceryl residue would not be worthwhile.

A six line pattern would be expected from the X proton of an ABX system and such a pattern is observed from the methine proton of the -CHVW group at 3.7 ppm. However this is probably only fortuitous since this proton will also be coupled to the methylene protons of group W and the hydroxyl proton of group V, and there-fore a highly complex spin-spin splitting pattern would be expected. However non-resolution and overlap of several of the theoretical lines has probably reduced this complex pattern to the sextet observed.

Coupling of the methylene protons of group W to the hydroxyl proton in the same group and to the proton of the CHVW group would be expected to give a quartet but overlapping of the two centre lines reduces this to the distorted triplet observed at 3.4 ppm.

CHAPTER VII

CONCLUSIONS

(I) Polymorphism of 1-monoglycerides

The polymorphic forms of MG18, obtained by thermal treatment, and their transition temperatures observed in this work are in good agreement with those reported previously. The polymorphic transitions are reversible, and the polymorphs are stable over their appropriate temperature ranges.

The polymorphism of 1-monoglycerides in the range MG8-MG12 is exceptionally complex since most of the polymorphic transitions are only reversible in the short term, and the majority of the polymorphs are metastable changing at various rates to the stable B-form.

PMR second moments and line-widths from the α' - phase (Lutton's α - phase (20)) are consistent with a structure in which the alkyl chains are rotating about their long axes. The experimental values are slightly lower than those predicted theoretically which agrees with the concept that the chains are possibly tilted instead of vertical, as in an α - phase, or that the chain motion is slightly more complex than just simple rotation.

Two new polymorphic forms produced by thermal treatment have been observed for MG8 and MG12. Characterisation of these forms has proved impossible due to their exceeding short life-

times.

In addition to the polymorphic forms reported previously, for 1-monoglycerides in the range MG8-MG12 an l.c. phase has been observed existing over a range of 2-3°C before the transition to α'- phase. Addition of small amounts of water (up to ca. 0.45 mole fraction) increases the range of stability of the l.c. phase and α'- phase, almost certainly by forming a hydrogen-bonding network with the polar end groups.

Broad-line PMR spectra of the metastable l.c. phase are very similar to those of the stable l.c. phase at high water contents, indicating that the structures of the two phases are probably very similar.

(II) Structure of the neat phases

(a) Water layer

The NMR results can be adequately explained in terms of a model for the water layer in which each water molecule possesses a small partial orientation caused by it spending part of its time hydrogen-bonded to the polar end groups of the lipid molecules.

The partial orientation is principally a function of the mole fraction of water present and is only slightly affected by the nature of the lipid in the systems studied.

Only slow exchange has been found to occur between 1-monoglyceride hydroxyl protons or deuterons and water, while rapid exchange occurs between OA amine protons or deuterons and water. For this reason the degree of order calculated for the water in the OA/water neat phase appears to be greater than that calculated for the water in the 1-monoglyceride/water neat phase.

(b) Lipid layer

NMR results have indicated that the lipid molecules in the

bilayer are undergoing rapid two dimensional diffusion at $\gtrsim$ ca. 3 kHz. Each individual lipid molecule is also rotating about its long axis with a significant increase in the complexity of this rotational motion occurring at ca. 4-5 methylene groups along the alkyl chain from the polar head group for the saturated lipids.

Calculation of the activation energy for the motion of the first few methylene groups of the MG11 and OA chains at low temperatures has indicated that virtually simple rotation of these methylene groups is occurring with the remaining methylene groups and terminal methyl group sweeping out a cone-shaped envelope.

The significant increase in motion for the MG//18 molecule probably occurs at the cis double bond. We consider that a significant twisting of the end part of the oleyl chain, to make it more cylindrical, will be necessary in order for it to rotate about its long axis without interfering with the motion of adjoining molecules in the bilayer.

(III) <u>1-monoglycerides in solution</u>

The resonance lines occurring in the high resolution PMR spectra of 1-monoglycerides in CCl_4 and d_6-DMSO have been assigned including those from the primary and secondary hydroxyl protons. Values of J_{HCOH}, and J_{AB}, J_{AX}, and J_{BX} appropriate to the protons of the glyceryl residue have been calculated.

Comparison of the chemical shifts of the primary and secondary hydroxyl protons with those from simpler but similar compounds, and the effect of concentration changes on the chemical shift has indicated that a large amount of intramolecular hydrogen-bonding occurs in the 1-monoglyceride molecules in solution. This has been confirmed by an infra-red study of the carbonyl band. Several possible hydrogen-bonded structures are discussed and

further experiments to determine which of these predominate are outlined.

APPENDIX I

Calculation of the number of protons contributing to the two broad-lines in the PMR spectra from non-oriented MG8/water and OA/water neat phases.

(I) <u>MG8 + 0.66 mole fraction of H_2O</u>

The total number of protons in the components of this system ($MG8.2H_2O$) is 26 divided up as follows:-

Groups	Number of protons
Methyl	3
Alkyl chain	12
Glyceryl residue	5
Hydroxyl	2
Water molecules	4

Since no T_2 value was observed corresponding to the widest line we assume that the signal due to the protons producing this line has been lost during the recovery time of the apparatus. We also assume that T_2(med.) and T_2(slow) originate from the methyl, hydroxyl, and water protons, and therefore these nine protons constitute 66% of the total intensity (table XX). This means that the total number of protons contributing to the decay curve is fourteen which gives a total of twelve protons left for the widest line. This corresponds to all six methylene groups of the MG8 chain.

To check the calculations we find that the five glyceryl

residue protons constitute 36% of the total number of protons contributing to the decay which agrees very well with the experimental intensity of T_2 fast of 34%.

(II) MG8 + 0.8 and 0.9 mole fractions of H_2O

Similar calculations to those described above have been carried out with the relaxation time intensities of the above two systems. It has been calculated that the protons of five methylene groups are contributing to the widest line.

The calculations have been checked as described above and we find that the five glyceryl residue protons and the remaining two methylene protons combined constitute 35% and 23% of the total number of protons contributing to the observed decays. These compare well with experimental values of 32% and 22%.

(III) OA + 0.8, 0.85, and 0.915 mole fractions of H_2O

Similar calculations to those described above have been carried out with the relaxation time intensities of the above three systems. It has been calculated that the protons of ca. four methylene groups are contributing to the widest line.

The calculations have been checked as described above and good agreement has been obtained between calculated and experimental percentages of the protons contributing to T_2(fast).

The slight variation of the intensities of the relaxation times with τ could make the above calculations somewhat suspect. However the percentages of protons constituting the most rigid part of the alkyl chain calculated above are in good agreement with those calculated using the line-shapes derived by integrating PMR spectra of the middle and outer doublet splittings from oriented samples of the appropriate systems.

REFERENCES

1. D.M. Small, J. Amer. Oil Chem. Soc., 45, 108, 1968.
2. A.S.C. Lawrence, Mol. Cryst. Liquid Cryst., 7, 1,1969.
3. D. Chapman, 'Introduction to Lipids', McGraw-Hill, 1969.
4. J.W. McBain, 'Colloid Chemistry', ed. J. Alexander, Chemical Catalog Company Inc., New York, 1926, p. 137.
5. A.S.C. Lawrence, A. Bingham, C.B. Cooper and K. Hume, J. Phys. Chem., 68, 3470, 1964.
6. F. Krafft and H. Wiglow, Ber., 28, 2566, 1895.
7. A.F. Hofmann, Gastroenterology, 48, 484, 1965.
8. R.D. Vold and J.W. McBain, J. Amer. Chem. Soc., 63, 1296, 1941.
9. D.M. Small, M. Bourges, and D.G. Dervichian, Biochim. Biophys. Acta., 125, 563, 1966.
10. D.M. Small, M. Bourges, and D.G. Dervichian, Nature, 211, 816, 1966.
11. A.F. Hofmann and D.M. Small, Ann. Rev. Med., 18, 333, 1967.
12. D. Chapman, Chem. Rev., 62, 433, 1962.
13. K. Larsson, Arkiv Kemi, 23, 29, 1964.
14. K. Larsson, Arkiv Kemi, 23, 35, 1964.
15. E. Fischer, M. Bergmann, and H. Barwind, Ber., 53, 1589, 1920.
16. R.S. Rewadikar and H.E. Watson, J. Indian Inst. Sci., 13A, 128, 1930.
17. T. Malkin and M.R. El Shurbagy, J. Chem. Soc., 1628, 1936.
18. B.F. Daubert and A.R. Baldwin, J. Amer. Chem. Soc., 66, 997, 1944.
19. M.G.R. Carter and T. Malkin, J. Chem. Soc., 554, 1947.
20. E.S. Lutton and F.L. Jackson, J. Amer. Chem. Soc., 70, 2445, 1948.

21. T. Malkin, 'Progress in the Chemistry of Fats and other Lipids', Pergamon Press, London, Vol. 2, Ch. 1, 1954.

22. A.T. Gros and R.O. Feuge, J.Amer. Oil Chem. Soc., 34, 239, 1957.

23. L.J. Filer, Jr., S.S. Sidhu, B.F. Daubert, and H.E. Longenecker, J. Amer. Chem. Soc., 66, 1333, 1944.

24. D. Chapman, Nature, 176, 216, 1955.

25. D. Chapman, J. Chem. Soc., 55, 1956.

26. D. Chapman, R.E. Richards, and R.W. Yorke, J. Chem. Soc., 436, 1960.

27. Bhide and Bhide, J. Univ. Bombay, 8, 220, 1939.

28. R.W. Crowe and C.P. Smyth, J. Amer. Chem. Soc., 72, 4427, 1950.

29. R.S. Stein and G.B.B.M. Sutherland, J. Chem. Phys., 22, 1993, 1954.

30. L. Robert and J. Favre, Compt. Rend., 234, 2270, 1952.

31. A. Muller, Proc. Roy. Soc., 138A, 514, 1932.

32. R.S. Stein, J.Chem. Phys., 23, 734, 1955.

33. T. Malkin, Trans. Faraday Soc., 29, 977, 1933.

34. J.D. Bernal, Z. Krist., 83, 153, 1932.

35. S. Abrahamsson, S. Aleby, G. Larsson, K. Larsson, Acta. Cryst., 13, 1044, 1960.

36. K. Larsson, Arkiv Kemi, 23, 23, 1964.

37. N.H. Kuhrt, E.A. Welch, W.P. Blum, E.S. Perry and W.H. Weber, J. Amer. Oil Chem. Soc., 29, 261, 1952.

38. J.R. Barcelo and C.S. Martin, J. Phys. Radium, 5, 403, 1954.

39. R.T. O'Connor, E.F. DuPre, and R.O. Feuge, J.Amer. Oil Chem. Soc., 32, 88, 1955.

40. D. Chapman, J. Amer. Oil Chem. Soc., 37, 73, 1960.

41. R.J. Warren, J.E. Zarembo, C.W. Chong and M.J. Robinson, J. Pharm. Sci., 59, 109, 1970.

42. D. Chapman, J. Chem. Soc., 131, 1963.

43. C.Y. Hopkins, 'Progress in the Chemistry of Fats and other Lipids', Pergamon Press, London, Vol.8, Pt.2, p. 213, 1965.

44. R. Virchow, Archiv., 6, 502, 1854.

45. Neubauer, Analyt. Zeit., 6, 189, 1863.

46. Neubauer, Liter. Centralbl., 491, 1863.

47a. G.H. Brown and W.G. Shaw, Chem. Rev., 57, 1049, 1957.

47b. G.H. Brown, J.W. Doane, V.D. Neff, Crit. Revs. in Solid State Sci., 1, 303, 1970.

48. I.G. Chistyakov, Soviet Physics Cryst., 5, 917, 1961.

49. P.A. Winsor, Chem. Rev., 68, 1, 1968.

50. A.S.C. Lawrence, Faraday Soc. Disc., 25, 51, 1958.

51. A.S.C. Lawrence, Nature, 183, 14, 1959.

52. A.S.C. Lawrence, Ch. 7 in 'Surface Activity and Detergency', Ed. K. Durham, London, 1961.

53. A.W. Ralston, C.W. Hoerr, and E.J. Hoffman, J. Amer. Chem. Soc., 64, 1516, 1942.

54. E.S. Lutton, J. Amer. Oil Chem. Soc., 43, 28, 1966.

55. K.D. Lawson and T.J. Flautt, Mol. Cryst., 1, 241, 1966.

56. F.K. Broome, C.W. Hoerr and H.J. Harwood, J. Amer. Chem. Soc., 73, 3350, 1951.

57. R.R. Balmbra, J.S. Clunie, and J.F. Goodman, Nature, 222, 1159, 1969.

58. J.S. Clunie, J.M. Corkhill, and J.F. Goodman, Proc. Roy. Soc., A285, 520, 1965.

59. E.S. Lutton, J. Amer. Oil Chem. Soc., 42, 1068, 1965.

60. A.S.C. Lawrence and M.P. McDonald, Mol. Cryst., 1, 205, 1966.

61. K. Larsson, Zeit., Phys. Chem., 56, 173, 1967.

62. N. Krog and J. Andreasen, Nord. Symp. Graensefladekemi, Fortryk Foredrag, 3rd, I, 1967.

63. N. Krog and K. Larsson, Chem. Phys. Lipids, 2, 129, 1968.

64. B. Ellis, M.P. McDonald, A.S.C. Lawrence and W.E. Peel, 'Liquid Crystals and Ordered Fluids', J.F. Johnson and R.S. Porter, Ed. Plenum Press, New York, 1970.

65. J.S. Clunie, J.F. Goodman, and P.C. Symons, Trans. Faraday Soc., 65, 287, 1969.

66. D.M. Small, J. Lipid Research, 8, 551, 1967.

67. F.B. Rosevear, J. Amer Oil Chem. Soc., 31, 628, 1954.

68. F.B. Rosevear, J. Soc. Cosmetic Chemists, 19, 581, 1968.

69. J. Stauff, Kolloidzeitschrift, 89, 224, 1939.

70. T. Doscher and R. Vold, J. phys. Colloid Chem. 52, 97, 1948.

71. W. Philippoff and J.W. McBain, Nature, 164, 885, 1949.

72. V. Luzzati, H. Mustacci, and A. Skoulios, Nature, 180, 600, 1957.

73. V. Luzzati, H. Mustacci, and A. Skoulios, Disc. Faraday Soc., 25, 43, 1958.

74. V. Luzzati, H. Mustacci, A. Skoulios and F. Husson, Acta. Cryst., 13, 660, 1960.

75. F. Husson, H. Mustacci and V. Luzzati, Acta Cryst., 13, 668, 1960.

76. V. Luzzati and F. Husson, J. Cell Biology, 12, 207, 1962.

77. B. Gallot and A.E. Skoulios, Kolloidzeitschrift, 208, 37, 1966.

78. R.R. Balmbra, J.S. Clunie, and J.F. Goodman, Mol. Cryst., 3, 281, 1967.

79. D.A.B. Bucknall, J.S. Clunie, and J.F. Goodman, Mol. Cryst. Liquid Cryst., 7, 215, 1969.

80. F. Reiss-Husson, J. Mol. Biology, 25, 363, 1967.

81. A. Skoulios, Advan. Colloid Interface Sci., 1, 79, 1967.

82. V. Luzzati, Ch. 3, 'Biological Membranes', ed. D. Chapman, Academic Press, 1969.

83. K.D. Lawson, A.J. Mabis and T.J. Flautt, J. Phys. Chem., 72, 2058, 1968.

84. R.R. Balmbra, J.S. Clunie, and J.F. Goodman, Proc. Roy. Soc., A285, 534, 1965.

85. J.W. McBain and S.S. Marsden, J. Chem. Phys. 15, 211, 1947.

86. S.S. Marsden and J.W. McBain, J. phys. Colloid Chem., 52, 110, 1948.

87. V. Luzzati, F. Reiss-Husson, E. Rivas, and T. Gulik-Krzywicki, Ann. N.Y. Acad. Sci., 137, 409, 1966.

88. T. Gulik-Krzywicki, E. Rivas, and V. Luzzati, J. Mol. Biology, 27, 303, 1967.

89. A.D. Bangham and R.W. Horne, J. Mol. Biology, 8, 660, 1964.

90. W. Stoeckenius, J. Cell Biol., 12, 221, 1962.

91. D. Chapman, Ch. 4 in 'Biological Membranes', ed. D. Chapman, Academic Press, 1969.

92. L.D.R. Wilford, Sheffield Polytechnic, unpublished results.

93. P. Byrne and D. Chapman, Nature, 202, 987, 1964.

94. D. Chapman, in 'The strucutre of Lipids', Methuen and Co. Ltd., London, 1965.

95. A.H. Maddy and B.R. Malcolm, Science, N.Y., 150, 1616, 1965.

96. J.L. Kavanu, Science, N.Y., 153, 213, 1966.

97. D.F.H. Wallach and P.H. Zahler, Proc. Natn. Acad. Sci., U.S.A., 56, 1552, 1966.

98. D. Chapman, V.B. Kamat, R.J. Levene, Science, N.Y., 160, 314, 1968.

99. J. Seelig, J. Amer. Chem. Soc., 92, 3881, 1970.

100. M.P. McDonald, Arch. Sci. (Geneva), 12,141, 1959.

101. K.W. Herrmann, J.G. Brushmiller and W.L. Courchene, J. Phys. Chem. 70, 2909, 1966.

102. C.A. Gilchrist, J. Rogers, G. Steel, E.G. Vaal, and P.A. Winsor, J. Colloid Interface Sci., 25, 409, 1967.

103. J.M. Corkhill, J.F. Goodman, and J. Wyer, Trans. Faraday Soc., 65, 9, 1969.

104. K.D. Lawson and T.J. Flautt, J. Phys. Chem., 72, 2066, 1968.

105. K.D. Lawson and T.J. Flautt, J. Phys. Chem., 69, 4256, 1965.

106. J. Charvolin and P. Rigny, J. Phys. (Paris) 30, C4-76, 1969.

107. R. Blinc, K. Easwaran, J. Pirs, M. Volfan and I. Zupancic, Phys. Rev. Letters, 25, 1327, 1970.

108. J.J. de Vries and H.J.C. Berendsen, Nature, 221, 1139, 1969.

109. E.R. Andrew, J. Chem. Phys., 18, 607, 1950.

110. T. Drakenberg, A. Johansson, and S. Forsen, J. Phys. Chem., 74, 4528, 1970.

111. J.R. Hansen and K.D. Lawson, Nature, 225, 542, 1970.

112. S.A. Penkett, A.G. Flook, and D. Chapman, Chem. Phys. Lipids, 2, 273, 1968.

113. J. Charvolin and P. Rigny, J. Magnetic Resonance, 4, 40, 1971.

114. N.J. Salisbury, D. Chapman and G. Parry-Jones, Trans. Faraday Soc., 66, 1554, 1970.

115. S. Kaufman, J.M. Steim, and J. H. Gibbs, Nature, 225, 743, 1970.

116. G.J.T. Tiddy, Nature, 230, 136, 1971.

117. S.I. Chan, G.W. Feigenson, and C.H.A. Seiter, Nature, 231, 110, 1971.

118. S. Meiboom and D. Gill, Rev. Sci. Instr., 29, 688, 1958.

119. A.Y. Carr and E.M. Purcell, Phys. Rev., 94, 630, 1954.

120. G.E. Pake, J. Chem. Phys., 16, 327, 1948.

121. E.R. Andrew and R. Bersohn, J. Chem. Phys., 18, 159, 1950.

122. J. Itoh, R. Kusaka, R. Kiriyama, Y. Yamagata and H. Ibamoto, J. Chem. Phys., 20, 1503; 21, 190, 1952.

123. J. Itoh, R. Kusaka, R. Kiriyama, Y. Yamagata, and H. Ibamoto, J. Phys. Soc. Japan, 8, 293, 1953.

124. K. Tomita, Progr. Theor. Phys., 8, 138, 1952.

125. K. Tomita, Phys. Rev., 89, 429, 1953.

126. R. Bersohn and H.S. Gutowsky, J. Chem. Phys., 22, 651, 1954.

127. J.H. van Vleck, Phys. Rev., 74, 1168, 1948.

128. H.S. Gutowsky and G.E. Pake, J. Chem. Phys., 18, 162, 1950.

129. E.R. Andrew, J. Chem. Phys., 18, 607, 1950.

130. E.R. Andrew and R.G. Eades, Proc. Roy. Soc., 216A, 398, 1953.

131. N. Bloembergen, E.M. Purcell, and R.V. Pound, Phys. Rev., 73, 679, 1948.

132. R.V. Pound, Phys. Rev., 79, 685, 1950.

133. M.H. Cohen and F. Reif, Solid State Phys., 5, 321, 1957.

134. D.C. Malins and H.K. Mangold, J. Amer. Oil Chem. Soc., 37, 383 and 576, 1960.

135. K. Randerath, Thin Layer Chromatography, (Verlag Chemie Academic Press), 1964.

136. D.A. Vassolo and J.C. Harden, Anal. Chem., 34, 132, 1962.

137. G. Friedel, Ann. de physique, 18, 300, 1922.

138. H.G. Olf and A. Peterlin, J. Polymer Sci., A-2, 8, 791, 1970.

139. A.S.C. Lawrence, M.A. Al-Mamun, and M.P. McDonald, Trans. Faraday Soc., 63, 2789, 1967.

140. M. Tasumi, T. Shimanouchi, A. Watanabe, and R. Goto, Spectrochimica Acta., 20, 629, 1964.

141. S. Friberg and L. Mandell, J. Pharm. Sci., 59, 1001, 1970.

142. P. Ekwall, L. Mandell, and K. Fontell, Mol. Cryst. Liquid Cryst., 8, 157, 1969.

143. A. Johansson and T. Drakenberg, Mol. Cryst. Liquid Cryst., 14, 23, 1971.

144. N. Persson and A. Johansson, Acta. Chem. Scand., 25, 2118, 1971.

145. P. Ducros, Bull. Soc. franc. Miner. Crist., 83, 85, 1960.

146. Y. Ayant, P. Ducros, X. Pare, and M. Soutif, Compt. Rend., 252, 550, 1961.

147. J. Graham, G.F. Walker, and G.W. West, J. Chem. Phys. 40, 540, 1964.

148. A.M. Hecht, M. Dupont, and P. Ducros, Bull Soc. franc. Miner. Crist., 89, 6, 1966.

149. D.E. Woessner and B.S. Snowden, Jr., J. Chem. Phys., 50, 1516, 1969.

150. D.E. Woessner and B.S. Snowden, Jr., J. Colloid and Interface Sci., 30, 54, 1969.

151. A.M. Hecht and E. Geissler, J. Colloid and Interface Sci., 34, 32, 1970.

152. D.E. Woessner, B.S. Snowden, Jr., and G.H. Meyer, J. Colloid and Interface Sci., 34, 43, 1970.

153. H.J.C. Berendsen, J. Chem. Phys., 36, 3297, 1961.

154. H.J.C. Berendsen and C. Migchelsen, Ann. N.Y. Acad. Sci., 125, 365, 1965.

155. H.J.C. Berendsen and C. Migvhelsen, Federation Proc., 25, 998, 1966.

156. C. Migchelsen and H.J.C. Berendsen, Colloque Ampere XIV, 762, North-Holland Publ. Co., 1967.

157. R.E. Dehl, J. Chem. Phys. 48, 831, 1968.

158. R.E. Dehl and C.A.J. Hoeve, J. Chem. Phys., 50, 3245, 1969.

159. B. Fung and P. Trautmann, Biopolymers, 10, 391, 1971.

160. A.A. Khanagov, Biopolymers, 10, 789, 1971.

161. A. Saupe, Z. Naturforsch., 19a, 161, 1964.

162. A.D. Buckingham and K.A. McLauchlan, 'Progress in NMR Spectroscopy', Vol II, J.W. Emsley, J. Feeney, and L.H. Sutcliffe, Ed., Pergammon Press, Oxford, 1967, p. 63.

163. P. Waldstein, S.W. Rabideau, and J.A. Jackson, J. Chem. Phys., 41, 3407, 1964.

164. D.W. Poesner, Aust. J. Phys., 13, 168, 1960.

165. E.B. Treacy and Y. Beers, J.Chem. Phys., 36, 1473, 1962.

166. J. Charvolin and P. Rigny, Mol. Cryst. Liquid Cryst., 15, 211, 1971.

167. W.L. Hubbell and H.M. McConnell, J. Amer. Chem. Soc., 93, 314, 1971.

168. P.J. Flory, 'Statistical Mechanics of Chain Molecules', Interscience, New York, N.Y., 1969.

[illegible]

[illegible]

[illegible]

169. R.D. Kornberg and H.M. McConnell, Proc. Nat. Acad. Sci. U.S.A., 68, 2564, 1971.

170. P.L. Jain, J.C. Lee, and R.D. Spence, J. Chem. Phys., 23, 878, 1955.

171. H. Lippman and K.H. Weber, Ann. Phys., 20, 265, 1957.

172. H. Eyring, J. Walter, and G. Kimball, 'Quantum Chemistry', John Wiley and Sons, Inc., New York, 1944, p. 358.

173. K.H. Weber, Z. Naturforsch., 14a, 112, 1959.

174. K.H. Weber, Ann. Phys., 3, 125, 1959.

175. J.C. Rowell, W.D. Phillips, L.R. Melby and M. Panar, J. Chem. Phys., 43, 3442, 1965.

176. M. Linzer and R.A. Forman, J. Chem. Phys., 46, 4690, 1967.

177. F. Hruska, T. Schaefer and C.A. Reilly, Can. J. Chem., 42, 697, 1964.

178. C.P. Rader, J. Amer. Chem. Soc., 88, 1713, 1966.

179. C.P. Rader, J. Amer. Chem. Soc., 91, 3248, 1969.

180. W.B. Moniz and C.F. Poranski, Jr., J. Amer. Chem. Soc., 88, 190, 1966.

181. O.L. Chapman and R.W. King, J. Amer. Chem. Soc., 86, 1256, 1964.

182. G.C. Pimentel and A.L. McClellan, 'The Hydrogen Bond', W.H. Freeman and Co., 1960, p. 167.

183. R.J. Abraham, 'The Analysis of High Resolution NMR Spectra', Elsevier Publishing Co., 1971, p. 58.

184. J. Delamu and C. Barbier, J. Chem. Phys., 41, 1106, 1964.

185. K.C. Raney and J. Messick, Tetrahedron Letters, 4423, 1965.

186. M. Karplus, J. Chem. Phys., 30, 11, 1959.

187. M.P. McDonald and W.E. Peel, Trans. Faraday Soc., 67, 890, 1971.

Postgraduate course of studies

The following series of lectures given to postgraduate students at the University of Sheffield were attended.

1. Principles of nuclear magnetic resonance and chemical applications, by Dr. W.T. Raynes (6 lectures).

2. Magnetic relaxation processes and lineshapes, by Dr. N. Atherton (6 lectures).

3. Structure of membranes, by Professor D. Chapman (6 lectures).